

✓  
**ISOTOPICALLY ANOMALOUS  
MERCURY IN METEORITES BY  
NEUTRON ACTIVATION ANALYSIS**

**A Thesis Submitted  
in Partial Fulfilment of the Requirements  
for the Degree of**

**DOCTOR OF PHILOSOPHY**

*by*

**ALAKH NIRANJAN THAKUR**

*to the*

**DEPARTMENT OF CHEMISTRY**

**INDIAN INSTITUTE OF TECHNOLOGY KANPUR**

**JANUARY, 1988**

106249

Dedicated to

**MATAJEE, BABUJEE AND DIDI**

who gave first priority to education and encouraged me to do research.

## STATEMENT

I hereby declare that the research work embodied in this thesis is the result of investigations carried out by me in the Department of Chemistry, Indian Institute of Technology, Kanpur under the supervision of Professor P.S. Goel.

In keeping with the general practice of reporting scientific observations, due acknowledgements have been made wherever the work described is based on the findings of other investigators.

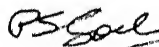


( Alakh Niranjana Thakur )

Kanpur, India.

January, 1988

Statement verified




( P.S. Goel )

Thesis Supervisor.



## C E R T I F I C A T E

Certified that the work contained in this thesis entitled "ISOTOPICALLY ANOMALOUS MERCURY IN METEORITES BY NEUTRON ACTIVATION ANALYSIS" has been carried out by Mr Alakh Niranjan Thakur under my supervision and the same has not been submitted elsewhere for a degree.

  
( P.S. Goel )  
Thesis Supervisor

DEPARTMENT OF CHEMISTRY  
INDIAN INSTITUTE OF TECHNOLOGY, KANPUR

CERTIFICATE OF COURSE WORK

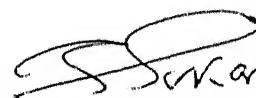
This is to certify that Mr Alakh Niranjana Thakur has satisfactorily completed all the course requirements for the Ph.D. degree programme in Chemistry. The courses include :

CHM505	PRINCIPLES OF ORGANIC CHEMISTRY
CHM524	MODERN PHYSICAL METHODS OF CHEMISTRY
CHM525	PRINCIPLES OF PHYSICAL CHEMISTRY
CHM543	INTRODUCTION TO NUCLEAR CHEMISTRY
CHM545	PRINCIPLES OF INORGANIC CHEMISTRY
CHM626	SOLID STATE CHEMISTRY
CHM642	APPLICATIONS OF NUCLEAR CHEMISTRY
CHM800N	GENERAL SEMINAR
CHM801N	SPECIAL SEMINAR
CHM900N	Ph.D. THESIS

Mr Alakh Niranjana Thakur was admitted to the candidacy of the Ph.D. degree in December, 1982 after he successfully completed the written and oral qualifying examinations.



( P.S. Goel )  
Head  
Department of Chemistry



( S. Sarkar )  
Convener  
Departmental Post-Graduate Committee  
Department of Chemistry  
I.I.T. Kanpur

## ACKNOWLEDGEMENT S

I am grateful to Professor P.S. Goel who introduced me to the exciting area of the study of meteorites and neutron activation analysis technique. His efficient guidance and encouragement during the course of this work lead to the successful completion of this thesis.

Financial support for this work from the Indian Space Research Organization is deeply appreciated.

I would like to thank the following persons and organizations for donation of valuable meteorite samples for this work.

Dr K Fredriksson, Prof T P Kohman, Prof J Arnold, Prof G Kurat, Dr B Mason, Prof C B Moore and the USSR academy of sciences.

Dr R G Deshpande of BARC is thanked for his cooperation in providing us timely bombardments in the reactors at BARC Bombay. This research at IIT Kanpur was supported by Department of Space.

The following persons are thanked for the help they provided in various ways :

Mr B Sairam, Mr M J Bhaskaran and Mr P R Subramanian of glass blowing shop for their efficient cooperation during the course of this work.

Mr T G Rao, Mr R K Jha and Mr R K Sharma for their skillful technical assistance and Mr V S Agnihotri for laboratory assistance.

To all the staff members of liquid Nitrogen Plant for making an untiring regular supply of liquid Nitrogen.

My laboratory colleague Mr Pradeep Kumar for his cooperation during the work and Lalita his wife, for her sympathetic attitude.

Dr Rakesh Jain for proof reading of some parts of this thesis.

My friends, particularly, Mr B B Pandey, Mr Udaya Kumar, Mr K Mohan Rao, Mr A K Dubey for their help at various stages.

My special appreciation to Ms Poonam Singh, Mrs Kalpana Choudhary and Ms Kalyani Choudhary for their moral support and pleasing temperament during the hours of distress, to Mrs Saroj Goel for her motherly approach, and to my brothers Khageshwar, Tarkeshwar, Akhileshwar and Gyaneshwar for their patience during the course of this work.

Above all my appreciation and regards goes to Rita bhabhi for her morale, encouragement and material help, which gave me enormous mental drive at accelerated completion of this thesis work.

The last but not the least I am thankful to Mr Firoz who spent several sleepless nights to type the thesis.

**Alakh Niranjana Thakur**

## TABLE OF CONTENTS

		Page
	LIST OF TABLES	vii
	LIST OF FIGURES	x
	SYNOPSIS	xv
Chapter 1	INTRODUCTION	1
1.1	Meteorite classes	1
1.1.1	Ordinary chondrites	2
1.1.2	Carbonaceous chondrites	2
1.1.3	Iron meteorites	3
1.1.4	Stony-Iron meteorites	4
1.1.5	Achondrites	5
1.1.6	Meteorites of Asteroidal, Lunar and Martian origin	5
1.2	Summary of isotopic anomalies in meteorites	6
1.2.1	Mass fractionation	6
1.2.2	Nuclear reactions	6
1.2.3	Radioactive decay products	7
1.2.4	Anomalies in stone meteorites	7
1.2.5	Anomalies in iron meteorites	8
1.2.6	D/H ratios in carbonaceous chondrites	9
1.2.7	$^{15}\text{N}/^{14}\text{N}$ ratios	10
1.2.8	Oxygen isotopic anomaly	10
1.2.9	Oxygen isotope fractionation in the laboratory	13
1.2.10	Kinetics and self shielding in $\text{O}_2$	15

1.2.11	Importance of noble gases	16
1.2.12	Neon-E	17
1.2.13	Xenon isotopic anomalies	19
1.2.14	CCF-xenon (SN-xenon or xenon-X)	20
1.2.15	S-process xenon	20
1.3	Mercury	23
1.3.1	Mercury in stars	25
1.3.2	Cosmic abundance of mercury	25
1.3.3	Mercury abundances in meteorites	28
1.3.4	Mercury isotopic anomaly in meteorites	29
1.3.5	Interpretation of mercury isotopic anomaly	31
1.4	Carrier phase(s) of the isotopic anomalies	34
1.4.1	Carbonaceous carrier : the acid insoluble residue	34
1.4.2	Cathodless glow discharge experiment	35
1.4.3	Allende inclusions CI and EK 1-4-1	36
1.4.4	Organic compounds bearing isotopic signatures	36
Chapter 2	<b>EXPERIMENTAL</b>	40
2.1	Introduction	40
2.2	Sample preparation	43
2.2.1	Acid dissolution of iron meteorites	43
2.2.2	Grain size separation	44
2.2.3	Magnetic phase separation	44

2.2.4	Relative densities of grains	45
2.2.5	Sampling of stone meteorites	45
2.2.6	Terrestrial standard : the monitor	46
2.3	Packing of samples and monitors	46
2.4	The neutron irradiation	47
2.5	Mercury distillation	47
2.6	Extraction of Hg using sodium diethyldithiocarbamate	49
2.6.1	Reagent preparation	51
2.6.2	Washing of distilled Hg from vacuum line	52
2.7	Radiochemical purification of mercury	52
2.8	Activity measurement	53
2.8.1	Energy calibration	55
2.8.2	Sample counting geometry	55
2.8.3	Shielding of the detector	56
2.8.4	Counting	56
2.8.5	Decay corrections	56
2.8.6	Errors	57
2.9	Precautions to avoid contamination	57
2.9.1	Blank level monitoring	59
Chapter 3	<b>RESULTS FROM METEORITE STUDIES</b>	60
3.1	Vial No. 1/85	60
3.2	Vial No. 2/85	61
3.3	Vial No. 3/85	64
3.4	Vial No. 4/85	69
3.5	Vial No. 5/85	73

## Page

3.6	Vial No. 6/85	73
3.7	Vial No. 7/85	77
3.8	Vial No. 8/85	81
3.9	Vial No. 9/85	81
3.10	Vial No. 1/86	90
3.11	Vial No. 2/86	98
3.12	Vial No. 3/86	103
3.13	Vial No. 4/86	109
3.14	Vial No. 5/86	127
3.15	Vial No. 6/86	133
3.16	Vial No. 7/86	137
3.17	Vial No. 8/86	143
3.18	Vial No. 9/86	153
3.19	Vial No. 10/86	168
3.20	Vial No. 1/87	170
3.21	Vial No. 2/87	173
3.22	Vial No. 3/87	173
3.23	Vial No. 4/87	177
3.24	Vial No. 6/87	177
3.25	Vial No. 7/87 : The organic extract	177

Chapter 4	<b>RESULTS FROM RE-IRRADIATION EXPERIMENTS</b>	183
4.1	Vial No. 1/87	183
4.2	Vial No. 2/87	185
4.3	Vial No. 3/87	190
4.4	Vial No. 4/87	191
4.5	Vial No. 5/87	191
4.6	Vial No. 6/87	199



	Page
Chapter 5 DISCUSSION	208
5.1 Absence of experimental artifacts	208
5.1.1 Matrix effect	209
5.1.2 Sample position in a vial	209
5.1.3 Counting geometry and sample volume	211
5.1.4 Dependence of ratio on counting rates	211
5.1.5 Interference from other gamma lines	214
5.1.6 Mass fractionation during distillation	214
5.1.7 Re-irradiation experiments	216
5.2 Anomalies in stone meteorites	216
5.2.1 Allegan (H5)	218
5.2.2 Allende (CV3)	218
5.2.3 Ambapur Nagla (H5)	218
5.2.4 Cold Bokveld (CM2)	228
5.2.5 Dhajala (H 3-4)	228
5.2.6 Elenovka (L5)	228
5.2.7 Forest Vale (H4)	228
5.2.8 Holbrook (L6)	230
5.2.9 Karkh (L6)	230
5.2.10 Menow (H4)	230
5.2.11 Rangala (L6)	230
5.2.12 Richardton (H5)	232
5.3 Anomalies in Iron meteorite residues	232
5.3.1 bear Creek (III B)	232
5.3.2 Campo del Cielo (IA)	234
5.3.3 Canyon Diablo (IA)	234
5.3.4 Carbo (II D)	234
5.3.5 Chinga (IV B ANOM)	234

## Page

5.3.6 Elga (II E) 237

5.3.7 Odessa (IA) 237

5.3.8 Sikhote Alin (II B) 237

5.3.9 Toluca (IA) 241

5.4 Constrains on the Origin of Meteorites 248

REFERENCES 251

GENERAL REFERENCES 266

## LIST OF TABLES

Table No.		Page
1.1	Mercury in Stars	24
1.2	Cosmic Abundance of Mercury	26
2.1	Nuclear activation parameters for Hg isotopes	42
3.1	$^{203}\text{Hg}/^{197}\text{Hg}$ Ratio in Vial No. 1/85	62
3.2	Results from Vial No. 2/85	65
3.3	Results from Vial No. 3/85	68
3.4	Mercury in Ambapur Nagla (Vial No. 4/85)	70
3.5	Results from Run No. 5/85	75
3.6	Results from Run No. 6/85	78
3.7	Vial No. 7/85 : Mercury from Ambapur Nagla and Carbo Meteorites	79
3.8	Results from Vial No. 7/85	80
3.9	Vial No. 8/85 Mercury from Ambapur Nagla	82
3.10	Vial No. 8/85 Total Mercury concentration in Ambapur Nagla samples	83
3.11	Results from Vial No. 9/85	85
3.12	Calculated gross ratios (Vial No. 9/85)	93
3.13	Activation energy of mercury released from Ambapur Nagla and Rangala (Vial No. 9/85)	97
3.14	Results from Dhajala, Vial No. 1/86	99
3.15	Results from Vial No. 2/86	101
3.16	Vial No. 3/86 : Mercury from Allende fragments	110
3.17	Vial No. 4/86 : Mercury from Ambapur Nagla	122
3.18	Results from Vial No. 5/86	128
3.19	Vial No. 6/86 Mercury from Iron Meteorite Residues	134

Table No.	Page
3.20	Vial No. 7/86 Mercury from Sikhote Alin Residues 139
3.21	Vial No. 8/86 Mercury from Ambapur Nagla fragments 150
3.22	Vial No. 9/86 Mercury from Sikhote Alin Residues 162
3.23	Vial No. 10/86 Mercury from Karkh and Rangala 169
3.24	Vial No. 1/87 Mercury from Rangala 171
3.25	Vial No. 1/87 Mercury from Chinga residues 172
3.26	Vial No. 2/87 Mercury from Holbrook and CdC residues 174
3.27	Vial No. 2/87 Mercury from CdC residues (supplementary data) 175
3.28	Vial No. 3/87 Results from Ambapur Nagla bulk 178
3.29	Vial No. 4/87 Irradiation of Hg distilled from Karkh fragments 179
3.30	Vial No. 6/87 Mercury from Odessa Residues 180
3.31	Vial No. 7/87 Solvent Extraction Experiment 182
4.1	Vial No. 1/87 Re-irradiation Control Experiment 186
4.2	$^{197}\text{Hg}/^{203}\text{Hg}$ Ratio in Acid Insoluble Residues 189
	(magnetic) of Sikhote Alin Iron Meteorite
4.3	$^{197}\text{Hg}/^{203}\text{Hg}$ Ratio in Sikhote Alin Magnetic Residues 192
4.4	$^{197}\text{Hg}/^{203}\text{Hg}$ Ratio in Ambapur Nagla 196
4.5	Vial No. 5/87, Re-irradiation of Sikhote Alin and Chinga 200
4.6	$^{197}\text{Hg}/^{203}\text{Hg}$ Ratio in Chinga Residues 201
4.7	$^{197}\text{Hg}/^{203}\text{Hg}$ Ratio in Sikhote Alin Residues 203
4.8	Vial No. 6/87 Re-irradiation of Hg Distilled from Sikhote Alin 205
4.9	$^{197}\text{Hg}/^{203}\text{Hg}$ Ratio in Sikhote Alin Magnetic Residues 206
5.1	Results of Isotopic Ratio of Hg Loaded on Different Matrices 210
5.2	Anomalies in Allende (Vial No. 3/86) : the summary 219
5.3	Gross values of $R/R^+$ and Hg contents in Ambapur Nagla 223
5.4	Summary of Anomalous Isotopic Ratios in Ambapur Nagla 224
5.5	Anomalies in Cold Bokeveld, Dhajala and 229
	Elenovka : the summary

Table No.		Page
5.6	Anomalies in Rangala and Richardton : the summary	231
5.7	Mercury from Chondrites	233
5.8	Summary of Anomalous Isotopic Ratios in Campo del Cielo, Canyon Diablo and Carbo residues	235
5.9	Summary of Anomalous Isotopic Ratios in Chinga, Elga and Odessa residues	236
5.10	Summary of Anomalous Isotopic Ratios in Sikhote Alin Residues	243
5.11	Gross values of $R/R^+$ and Hg contents in Sikhote Alin	246
5.12	Mercury Concentration Ranges in different Iron Meteorite samples	247

## LIST OF FIGURES

Figure No.		Page
1.1	Graph of $^{17}\text{O}/^{16}\text{O}$ vs. $^{18}\text{O}/^{16}\text{O}$ for terrestrial and meteoritic samples	11
1.2	Neon isotopic anomaly in Orguil meteorite	18
1.3	Comparison of anomalous Xenon and anomalous Krypton	21
1.4	CCF-Xe and s-Xe	22
2.1	Nuclides chart of mercury	41
2.2	Mercury distillation arrangement	48
2.3	Mercury distillation apparatus	50
2.4	Photon detection recording set-up	54
2.5	Counting rate vs. distillation sequence	58
3.1	The Hg isotopic ratio in samples from Bear Creek and Campo del Cielo meteorites	63
3.2	The isotopic ratio data from Vial No. 2/85	66
3.3	Photon spectra of Sikhote Alin residue samples	67
3.4	$R/R^+$ values for Ambapur Nagla samples	71
3.5	Photon spectra of anomalous and normal Hg samples of Ambapur Nagla and the reagent mercury	72
3.6	Decay lines of $^{197}\text{Hg}$ and $^{203}\text{Hg}$ from samples of Ambapur Nagla	74
3.7	Mercury concentration (left scale) and its Hg isotopic ratios (right scale) measured at different temperatures in samples of Ambapur Nagla	87
3.8	Mercury concentration (left scale) and its Hg isotopic ratios (right scale) measured at different temperatures in samples of Ambapur Nagla	88
3.9	Mercury concentration (left scale) and its Hg isotopic ratios (right scale) measured at different temperatures in samples of Rangala	89

Figure No.	Page
3.10 Photon spectra of Hg distilled from Ambapur Nagla chondrules	91
3.11 Decay measurements on $^{197}\text{Hg}/^{203}\text{Hg}$ ratio from some Ambapur Nagla samples	92
3.12 Arrhenius plot for mercury released	94
3.13 Arrhenius plot for mercury released	95
3.14 Arrhenius plot for mercury released	96
3.15 Photon spectra of Cold Bokeveld samples	104
3.16 Photon spectra of Hg released from some samples in Vial No. 2/86	105
3.17 Decay line of $^{203}\text{Hg}$ from Cold Bokeveld	106
3.18 Decay line of activity ratio of Hg isotopes from Sikhote Alin inclusion	107
3.19 Decay lines of $^{197}\text{Hg}$ and $^{203}\text{Hg}$ from Sikhote Alin inclusion	108
3.20 Mercury isotopic ratio (left scale) and its concentration (right scale) measured in samples of Allende at different temperatures	112
3.21 Photon spectra of some Hg distillates from Allende	113
3.22 Photon spectra of some Hg samples isolated from Allende	114
3.23 Photon spectra of some Hg samples isolated from Allende	115
3.24 Photon spectra of some Hg samples isolated from Allende	116
3.25 Decay line of activity ratio of Hg isotopes from Allende sample	117
3.26 Decay lines of $^{197}\text{Hg}$ and $^{203}\text{Hg}$ from Allende sample	118
3.27 Decay line of activity ratio of Hg isotopes from Allende	119
3.28 Decay lines of $^{197}\text{Hg}$ and $^{203}\text{Hg}$ from Allende	120

Figure No.	Page
3.29 The isotopic ratio data from Vial No. 4/86	124
3.30 Photon spectra of some Hg samples of Ambapur Nagla	125
3.31 Photon spectra of some Hg samples of Ambapur Nagla	126
3.32 Photon spectrum of an anomalous sample of Richardton	130
3.33 Mercury concentration (left scale) and its isotopic ratio (right scale) measured at different temperatures in samples of Allegan and Richardton	131
3.34 Mercury concentration (left scale) and its isotopic ratio (right scale) measured at different temperatures in samples of Dhajala and Allende	132
3.35 The isotopic ratio data from Vial No. 6/86	136
3.36 The photon spectra of Hg distillates from some samples of Elga	138
3.37 Photon spectra of normal and anomalous samples from Sikhote Alin acid residues	141
3.38 Photon spectra of some samples of Sikhote Alin residue	142
3.39 Photon spectra of some samples of Sikhote Alin residue	144
3.40 Decay lines of $^{203}\text{Hg}$ from samples of Sikhote Alin	145
3.41 Decay lines of $^{203}\text{Hg}$ from samples of Sikhote Alin	146
3.42 Mercury concentration (left scale) and its isotopic ratio (right scale) measured at different temperatures in samples of Ambapur Nagla	148
3.43 Mercury concentration (left scale) and its isotopic ratio (right scale) measured at different temperatures in samples of Ambapur Nagla	149
3.44 Photon spectra of some samples of Ambapur Nagla	151
3.45 Photon spectra of some samples of Ambapur Nagla	152
3.46 Photon spectra of some samples of Ambapur Nagla	154
3.47 Photon spectra of some samples of Ambapur Nagla	155
3.48 Arrhenius plot for mercury released	156
3.49 Arrhenius plot for mercury released	157



Figure No.	Page
3.50 Decay lines of activity ratios of Hg in some samples from Ambapur Nagla	158
3.51 Decay line of $^{203}\text{Hg}$ from some samples of Ambapur Nagla	159
3.52 Decay line of $^{203}\text{Hg}$ from some samples of Ambapur Nagla	160
3.53 Photon spectra of an anomalous sample of Sikhote Alin	163
3.54 Decay lines of activity ratios of Hg from samples of SikhoteAlin residue	164
3.55 Decay lines of $^{197}\text{Hg}$ from samples of Sikhote Alin residue	165
3.56 Decay lines of $^{203}\text{Hg}$ from some samples of Sikhote Alin residue	166
3.57 Decay lines of $^{203}\text{Hg}$ from some samples of Sikhote Alin residue	167
3.58 Decay lines of activity ratios of Hg isotopes from Campo del Cielo residue samples	176
4.1 Micro shaking flask	184
4.2 Ratio vs. count-rate of re-irradiated normal sample (1/87)	187
4.3 Count-rate before re-irradiation vs. count-rate after re-irradiation (1/87)	188
4.4 Photon spectra of re-irradiated samples of Sikhote Alin (3/87)	193
4.5 Decay lines of ratio of re-irradiated samples (3/87)	194
4.6 Decay lines of $^{197}\text{Hg}$ of re-irradiated samples (3/87)	195
4.7 Count-rate in Vial No. 8/86 vs. count-rate in Vial No. 4/87 of Ambapur Nagla samples	197
4.8 Photon spectra of re-irradiated anomalous sample of Ambapur Nagla and monitor (4/87)	198
4.9 Count-rate in Vial No. 1/87 vs. count-rate in Vial No. 5/87 of Chinga samples	202
4.10 Mercury $\mu\text{g}$ in Vial No. 7/86 vs. count-rate in Vial No. 5/87 of Sikhote Alin samples	204
4.11 Count-rate in Vial No. 9/86 vs. count-rate in Vial No. 6/87 of Sikhote Alin samples	207

Figure No.		Page
5.1	$^{197}\text{Hg}/^{203}\text{Hg}$ Ratio vs. counting volume in reagent mercury	212
5.2	$^{197}\text{Hg}/^{203}\text{Hg}$ vs. activity of $^{203}\text{Hg}$ in reagent mercury	213
5.3	Ratio deviation (%) based on 77 keV and 68 keV photons (from $^{197}\text{Hg}$ ) and 279 keV gamma energy (from $^{203}\text{Hg}$ ) in iron meteorite residues	215
5.4	Photon spectra of re-irradiated samples of Sikhote Alin	217
5.5	$R/R^+$ vs. temperature in Allende	220
5.6	ppb-Hg vs. temperature in Allende	221
5.7	$R/R^+$ vs. temperature in Ambapur Nagla	226
5.8	ppb-Hg vs. temperature in Ambapur Nagla	227
5.9	$\delta$ values of $R/R^+$ vs. sample number of Sikhote Alin	238
5.10	$R/R^+$ variation in Sikhote Alin samples (7/86)	239
5.11	Photon spectra of anomalous and normal samples of Sikhote Alin	240
5.12	Variation of $R/R^+$ vs. temperature in Sikhote Alin (9/86)	242
5.13	$R/R^+$ vs. temperature in Sikhote Alin	244
5.14	ppm-Hg vs. temperature in Sikhote Alin.	245

## SYNOPSIS

Isotopic ratio of  $^{196}\text{Hg}/^{202}\text{Hg}$  has been measured in a large number samples obtained from meteorites by neutron activation analysis. Irradiated samples have been heated stepwise to distill the radionuclides for isotopic ratio measurements. While many samples give a normal ratio, in some cases huge anomalies are found.

The stone meteorites were studied as bulk, separated into magnetic and non-magnetic fractions, and chondrules. Acid insoluble residues of iron meteorites were obtained by slow dissolution of metal in 2M  $\text{H}_2\text{SO}_4$ . The residues were further separated into different size fractions, magnetic and non-magnetic. Typically 100 mg size samples packed in quartz capsules were irradiated to a neutron flux of  $10^{13}\text{n/sec/cm}^2$  along with reagent monitor. Hg was vacuum distilled at various temperatures ( $100^\circ\text{C}$  to  $600^\circ\text{C}$ ). The distillates trapped in the cold finger at liquid nitrogen temperature, were washed with aqua regia or, in later experiments, were extracted into diethyl dithio carbamate complex in carbon tetrachloride.

The samples were counted in liquid form under reproducible geometry. Photons of  $^{197}\text{Hg}$  (2.67 days, 77.3 keV  $\gamma$  and 77.9 keV X) and  $^{203}\text{Hg}$  (46.6 days, 279 keV  $\gamma$ ) were spectrum analysed on a high purity germanium detector coupled with multichannel analyser.

Absence of experimental artifacts during irradiation or during counting has been demonstrated by devising a number of experiments.

A total of fifteen stone meteorites and nine iron meteorites residues have been studied in twenty-six different irradiations. The Hg content ranges from 1 ppb to 50 ppm. In almost all meteorites (stones and irons) in some phase and at some temperature we find anomalous ratio of  $^{196}\text{Hg}/^{202}\text{Hg}$ . Both positive and negative deviations are observed and the anomalous component is highly sporadic and minor in nature. In Ambapur Nagla chondrite in most cases upto  $300^\circ\text{C}$ , Hg is at about 1 ppm level and the isotopic ratio is normal or, sometimes, slightly higher than normal. In the high temperature fractions we get 10 to 100 ppb Hg with the isotopic ratio of  $^{196}\text{Hg}/^{202}\text{Hg}$  only 50 % of the normal value. If one were to make a one temperature measurement one may get almost normal value due to over-abundance of the normal low temperature mercury. A few other chondrites have also registered a similar temperature profile but all profiles are not necessarily identical. The most spectacular deviation was found in fine grained magnetic particles of Ambapur Nagla at  $100^\circ\text{C}$ . The  $^{196}\text{Hg}$  is apparently absent, a  $2\sigma$  value estimated for normalised ratio is only 2 % of the normal value. Iron meteorites, on the other hand, do not show any regular temperature profile. But the anomalies are found there as well. One sample of Sikhote Alin iron meteorite residue (45-75  $\mu\text{m}$ , magnetic) also showed a complete absence of  $^{196}\text{Hg}$ .

The extreme positive value obtained in the case of stone meteorites is for bulk Allende having 1.5 times of the normal value and the largest in the case of iron is for a residue from Campo del Cielo which is 1.3 times of normal isotopic ratio.

Some of the distilled radioactive condensates of Hg from several runs were reirradiated to ensure absence of artifacts during irradiation. Our results demonstrate that we were able to obtain Hg condensates from meteorites without any contamination from the laboratory. The re-irradiated samples showed the activity ratios of  $^{197}\text{Hg}/^{203}\text{Hg}$  of the same pattern as was expected on the basis of the results of the previous runs. In these re-irradiation experiments all samples of Hg (monitor, normal, anomalous, isotopically diluted and blank) were in identical chemical forms and were bombarded under similar conditions. Further, the Hg contents of the normal and anomalous samples were comparable. In all cases the anomaly persisted showing that any artifacts introduced during irradiation due to such causes as neutron energy spectrum variation, interference from the matrix element, self-shielding effects, are not responsible for the observed isotopic variations.

Existence of isotopically anomalous Hg in iron meteorites along with other results obtained in this laboratory suggests that these objects contain presolar grains and might not have been formed by a magmatic differentiation. Also to retain the memory of this volatile elements isotope variations, they must not have been heated to high temperatures for long time.

Another possible explanation for the existence of Hg isotopic anomaly in meteorites (both iron and stones) would be that the anomalous components might have been introduced late in the history of the meteorite parent body during its collisions with other cosmic objects (for example, a comet) with presumably different isotopic ratio of Hg.

## Chapter I

### INTRODUCTION

Until several years ago it was widely believed that the planetary objects of our solar system including meteorites were formed from a well mixed primordial nebula of chemically and isotopically uniform composition, as a result of complete mixing of atoms of diverse nucleosynthetic origin, either in interstellar space prior to formation of the nebula or in the nebula itself prior to condensation. However, recent measurements have shown this conception to be erroneous. Anomalies have been discovered in the isotopic composition of a number of elements, found in some phases of meteorites. These isotopic anomalies cannot be ascribed to any process active within the solar system today. In a few specific cases the nuclear reactions responsible for the anomalous abundances might have taken place in the early solar system. However, most anomalies appear to predate the formation of the solar system and to be the result of nuclear reactions in other stars. The occurrence of such anomalies also requires incomplete mixing of the solar system material prior to condensation and/or survival of presolar grains. These nuclear isotopic anomalies which may influence one or several isotopes of an element are often accompanied by systematic isotopic abundance variations due to mass dependent fractionation processes.

Many samples of solar system matter are available for study, either in the laboratory or by remote sensing methods. These include the sun and the solar wind, planets and their satellites, asteroids, comets and meteorites. For the observation of isotopic variations in the laboratory

with sufficient precision, meteorites are probably the best source of information (Sears, 1986; Lipschutz, 1986).

## 1.1 Meteorite classes

There are five main classes of meteorites : ordinary chondrites, carbonaceous chondrites, achondrites, irons and stony-irons, each including a number of chemically distinct sub-classes.

### 1.1.1 Ordinary chondrites

These abundant meteorites are aggregates of chiefly ferromagnesian silicate minerals, grains of metallic nickel-iron, and chondrules (e.g. Semenenko et al., 1986; Scott et al., 1985). Chondrules are spheroidal bodies, few mm in diameter, consisting mainly of olivine  $[(\text{Mg}, \text{Fe})_2\text{SiO}_4]$  and pyroxene  $[(\text{Mg}, \text{Fe}) \text{SiO}_3]$ , with or without glass. They appear to be droplets of silicate melts that congealed before they could accumulate into the parent bodies of chondrites (McSween, 1985; Ashworth, 1979; 1980; Ashworth et al., 1984). Alternative views suggesting that most chondrules are melted aggregates of interstellar dust or are formed by impact have also been put forward (Rubin et al., 1983).

### 1.1.2 Carbonaceous chondrites

There are three main types of carbonaceous chondrites, designated C1, C2 and C3. The C1 chondrites are soft, black meteorites consisting almost entirely of layer lattice hydrous silicates, such as clays and serpentine, ranging in grain size from a few angstroms to a few microns (Barber, 1985). Grains and spherules of magnetite ( $\text{Fe}^{++}\text{Fe}_2^{+++}\text{O}_4$ ) are also present, indicating formation under oxidising conditions. C1 chondrites are known to contain hydrocarbons which form and survive only at

low temperature. The structure and stereochemistry of the meteoritic hydrocarbons exclude a biological origin (Mullie and Reisse, 1987). C1 chondrites contain no chondrules. However, some scattered grains of high temperature minerals, such as olivine, (some of which display solar flare particle tracks, Macdougall, 1977) are found. Although they show evidence of some post-accretion processing, C1 chondrites are believed to be the most primitive meteorites.

The C2 chondrites consist of about equal proportions of C1 type matrix material and high temperature condensates, including chondrules, individual olivine and pyroxene grains, olivine aggregates, and about 1% inclusions rich in calcium-aluminium silicates. The C3 chondrites consist of 35-40 % matrix (Scott et al., 1984; Nagahara, 1984), largely made-up of Fe-rich olivine, 60-65 % high temperature components, and only about 0.4 % C. The Ca-Al-rich inclusions (CAIs), have gained extraordinary importance for the indications they give of nebular and interstellar components (Kornacki and Fegey, 1986). CAIs inclusions obtained from Allende meteorite, are assemblages of anorthite ( $\text{CaAl}_2\text{Si}_2\text{O}_8$ ), Ca-Al-Ti-rich pyroxene, melilites (solid solutions of  $\text{Ca}_2\text{Al}_2\text{SiO}_7$  and  $\text{Ca}_2\text{MgSi}_2\text{O}_7$ ), spinel ( $\text{Mg}_2\text{SiO}_4$ ), perovskite ( $\text{CaTiO}_3$ ) and other highly refractory minerals (MacPherson and Grossman, 1984). Some of them contain 'nuggets' of platinum group metals, and all show enhancements in non volatile trace elements.

### 1.1.3 Iron meteorites

Iron meteorites are masses of metallic nickel-iron with minor accessory minerals, chiefly sulfides, graphite, schreibersite, carbides and phosphides. Most irons appear to have crystallised from cores or pods of molten metal within chondritic parent bodies. Cooling rates, ranging from



less than  $1^\circ$  to about  $6000^\circ\text{C}$  per million years, have been calculated from the textures and Ni distributions within iron meteorites (Narayan and Goldstein, 1985). Such rapid rates (by planetary standards) could occur only within small, poorly-insulated bodies. Additional evidence for rapid cooling comes from radiometric age determinations showing that iron meteorites solidified within a few tens of millions of years after the birth of the solar system. Trace element analyses show that iron meteorites belong to about 60 chemical groups, suggestive of derivation from a large number of different parent bodies. Although, as noted above, most irons are postulated to have originated from melts, some of them show chemical variations over distances of few centimeters indicating that the metal never completely melted and homogenized. Indeed, instead of having formed as molten pools within a predominantly silicate-rich planetoid, certain irons may record a history of primary metal grain condensation and accretion in the cooling solar nebula.

#### **1.1.4 Stony-Iron meteorites**

This less common class of meteorites contains silicates and metal in roughly equal proportion. These meteorites occur in two main varieties : pallasites and mesosiderites. Pallasites consist chiefly of coarse grains of olivine, ranging in size upto about one centimeter, embedded in a meshwork of metallic Ni-Fe. Textural relations suggest that a mass of olivine grains segregated from a silicate melt, was engulfed by molten metal. Mesosiderites are admixtures of silicates and nodular masses of Ni-Fe metal, plus minor oxides, phosphates and sulphides (Wasson and Rubin, 1985). Many show evidence of metamorphism, brecciation and even late-stage partial re-melting.

### 1.1.5 Achondrites

Achondrites are stone-meteorites free of chondrules, resembling magmatic rocks or, sometimes, basaltic lavas (e.g. Wolf et al., 1983; Hertogen et al., 1983). Some of these are formed by crystal settling in cooling melts. All achondrites have been brecciated and metamorphosed to some degree, and some show shock effects due to collisions. The most common type of achondrites are eucrites and howardites.

### 1.1.6 Meteorites of Asteroidal, Lunar and Martian origin

Some meteorites are believed to be derived from earth crossing comets or asteroids as indicated by several lines of evidence (e.g. Wasson and Wetherill, 1979; Drake, 1979; Larson et al., 1983; Gaffey, 1986). There are four Antarctica meteorites (Allan Hills 81005, Y-791197, Y-82192 and Y-82193) identified as originating from moon (Bogard, 1983; Marvin, 1983). All four lunar meteorites are rather small: 31, 52, 37 and 27 g respectively. Various properties of these meteorites were studied by a number of authors (e.g. Sutton and Crozaz, 1983; Crozaz, 1985; Sutton, 1985; Nishiizumi et al., 1986; Nagata and Funaki, 1985; Nakamura et al., 1985; Chen and Wasserburg, 1985; Takaoka, 1986; Clayton et al., 1984; Warren and Kallemeyn, 1986) and have been reviewed in a recent article by Ryder (1987).

Evidence indicated the possibility of a martian origin for six non - Antarctic SNC (two shergottites, three nakhlites and a chassignite) meteorites (e.g. Wood and Ashwal, 1981; Walker et al., 1979; Nyquist et al., 1979; McSween, 1985). An additional shergottite, found in Victoria Land, Antarctica, has shown noble gases and nitrogen with isotopic compositions that indicate a mixture of martian (data from Viking lander results)

and terrestrial atmospheric components (Bogard and Johnson, 1983). Various ejection models of the lunar, martian and other asteroidal type of meteorites have been discussed by Melosh (1984).

## **1.2 Summary of the isotopic anomalies in meteorites**

When the isotopic ratio of an element differs from the standard cosmic ratio, it is called anomalous. An account for the search of isotopic anomalies in meteorites has been given in recent review articles by Lewis and Anders, 1983; Lee, 1979; Wasserburg et al., 1980; Adler, 1986; Barber, 1985; Shima, 1986; R.N. Clayton, 1978; D.D. Clayton, 1982; Anders, 1981; Begemann, 1980; 1986; Fowler, 1984; Geiss and Bochsler, 1982; Pillinger, 1984; Widenbeck, 1983; Rolfs et al., 1987. To-date isotopic anomalies have been reported in about one third of the elements covering the periodic table, and more elements are being added to the list. Isotopic variations can be categorized in terms of fractionation, nuclear reactions, decay of primordial radionuclides and presolar nebular heterogeneities.

### **1.2.1 Mass fractionation**

The mass dependent fractionation might have occurred both before and after the formation of the solar system. Fractionation may be caused by volatilization and condensation or by chemical processes including special cases such as the production of organic matter.

### **1.2.2 Nuclear reactions**

This term includes nucleosynthesis, spallation reactions, the nuclear reactions induced by galactic and solar cosmic ray bombardment and low energy neutron capture reactions from their secondaries prior to the fall of meteorite.

### 1.2.3 Radioactive decay products

There are at least two different ways this could be responsible for the observed isotopic anomalies in meteorites. (i) Product from extinct nuclides : when the solar system had evolved to the point where the meteorites became isotopically a closed system, about  $4.6 \times 10^9$  years ago, some radioactive nuclides, now extinct in the solar system were still present. Daughter products of such nuclides are responsible for the anomalous isotopic composition of certain elements. (ii) Enrichment in the daughter products of long-lived radioactive nuclides which are commonly used for geochronology and other fission products.

Other processes responsible, at least in some cases, could be the survival of presolar (extrasolar) grains having a different isotopic composition and its subsequent insertion in the meteoritic parent body.

Isotopic anomalies have been observed in both stone and iron meteorites. This is being summarised here with special reference to volatile elements since their preservation indicates that some information about presolar interstellar grains is still preserved in meteorites.

### 1.2.4. Anomalies in stone meteorites

Isotopic ratio measurements in stone meteorites have provided a wealth of information on early chemistry of the solar system, the carbonaceous chondrites are particularly considered to represent the most pristine samples of solar system material. Of these the samples of Allende (C3) and Murchison (C2) have been studied extensively. Isotopic anomalies have so far been observed for hydrogen (Yang and Epstein, 1983); helium (Reynolds et al., 1978); carbon (Halbout et al., 1986; Zinner and Epstein, 1987);

nitrogen (Lewis et al., 1983; Kuroda, 1985; Franchi et al., 1986); oxygen (Clayton and Mayeda, 1984; Halbout et al., 1986); neon (Ne-E, Jungck and Eberhardt, 1979); magnesium (Hutcheon et al., 1984; Ireland et al., 1986; Ireland and Compston, 1987); silicon (Becker and Epstein, 1981); sulphur (Rees and Thode, 1977); argon (Gobel et al., 1982); potassium (Hutcheon et al., 1984); calcium (Lee et al., 1979; Niederer and Papanastassiou, 1984); titanium (Niemeyer and Lugmair, 1984; Ireland et al., 1985); chromium (Birck and Allegre, 1985); krypton (Gobel et al., 1982); strontium (Papanastassiou and Wasserburg, 1978; Patchett, 1980); cadmium (Rosman et al., 1980); xenon (Frick and Pepin, 1981; Ott et al., 1985); barium (McCulloch and Wasserburg, 1978); neodymium (Lugmair et al., 1983); Samarium (Lugmair et al., 1978); mercury (Jovanovic and Reed, 1976a; 1976b; 1987; Goel and Thakur, 1987); lead (Chen and Wasserburg, 1981) and osmium (Goel, 1986; unpublished).

### 1.2.5 Anomalies in iron meteorites

Relatively much less effort has been made to search for the isotopic anomalies in iron meteorites. So far the anomalies are reported for helium (Hintenberger and Wanke, 1964); lithium (Voshage, 1981); neon (Voshage and Feldmann, 1978); sulphur (Hulston and Thode, 1965); argon (Lammerzahl and Zahringer, 1966); potassium (Voshage and Hintenberger, 1961); calcium (Shima et al., 1969; Hintenberger et al., 1965); vanadium and titanium (Imamura et al., 1980); chromium (Shima and Honda, 1966). All these have been explained in terms of spallation reactions, most probably by galactic and solar cosmic rays and other energetic particles.

Huge excess of  $^{107}\text{Ag}$  ( $107/109 = 2.94$ ) was reported in iron meteorite Hoba no. 4213 by Kaiser and Wasserburg (1983). This has

been explained as a result of decay of  $^{107}\text{Pd}$ , a nuclide that is extinct at present (Kaiser et al., 1980; Wasserburg, 1985; Teshima et al., 1986). Goel and Murty (1983) and Goel (1987), reported xenon and osmium anomalies, in samples of acid insoluble residues of iron meteorites, indicating that these objects might contain presolar grains that have not been completely homogenised. Some of the anomalies are discussed further with their cosmochemical inferences.

### **1.2.6 D/H ratios in carbonaceous chondrites**

Kerogen found in the insoluble residues of carbonaceous chondrites (Kerridge, 1983) shows striking isotopic heterogeneities. Different microsamples of the same residue vary widely in their ratios of D/H,  $^{13}\text{C}/^{12}\text{C}$  and  $^{15}\text{N}/^{14}\text{N}$ . Robert and Epstein (1982) measured enrichments in deuterium (relative to the average galactic value of  $2 \times 10^{-5}$ ) of  $5.4 \times 10^{-4}$  and still higher values ( $7 \times 10^{-4}$ ) during stepwise extractions. In a study of 19 carbonaceous and unequilibrated ordinary chondrites, Yang and Epstein (1983) measured D excess upto about 2000 per mill in insoluble carbonaceous residues and an inferred isotopic composition of D excess equalling 10,000 per mill in acid soluble material.

Such high D/H ratios can not be attributed to nuclear processes and must be due to ion-molecular exchange reactions at temperatures below 40 K (Geiss and Reeves, 1981). Yang and Epstein argued that the D-rich carbonaceous matter must have formed in interstellar clouds where ionising conditions and low temperatures both existed. McKeegan et al. (1985) supported this idea stating that deuterated organic matter in primitive meteorites actually may be a sample of preserved molecular cloud material which has not been equilibrated isotopically with average solar

system material . In this model other isotopic anomalies are also expected.

### 1.2.7 $^{15}\text{N}/^{14}\text{N}$ ratios

Carbonaceous chondrites often show widely variable values of  $^{15}\text{N}/^{14}\text{N}$ . However, the largest enrichments in  $^{15}\text{N}$  ever found in any meteorite were recently reported by Prombo and Clayton (1985) in Bencubbin and Weatherford stony iron meteorites. They made measurements on silicate fractions, the metal fractions and bulk samples and reported  $^{14}\text{N}$  values ranging from + 414 to + 973 per mill. Indeed the bulk meteorite showed a greater enhancement than any of the fractions, implying the presence of a component with extraordinary high  $^{15}\text{N}/^{14}\text{N}$  ratio. Previous whole rock  $^{15}\text{N}$  values measured in meteorites ranged from - 90 to + 335 per mill, with the great majority lying between - 90 and + 50 per mill. Prombo and Clayton concluded that the excess  $^{15}\text{N}$  may be an unhomogenized product of nova explosions, or else it originated by extreme isotopic fractionation at temperatures below 40 K in presolar molecular cloud. Kuroda (1985) attributed these light elements (H,C, N etc.) anomalies to the by product of x-process nucleosynthesis of light elements : D, Li, Be and B.

### 1.2.8 Oxygen isotopic anomaly

R.N. Clayton et al. (1973) discovered that the variations of the  $^{17}\text{O}/^{16}\text{O}$  versus  $^{18}\text{O}/^{16}\text{O}$  ratios show a slope of 1 in the refractory minerals of the carbonaceous meteorites, while it is 0.5 (as it is expected from chemical fractionation) in terrestrial samples and also in ordinary meteorites. This was of great significance because the anomaly was seen in a major constituent. Since then the oxygen isotopes have been extensively used to describe genetic relations between meteorites and between differ-

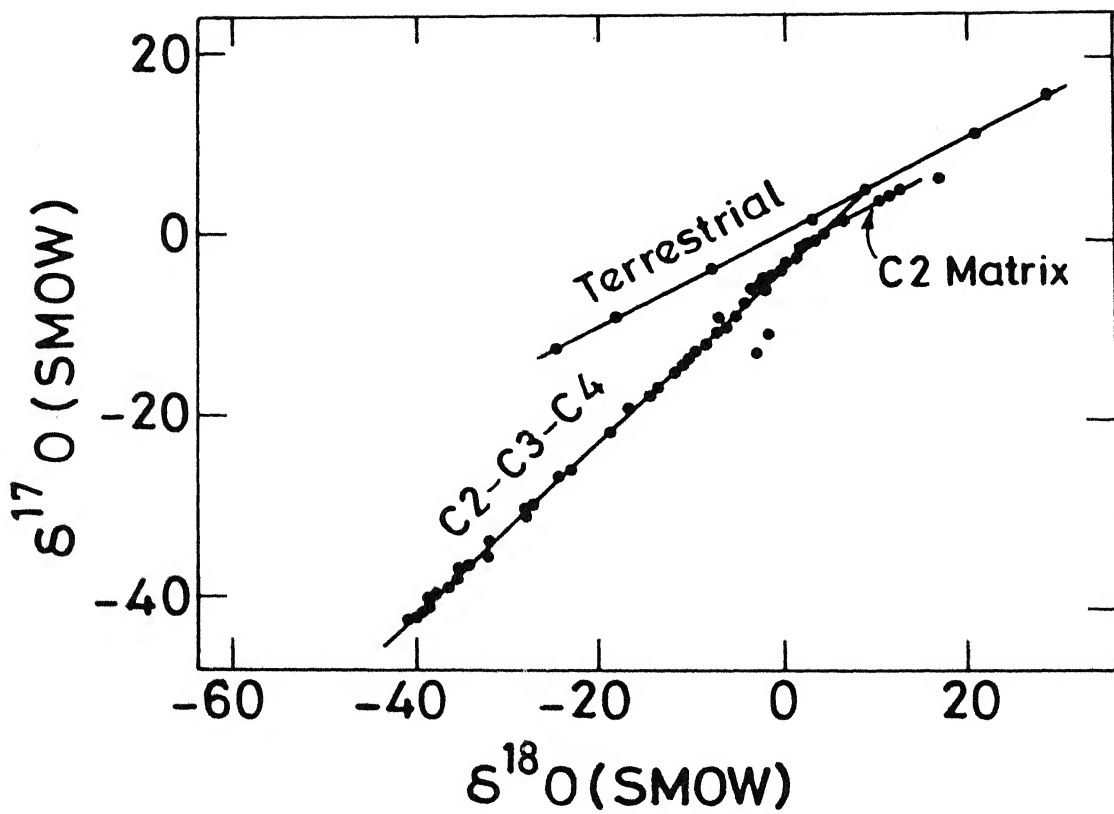


Fig. 1.1 Graph of  $^{17}\text{O}/^{16}\text{O}$  vs.  $^{18}\text{O}/^{16}\text{O}$   
for terrestrial and meteoritic samples  
(After Clayton et al., 1978)



ent phases of the same meteorite (e.g. Clayton and Mayeda 1984; Halbout et al., 1986)

Figure 1.1 illustrates the relationship between the fractional excesses in the  $^{17}\text{O}/^{16}\text{O}$  ratios of the anhydrous minerals found in type C2, C3 and C4 carbonaceous chondrites as compared to standard mean ocean water (SMOW). The fractional excess

$\delta = \left[ \left( \frac{^{17}\text{O}}{^{16}\text{O}} \right)_{\text{Sample}} / \left( \frac{^{17}\text{O}}{^{16}\text{O}} \right)_{\text{SMOW}} - 1 \right] \times 10^3$  is expressed in parts per thousand so that a value of  $\delta$  equal to -50 corresponds to a 5 % deficiency in that ratio compared to SMOW. The well known mass-fractionation line for terrestrial material is shown that has a slope of 0.5 as expected. Clayton's group interpreted such precisely correlated decreases in the  $^{17}\text{O}/^{16}\text{O}$  and  $^{18}\text{O}/^{16}\text{O}$  ratios as due to admixture of pure  $^{16}\text{O}$  carried by interstellar grains. In their abstract they state " This component may predate the solar system and may represent interstellar dust with separate history of nucleosynthesis". This explanation is consistent with (Audouze, 1980) the determinations made by Chevalier and Kirshner (1978) of large oxygen enhancement in the cas A supernova remnant. As suggested by various authors (Reeves, 1978; Cameron and Truran, 1978; Schramm, 1978) this discovery is a strong argument in favour of the triggering of a solar system formation by the explosion(s) of nearby supernova(e). Don Clayton has suggested alternate models.

There are other interesting facts : (i) There is no apparent correlation of  $^{16}\text{O}$  richness with other isotopic anomalies. (ii) The exotic admixture component is not pure  $^{16}\text{O}$ . A least squares linear fit to the data has a slope of  $0.94 \pm 0.01$  ( $2\sigma$ ). According to the authors it is conceivable, however, that systematic errors in the  $\delta(^{17}\text{O})$  determina-

tions are large enough that the apparent departure from unity is insignificant and hence an extrapolation of the mixing line passes through or close to the point with  $\delta^{17}\text{O} = \delta^{18}\text{O} = -1000$  which would correspond to pure  $^{16}\text{O}$ . Begemann (1980) and D.D. Clayton (1982) argue against this idea and suggest that although the exotic component is very deficient in both  $^{17}\text{O}$  and  $^{18}\text{O}$ , it is more deficient in  $^{18}\text{O}$ . The most extreme end member for the mixing line would consist of  $^{16}\text{O}$  and  $^{17}\text{O}$  only, and in the ratio  $(^{17}\text{O}/^{16}\text{O})^* = 0.006 (^{17}\text{O}/^{16}\text{O})_{\text{SMOW}}$ , where the asterisk denotes the  $^{18}\text{O}$  free end member of the mixing line. (iii) Although different classes of meteorites show internal fractionation lines of slope 0.5 connecting distinct phases that have chemically evolved from one another, these fractionation lines of separate objects do not overlap (Clayton et al., 1976). For example, the somewhat different fractionation lines for chondrites of varying type lie slightly above the terrestrial line, whereas that of the C2 matrix is shown originating slightly below the terrestrial line. The simplest interpretation, given by D.D. Clayton (1979) is that the presolar  $^{16}\text{O}$  bearing component has different concentration at different parts of the solar system.

### 1.2.9 Oxygen isotope fractionation in the laboratory

Mass-independent fractionation of oxygen has been observed in the laboratory (Thiemens and Heidenreich, 1983; Thiemens et al., 1983; Heidenreich and Thiemens, 1983; 1986). Models for "non nuclear" origin of mass-independent fractionation have since been proposed (Navon and Wasserburg, 1985; Heidenreich and Thiemens, 1985; Thiemens and Jackson, 1985; Robert, 1985). Such fractionations, whatever may be the mechanism, provide interesting alternatives for the formation of reservoirs of various

$^{16}\text{O}$  contents which do not require a component of different nucleosynthetic history.

Thiemens and Heidenreich discovered a non-mass-dependent isotope effect in the production of ozone from molecular oxygen. Briefly, the experiment was done as follows. Ozone production was initiated by a high frequency tesla coil in oxygen expanded into a reaction tube. Ozone was immediately collected as liquid on the refrigerated walls of the vessel at liquid nitrogen temperature. After achieving the desired degree of completion, excess oxygen from the reaction tube was removed. The ozone was collected on a molecular sieve 13 X pellets at  $-196^\circ\text{C}$ , then released and decomposed to molecular oxygen by baking the sieve. The molecular oxygen was expanded in a glass sample tube for isotope ratio mass spectrometric analysis of  $^{16}\text{O}$ ,  $^{17}\text{O}$  and  $^{18}\text{O}$ . By performing the electrosynthesis of  $\text{O}_3$  from  $\text{O}_2$ , these authors found a slope of 1 for the resulting  $^{17}\text{O}/^{16}\text{O}$  versus  $^{18}\text{O}/^{16}\text{O}$  variations. Heidenreich and Thiemens (1983, 1986), based on the above experiment, suggested that the meteoritic oxygen isotope data may be a result of a process of photodissociation of molecular oxygen with subsequent removal by a scavenging species of the atomic products. The first step of electrosynthesis of  $\text{O}_3$  consists in the breaking of some  $\text{O}_2$  molecules ( $\text{O}_2 = \text{O} + \text{O}$ ). The atomic oxygen is absorbed by a molecular oxygen in the second step. In the first step only three different molecules,  $^{16}\text{O}^{16}\text{O}$ ,  $^{16}\text{O}^{17}\text{O}$  and  $^{16}\text{O}^{18}\text{O}$ , have to be considered due to the low abundance of  $^{17}\text{O}$  and  $^{18}\text{O}$  relative to  $^{16}\text{O}$ . Since the asymmetric molecules  $^{16}\text{O}^{17}\text{O}$  and  $^{16}\text{O}^{18}\text{O}$  have twice more states which can be populated (starting from the ground state) than the symmetric  $^{16}\text{O}^{16}\text{O}$  molecule, the rates of breaking of  $^{16}\text{O}^{17}\text{O}$  and  $^{16}\text{O}^{18}\text{O}$  are

equal and are twice more rapid than that of  $^{16}\text{O}^{16}\text{O}$ . Therefore one can assume (as discussed by Reeves, 1978) that the solar system was formed in an OB association where many stars were providing the UV flux able to dissociate the  $\text{O}_2$  molecules present in the interstellar medium. In these conditions, the  $^{17}\text{O}/^{16}\text{O}$  versus  $^{18}\text{O}/^{16}\text{O}$  variation pattern observed in some meteoritic samples might be simply due to the incorporation of  $\text{O}_2$  into grains floating around the OB association. Therefore it might not be necessary to invoke nuclear effects to account for such an isotope variation pattern. Moreover this alleviates the difficulty encountered by the "nuclear" hypothesis to explain the fact that the oxygen anomalies are not correlated with other anomalies (Wasserburg and Papanastasiou, 1983).

#### 1.2.10 Kinetics and self-shielding in $\text{O}_2$

Navon and Wasserburg (1985) analysed the isotope shifts in the  $\text{O}_3$  resulting from photodissociation of  $\text{O}_2$  and competition between formation of  $\text{O}_3$  and isotopic exchange reaction at different gas compositions and temperatures. According to the kinetic model of self-shielding (Navon and Wasserburg, 1985; Sander et al., 1977) during photodissociation of  $\text{O}_2$  the remaining  $\text{O}_2$  is correspondingly enriched in  $^{16}\text{O}$ . These large shifts are quenched at temperatures higher than 500 K, or if water is present in higher relative concentration than  $\text{O}_2$ . Following dissociation, fast isotopic exchange reactions (e.g.  $^{17}\text{O} + ^{16}\text{O}_2 \rightarrow ^{16}\text{O} + ^{17}\text{O}^{16}\text{O}$ ) may destroy the effect unless the atomic oxygen is efficiently trapped. Trapping of O by metal atoms, combination with hydrogen or formation of  $\text{O}_2$  cannot compete with the exchange reaction, whereas trapping on dust grains may be efficient. However, the extinction of radiation by the dust is

likely to quench the self-shielding effect itself. To achieve an  $^{16}\text{O}$  enrichment, of the pattern observed in meteorites, two stage process is suggested : (i) trapping of the atomic oxygen produced by the photodissociation and (ii) subsequent removal of trapped species, to leave behind a reservoir depleted in  $^{17}\text{O}$  and  $^{18}\text{O}$ , which requires cycling of large quantities of nebular gases. It seems that self-shielding of photolysing radiation by  $\text{O}_2$  is not a satisfactory explanation for the oxygen anomalies in meteorites in the light of the difficulties throughout many stages of the process. Also other photochemical processes as well as self-shielding in other oxygen bearing molecules have been considered as possible explanations for the oxygen anomalies in meteorites. The CO molecule is a suitable candidate for such processes. Jaffe and Klein (1966) reported the isotopic exchange reaction of CO is three orders of magnitude slower than that of  $\text{O}_2$  at 300 K. Bally and Langer (1982) studied isotopic selective photodissociation of CO and suggested self-shielding in CO as the source of large isotopic fractionation in molecular clouds. This needs further investigation.

### **1.2.11 Importance of noble gases**

The chemical heterogeneity that existed prior to condensation was in many cases obscured by chemical separation of elements into different minerals during condensation. However, a few elements with very similar chemical properties have retained a record of the chemical heterogeneities that existed prior to redistribution of elements during condensation. The five inert gases have similar physical properties and are essentially inert to chemical reactions. It is not surprising then that these elements provided the first clear evidence of chemically and isotopically distinct regions in the primitive solar nebula.

Meteoritic noble gases are mixture of various components consisting of (i) a trapped component at the time of condensation, (ii) an implanted component such as from solar wind, best preserved in lunar soils (Pillinger, 1979), (iii) a spallogenic component due to cosmic ray bombardment, (iv) a fissiogenic component from spontaneous fission of U and Th, (v) a radiogenic component from the decay of now extinct nuclides like  $^{129}\text{I}$ ,  $^{224}\text{Pu}$  and possibly extinct superheavy elements (SHE) and (vi) a component carried by the presolar grains. It is fortunate that these various components reside at different sites which have different thermal retentivities and different resistivities to chemical attack. Stepwise heating techniques have made it possible to separate each noble gas into its various components.

#### 1.2.12 Neon - E

If one plots the ratio of neon 20 to neon 22 against the ratio of neon 21 to neon 22 for each temperature step of neon extraction, one gets a data plot shown in Figure 1.2 . Neon in meteorites is a mixture of atleast three components : primordial neon A, which comes from the solar nebula; solar neon B, implanted in the meteorite by the wind of ions flowing outward from the sun; and cosmogenic neon S, produced by the cosmic ray bombardments upon atomic nuclei inside the meteorite.

All meteoritic neon data measured upto the time of Black and Pepin (1969) fell within the triangle bounded by neon A, neon B and neon S, as expected. Black (1972) discovered that the neon released from carbonaceous chondrite Ivuna between 800 and 1100°C clearly fell below the triangle. Evidently a new neon component was present, with a ratio of  $^{20}\text{Ne}/^{22}\text{Ne}$  that was 3.4 (a factor of three lower). Black named it

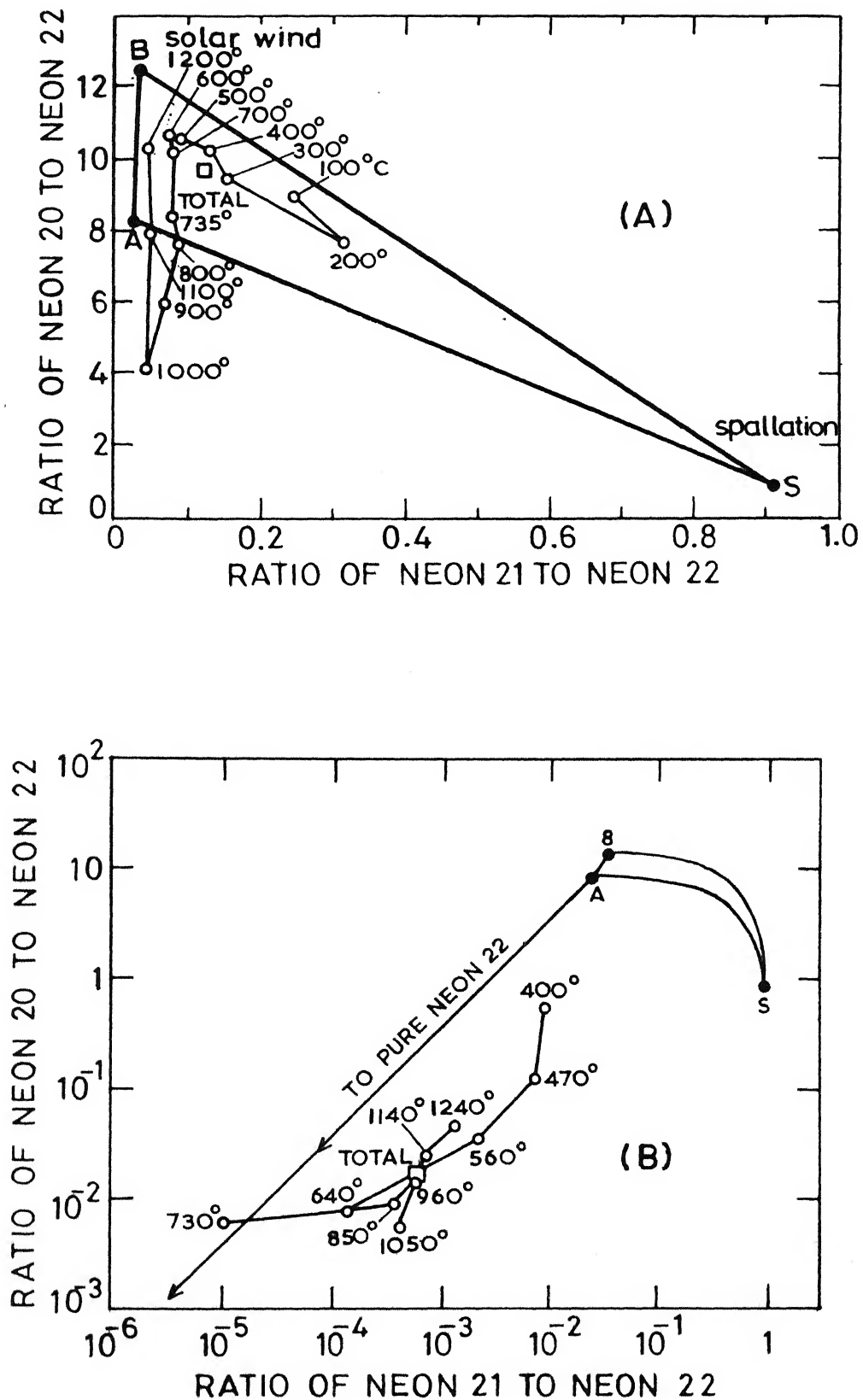


Fig. 1.2 Neon isotopic anomaly in Orgueil meteorite  
(from Lewis and Anders 1983)

neon-E. Jungck and Eberhardt (1979) studied a tiny mineral sample of Orgueil meteorite and obtained greatly enriched neon-E. The neon-E proved to be essentially pure neon-22 (more than 99 percent for the fractions released from 640 through 1,050°C). Subsequently, refined measurements of grains of Orgueil meteorite led Eberhardt et al. (1981) to extreme ratios of  $^{20}\text{Ne}/^{22}\text{Ne}$  0.15 (and  $^{21}\text{Ne}/^{22}\text{Ne}$  0.0022) and it was suggested that Ne-E is essentially fossil material of extinct  $^{22}\text{Na}$ . Since the half life of  $^{22}\text{Na}$  is only 2.6 years, the results produce rather severe constraints on any astrophysical scenario which might explain its origin (Rolfs et al., 1987). Fowler (1985) suggested that active  $^{22}\text{Na}$  might be present in the interstellar medium and  $\gamma$ -ray astronomy could be fruitful. The short life time of  $^{22}\text{Na}$  would prevent significant spreading from the source through the galaxy, and thus lead to localised ('spotty')  $\gamma$  - ray source.

### 1.2.13 Xenon isotopic anomalies

Xenon has turned out to be the most prolific single element. The reasons are manyfold. Xe has nine stable isotopes covering, in atmospheric xenon, a wide range of abundances from about 0.1 % for  $^{124,126}\text{Xe}$  to 27 % for  $^{129,132}\text{Xe}$ . Two isotopes each are pure p-, r- and s- products of nucleosynthesis and three are mixtures of s- and r- products. Notably, all r- products can be produced by fission as well. Being a rare gas Xe is depleted in meteorites by atleast five orders of magnitude. Consequently, if for Xe and any of its neighbours, effects of comparable absolute magnitude are produced after this depletion has occurred the relative anomalies will be correspondingly higher for Xe. Further, with modern high vacuum technology the detectibility for excess xenon achieved so far has been set at about 20000 atoms (Begemann, 1986). Fortunately different xenon



components reside in different host minerals or phases. Heating a sample and extracting the xenon in steps often results in an effective separation of different components. Similarly, the different resistivities to chemical attack of the host phases make possible a preferential decomposition of certain carriers and at the same time enhancement of others. The latter approach in particular has yielded two kinds of highly anomalous Xe.

#### 1.2.14 CCF-Xenon (SN-Xenon or Xenon-X)

Xenon with excess of four heaviest xenon isotopes is called "carbonaceous chondrite fission xenon (Pepin, 1968) or CCF for short. Since the excess heavy isotopes are always accompanied by an excess of two lightest shielded isotopes ( $^{124}\text{Xe}$  and  $^{128}\text{Xe}$ ), which cannot be made by fission, it might be a supernova xenon. Although opinion on this point do not appear to be unanimous (Ballad et al., 1979; Anders, 1981), this idea of supernova injection is supported by the cold accretionary model (Alfven and Arrhenius, 1974; Audouze, 1985). Frick (1977) identified a krypton component, depleted in light isotopes ( $^{78}\text{Kr}$  and  $^{80}\text{Kr}$ ) and rich in heavy isotopes ( $^{83}\text{Kr}$ ,  $^{84}\text{Kr}$  and  $^{86}\text{Kr}$ ), which is linked to excess of light xenon (124 and 126) and excess of heavy xenon (131, 132, 134 and 136) as shown in Figure 1.3 . The positive xenon and negative Kr anomaly does not favour the mass fractionation explanation.

#### 1.2.15 s-Process xenon

The xenon in Figure 1.4 b is characterised by the absence of two lightest and two heaviest isotopes. Since these are the p-process and r-process isotopes, respectively, this xenon consists only of isotopes which originate in the s-process of nucleosynthesis. In a sense this xenon

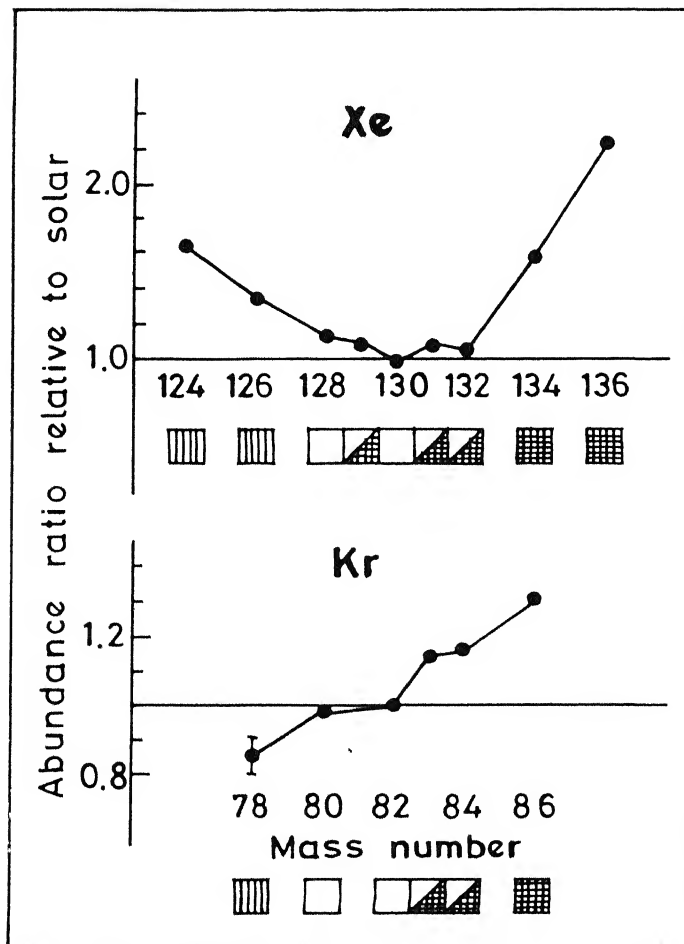


Fig. 1.3 Comparison of anomalous xenon and anomalous Krypton  
(from Begemann, 1980)

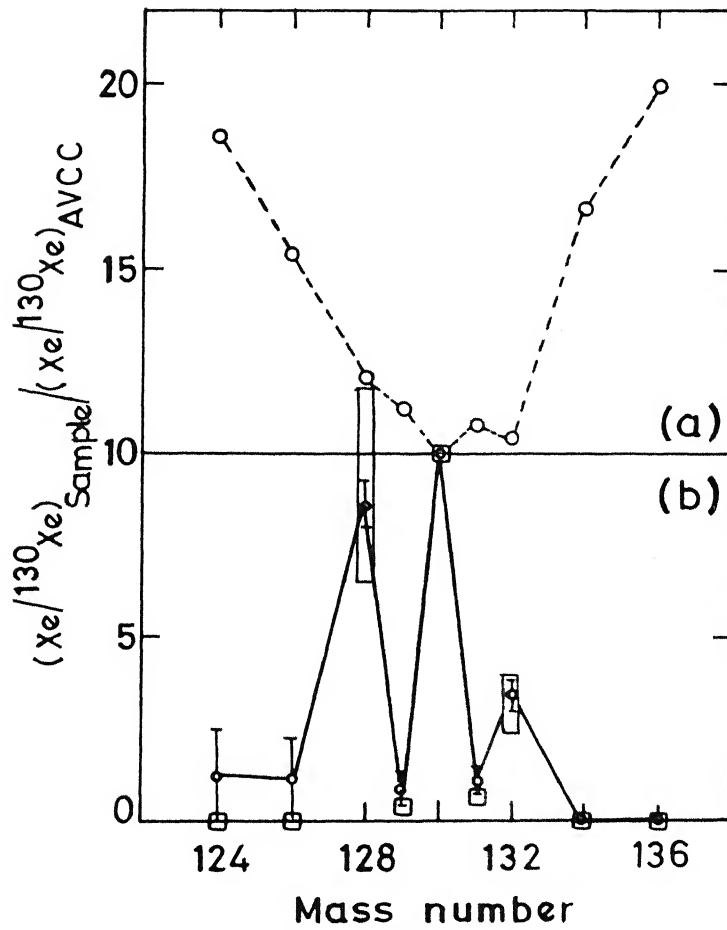


Fig. 1.4 (a) CCF-Xe (b) s-Xe Boxes indicate  
Xe-s calculated for red-giants (from Begemann, 1985)  
AVCC : Average Carbonaceous Chondrite

is complementary to CCF-xenon since in that the p- and r-process isotopes are missing (or the s-process isotopes are overabundant). s-Xe is usually accompanied by similarly enriched s- isotopes of Kr, and also is enriched in  $^{22}\text{Ne}$  (Srinivasan and Anders, 1978).

Murty et al. (1983) studied several samples of the acid residues of iron meteorites and reported, (i) higher total xenon in the non-magnetic residue as compared to magnetic phase; (ii) enrichment of  $^{129}\text{Xe}$  presumably due to extinct radionuclide  $^{129}\text{I}$ ; (iii) depletion of  $^{124}\text{Xe}$  and  $^{126}\text{Xe}$  in some non-magnetic residues and (iv) enrichment of  $^{124}\text{Xe}$  and  $^{126}\text{Xe}$  in some non-magnetic residues. This has been attributed to the presolar nebular matter which was trapped during the formation of iron meteorites (Goel and Murty, 1983; Shukolyukov et al., 1984).

The three components of noble gases Ne-E, s-process Xe and s-process Kr must be presolar condensates from highly evolved stars that found their way into the early solar system and survived in the primitive meteorites (Anders, 1981; Lewis and Anders, 1983). The CCF-Xe has been more controversial. According to Anders and coworkers the W pattern (Figure 1.4 a) is due to the superposition of fission xenon and strongly mass-fractionated xenon favouring the light isotopes (e.g. Alaerts et al., 1980).

### 1.3 Mercury

Mercury is one of the few elements for which no reliable experimental data on its solar system abundances are available. The isotopes of mercury are produced by a mixture of two processes of nucleosynthesis, the s-process and the r-process in addition to a small ( $\sim 1\%$ ) p-process contribution (Beer and Macklin, 1985; Audouze and Truran,

Table 1.1 Mercury in Stars

Mercury Isotopes	Wavelength Å 3980 +	Abundance (%)				Terrestrial
		Iota Cr B	HR 4074	HR 5883	HR 465	
196	3.769	~0	~0	~0	~0	0.15
198	3.838	6	0	0	10	10.0
199	3.838					16.8
	3.849					
200	3.909	16	4	0	45	23.1
201	3.930					13.2
	3.941					
202	3.990	45	37	3	45	29.8
204	4.071	33	59	97		6.9

1975; Arnould, 1976; Woosly and Howard, 1977).

### 1.3.1 Mercury in stars

Observational evidence shows (Dworetsky et al., 1970; Preston, 1971; Cowley and Aller, 1971) variable isotopic composition of mercury in stars. A relative Hg over-abundance of  $4 \times 10^4$  has also been reported (Sargent, 1964; Aller and Ross, 1967; Jaschek and Jascheck, 1967; Bidelman, 1968) in several stars. The isotopic abundances (of Hg II) can be determined at wavelengths 3980-3985 Å as presented in Table 1.1. (White et al., 1976). Data points at 198.5 and 200.5 represent sums of abundances of 198+199 and 200+201, that cannot be resolved in stellar spectra (M.I.T. Wavelength table). More than 50 stars (showing Hg II line) have extensively been studied for the distribution of mercury isotopes. The results show wide variations which range from almost pure  $^{204}\text{Hg}$  to that of the terrestrial isotopic ratio.

### 1.3.2 Cosmic abundance of mercury

The extreme variability observed, between different meteorites of the same type, seems to be more pronounced in mercury than in any other element. Calculation of the atomic abundance of mercury on the basis of various chondrite models are made difficult due to this variability. The abundances determined are much higher than any possible value which would be consistent with our understanding of the s- and r- processes of nucleosynthesis (Mathews and Ward, 1985; Rolfs et al., 1987). The available data have been summarised in Table 1.2. The carbonaceous chondrite values are about two orders of magnitude higher than the values expected from nuclear systematics. The mercury values in the cosmic abundance tables of Suess and Urey (1956) and Cameron

Table 1.2 Cosmic Abundance of Mercury

Reference model	Mercury atomic abundance <sup>*</sup> ( relative to Si = $10^6$ atm. )	
	Range	Mean
Type I carbonaceous chondrites	22 - 148	2.9 <sup>a</sup>
Type II carbonaceous chondrites	1.6 - 6.82	4.4 <sup>b</sup>
Type III carbonaceous chondrites	0.009 - 7.3	2.8 <sup>c</sup>
Type A enstatite chondrites	1.3	1.3 <sup>d</sup>
Type B enstatite chondrites	0.35 - 0.59	0.47 <sup>e</sup>
Ordinary chondrites	0.02 - 13.92	2.5 <sup>f</sup>
Suess and Urey (1956)		0.284
Cameron (1963)		0.27
Clayton and Fowler (1961)		0.62
Cameron (1973)		0.40
Anders and Ebihara (1982)		0.52
Cameron (1983)		0.21
Beer and Macklin (1985)		0.34

<sup>\*</sup> Using silicon abundances largely from the compilation of Voigt and Ehmman(1965).

a Assuming Orgueil = 22 ppm Hg.

b Mean of Mighei and Murray.

c Mean of Karoonda, Mokoia I and Mokoia II.

d Assuming Abeo = 1.52 ppm Hg.

e Mean of Hvittis and St Marks

f Mean of 15 ordinary chondrite analyses.

(1963) are similar, because both mercury values were obtained by interpolation of similar abundance curves of the bracketing elements Au and Tl. The value predicted by Clayton and Fowler (1961) is slightly higher. Cameron (1983) set  $^{198}\text{Hg}$  equal to the geometric mean of  $^{192}\text{Pt}$  and  $^{204}\text{Pb}$ . Anders and Ebihara (1982) also used Cameron's (1983) method and calculated a higher Hg abundance due to the fact that the Pb abundances that they used were higher. The value given by Beer and Macklin (1985) was from an independently studied nuclear systematics of s- process branching and termination processes.

There are many reasons for believing that the type I carbonaceous chondrites represent the closest approach to primitive solar system material (e.g. Greenland and Lovering, 1965; Anders, 1971; Rubin, 1985; Hanan and Tilton, 1985; Molini-Velsko et al., 1986). However, if the very high mercury abundances measured in the type I carbonaceous chondrites approach the true cosmic abundance of mercury, the abundance curves in the vicinity of mass number 202 should be drastically revised. It would then be necessary to re-examine the nuclear processes suggested for the production of the isotopes of mercury to see how it would be possible to produce the high abundances observed in type I carbonaceous chondrites (Ehmann and Lovering, 1967). If the high mercury abundances in meteorites are not due to terrestrial contamination, as many authors believe (Ehmann and Lovering, 1967; Reed, 1971; Jovanovic and Reed, 1985), there should be some nuclear astrophysical or cosmochemical processes that give rise to an enrichment of Hg in meteorites. It was pointed out that the elemental sulphur if present in the early stages of condensation, could have preferentially concentrated mercury from



the primitive solar nebular material (Jovanovic and Reed, 1980) from which a substantial proportion of these meteorites condensed. Under these circumstances the abundance of mercury would be enriched relative to primitive solar system and would not reflect the true cosmic abundance value. If condensation of elements occurred in dis-equilibrium conditions from cosmic plasma, the problem of disparity between the measured meteoritic abundance of Hg and its estimated cosmic abundance would get alleviated (Arrhenius and Alfven, 1971).

### 1.3.3 Mercury abundances in meteorites

Reed and Jovanovic (1967) and Reed (1971) tabulated the results of replicate analysis of Hg on a number of meteorites, mostly by the use of neutron activation analysis technique. The extremely large range observed within a given class of meteorite makes averaging meaningless. Even for a given meteorite large variations are found. For example, in Orgueil Hg was found to vary from 2.4 to 213 ppm. Ehmann reported values for Orgueil at 17.3 (Ehmann and Huizenga, 1959) and 114 ppm (Ehmann and Lovering 1967). Ehmann and Lovering (1967) also reported 0.69 and 7.3 ppm for Mokoia. The fractionation of Hg between chondrite classes do not follow the patterns, observed for other elements. Even the ordinary chondrite classes exhibit differences. Jovanovic and Reed (1985) suggested that the concentration of Hg observed do not reflect an initial distribution but are result of re-distribution. Considering the volatility of Hg it is of interest that chondrules which are most probably high temperature condensates and the total meteorite including the fine grained crystalline matrix have very similar total Hg concentration.

Hg in achondrites, as reported by Ehmann and Lovering (1967) and Jovanovic and Reed (1987), varies between 1 ppb to 9 ppm. Mercury in troilite from iron meteorites has been reported by Reed et al., (1960); Reed and Jovanovic (1967) and Kiesel and Hecht (1969). It varies between 6 ppb to 2 ppm. No measurements of total Hg contents of iron meteorites have yet been reported.

#### 1.3.4 Mercury isotopic anomaly in meteorites

Reed and Jovanovic (1969) using neutron activation methods, reported an anomaly in the  $^{196}\text{Hg}/^{202}\text{Hg}$  abundance ratio in bulk samples of several chondritic meteorites. They suggested that the anomaly could be due to the meteorites containing genetically different materials. The anomalies were observed in the meteorites Orgueil-1, Orgueil-2, Hollingsberg, Tieschitz and Allegan. In further studies, Jovanovic and Reed (1976 a, b) observed anomalies in Murchison and Allende. In general the  $^{196}\text{Hg}/^{202}\text{Hg}$  ratio differed from the normal terrestrial value by about 20 percent. In one sample of Allegan chondrules the ratio measured, in the 300°C temperature release fraction, was about twenty two times lower than the terrestrial  $^{196}\text{Hg}/^{202}\text{Hg}$  ratio. The anomaly was attributed to a deficiency in  $^{196}\text{Hg}$  rather than an excess of  $^{202}\text{Hg}$ .

Recently Jovanovic and Reed (1987) reported anomalous isotopic ratio in Hg obtained in the 130°C fraction from Shergottite EETA 79001, 238 and Polymict eucrite ALHA 78132, 67. The  $^{197}\text{Hg}/^{203}\text{Hg}$  ratio measured relative to terrestrial was  $0.31 \pm 0.02$ . EETA 79001, 238 is a SNC meteorite postulated to be Martian ejecta. Isotopic homogenisation would be expected in such a geologically active planet. Also

in lunar samples studied by Jovanovic and Reed (1977) the isotopic composition of  $^{196}\text{Hg}/^{202}\text{Hg}$ , in mercury released during stepwise heating the samples of Apollo 14 breccia 14305 and 14321, was measured. The isotopic variation appears as an approximately 25 % depletion in  $^{196}\text{Hg}$  or excess in  $^{202}\text{Hg}$  in some samples. A possible explanation given by the authors is the presence of extra lunar material in the breccias. However, the evolution of moon is such that this must have occurred at a very late stage of breccia formation. A similar suggestion that the moon may have accreted grains of extra-solar system matter was made by D.D. Clayton (1975) as a possible explanation for the presence of excess fission Xe (Behram et al., 1973; Drozd et al., 1976; Reynolds et al., 1974) in Apollo 14 samples.

Early attempts to observe an anomaly using mass spectrometry have not been successful. The problem is complicated by the fact that  $^{196}\text{Hg}$  is a relatively rare isotope having an abundance of less than 0.2 percent. Von Helden and Begemann (1976) heated samples of Allegan and Tieschitz to 1000°C and found no anomalies in the abundance ratios of  $^{198}\text{Hg}$  and other heavier isotopes. But interference by hydrocarbon impurities prevented a measurement of rare isotope  $^{196}\text{Hg}$ . In another investigation (Lugmair et al., 1978), the mercury extracted from an Allende inclusion, EK 1-4-1, heated to various temperatures lay near blank levels and had an isotopic composition agreeing within error limits with terrestrial mercury. Since their measurements lay near blank levels, no claim was made for the existence or non-existence of an anomaly. Recently Nier and Schlutter (1986) reported isotopic abundance ratios for mercury in six samples of bulk material and in one sample of chond-

rules from Allende meteorite. Most measurements were made on the mercury released at temperatures of 250°C, 450°C, 600°C and in some cases at higher temperatures. The experiment failed to show any anomaly in the  $^{196}\text{Hg}/^{203}\text{Hg}$  abundance ratio within the error limits of measurement. Anomaly reported for this element is generally looked on with suspicion (Wasson, 1974; Begemann, 1980).

### 1.3.5 Interpretation of mercury isotopic anomaly

The Hg isotopic variations observed in stars can be understood from various nucleosynthesis processes (Guthrie, 1972; 1984). The Hg may have been formed in the cyclic part of the r- process and accreted by the stars. A cyclic process is the process to add neutrons rapidly until  $(n,\gamma)$ ,  $(\gamma,n)$  equilibrium is achieved. Then  $\beta$ -decay leakage to higher Z will allow further  $(n,\gamma)$  and  $(\gamma,n)$  equilibrium (Burbridge et al., 1957; Seegar et al., 1965; Schramm, 1983). If the neutron flux was removed gradually so that the final  $\beta$ -decay took place in neutron rich environment, the Hg produced would be dominated by heavier isotopes. This model has been criticized. It does not provide an obvious explanation for the probable dependence of the isotopic composition of Hg on effective temperature of the equilibrium process (White et al., 1976). Another problem is that the Hg in some stars, like  $\chi$  Lup pr, is found to be concentrated in the heaviest stable isotope  $^{204}\text{Hg}$ , instead of being distributed as expected among several of the heavier isotopes. Cowley and Aikman (1975) and White et al. (1976) presented some arguments against the possibility that the shifts in the Hg line (Hg II at 3984 Å) are due to blending with lines of other elements, and the consistent shifts of Hg II lines suggest real, though unexplained, variations in the isotopic composi-

tion. The separation of Hg - isotopes by diffusion as proposed by Michaud et al. (1974) would require very stable atmosphere and was ruled out (Guthrie, 1984).

The observed isotopic anomalies of Hg obtained from meteorites have been interpreted in various ways. Some nucleogenetic origin for Hg isotopes have been postulated. In one, the normal range of elements synthesis processes occurred, yielding the dominant "normal" Hg found in most solar system samples measured (Burbridge et al., 1957). In a second, a different balance between r- and p- processes caused a relative depletion in p- process produced  $^{196}\text{Hg}$ . An excess of samarium-144 in Ek 1-4-1, from Ca-Al rich inclusions of Allende, has been explained on the basis of p- process nucleosynthesis (Lugmair et al., 1978) that might have affected the isotopic composition of pre-solar nebula. Noting that this interpretation is not consistent with the normal abundance of two barium isotopes (McCulloch and Wasserburg, 1978a) produced only by the p- process, it was suggested that the effects of the classical p- process are different for different elements (McCulloch and Wasserburg, 1978b). In a third,  $^{202}\text{Pb}$  was produced during the p- process and became incorporated into condensed phases before decaying to  $^{202}\text{Hg}$  (Jovanovic and Reed, 1976). But the suitable target nuclide to produce  $^{202}\text{Pb}$  ( $t_{1/2} \approx 3 \times 10^5$  years) and its energetics requirements etc. are not known (Arnould, 1976; Woosley and Howard, 1978).

Burn up of  $^{196}\text{Hg}$  by exposure to an intense neutron flux in the envelope of a supernova ( $\sigma_{n\gamma} \approx 3000$  barn) could produce a sample deficient in  $^{196}\text{Hg}$  (Jovanovic and Reed, 1976a; Heymann and Liffman, 1986). To ascertain this irradiation effect, Pallas et al. (1973) made

track studies on several samples studied by Jovanovic and Reed. They did not observe differences in track densities. Based on this observation the authors preclude the possibility that the postulated neutron irradiation took place after the chondrule formation.

Other processes leading to a separation of isotopes are possible such as photochemical separation of Hg isotopes. Isotopically selective photoionisation of mercury has been reported (Dyer et al., 1983; Pertel and Gunning, 1959). Pertel and Gunning investigated the photoexcitation of  $^{202}\text{Hg}$  in natural mercury vapour in presence of several HgO forming substrates, including water vapor, nitrous oxide and oxygen. The reactions were carried out under flow conditions, at 25°C temperature, in a high vacuum optical quartz cell. The light source was a quartz electrodeless discharge arrangement sustained with a microwave exciter. The HgO deposited was removed from the cell by solution in hydrochloric acid. The fraction of  $^{202}\text{Hg}$  in the recovered mercury was determined by Resonance Radiation Absorbiometry and Mass-spectrometry. The results obtained were very exciting. In the reaction with nitrous oxide and oxygen, it was found that the HgO product contained the normal abundance of  $^{202}\text{Hg}$ . With water vapor, a product containing upto 35 %  $^{202}\text{Hg}$  was obtained, compared to the normal abundance of 29.8 %. The addition of 1,3 - butadiene to the water vapor substrate was found to have a marked effect on the enrichment of  $^{202}\text{Hg}$  in the HgO product. A product containing 85 %  $^{202}\text{Hg}$  was recovered when the substrate contained 21 mole % of added butadiene. On the basis of this observation the authors recommended a simple method for preparing  $^{202}\text{Hg}$  from natural mercury. Dyer et al. (1983) used pulsed laser radiation for isotopically

selective ionisation of pure mercury vapor, at a density of  $6.6 \times 10^{12}$  atoms  $\text{cm}^{-3}$ , in a cell containing electrodes to which the ions were drawn by an electric field. They concluded that the clean separation of isotopes were possible because the exchange charge loss was negligible in the case of Hg at the experimental density.

These observations of photochemical separation of mercury isotopes may be important in astrophysical settings. However, further investigations are needed for a meaningful understanding of these implications. If Hg in space, particularly in cold molecular clouds, can form substrates that are suitable for the above mechanism to operate, one may get some isotopic fractionation, particularly since photons and ions are readily available. The incorporation of isotopically different grains in the meteorites may occur at the later stage of condensation.

#### **1.4 Carrier phase(s) of the isotopic anomalies**

Isotopic studies on separated phases of meteorites may prove rewarding in understanding the nebular processes and the heterogeneities in the solar nebula, which is very important for the understanding of the origin and evolution of the solar system.

##### **1.4.1 Carbonaceous carrier: the acid insoluble residue**

One of the novel techniques begins with the placing of meteoritic samples in acid solutions. The common meteoritic minerals can thereby be dissolved, leaving only a small residue that appears to be primarily carbonaceous. The exact nature of the carbon, and whether it is altered by the acid solution, is not known (D.D. Clayton, 1982; Lewis and Anders, 1983) but noble gases isotopes are often trapped within

the carbonaceous matter (e.g. Ott et al., 1984). Prominent among these are xenon-X, a r- and p- process rich pattern, xenon-s a s- process rich pattern and neon-E virtually pure  $^{22}\text{Ne}$ . Treating bulk samples with non-oxidizing acids (HF, HCl) leaves a black residue which, depending on petrologic type amounts to between 0.5 and 5 % by weight but which contains most of the trapped noble gases. Further mild treatment with oxidising agents (acids,  $\text{H}_2\text{O}_2$ , atomic oxygen) results in the opposite effect, namely a mass loss of 10 % or less but the removal of 90 % or more of Kr and Xe. Most significantly, the isotope abundance pattern is changed drastically. Normalised to  $\beta$ -shielded  $^{130}\text{Xe}$  the light and heavy isotopes are strongly enhanced, in extreme cases by up to a factor of two or more (Lewis and Anders, 1983). Goel and Murty (1983) identified anomalous xenon and osmium in the acid insoluble residues of iron meteorites and Goel (1987) reported osmium isotopic anomalies in iron meteorite residues.

#### 1.4.2 Cathodless glow discharge experiment

Bernatowicz and Fahey (1986) performed two interesting experiments : one in which pre-existing carbonaceous material (activated charcoal) was exposed to a cathodless glow discharge in rarefied air, and a second in which similar discharge was maintained in an empty pyrex container. Residual gas phase Xe and trapped Xe were found to be fractionated. The trapped xenon compositions were fractionated up to 1 % per amu. The results show that plasma synthesis of carbonaceous material (e.g. Dziczkaniec et al., 1981) is not necessary for producing xenon fractionations. If adsorption is responsible for the elemental and isotopic noble gas pattern in meteorites, the heavy noble gas isotopic



fractionation between them must have been produced prior to and by a different process than equilibrium adsorption (Bernatowicz and Podosek, 1986; Bernatowicz and Hagee, 1987).

#### **1.4.3 Allende inclusions C1 and EK 1-4-1**

These two inclusions which are rounded, about one centimeter in diameter, and are composed primarily of relatively coarse crystals of melilite, pyroxene and spinel, need special discussion. They have anomalous isotopic composition for almost every element that has been analysed. The inclusions were first recognised by oxygen isotope abundances (Clayton et al., 1977; Clayton and Mayeda, 1977), which have been modified by a mass fractionation process, superimposed on the commonly observed  $^{16}\text{O}$  additions (Clayton, 1978). Lugmair et al. (1978) in their analysis of inclusion EK 1-4-1 found that the isotopic composition of Hg agrees within error limits with terrestrial Hg, with some uncertainty in the measurements.

#### **1.4.4 Organic compounds bearing isotopic signatures**

C1 and C2 carbonaceous chondrites contain several percent of organic matter (Hayatsu and Anders, 1981; Mullie and Risse, 1987), mainly as bridged aromatic polymers containing COOH, OH and CO groups, as well as heterocyclic rings containing N, O and S. The remaining 5-30 % includes the following compound classes, either present initially or generated by solvolysis : alkanes (mainly normal), alkenes, arenes, alicyclics, alcohols, aliphatic carboxylic acids, purines, pyrimidines and other basic N-compounds, amino acids, porphyrin-like pigments, carbynes etc.

Isotopic analysis of some of the extracted organic compounds reveal large variations.  $^{12}\text{C}/^{13}\text{C}$  ratio between carbonate and organic carbon lies between 60 - 80 ‰ (Boato, 1953; Briggs, 1963; Clayton, 1963; Smith and Kaplan, 1970). Swart et al. (1983) found carbon (probably present as elemental carbon) highly enriched in  $^{13}\text{C}$  in some acid insoluble residues obtained from samples of Murchison and Allende. Zinner and Epstein (1987) reported  $\delta^{13}\text{C}$  value of upto + 7000 per mill in individual oxide grains from Murchison, which correspond to  $^{12}\text{C}/^{13}\text{C} = 11$  compared to a value of 88 to 93 for terrestrial carbon. This "heavy" carbon is associated with neon-22 and anomalous krypton and xenon showing the signature of the s- process, representing interstellar grains ejected from late type stars.

The value of  $^{13}\text{C}$  varies from one class of molecules to another. For example,  $\delta^{13}\text{C}$  values of amino acids are positive ( $\sim + 30$  ‰) whereas that of more reduced hydrocarbons are negative. The  $^{13}\text{C}/^{12}\text{C}$  ratio for individual hydrocarbons and monocarboxylic acids decreases with increasing carbon number in a roughly parallel manner. In the case of the same number of carbon atoms, a higher  $\delta^{13}\text{C}$  value is observed in carboxylic acids than in hydrocarbons. Fischer - Tropsch type of reaction is proposed to be responsible for isotopic fractionation (Lancet and Anders, 1970; Lancet, 1972).

Hydrogen isotopic composition of the organic fractions was first measured by Briggs (1963). He found that benzene-methanol extracts of four C1, C2 and C3V chondrites had variable isotopic composition. Other studies by stepped heating (Robert et al., 1979; 1980), oxidation

in an oxygen plasma (Kolodny et al., 1980) or prior enrichment of organic matter by solvent extraction (Robert et al., 1980; Robert and Epstein, 1980), show the organic matter having large deuterium enrichments upto  $\delta D = 150\text{‰}$  for Orgueil and  $310\text{‰}$  for Renazzo. C and N isotopes also vary but do not correlate with D. Yang and Epstein (1984) found  $\delta D$  values upto  $+2860\text{‰}$  in a sample of stepwise pyrolysed Murchison acid residues. This very abnormal  $\delta D$  value is associated with  $\delta^{13}C$  which is also very high ( $\sim +508\text{‰}$ ). Various possible mechanisms have been discussed by the respective authors and most comprehensively by Geiss and Reeves (1981) who have suggested that the deuterium enrichment was caused by ion-molecule gas phase reaction at low temperatures (10-50K). Certain interstellar molecules such as  $HCO^+$ , HCN or HNC are enriched in D by a factor of  $10^2$  to  $10^5$  (Penzias, 1979; 1980; Snell and Wooten, 1979). These are attributed to ion molecule reactions (Watson, 1976; Huntress, 1977; Wannier, 1980). The D enrichment in meteoritic organic matter is upto four orders of magnitude smaller than in interstellar molecules (Winnewisser and Herbst, 1987). Thus, probably, it is mainly of local origin that was slightly mixed with D rich interstellar matter or the presolar grains (Eberhardt, 1979; Lewis et al., 1979).

In carbonaceous chondrites, nitrogen is essentially part of organic molecules, compared to other meteorites where it is mostly in the inorganic form. The  $CH_3OH$  extracted organic molecules from Murchison show  $\delta^{15}N$  upto  $+90\text{‰}$  (Becker and Epstein, 1982; Epstein et al., 1987). Observation during the stepwise oxidation of organic matter proves that the  $^{15}N$  content is dependent on the type of host organic molecules. Acid resistant residues from Murchison, after removal of

organic polymers by the use of oxidative treatment show very low  $\delta^{15}\text{N}$  (upto  $-274\text{‰}$ , Pillinger, 1984; Lewis et al., 1983). Two other interesting elements with respect to the study of isotopic ratios in organic matter are oxygen and sulphur but unfortunately the information remains very sparse (Briggs, 1963; Hulston and Thode, 1965). Heavier elements in the form of organometallic compounds (if found in meteorites) could be very interesting to study for their isotopic ratios.

In order to identify the carrier phase of isotopic anomalies other physical separation methods have also been tried. Kuznetsov et al. (1985) reported a systematic correlation of concentration of volatile elements (excluding mercury) in grain size fractions and magnetic or non-magnetic fractions. Eugster et al. (1986) observed concentration of trapped noble gases to be grain size correlated. But the isotopic ratio studies gave normal values. Ott et al. (1981) combined acid residue separation methods with density separation, sedimentation separation, settling rate separation and colloidal separation. Isotopic data for carbon showed little variation ( $\lesssim 5\text{‰}$ ); isotopic data for noble gases show that the host phase of the anomalous component was not clearly separated.

## EXPERIMENTAL

## 2.1 Introduction

Most isotopic ratio measurements are done by mass spectrometry (e.g. Clayton et al., 1973; Morand and Allegre, 1983; Niemeyer and Lugmair, 1985; Kuroda, 1985; Esat et al., 1986; Huss and Alexander, 1987). While neutron activation analysis technique has been extensively used for reliable measurements of trace elements in extraterrestrial matter (e.g. Dybezynski, 1985; Prutt, 1986), its application to isotopic ratio determination has been rather limited. In meteorites, isotopic ratios have been measured by RNA (Radiochemical Neutron Activation) for Hg (Jovanovic and Reed, 1969; 1976a; 1976b; 1987), Os (Takahashi et al., 1976; Goel and Murty, 1983; Goel, 1987) and Te (Oliver et al., 1981). With the availability of high resolution gamma-ray spectrometry system (Ehmann and Yates, 1986), the RNA method stands to be developed into a powerful technique for isotopic ratio measurements. Following the method of Jovanovic and Reed (1976a; 1976b; 1987) we have measured the Hg isotopic ratios in stone meteorites and in the separated phases of stone and iron meteorites.

Of the seven stable isotopes of Hg, shown in Figure 2.1,  $^{196}\text{Hg}$  and  $^{202}\text{Hg}$  can be conveniently measured by RNA. The basis for determination of isotopic ratio for the above mentioned two Hg isotopes can be seen from the nuclear data presented in Table 2.1. When a sample is bombarded to thermal neutrons the isotopes  $^{196}\text{Hg}$  and  $^{202}\text{Hg}$  are converted to  $^{197}\text{Hg}$  and  $^{203}\text{Hg}$  respectively which have convenient half lives. Their

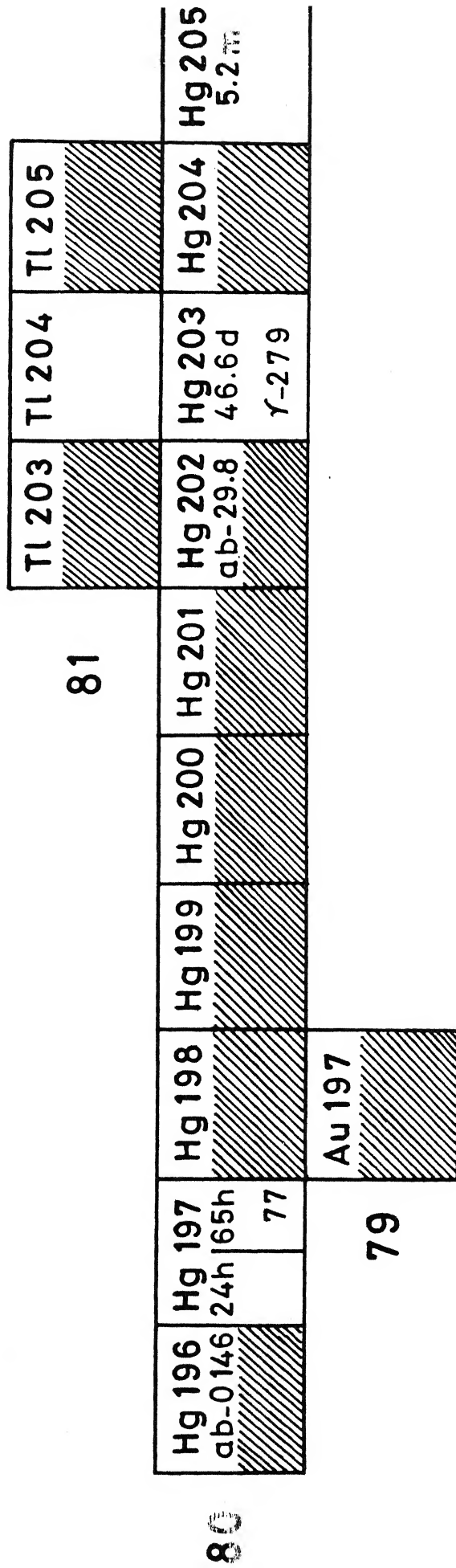


Fig. 2.1 Nuclides chart of mercury

Table 2.1 Nuclear activation parameters for Hg isotopes

Isotope	$^{196}\text{Hg}$	$^{202}\text{Hg}$
Abundance (%)	0.146	29.799
Thermal neutron cross section	3000 barn	5 barn
Neutron Activation Products		
Nuclide	$^{197}\text{Hg}$	$^{203}\text{Hg}$
Half life	2.67 day	46.58 day
Energies of X and $\gamma$ rays (keV) followed by intensities (%)	67.0 X    21.2	70.8 X    3.75
	68.8 X    36.2	72.9 X    6.35
	77.3 $\gamma$ 18.1	82.5 X    2.20
	77.9 X    12.5	84.9 X    0.63
	80.2 X    3.37	279.2 $\gamma$ 81.5

photon spectra are analysed at energies of  $(67.0 + 68.8)$  keV and  $(77.3 + 77.9)$  keV for  $^{197}\text{Hg}$  and of 279.2 keV for  $^{203}\text{Hg}$ , using a high purity germanium detector. A description of sample preparation, packing, irradiation, and detection is given here.

## 2.2 Sample preparation

There are some differences in the sample preparation procedures of stone meteorites and iron meteorites. Iron meteorites are always taken as acid insoluble residues. These residues are then separated into various grain sizes and magnetic fractions. Stone meteorites are crushed into powder and separated into different fractions.

### 2.2.1 Acid dissolution of iron meteorites

Pieces of iron meteorites, cleaned and etched, are dissolved in 2M  $\text{H}_2\text{SO}_4$  (Murty et al., 1982; 1983; Goel and Murty, 1983) with occasional stirring and periodic addition of fresh acid. This process lasts for four to eight weeks. Sufficient quantity of residual matter is always found upon dissolution.

The acid dissolution is considered complete when bubbles cease. The insoluble residue is filtered using a Millipore filtration assembly. This is washed free of acid, with water, then once with ethyl alcohol. Ethyl alcohol prevents aggregation of the grains during the drying process. The filtrate, containing unused excess acid and dissolved salts is saved.

Drying is done by either of the two ways, (i) by keeping the residue at room temperature for sufficiently long time, usually it takes four to six hours to dry; (ii) or by placing the residue under infrared heat



lamp, at sufficient height to avoid over-heating. Since mercury is one of the pollutant in the atmosphere and in the laboratory, care is taken during drying process to minimise the addition of dust etc. to the residue. The insoluble residues were often found to contain milimeter size brittle pieces and thin mettalic flakes. Most of the material was black powder of sub-metalllic lustre.

### **2.2.2 Grain size separation**

In a mixture of meteoritic material of different minerals, it is plausible that some mineral might get more concentrated into small or big size grains depending on their hardness and fracture properties. With this hope, we carried out sieving of residues and crushed meteorites. Sieving is done manually as well as by using ultrasonic sifter. In ultrasonic method sieves of different sizes are stacked together, in an ascending order, with the coarsest at the top where the sample is placed. Ultrasonic wave comes from the top. A transverse shock wave is also given to the lowest sieve to remove the cohesion and adhesion effects. Using this method we have separated grain sizes from  $<38\text{ }\mu\text{m}$  to  $>150\text{ }\mu\text{m}$ . Ultrasonic sifter has only been used in pre-irradiation cases to avoid contamination problem. For post-irradiation separation, and samples of small masses, manual sieving was done. Samples are taken on sieves (commercial as well as home made) and shaken gently with mild tapping. In many cases, upon visual inspection, flakes and inclusions are seen particularly in the coarser sizes. These are separated with the help of a forceps.

### **2.2.3 Magnetic phase separation**

We further separated the residues into magnetic, weakly magnetic and non-magnetic fractions with the help of a hand magnet. Grains

that are clearly attracted from a distance ( $\sim 2$  cm), are termed magnetic and those attracted only from very close distance (few mm) are weakly magnetic. Precautions are taken to minimise adhesion of particles of different magnetic behaviour. Tapping of powder and repeated separations are found useful. Interestingly in many cases the non-magnetic samples, after heating for Hg-extraction, were converted into magnetic, while the magnetic remains unaltered on heating.

#### **2.2.4 Relative densities of grains**

Sometimes a low density fraction (L) is separated in the form of slurry with water. The grains in the high density fraction (H) are more shiny (Goel, 1987) we have not attempted to find the absolute densities of the samples packed for irradiation. Crude estimation of relative densities are done by measuring the sample column height in irradiation quartz tubes, of equal bore size, used for packing after a little tapping.

#### **2.2.5 Sampling of stone meteorites**

Unlike irons, stones are not dissolved in acids. These are taken as bulk or crushed and separated into chondrules, sieve sizes and magnetic fractions.

Pieces of stone meteorites weighing 100-500 mg are wrapped in an aluminium foil. The irradiated pieces are ground using steel or agate mortar and pestle. When this powder is directly used for mercury distillation, it is termed as bulk sample. Irradiated sample cans are opened in a hot laboratory where grinding, sieving and separation of phases are done. Gently ground stone meteorites often separate into chondrules. Millimeter size round and relatively hard grains are picked up with the help of forceps.

Sometimes it may also contain some grains other than chondrules. A crushed stone meteorite is further separated into various sieve sizes and magnetic fractions following the procedures similar to those used for iron meteorite residues. Chondrules in most cases are magnetic in nature.

### 2.2.6 Terrestrial standard : the monitors

To compare the values of Hg-isotopic ratios measured in meteorites, a terrestrial standard sample of Hg is needed. Hg monitors are prepared by loading reagent  $\text{Hg}(\text{NO}_3)_2$  solution on alumina or magnesium oxide matrix. The amount of Hg in a monitor varied between 0.1 to 20  $\mu\text{g}$ . The concentrations between 0.1 to 1.0  $\mu\text{g}$  of Hg were more suitable since these gave comparable counts with the meteoritic samples. Otherwise a high activity monitor had to be diluted before it could be compared with the samples. Magnesium oxide matrix is preferred over alumina matrix because the later, due to its insolubility, creates some problems in chemical separations. Hg loaded matrices were dried at room temperature in quartz tubes and were sealed carefully to avoid appreciable heating of the powder.

### 2.3 Packing of samples and monitors

To avoid contamination, sample handling is kept to a minimum. However, for unavoidable steps, extreme precautions are taken by using clean apparatus and reagents of "GR" grade. Monitor(s) and separated phases of stone and iron meteorites are sealed in thin bore ( $\sim 2$  mm I.D.) quartz tubes which are finally kept in screw capped aluminium can. Sometimes pieces of stone meteorites, wrapped in aluminium foils, are also packed alongwith other samples and monitors. Heat sealing of quartz tubes results in loss of mercury. Thus in vials, packed in later runs, either the sealing was avoided or, if needed was done after putting a cover of wet asbestos

around a tube. The quartz tubes were firmly capped with aluminium revets in the former case. Removal of aluminium foils and thorough cleaning of the outer surface of the quartz ampules after irradiation ensured a freedom from external contamination during irradiation. Masses of samples packed, usually, varied from 10 to 1000 mg.

## 2.4 The neutron irradiation

A set of samples packed for neutron irradiation is termed a **vial**. For identification, each vial is given a serial number and the year of experimentation. Irradiations were carried out at the Bhabha Atomic Research Centre, Bombay. Vials were irradiated in the CIRUS reactor to a thermal neutron flux of  $10^{13} \text{ n cm}^{-2} \text{ sec}^{-1}$  for one week. It takes almost a week after the end of irradiation to reach the vial in our laboratory. Samples were processed without further cooling. During this transfer period many undesirable short-lived nuclides decay off (Alian et al., 1984). In CIRUS which is a deuterated - water moderated reactor, the temperature at the bombardment site is not expected to be undesirably high. The position where our samples are normally irradiated has the fast ( $E > 1 \text{ MeV}$ ) to the thermal neutron ratio of  $< 0.01$  and the epithermal ( $E > 100 \text{ keV}$ ) to the thermal ratio is  $< 0.1$ .

## 2.5 Mercury distillation

Mercury can be extracted from a sample by heating it for about four hours at  $400^\circ\text{C}$  under vacuum (Rozanska and Lachowicz, 1984; Dusan et al., 1984). This technique was followed, in earlier vials, to distill mercury from an irradiated sample. Later vials were processed by stepwise heating (Jovanovic and Reed, 1987). The temperature generally ranged from  $100^\circ\text{C}$  to  $600^\circ\text{C}$ . The heating time varied from one to four hours depending

on the amount of mercury released, as seen from the counting rate of the extracted sample. The arrangement for distillation is shown diagrammatically in Figure 2.2 . The distillate is condensed in a trap cooled with liquid nitrogen. The system is flamed thoroughly to ensure that all the released Hg is collected. Condensed Hg is isolated from the detached cold finger by washing with few drops of conc.  $\text{HNO}_3$  and conc.  $\text{HCl}$ .

Often we were interested in making measurements on large size sample ( $\sim 1$  gm). In such a case the Hg was distilled prior to activation. This has two advantages : (i) it minimises the radiation hazard from radioactive sample and (ii) the remaining heated sample can be saved for future experiments. The apparatus used is shown in Figure 2.3 . The quartz combustion tube, having a cold finger, was mounted horizontally and connected to the vacuum line. The cold finger was cut off, after each distillation, either by heat sealing process or by the use of a file and a new quartz tube was connected in its place. Vials 5/85, 6/85 and 7/85 contained Hg samples distilled in this way. Because of impurities these Hg distillates were once again distilled after activation, as described earlier. These experiments were not successful and gave poor yields.

## 2.6 Extraction of Hg using sodium diethyldithiocarbamate

It was observed that the Hg distillate washed with aqua regia resulted in a loss of its Hg content upon storage. A suitable organic chelating reagent was sought for, which could form more stable complex with Hg and could be easier to handle. Sodium diethyldithiocarbamate (cupral) is one of the best known organic reagents which form extractable chelates with many metals (Stary and Kratzer, 1968; Sekine and Hasegawa, 1977; Hakkila and waterbury, 1960). These chelated complexes, known as Metal-

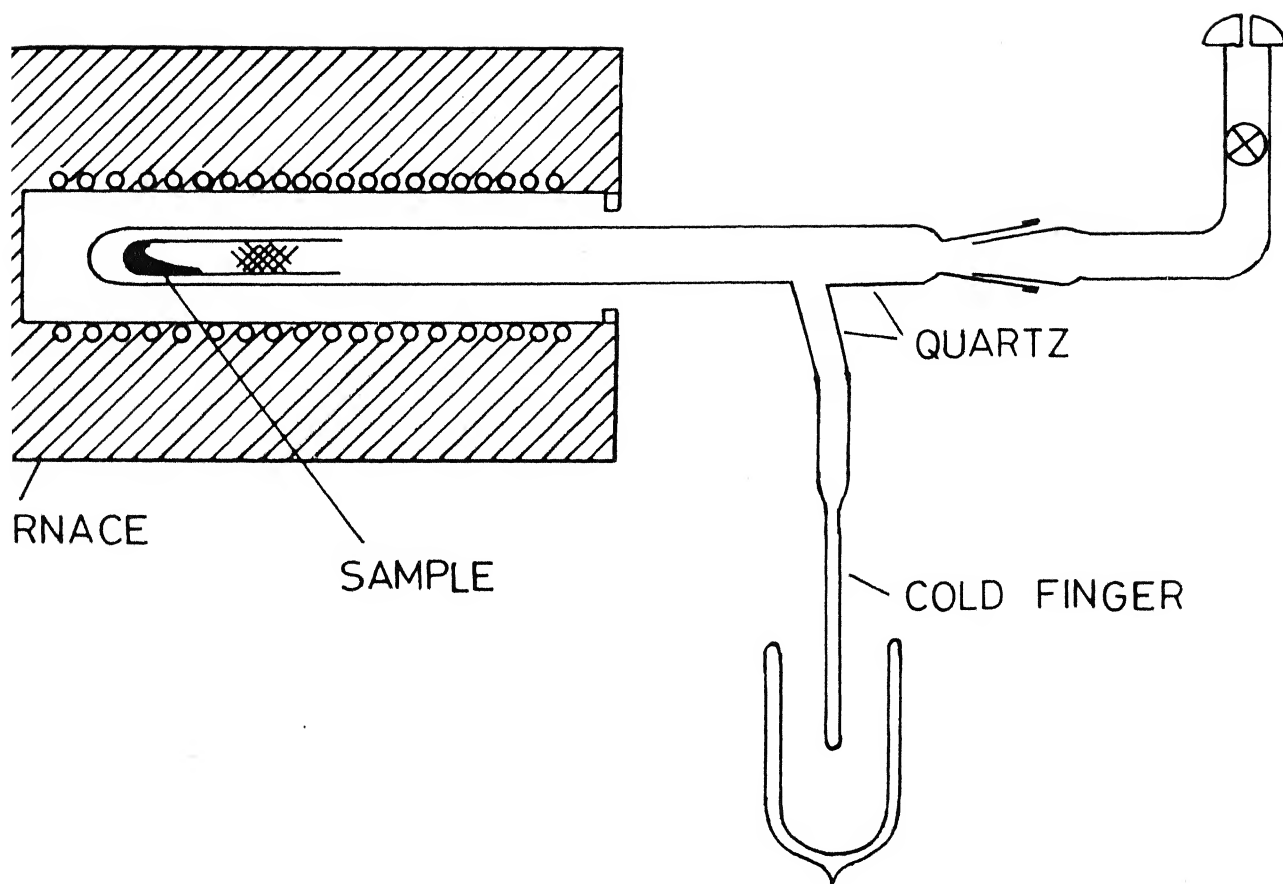


Fig. 2.3 Mercury distillation apparatus

DDTC complexes, are stable, soluble in organic solvents (e.g. chloroform, carbon tetrachloride) and the solution can be conveniently dried at room temperature without any appreciable loss of the metal (Yeh et al., 1984). The extractability of metal diethyl dithiocarbamate, as determined by Stary and Kratzer (1968), decreases in the following order :  $\text{Pd}^{+2}$ ,  $\text{Hg}^{+2}$ ,  $\text{Ag}^{+}$ ,  $\text{Cu}^{+2}$ ,  $\text{Ni}^{+2}$ ,  $\text{Bi}^{+3}$ ,  $\text{Pb}^{+2}$ ,  $\text{In}^{+3}$ ,  $\text{Cd}^{+2}$ ,  $\text{Zn}^{+2}$ ,  $\text{Co}^{+2}$ ,  $\text{Fe}^{+2}$ ,  $\text{Tl}^{+}$  and  $\text{Mn}^{+2}$ . The typical values of extraction constant,  $\log k$ , for  $\text{Pd}^{+2}$ ,  $\text{Hg}^{+2}$ ,  $\text{Ag}^{+}$  and  $\text{Cu}^{+2}$  were 32, 32, 11.9 and 13.7 respectively. Yu et al. (1983) selectively extracted mercury from sea water using this reagent. The dried samples were neutron activated and  $^{197}\text{Hg}$  tracer was used for  $\gamma$ -spectrometry. The detection limit was established as  $0.01 \mu\text{g l}^{-1}$ . Yeh et al. (1984) used  $^{197}\text{Hg}$  tracer and showed that preconcentration of Hg offers better sensitivity for neutron activation analysis. Stary and Kratzer (1968) used  $^{203}\text{Hg}$  tracer to determine the extraction constants of mercury.

Na-DDTC reagent has been used in this work to wash and collect the Hg distillates from meteorites and also to extract Hg from aqua regia washed distillates. The later was meant for reirradiation experiment as discussed in Chapter 4.

### 2.6.1 Reagent preparation

All the chemicals used were of A.R. purity. The extracting reagent is prepared freshly before each set of experiments. About 0.1 gram of sodium diethyl dithiocarbamate reagent is shaken with 50 ml of carbon tetrachloride for 3-4 hours. The undissolved part is filtered off and the filtrate is stored in a dark bottle. The reagent is unstable in acid solution, the half life being 0.5 minutes and 4.9 minutes at pH 4.0 and 5.0 respectively, but 498 minutes and 5050 minutes at pH 7.0 and 9.0 respectively,

CENTRAL LIBRARY

106249

at room temperature (Bode, 1954; Bode and Neumann, 1959). Therefore it is normally used at high pH in the presence of a suitable masking agent to prevent the formation of precipitates of hydroxides or basic salts.

### 2.6.2 Washing of distilled Hg from vacuum line

The condensate in the liquid nitrogen trap was shaken with 0.5 ml of the reagent for half an hour, washed once more with 0.5 ml of carbon tetrachloride, and transferred to the counting vial. It was found that almost all of the distilled Hg could be washed in just one shaking with the extracting reagent. A second extraction failed to give any count rate of Hg.

### 2.7 Radiochemical purification of mercury

In many cases, e.g. for monitors, it was desired to separate Hg from irradiated samples by a suitable radiochemical procedure. The adopted procedure consisted of the following steps :

- i. The quartz ampule, after its surface has been cleaned, is cut open and the powder is transferred to a small beaker.
- ii. The powder is dissolved in few drops of conc. HCl and minimum amount of  $\text{HNO}_3$  by slight warming, if needed. 10 to 50 mg Hg carrier is added and is left for one hour for equilibration.
- iii. The solution is evaporated at low heat to near dryness to remove excess  $\text{HNO}_3$  after addition of 1 ml of conc. HCl. This process is repeated till brown fumes of  $\text{NO}_2$  are given off.
- iv. The solution is made to 5 ml with distilled water and several drops of freshly prepared  $\text{SnCl}_2$  solution are added.
- v. The solution is warmed to  $60^\circ\text{C}$  for 10 minutes to complete



the precipitation of Hg and is cooled in a water bath for a few minutes. The white precipitate of  $\text{Hg}_2\text{Cl}_2$  (further reduction causes the precipitate to darken due to the formation of elemental mercury) is centrifuged and washed twice with 5 ml aliquots of 0.5 M HCl and, once with water.

vi. The  $\text{Hg}_2\text{Cl}_2$  precipitate is dissolved in a few drops of aqua regia and a few drops of  $\text{AgNO}_3$  solution are added. The precipitate of AgCl, which acts as a scavenger, is centrifuged and discarded.

vii. Mercury is re-precipitated using  $\text{SnCl}_2$  solution as in step iv. The precipitate is digested at  $60^\circ\text{C}$  for fifteen minutes and is washed several times with dil. HCl, distilled water and once with ethyl alcohol.

viii. The precipitate is then dissolved in a few drops of aqua regia and is transferred to the counting vial where it is diluted to the required volume.

Any extended heating of solution containing both mercury and chloride ions or its evaporation to dryness greatly decreases the chemical yield (Ehmann and Lovering, 1967) and was avoided.

## 2.8 Activity measurement

The washed mercury distillate is transferred to a 25 ml screw-capped glass vial. All samples are made upto the same volume of 1 ml ( $\pm 0.1$  ml) using distilled water or carbon tetrachloride, whatever is suitable, to prevent absorption effects (Gijbels, 1967). The detection-recording system for measurements of the photon spectra of irradiated sample is shown diagrammatically in Figure 2.4. High purity germanium crystal detectors (supplied by Canberra and ORTEC) were used in conjunction with a stabilised d.c. power supply. The signal from detector preamplifier is fed into a multichannel analyser. The dimensions of the crystal of ORTEC (gamma-X)

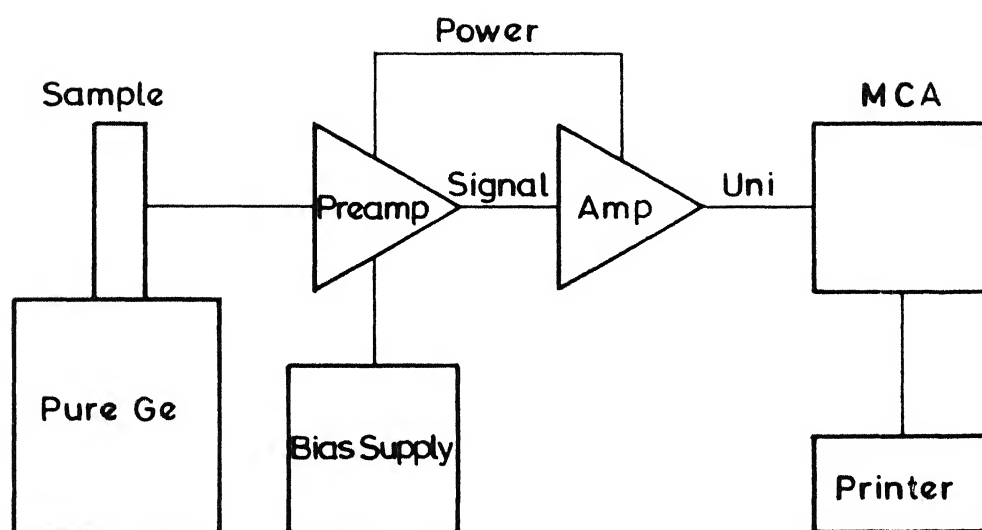


Fig.2.4 Photon detection recording set-up.

are : diameter = 45.2 mm; length = 52.7 mm with a 0.5 mm thick beryllium window. The crystal is cooled by conduction from a copper finger protruding from the bottom of the detector and maintained in liquid nitrogen. The Canberra detector does not have a beryllium window. It has a crystal length of 28 mm; active area =  $12.5 \text{ cm}^2$ ; distance from window = 5 mm and thickness of n-layer = 0.5 mm .

The multichannel Nuclear Data analysers (model ND65 and ND66) incorporate a video-screen display, automatic timing and numerous programmable control facilities and are interfaced to dot-matrix printers. The analyser energy scale was varied between 0.1 keV per channel to 1.0 keV per channel in different vials. In most cases it was kept at 0.5 keV per channel. Most of the work was done on the Canberra detector.

### **2.8.1 Energy calibration**

To encompass all the regions, the following calibration standards are used :  $^{57}\text{Co}$  (122 and 136 keV),  $^{137}\text{Cs}$  (662 keV),  $^{22}\text{Na}$  (511 and 1274 keV) and  $^{60}\text{Co}$  (1173 and 1332 keV). A very good linear energy calibration is obtained (Murty, 1981). Calibration is checked periodically to ensure stability of the amplifier gain.

### **2.8.2 Sample counting geometry**

Sample vials are placed in a perspex sample holder which snugly slips onto the detector. This sample holder has a circular groove, concentric with the crystal to allow reproducible positioning of the sample vials.

### 2.8.3 Shielding of the detector

To reduce the background due to radiations from natural radioactivity, the detector is positioned inside a thick (~2 inch wide) lead housing. The lead shielding around the detectors is lined with successive layers of steel and mercury. These coverings are to avoid the presence of lead X-rays in the spectra (Parry, 1984). About six inches thick steel shielding is placed below the detector vessel too.

### 2.8.4 Counting

The multichannel analyser recorded automatically a net integral count and its statistical variation. The radionuclides were counted for different times, 1 minute to 12 hours, depending on the counting rate. In most cases only  $\gamma$  and X rays from  $^{197}\text{Hg}$  and  $^{203}\text{Hg}$  are observed. Typically channels 550 to 569, accumulating in the range of 275 - 285 keV, were pre-set for  $^{203}\text{Hg}$ . Similarly channels 133 to 142 and channels 151 to 160 were pre-set to cover the energies of 66.5 to 71 keV, and 77.5 to 80 keV, respectively for  $^{197}\text{Hg}$ . Normally 77 keV (77.3 keV  $\gamma$  + 77.9 keV X) peak area for  $^{197}\text{Hg}$  and 279.2 keV for  $^{203}\text{Hg}$  were taken for isotopic ratio calculations. Generally the photon spectrum of a sample initially showed a 77 keV peak higher than the 279 keV peak. After several days the shorter half life of the former resulted in a "noisy" sloping background in that region.

### 2.8.5 Decay corrections

Reproducibility has been checked by repeated counting. Decay corrections have been applied for both  $^{197}\text{Hg}$  and  $^{203}\text{Hg}$  during the counting period. The activity ratios of all the samples are calculated for the same time base by multiplying with a proper decay factor.

### 2.8.6 Errors

Only statistical errors due to counting are considered and are computed by simple statistical laws. Homogenous samples, identical geometry and counting conditions have been employed in all cases to eliminate relative errors. The counting time in most cases is chosen such that the errors lie between 1 to 5 %. The quality of analytical results have often been described by terms such as A (excellent), B (acceptable) or C (poor) depending on the shape of spectra (McFarren et al., 1970).

### 2.9 Precautions to avoid contamination

Since contamination of Hg from various sources is a serious possibility (Jovanovic and Reed, 1980; Byrne et al., 1983; Heimbürger et al., 1986) and could affect our measurements in various ways, some preventive measures have been taken as outlined below :

- i. Quartz irradiation tubes, before filling the meteorite sample powders, are cleaned with nitric acid and heated at 600°C for few hours in vacuum.
- ii. All glass vials used for sample counting are washed thoroughly, before any set of experiments, using boiling soap solution, rinsed with distilled water and then decontaminated using EDTA solution. Other apparatus e.g. cold fingers, combustion tubes and droppers are kept in an air oven at 150°C for few hours after washing.
- iii. Thorough cleaning of vacuum line before and after each set of experiments is undertaken.
- iv. All the reagents, apparatus and meteorites are stored in strictly closed conditions.

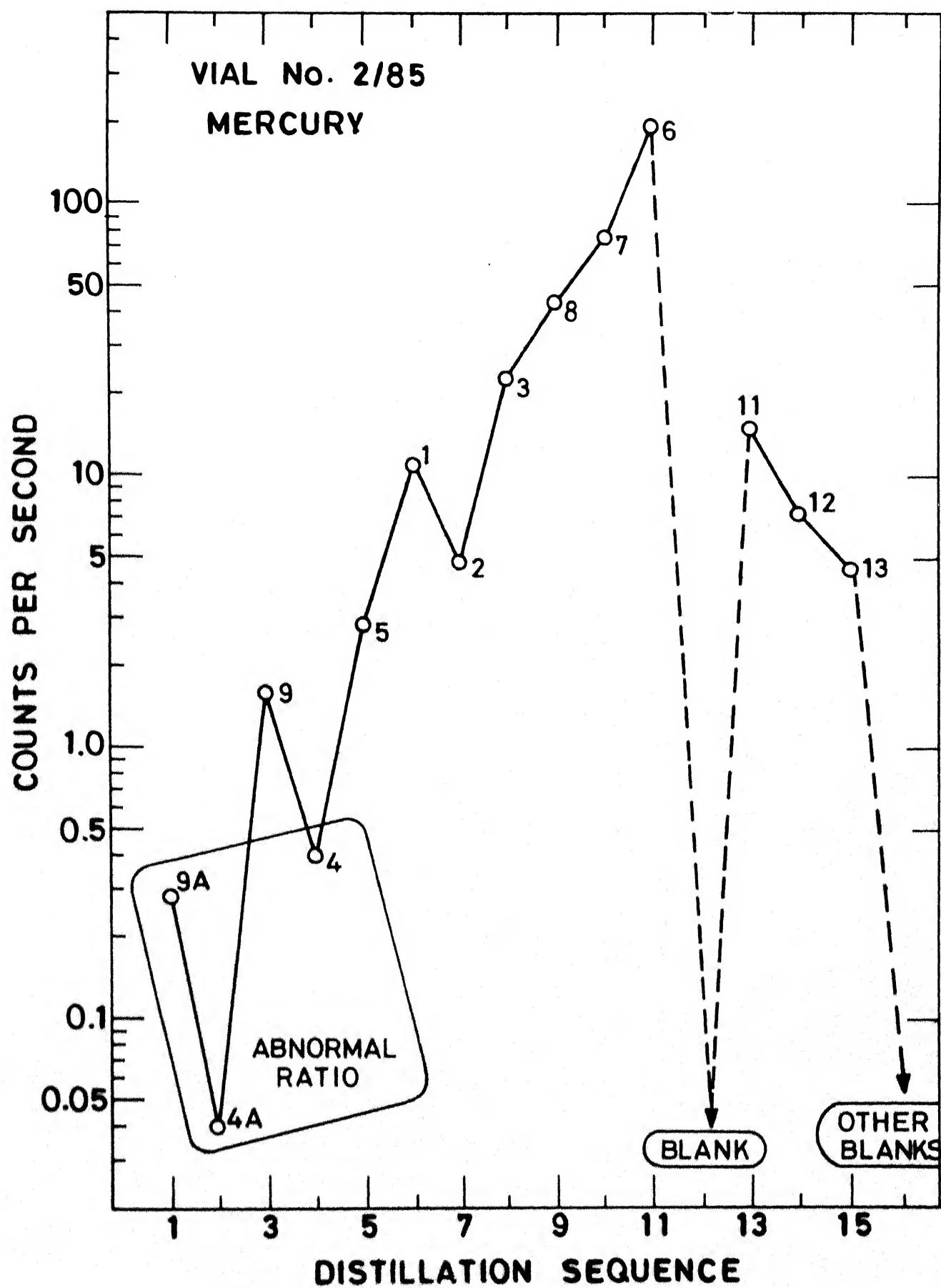


Fig. 2.5 Counting rate vs. distillation sequence (2/85)

- v. Monitor preparation is a completely isolated process.

### 2.9.1 Blank level monitoring

To monitor the level of contamination it is essential to study blank samples. The following different types of blanks have been investigated.

- i. Meteorites already heated to extract mercury (prior to irradiation) were packed alongwith other samples and processed similarly.
- ii. During the distillation of mercury from meteorites, distillation was done without placing actual sample but all the processes of flaming, acid addition etc. were done in the usual fashion.
- iii. Blank run samples were occasionally distilled between two meteorite samples to see any residual activity left in the line. Efforts were made to distill lowest level activity first to minimise the effect of cross contamination. The blanks distilled after high activity samples showed (Figure 2.5) that the problem of memory and contamination is also unimportant.
- iv. Empty quartz irradiation tubes, used for sample packing, were irradiated and Hg was vacuum distilled. No Hg - activity was found in those tubes.
- v. Occasional counting of the background was done to ascertain the absence of any contamination around the detector.
- vi. Na-DDTC/ $\text{CCl}_4$  reagent also showed an absence of Hg - activity upon neutron irradiation.

## Chapter 3

### RESULTS FROM METEORITE STUDIES

Twenty four different irradiations were carried out for Hg-isotopic studies in meteorites. There were some variations in the sample preparation, packing, Hg-distillation etc. of some of the runs. These are described with the results in each case. Hg abundances, wherever presented, are based on  $^{203}\text{Hg}$  activity assuming a normal isotopic ratio.

#### 3.1 Vial No. 1/85

In this vial we packed  $\text{H}_2\text{SO}_4$  acid insoluble residues of iron meteorites Bear Creek and Campo del Cielo. Sieving was done through a 32  $\mu\text{m}$  size hand-sieve, to yield coarse and fine fractions. These were heat sealed in quartz capsules and irradiated. There was no mercury monitor present. After neutron irradiation more samples were prepared by dividing them into aliquots and crushing four of them (representing all four samples as packed) in an agate mortar. Hg was extracted from all the samples by heating each in vacuum at a temperature of  $400^\circ\text{C}$ , for about four hours.  $^{203}\text{Hg}$  was measured in 10 channels (0.5 keV per channel) at 279 keV.  $^{197}\text{Hg}$  was measured from two different photon peak areas (i) 77.3 keV  $\gamma$  and 77.9 keV X in 6 channels and (ii)



67.0 and 68.8 keV X in 10 channels. The details along with the results on this vial are given in Table 3.1. The counting rate tabulated is on the basis of long lived  $^{203}\text{Hg}$  isotope. All the values of  $^{203}\text{Hg}/^{197}\text{Hg}$  ratio are, apparently, uniform within the limits of a conservative error of  $\pm 10\%$  (Figure 3.1). Since there was no mercury monitor present, it was not possible to compare the isotopic ratios with the terrestrial value and also to obtain the Hg abundances. In sample No. 3 the geometry differs in the first three countings because the vial was slightly off the perspex holder over the detector mount. The counting rate in the first three countings were 18 cps, whereas in the correct geometry the count rate was 23 cps. This, however, does not affect the isotopic ratio seriously. Since the counting rate in the high temperature fraction of sample No. 1 was very low, no high temperature extractions for the other samples were done.

### 3.2 Vial No. 2/85

Since the Os anomaly was most pronouncely found in the inclusion of Sikhote Alin meteorite (Murty et al., 1983; Goel, 1987), this run was planned to investigate these residues for Hg isotopic ratios with larger sample sizes. During the dissolution of Sikhote Alin iron meteorite, there were obtained many large size (few mm) inclusions with a density of about  $6.5 \text{ g cm}^{-3}$ . These could be easily crushed into powder. During this crushing process, we found two fragments of magnetic material that did not crush, and examined these malleable pieces for Hg isotopic

Table 3.1  $^{203}\text{Hg}/^{197}\text{Hg}$  Ratio in Vial No. 1/85

Sample		c/s	c/mg/s	$^{203}\text{Hg}/^{197}\text{Hg}$ Ratio		
No.	Description			Mass (mg)	Replicate	Best*
<u>Bear Creek</u>						
1.	< 32 $\mu\text{m}$	160.0	21	0.13	1.3, 1.4, 1.4, 1.4	1.4
1	HT.** < 32 $\mu\text{m}$	160.0	0.6	0.004	1.3	1.3
2.	Crushed, < 32 $\mu\text{m}$	170.0	39	0.23	1.5, 1.4, 1.4	1.4
3.	Crushed, > 32 $\mu\text{m}$	230.0	23	0.10	1.3, 1.3, 1.3, 1.3, 1.4	1.3
<u>Campo del Cielo</u>						
4.	Mag., Heavy, < 32 $\mu\text{m}$	142.7	45	0.32	1.46, 1.48	1.47
5.	Mag., Heavy Crushed, < 32 $\mu\text{m}$	64.0	41	0.64	1.4, 1.4	1.4
6.	Mag., Heavy Crushed, > 32 $\mu\text{m}$	146.0	24	0.17	1.4, 1.4	1.4
7.	Mag., Light, < 32 $\mu\text{m}$	43.5	32	0.74	1.4, 1.4	1.4
8.	Mag., Light, > 32 $\mu\text{m}$	22.5	14	0.61	1.4	1.4
9.	Mag., Light, < 32 $\mu\text{m}$	26.0	17	0.64	1.4	1.4

\*Errors are less than  $\pm 10\%$ . \*\*This sample was distilled at  $1000^\circ\text{C}$  whereas all others were distilled at  $400^\circ\text{C}$ .

c/s = counts/second/5 keV at 279 keV.

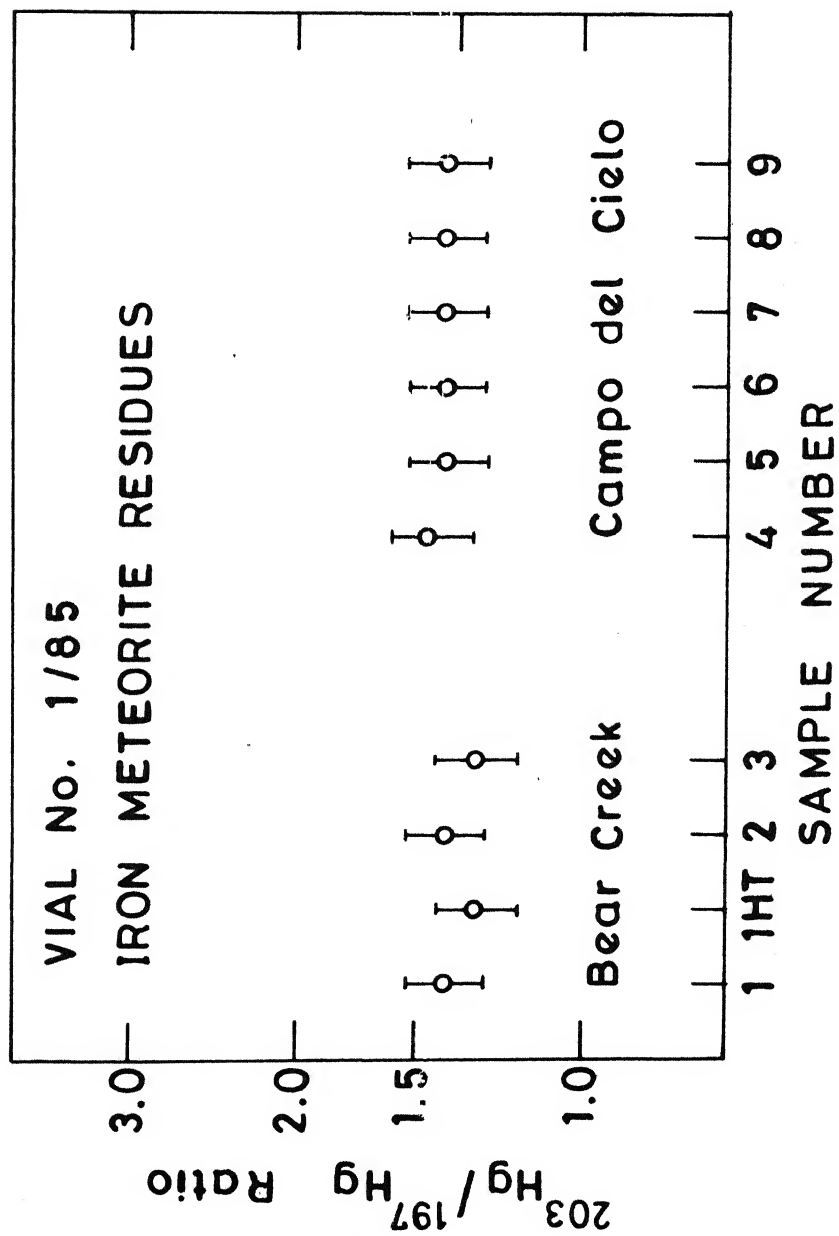


Fig. 3.1 The Hg isotopic ratio in samples from Bear Creek and Campo del Cielo meteorites

anomaly. For lack of any proper identification and better name, these we have called "nuggets". The nuggets were irradiated in capsules containing powdered masses of the inclusions to optimise space in the vial. Thus No. 9 nugget was sealed in the capsule containing powder of the inclusion No. 9, and No. 4 nugget was irradiated with 160 mg of the inclusion powder in capsule No. 4.

This vial also contained samples from Toluca acid insoluble residue, but there was no terrestrial standard of mercury present in it. All samples were distilled at 400°C only, for about three hours each. The results are given in Table 3.2 and Figure 3.2. It is found that sample No. 4 (inclusion), 4A (inclusion nugget) and 9A (inclusion nugget) have a lower value of  $^{197}\text{Hg}/^{203}\text{Hg}$  isotopic ratio. Most other samples are showing indistinguishable values within error limits. The photon spectra of some of the samples are shown in Figure 3.3.

### 3.3 Vial No. 3/85

Samples from stone meteorites Dhajala, Allende, Ambapur Nagla and from iron meteorite residues of Sikhote Alin, Campo del Cielo, Canyon Diablo and Elga were packed. Mercury distillation temperature was 500°C. The slope, for counting, was fixed as 0.25 keV per channel. The 68 keV and 77 keV photons were both measured in 6 channels, and the 279 keV  $\gamma$  in 25 channels. Unfortunately due to power breakdown, and delays in its restoration, the  $^{197}\text{Hg}$  activity decayed off for any reliable measurements. The results are presented in Table 3.3. Since

Table 3.2 Results from Vial No. 2/85

<div>Sample</div>		Mass (mg)	c/sec	c/mg/s	<div><math>^{203}\text{Hg}/^{197}\text{Hg}</math> Ratio</div>	Best*
No.	Description				Replicate	
<u>Sikhote Alin residues</u>						
1	Magnetic ( < 30 μm)	55	11	0.200	1.1; 1.1; 1.1; 1.1	1.1
2	Mag. crushed ( < 30 μm)	18	4.9	0.269	1.1; 1.1; 1.1	1.1
3	Mag. crushed ( > 30 μm)	54	23	0.423	1.1; 1.2; 1.3	1.2
4	Inclusion Powder	155	0.4	0.003	2.05; 1.95; 2.6	1.9 ±0.2
4A	Inclusion Nugget	7	0.04	0.005	>1.84; 1.79; 3.1	2.5 ±0.6
5	Inclusion	245	2.82	0.012	1.1; 1.1; 1.1	1.1
6	Non-mag. ( > 30 μm)	29	191	6.6	1.1; 1.2; 1.2	1.2
7	Non-mag. ( < 30 μm)	11	75	6.8	1.1; 1.1; 1.3	1.2
8	Non-mag. ( < 30 μm) no grinding	6.5	44	6.8	1.1; 1.2; 1.2	1.2
9	Inclusion Powder	51	1.6	0.03	1.1; 1.1; 1.1	1.1
9A	Inclusion Nugget	8	0.28	0.04	>4; 2.0; 3.1; 2.2	2.1 ±0.5
<u>Toluca residues</u>						
11	Mag. ( < 30 μm) no grinding	27	15	0.56	1.1; 0.95; 1.26	1.1
12	Mag. ( < 30 μm) grounded	23	7.3	0.32	1.0; 0.97; 1.2	1.1
13	Mag. ( > 30 μm) grounded	40.5	3.8	0.09	1.0; 1.0; 1.25	1.1

\* Errors are less than  $\pm 10\%$  unless otherwise stated.

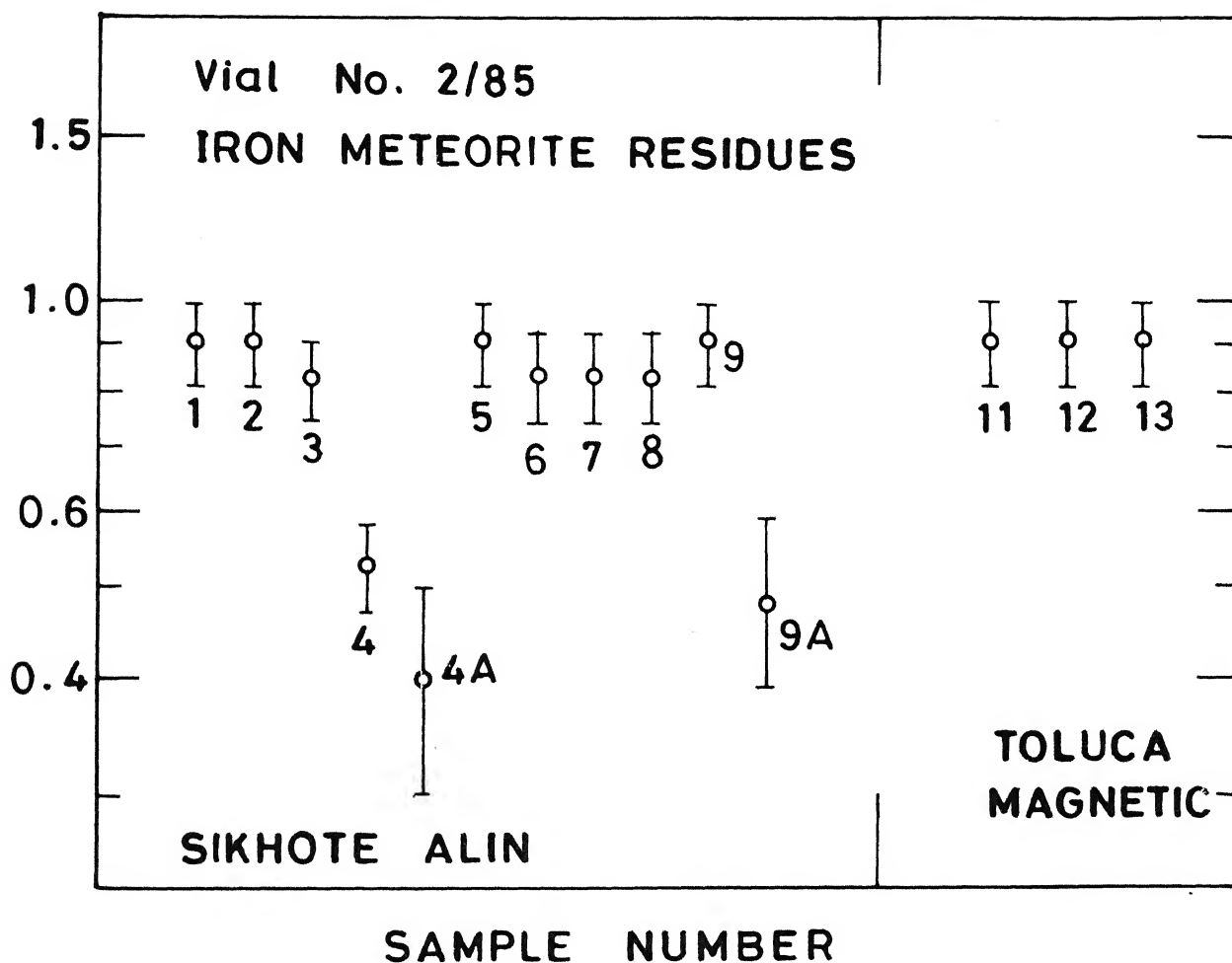


Fig. 3.2 The isotopic data from Vial No. 2/85

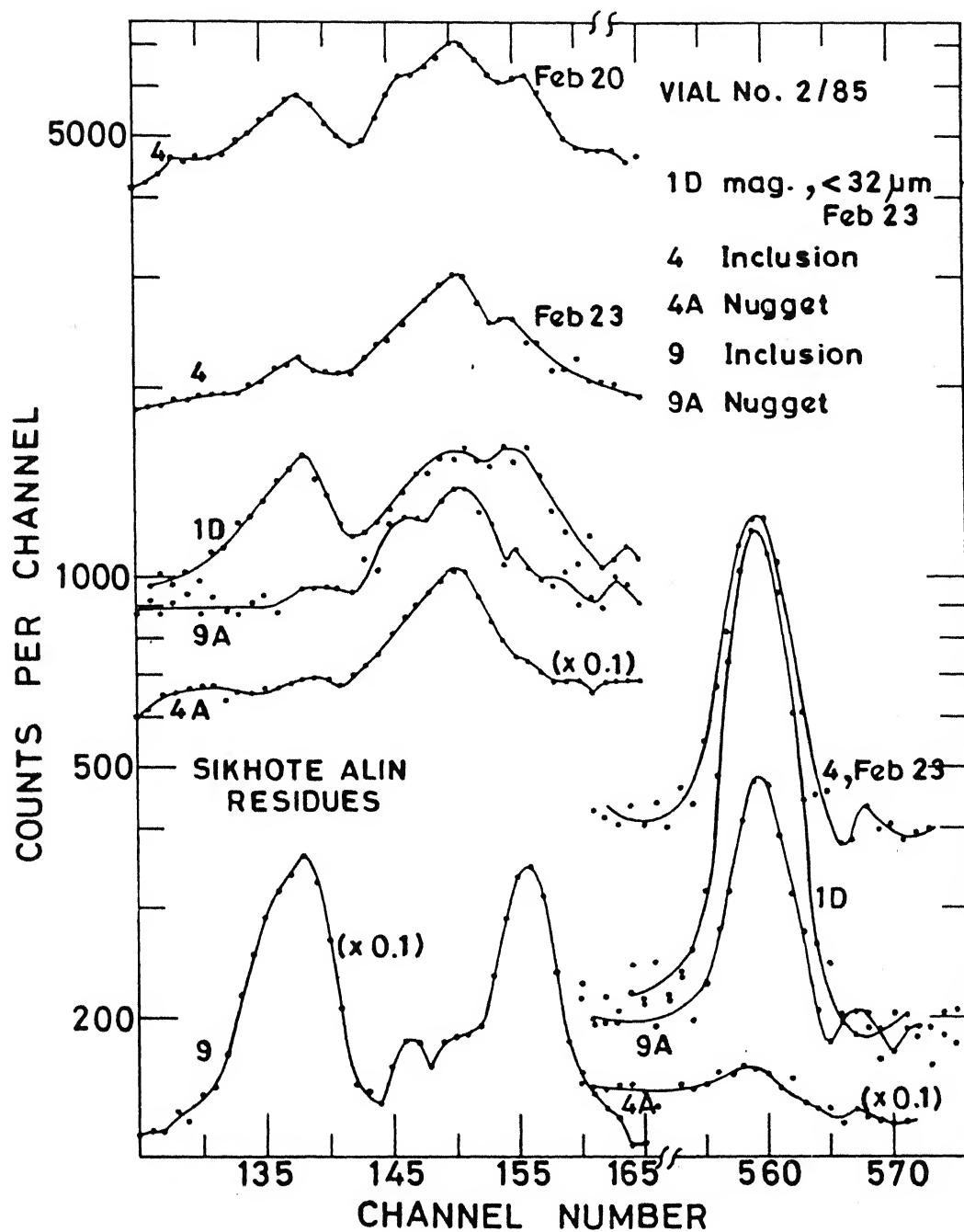


Fig. 3.3 Photon spectra of Sikhote Alin residue samples 4.4A and 9A are clearly anomalous

Table 3.3 Results from Vial No. 3/85

Sample	Mass (mg)	Code	Hg (ppm)	R/R <sup>+</sup>
<u>Residues from irons</u>				
Sikhote Alin Inclusion	105.5	1	1.03	0.93 (5)
Sikhote Alin Fragment	49.5	2	8.24	0.96 (6)
Sikhote Alin Inclusion	70.1	3	0.35	1.00 (10)
Sikhote Alin Inclusion	99.4	15	0.47	0.87 (9)
Campo del Cielo				
mag, >32 $\mu$ m	46.7	11	4.06	0.99 (5)
mag-H, < 32 $\mu$ m	51.2	4	67.56	1.03 (5)
Canyon Diablo				
75-105 $\mu$ m, mag	23.9	5	0.65	0.63 (8)
105-125 $\mu$ m, mag	28.4	6	2.47	0.98 (3)
Elga, mag	13.9	7	0.79	0.43 (8)
Elga, non-mag	24.1	8	4.18	0.90 (5)
<u>Chondrites</u>				
Dhajala				
olivines, 75-210 $\mu$ m	488.5	12	0.72	4.30 (87)
bulk, 75-210 $\mu$ m	513.2	13	3.15	1.00 (7)
Allende, 75-210 $\mu$ m	528.4	9	4.11	1.10 (6)
Ambapur Nagla, 75-210 $\mu$ m	515.7	10	5.84	1.07 (5)

All samples were distilled at 500°C. Numbers in parentheses indicate the errors.

$$R/R^+ = (^{197}\text{Hg}/^{203}\text{Hg})_{\text{sample}} \div (^{197}\text{Hg}/^{203}\text{Hg})_{\text{monitor.}}$$



large errors were associated with the ratio measurements, these have not been stressed. Some of the samples indicated an anomalous trend with respect to the isotopic ratio. On this basis repeat measurements on other aliquots of these samples were performed later.

### 3.4 Vial No. 4/85

Huge isotopic anomaly in Os in Ambapur Nagla from vial No. 3/85, prompted us to separate this meteorite into several fractions and irradiate a vial full of these samples alone. During opening of the irradiated can some of the sealed capsules kept inside were broken. As a result a mixture of powder was recovered from the bottom of the can. On the basis of weight calculation we ascertained this to be from sample Nos. 1, 3 and 4. It was given code No. 2 (Table 3.4). All samples were distilled at  $400^{\circ}\text{C}$  for a period of four hours each. 68 keV, 77 keV and 279 keV peak areas were calculated in 18, 10 and 10 channels, respectively with a gain of 0.25 keV per channel. There is a large variation in the Hg-abundance values. The ratio normalised to reference is drawn against sample numbers in Figure 3.4. Sample No. 2 is clearly anomalous. The photon spectrum of this sample was compared with standard and a decayed normal sample (No. 17). This is shown in Figure 3.5. The spectrum of anomalous sample No. 2 matches with the decayed sample, indicating that short lived  $^{197}\text{Hg}$  nuclide is depleted in the anomalous case. Samples Nos. 3 and 5 are also showing

Table 3.4 Mercury in Ambapur Nagla (Vial No. 4/85)

Sample	Code	Mass (mg)	c/s	Hg (ppm)	$\frac{^{197}\text{Hg}}{^{203}\text{Hg}}$	$\frac{^{203}\text{Hg}}{^{197}\text{Hg}}$	R/R <sup>+</sup>
Non-magnetic							
<38 $\mu\text{m}$	3	4	0.06	5.3	$2.5 \pm 0.2$	$0.40 \pm 0.03$	0.56 (5)
38-75 $\mu\text{m}$	5	34	2.85	1.7	$2.8 \pm 0.2$	$0.36 \pm 0.03$	0.62 (5)
75-106 $\mu\text{m}$	1	13	0.14	3.7	$4.0 \pm 0.4$	$0.25 \pm 0.03$	0.89 (7)
106-125 $\mu\text{m}$	16	50	0.36	2.3	$4.8 \pm 0.2$	$0.21 \pm 0.01$	1.07 (5)
125-150 $\mu\text{m}$	13	36	0.59	5.7	$4.4 \pm 0.2$	$0.23 \pm 0.01$	0.98 (5)
150-295 $\mu\text{m}$	9	54	0.27	1.7	$4.4 \pm 0.3$	$0.23 \pm 0.02$	0.98 (5)
Magnetic							
<38 $\mu\text{m}$	6	13	0.08	2.0	$3.5 \pm 0.3$	$0.29 \pm 0.02$	0.78 (7)
38-75 $\mu\text{m}$	4	36	9.35	86.3	$4.5 \pm 0.2$	$0.22 \pm 0.01$	1.00 (5)
75-106 $\mu\text{m}$	8	26	0.32	4.3	$3.7 \pm 0.3$	$0.27 \pm 0.02$	0.82 (7)
106-125 $\mu\text{m}$	15	49	34.1	234.3	$4.8 \pm 0.2$	$0.21 \pm 0.01$	1.07 (5)
125-150 $\mu\text{m}$	14	65	1.04	5.3	$4.7 \pm 0.2$	$0.21 \pm 0.01$	1.04 (5)
Weakly magnetic							
38-75 $\mu\text{m}$	10	46	0.10	0.7	$4.2 \pm 0.2$	$0.24 \pm 0.01$	0.93 (5)
75-106 $\mu\text{m}$	7	46	0.22	1.7	$4.4 \pm 0.2$	$0.23 \pm 0.01$	0.98 (5)
106-125 $\mu\text{m}$	12	51	2.86	19.0	$4.8 \pm 0.2$	$0.21 \pm 0.01$	1.07 (5)
125-150 $\mu\text{m}$	17	50	4.55	30.0	$4.7 \pm 0.2$	$0.21 \pm 0.01$	1.04 (5)
150-295 $\mu\text{m}$	11	33	0.87	8.7	$4.2 \pm 0.2$	$0.24 \pm 0.01$	0.93 (5)
Mix (1+3+4)	2	52	1.16	7.3	$1.4 \pm 0.1$	$0.71 \pm 0.05$	0.31 (3)
Monitor average					$4.5 \pm 0.2$	$0.22 \pm 0.01$	1.00 (5)

$$R/R^+ = (^{197}\text{Hg}/^{203}\text{Hg})_{\text{sample}} \div (^{197}\text{Hg}/^{203}\text{Hg})_{\text{reference}}$$

Numbers in the parentheses indicate the errors in R/R<sup>+</sup> values.

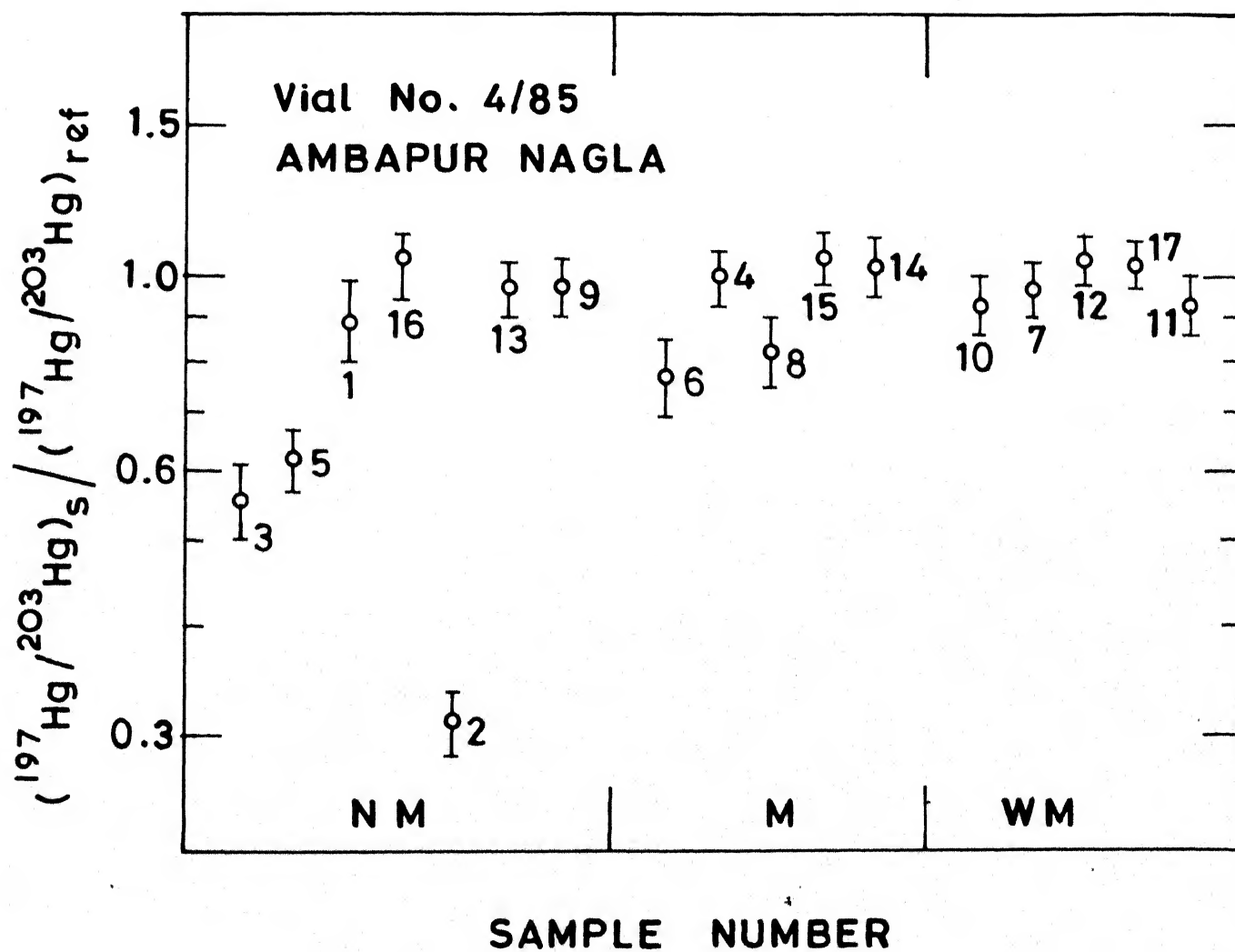


Fig. 3.4  $R/R^+$  values for Ambapur Nagla samples

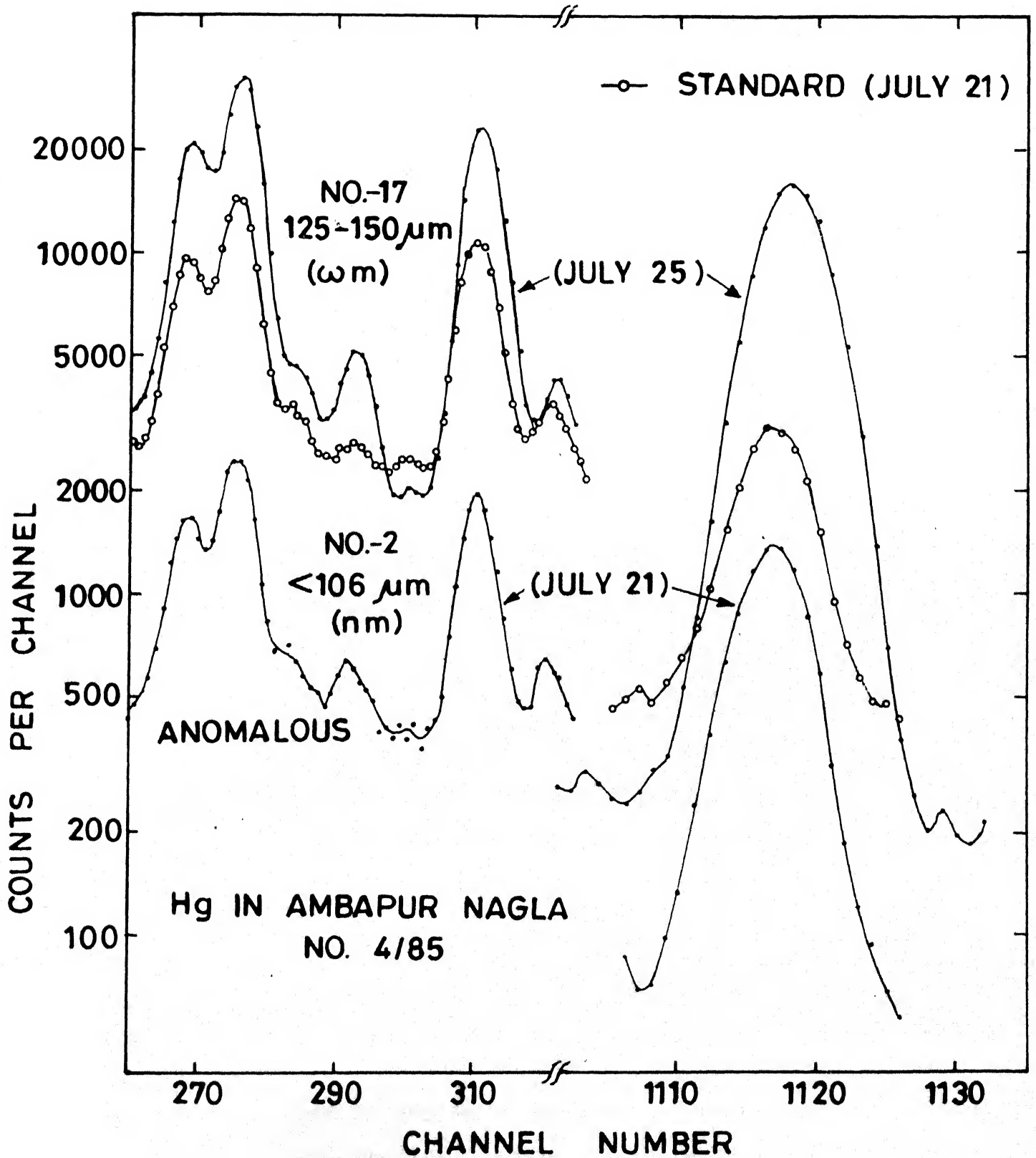


Fig. 3.5 Photon spectra of anomalous and normal Hg samples of Ambapur Nagla and the reagent mercury. Sample No.2 is clearly anomalous

negative anomaly of about 40%. The decay curves are found to be consistent with the half lives of  $^{197}\text{Hg}$  and  $^{203}\text{Hg}$ . Some of the decay curves for anomalous and normal samples are given in Figure 3.6.

### 3.5 Vial No. 5/85

A major change was made in sampling technique for this vial. Hg was distilled from stone meteorites and acid insoluble residues of iron meteorites, prior to activation, directly into quartz irradiation capsules which were heat sealed. Two monitors were packed to check the internal consistency. Since there were unwanted peaks from other volatile elements, samples were again distilled to purify Hg. Also carrier chemistry was performed to purify the two reagent standards. The results are presented in Table 3.5. The mercury content was found to be exceptionally low probably because of the loss during heat sealing. The ratios, however, showed a uniform value for all irons as well as stone meteorites. Since the sample size is large, we suspect that averaging effect might be responsible for uniformity of the values of isotopic ratios.

### 3.6 Vial No.6/85

Another major change was adopted in this vial in the sealing procedure of the irradiation capsules. Aluminium caps were used instead of heat sealing thereby minimising the loss of volatile mercury. After irradiating the distilled Hg and volatiles from

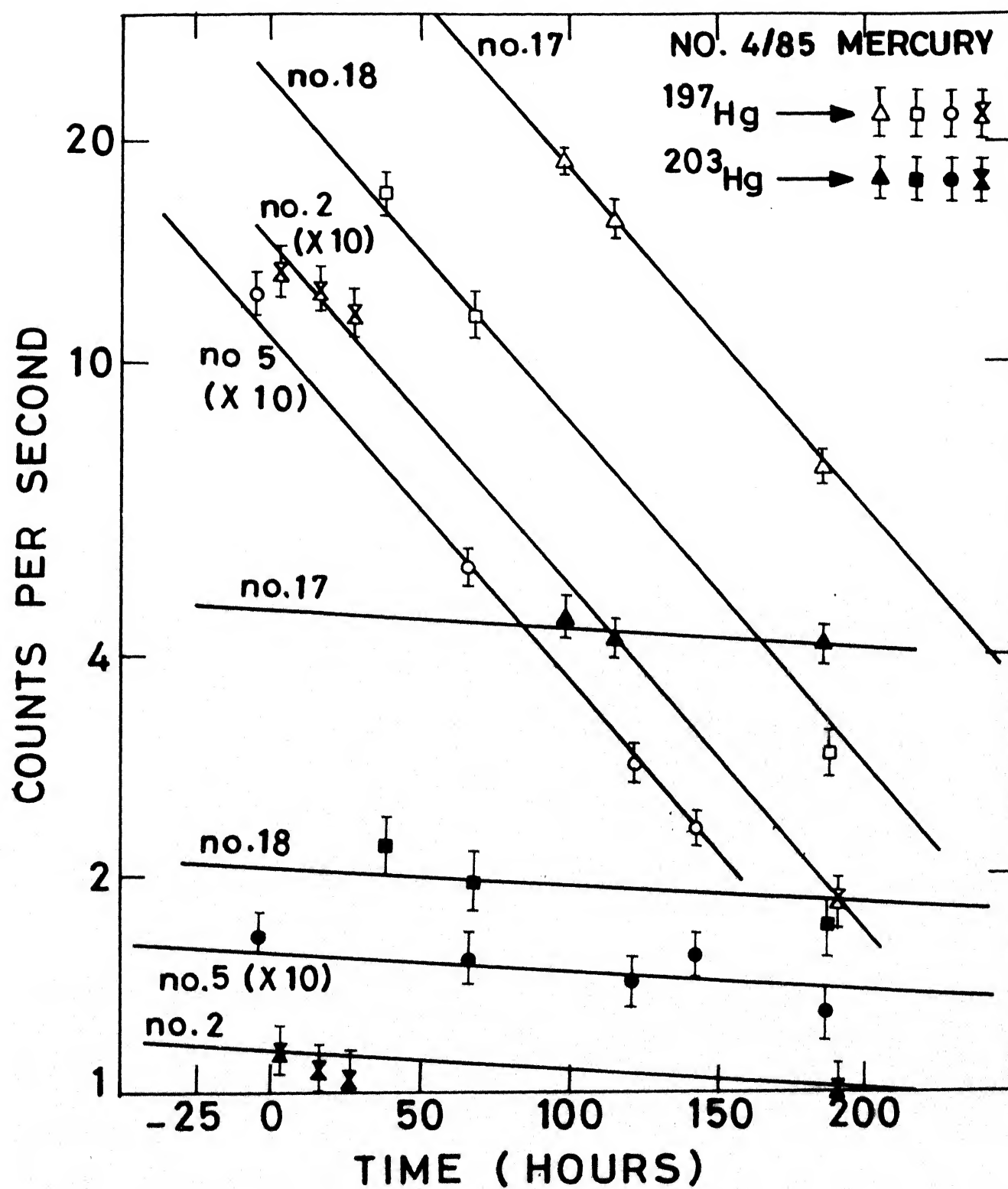


Fig. 3.6 Decay lines of  $^{197}\text{Hg}$  and  $^{203}\text{Hg}$  from samples of Ambapur Nagla

No.	Sample Description	Mass (mg)	cps/2.5	ppb (Hg)	197 Hg/ 203 Hg		R/R <sup>+</sup>
					Replicate	Average	
1	Forest Vale	245.3	2.54	129.1	12.05, 11.9	11.98	0.99
2	Allende (75-210 μm)	853.4	16.38	2313.0	12.16, 12.3	12.23	1.02
3	CdC nugget (insoluble fragment)	1700.8	8.89	65.0	12.49, 12.03	12.26	1.02
4	CdC surface coarse unattacked	406.1	12.8	391.2	12.06, 12.18	12.12	1.01
5	CdC surface very coarse unattacked	1478.7	0.35	2.9	11.56, 11.97, 11.36	11.63	0.97
6	CdC surface <0.2 mm	356.3	0.41	14.3	11.72, 12.03, 13.2	12.3	1.03
7	CdC, GM, MH <32 μm(H <sub>2</sub> SO <sub>4</sub> )	386.2	0.04	1.3	12.77	12.77	1.06
8	CD graphite crushed, nm	915.0	0.01	0.2	unmeasurable	-	-
9	Ambapur Nagla, 150-295 μm(nm)	1007.8	4.0	49.3	12.15, 12.02	12.14	1.01
10	Ambapur Nagla, 150-295 μm(m)	506.6	0.3	7.4	12.07, 12.45	12.26	1.02

Contd.....

No.	Sample Description	Mass (mg)	cps/2.5	ppb (Hg)	$^{197}\text{Hg}/^{203}\text{Hg}$		R/R <sup>+</sup>
					Replicate	Average	
11	Ambapur Nagla, 150-295 $\mu\text{m}$ (wm)	558.4	1.86	41.4	12.32, 11.85	12.09	1.01
12	CdC-J >180 $\mu\text{m}$ ( $\text{HNO}_3$ ), nm	1084.7	0.68	7.8	14.48, 15.15, 12.7	14.11 $\pm 1.5$	1.18
13	CdC-J ( $\text{H}_2\text{SO}_4$ ) oxidized crust, nm	2031.1	6.06	37.1	12.36, 12.23	12.3	1.03
14	CdC-J ( $\text{HNO}_3$ ) <180 $\mu\text{m}$ , nm	2209.3	0.3	1.7	unmeasurable	-	-
15	Hg Monitor	17.6 $\mu\text{g}$	1417	-	12.03, 11.63, 12.3	12.00	1.00
16	Hg Monitor	unknown	-	-	12.09, 11.98	12.04	1.00

\*Distillates were heat sealed in quartz tubes and irradiated.

cps/2.5 = c/sec/2.5 keV at 279 keV;  $\text{R/R}^+ = \text{Ratio}_{\text{sample}}/\text{Ratio}_{\text{monitor}}$



Ambapur Nagla and Campo del Cielo, radiochemical separation was done to purify them using carrier mercury. The results (Table 3.6) again showed a normal value for all the samples indistinguishable from terrestrial ratio.

### 3.7 Vial No. 7/85

Sample size was kept small in this vial. There were two types of packing: (i) Distilled mercury from Ambapur Nagla, Forest Vale and Menow meteorites were aluminium capped in quartz irradiation tubes. After irradiation radiochemical purification was required. (ii) Another set of samples consisting of distilled Hg from Ambapur Nagla and acid insoluble residues from Carbo were heat sealed. The distillation for this set was performed in two temperature steps of 200°C and 500°C of two hours each. These samples after irradiation had to be distilled again to remove contaminating peaks. The results are presented in Tables 3.7 and 3.8. The mercury content was very low from the heat sealed samples compared to the aluminium capped ones. In spite of high counting errors, the high temperature fraction of Ambapur Nagla and Carbo showed a trend of lower value of  $^{197}\text{Hg}/^{203}\text{Hg}$  ratio. One sample of Carbo (38-75  $\mu\text{m}$ ) gave a lower value of isotopic ratio for both higher as well as lower temperature fractions. Results from the other set (aluminium capped) may not have any significance since the blank level itself is very high, nearly 50% of the sample values.

(Distilled mercury, Al-capped in quartz tubes, irradiated)

Code	Sample Description	Mass (mg)	c/sec	ppb (Hg)	$^{197}\text{Hg}/^{203}\text{Hg}$ Ratio Replicate	Average	R/R*
1	Amb. Nagla <38 $\mu\text{m}$ , nm	89.5	0.77	90.4	1.86, 2.07, 2.08	2.00	0.98
2	Amb. Nagla 38-75 $\mu\text{m}$ , nm	113.3	0.50	45.2	2.06, 2.15	2.11	1.03
3	CdC-J (HNO <sub>3</sub> ) >180 $\mu\text{m}$ mag	85.4	0.42	51.5	2.15, 1.90, 2.19	2.08	1.01
4	CdC-J (HNO <sub>3</sub> ) >180 $\mu\text{m}$ , nm	84.2	1.08	134.5	1.96, 2.26, 2.04	2.09	1.02
5	CdC-J <180 $\mu\text{m}$ mag	65.5	2.41	386.8	2.11, 2.03, 2.13	2.10	1.02
6	CdC-J >180 $\mu\text{m}$ mag	94.4	0.23	25.2	1.85, 1.76, 1.92	1.84	0.90
Monitor 1		2.8 $\mu\text{g}$	325.69	-			
Monitor 2		5.9 $\mu\text{g}$	758.72	-			
Monitor 1D (diluted)		-	1.23	-	2.09, 2.08, 2.13	2.10	1.02
Monitor 2D (diluted)		-	3.76	-	2.05, 2.04, 2.06	2.05	1.00

\*Errors are less than  $\pm 10\%$ . c/sec = c/sec/3 keV at 279 keV.

Table 3.7 Vial No. 7/85 : Mercury from Ambapur Nagla and Carbo Meteorites  
(Heat sealed in quartz tubes, irradiated)

Sample			Temp (°C)	cps/2.5	Hg (ppb)	<sup>197</sup> Hg/ <sup>203</sup> Hg	R/R <sup>+</sup>
Description	Mass (mg)	Code					
Magnetic							
Ambapur Nagla, 150-295 μ m	55.5	10	200	31	6571	4.2±0.1	0.83
		11	500	0.04	9	2.34±0.4	0.46
Carbo, <38 μ m	38.2	12	200	5.04	1552	5.2±0.1	1.03
		13	500	0.12	38	2.7±0.3	0.54
Carbo, 38-75 μ m	37.2	14	200	0.05	17	1.8±0.3	0.36
		15	500	0.06	19	2.46±0.4	0.49
Carbo, 75-125 μ m	25.2	16	200	0.006	3	3.88±1.9	*
		17	500	0.063	29	-	*
Monitor	2.0 (μ m)	-	-	170	-	5.04±0.1	1.00

\* Large errors due to delay in counting.

Table 3.8 Results from Vial No. 7/85 (Distillates irradiated in aluminium capped quartz tubes)

Sample		Code	Temp (°C)	cps/2.5	Hg (ng)	$^{197}\text{Hg}/^{203}\text{Hg}$	R/R <sup>+</sup>
Description	Mass (mg)						
Blank	-	1	600	0.58	6.8	6.7±0.6	0.83
Blank	-	2	600	0.56	6.5	7.2±0.5	0.89
Ambapur Nagla 75-210 $\mu\text{m}$	71.9	3	550	1.26	14.7	7.7±0.5	0.96
Ambapur Nagla 75-210 $\mu\text{m}$	56.3	5	500	1.26	14.7	7.2±0.2	0.89
Forest Vale 50-100 mesh	102.5	7	500	1.10	12.9	8.8±0.5	1.09
Menow 75-210 $\mu\text{m}$	150.8	9	500	2.15	25.1	7.72±0.5	0.96
Monitor	2.0 ( $\mu\text{g}$ )	-	-	171.0	-	8.06±0.2	1.00

### 3.8 Vial No. 8/85

About 2 g crushed Ambapur Nagla was irradiated in a sealed quartz ampule. This, after irradiation, was separated into chondrules, sieve sizes and magnetic fractions. Stepwise heating technique was used as given in Table 3.9. First few samples (Code Nos. 1, 2, 3, 4, 6 and 7), heated in two temperature steps for two hours each, showed a decreasing trend in the isotopic ratios. Since the sample size of No. 5 was very small, only one heating step at 500°C was performed. Next sample when heated for two additional hours at 500 °C temperature, showed similar mercury content. It was not possible to measure the isotopic ratio of sample No. 9 because of lower Hg-abundance. Two subsequent samples were heated in larger number of heating steps and decreasing the distillation time to one hour. For last sample only two temperature heating could be performed. The overall Hg content varied between 0.1 to 2.5 ppm (Table 3.10). One fine fraction (<32  $\mu$ m, nm) showed abnormally high Hg-abundance. The most anomalous sample found (No. 10) showed a  $^{197}\text{Hg}/^{203}\text{Hg}$  isotopic ratio of only 40% of the reagent standard with some uncertainty in the measurement.

### 3.9 Vial No. 9/85

To minimise the handling of meteorite before neutron activation, few fragments of stone meteorites (Ambapur Nagla and Rangala) were wrapped in aluminium foil and packed for irradiation. Sample preparation was done as follows. Three

Table 3.9 Vial No. 8/85 Mercury from Ambapur Nagla (Powder irradiated)

Sample	Mass (mg)	Code	T (°C)	cps/2.5	$^{197}\text{Hg}/^{203}\text{Hg}$ Ratio*		R/R <sup>+</sup>
					Replicate	Best	
Chondrules	226.9	1	200	2.84	4.87, 5.09, 5.1	5.0	0.96
		2	500	0.05	2.55, 2.90, 1.22±0.4	2.5	0.48
>38 µm, nm	89.2	3	200	0.34	4.48, 4.62	4.6	0.88
		4	500	0.69	2.91, 2.99	2.9	0.55
<38 µm, m	8.2	5	500	0.05	2.52, 3.9±0.8	2.5	0.48
<38 µm, nm	55.5	6	200	1.95	5.29, 5.47	5.3	1.01
		7	500	5.56	5.28, 5.37	5.3	1.01
>38 µm, m	62.9	8	200	2.49	5.51, 5.2	5.5	1.05
		9	500	0.03	-	-	-
		10	500	0.04	1.5±0.3, 2.92	2.0	0.38
>38 µm, nm	243.2	11	150	4.81	5.04, 5.36	5.2	1.00
		12	300	0.63	4.54, 4.2	4.4	0.84
		13	450	1.06	4.26, 7.2	5.0	0.96
		14	600	0.33	3.26, 3.44	3.3	0.63
<38 µm, nm	227.9	15	100	2.19	5.16	5.2	0.99
		16	200	0.02	-	-	-
		17	300	15.79	5.52	5.5	1.06
		18	400	12.38	5.54	5.5	1.06
		19	500	1.12	4.40	4.4	0.84
>38 µm, m	89.5	20	200	0.007	-	-	-
		21	500	2.00	5.6	5.6	1.07
Monitor-Hg	0.06 µg	-	-	3.27	4.98, 5.25, 5.24	5.2	1.00

\*Errors are less than ±10% unless otherwise stated.

Table 3.10 Vial No. 8/85 Total Mercury Concentrations in Ambapur Nagla samples

Sample	Mass (mg)	c/sec/2.5 keV (279 keV)			Mercury (ppm)
		L.T.	H.T.	Total	
Chondrules	227	2.84	0.05	2.89	0.23
<38 $\mu\text{m}$ , m	8.2	-	0.05	0.05	0.11
<38 $\mu\text{m}$ , nm	55.5	1.95	5.56	7.51	2.48
>38 $\mu\text{m}$ , m	62.9	2.49	0.07	2.56	0.75
>38 $\mu\text{m}$ , nm	89.2	0.34	0.69	1.03	0.21
Monitor	-	-	-	3.27	0.06 $\mu\text{g}$

pieces of Ambapur Nagla were ground separately (bulk samples, I, [I and III]). Rest were powdered, mixed and then separated into chondrules, non-magnetic and magnetic parts. Two pieces of Rangala were crushed separately for the bulk samples (I and II) only. Stepwise heating for Hg-extraction was exercised in more details, upto six temperature steps.

The concentrations of Hg and the isotopic ratios are given in Table 3.11. There are variations in the abundances as well as ratios with temperature. The Ambapur Nagla bulk I registered a low concentration of Hg at all temperatures. The isotopic ratios were lower than the monitor values and tended to increase with temperature. The magnetic sample showed a ratio almost indistinguishable from the monitor except the 300°C fraction that was below normal (the terrestrial values). Because of very low counting rate, ratio of the 200°C fraction could not be measured. All other samples of Ambapur Nagla showed somewhat similar profiles with temperature (Figures 3.7 and 3.8 ). The ratios are below normal in the 100°C fraction. As the temperature increases, the ratio increases and nearly equals (or even exceeds) the terrestrial value. It again comes down gradually. Sometimes (as in case of bulk II) the first lower value is probably masked from the Hg of the second fraction having normal isotopic ratio. The two bulk samples of Rangala showed a consistently decreasing isotopic ratio as well as the abundance with temperature (Figure 3.9 ). The lowest value observed was only 37% of the monitor. Photon spectra were recorded in



Table 3.11 Results from

Sample	Mass (mg)	Code	T(°C)	cps/2.5	ppb (Hg)	$^{197}\text{Hg}/^{203}\text{Hg}$ Ratio	R/R <sup>+</sup>
Amb. Nagla Bulk I	201.5	1-1	100	0.13	25	1.4±0.1	0.25±0.02
		1-2	200	0.05	10	2.2±0.3	0.39±0.05
		1-3	300	0.05	10	2.3±0.8	0.41±0.14
		1-4	400	0.13	26	3.7±0.4	0.66±0.07
		1-5	500	0.02	3	-	-
Amb. Nagla (Magnetic)	183.3	2-1	100	0.05	10	5.5±0.3	0.98±0.05
		2-2	200	0.02	5	-	-
		2-3	300	0.05	10	3.0±0.4	0.54±0.07
		2-4	400	2.55	512	5.1±0.2	0.91±0.04
Amb. Nagla Chondrules	217.7	3-1	100	1.70	300	4.4±0.2	0.79±0.04
		3-2	200	4.69	830	5.0±0.1	0.89±0.02
		3-3	300	1.34	236	4.4±0.1	0.78±0.02
		3-4	400	0.27	47	3.9±0.1	0.69±0.02
		3-5	500	1.11	196	2.7±0.03	0.48±0.01
Amb. Nagla (Non-mag) Fine	340.5	4-1	100	7.14	807	5.4±0.1	0.97±0.02
		4-2	200	13.82	1562	5.5±0.1	0.97±0.02
		4-3	300	18.41	2080	5.5±0.2	0.99±0.04
		4-4	400	1.01	115	4.9±0.2	0.88±0.04
		4-5	500	1.16	131	3.7±0.2	0.66±0.04
		4-6	600	0.53	60	3.5±0.3	0.63±0.05
Amb. Nagla Bulk II	145.0	5-1	100	1.96	523	5.8±0.2	1.04±0.04
		5-2	200	5.12	1370	5.4±0.2	0.96±0.04
		5-3	300	3.66	978	5.3±0.1	0.94±0.02
		5-4	400	0.35	95	4.3±0.3	0.77±0.05
		5-5	500	0.22	60	3.1±0.2	0.55±0.04
		5-6	600	0.43	115	3.0±0.2	0.54±0.04

Contd.....

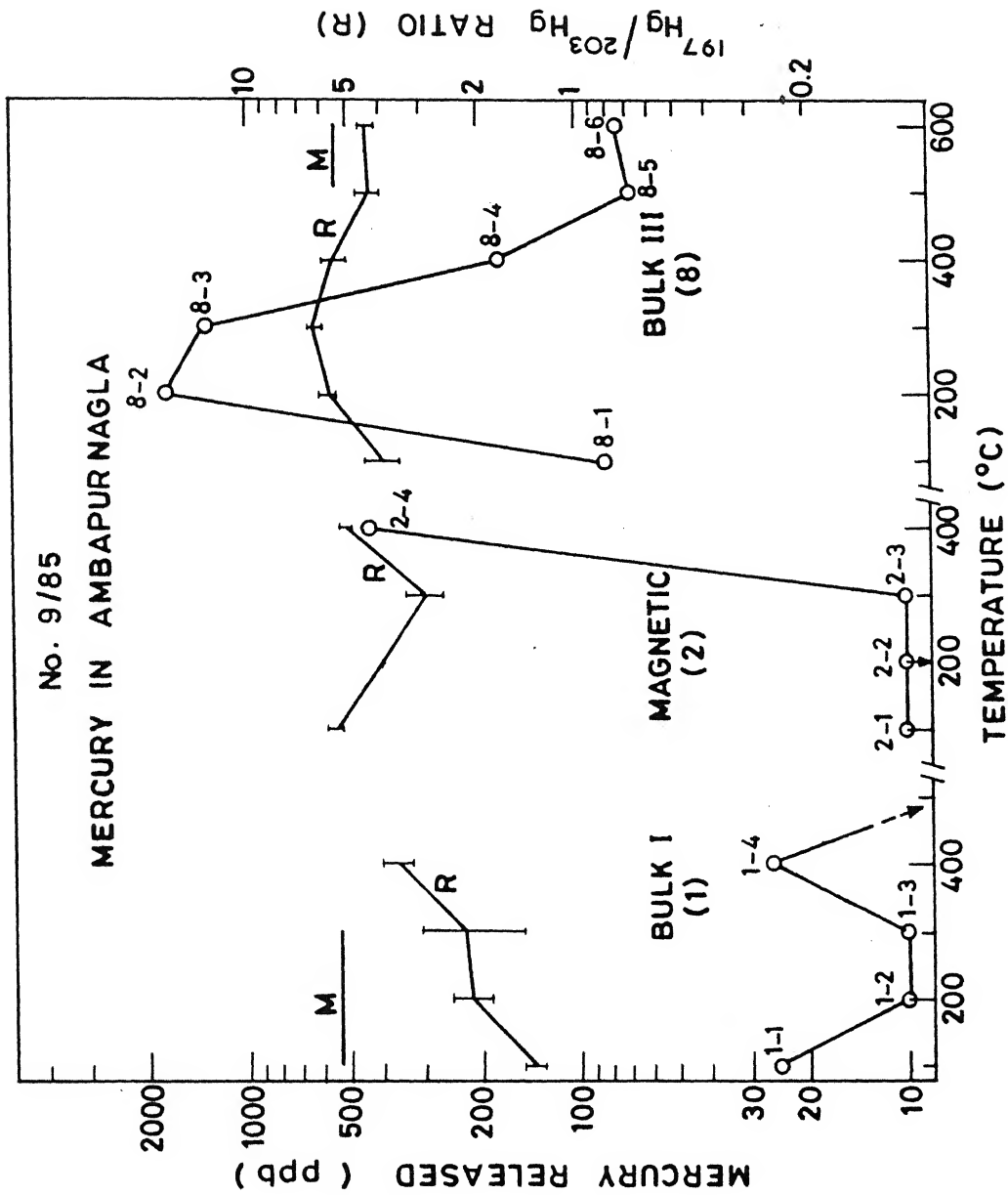


Fig. 3.7 Mercury concentration (left scale) and its isotopic ratios (right scale) measured at different temperatures in samples of Ambapur Nagla

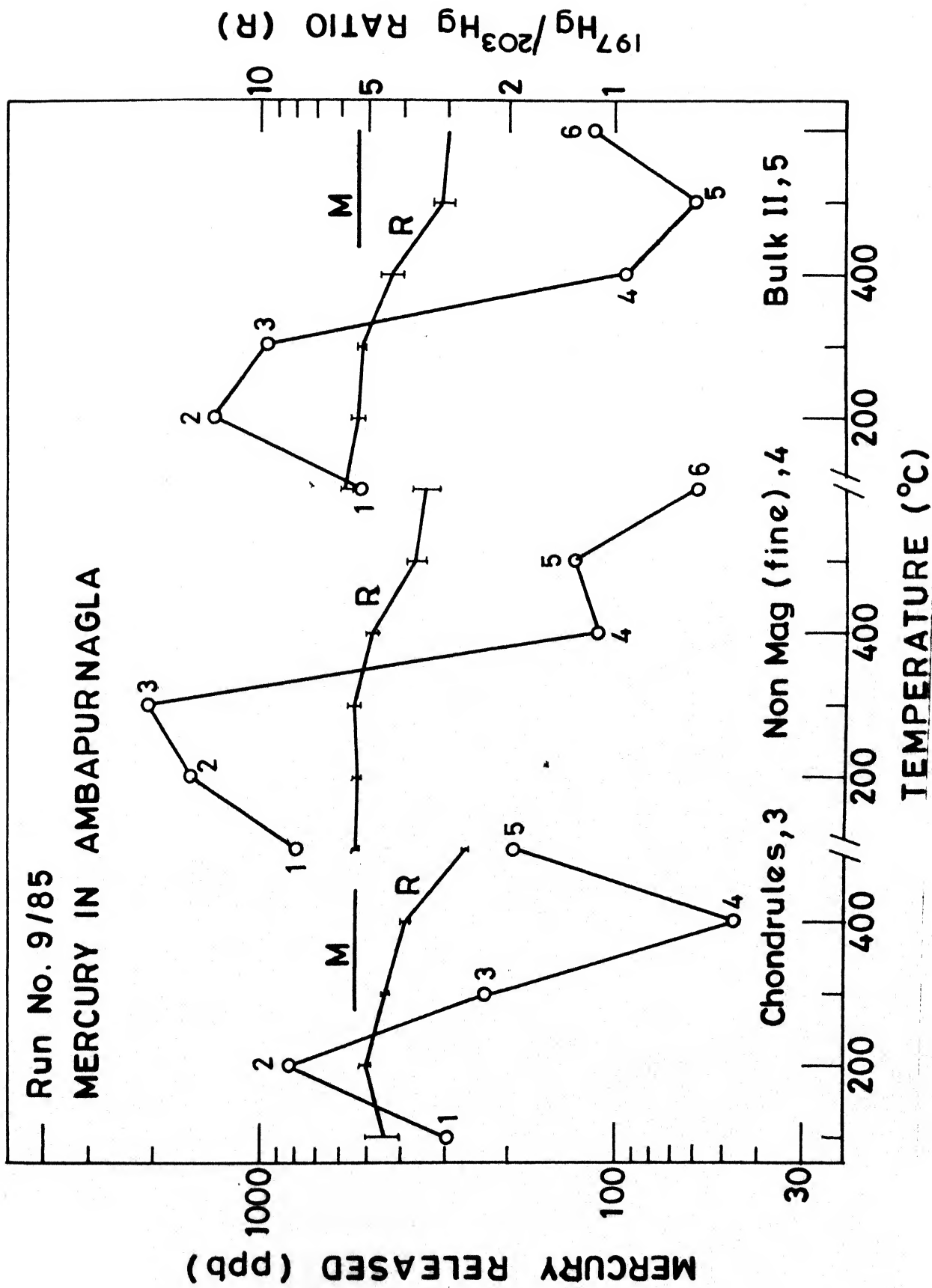


Fig. 3.8 Mercury concentration (left scale) and its isotopic ratios (right scale) measured at different temperatures in samples of Ambapur Nagla

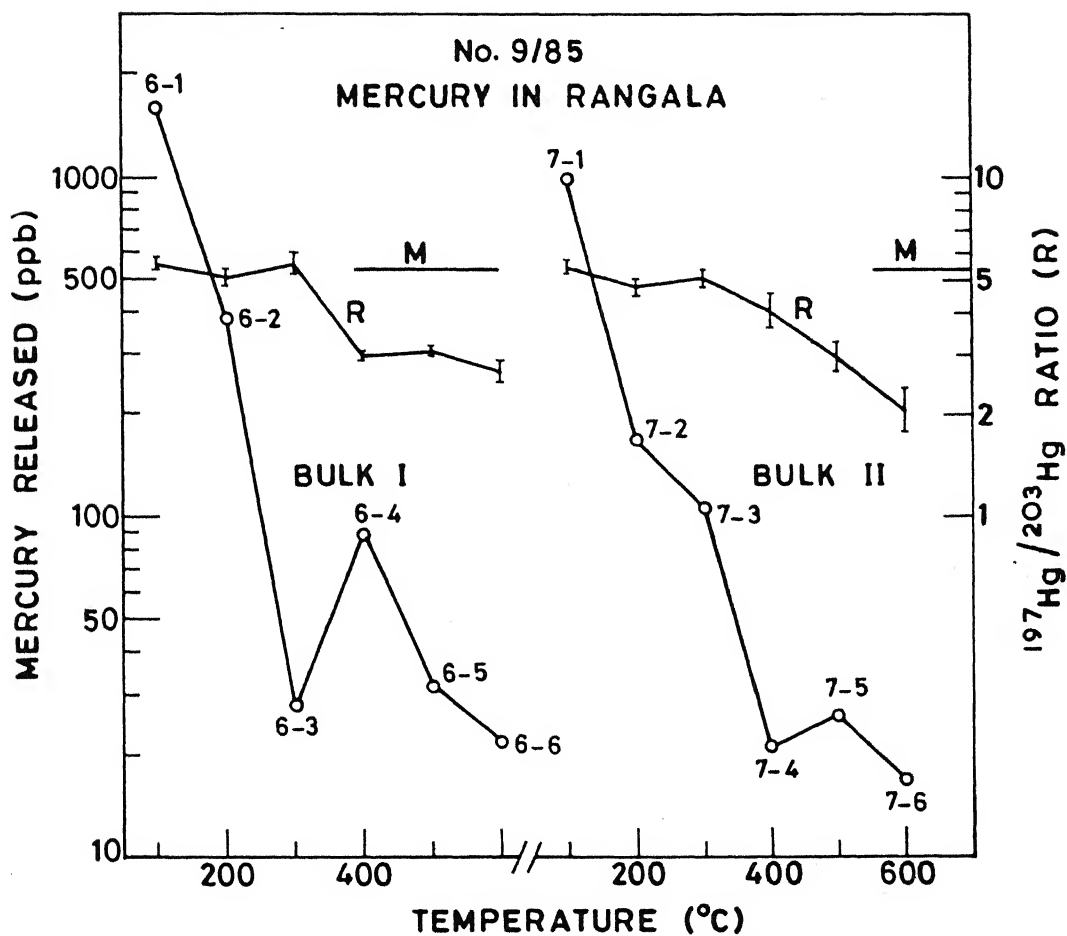


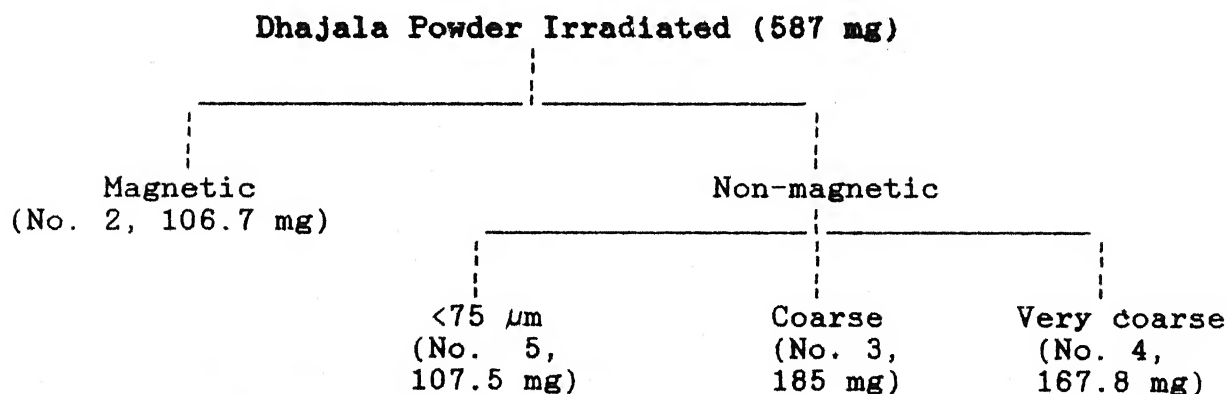
Fig. 3.9 Mercury concentration (left scale) and its isotopic ratios (right scale) measured at different temperatures in samples of Rangala

all cases. In Figure 3.10 the spectrum of sample No. 3-5 (anomalous) is compared with that of near normal sample 3-2. There is an obvious depletion in the  $^{197}\text{Hg}$  isotope at channel Nos. ~275 and ~310 whereas  $^{203}\text{Hg}$  is having similar counts at ~1115 channel number. This observation is further supported by the following of decay line of the ratio of these two samples, shown in Figure 3.11. The weighted average of isotopic ratios are calculated and given in Table 3.12. It is observed that if these samples were heated at one temperature only, to extract all Hg then all samples would have given uniformly normal value except the first one.

The activation energies calculated on the basis of Arrhenius plot (Figures 3.12, 3.13 and 3.14) are given in Table 3.13. The values match with those reported by Jovanovic and Reed, 1980; 1985 (6 to ~14 kcal per mole for ordinary chondrites).

### 3.10 Vial No. 1/86

In this vial we have analysed Dhajala stone meteorite:



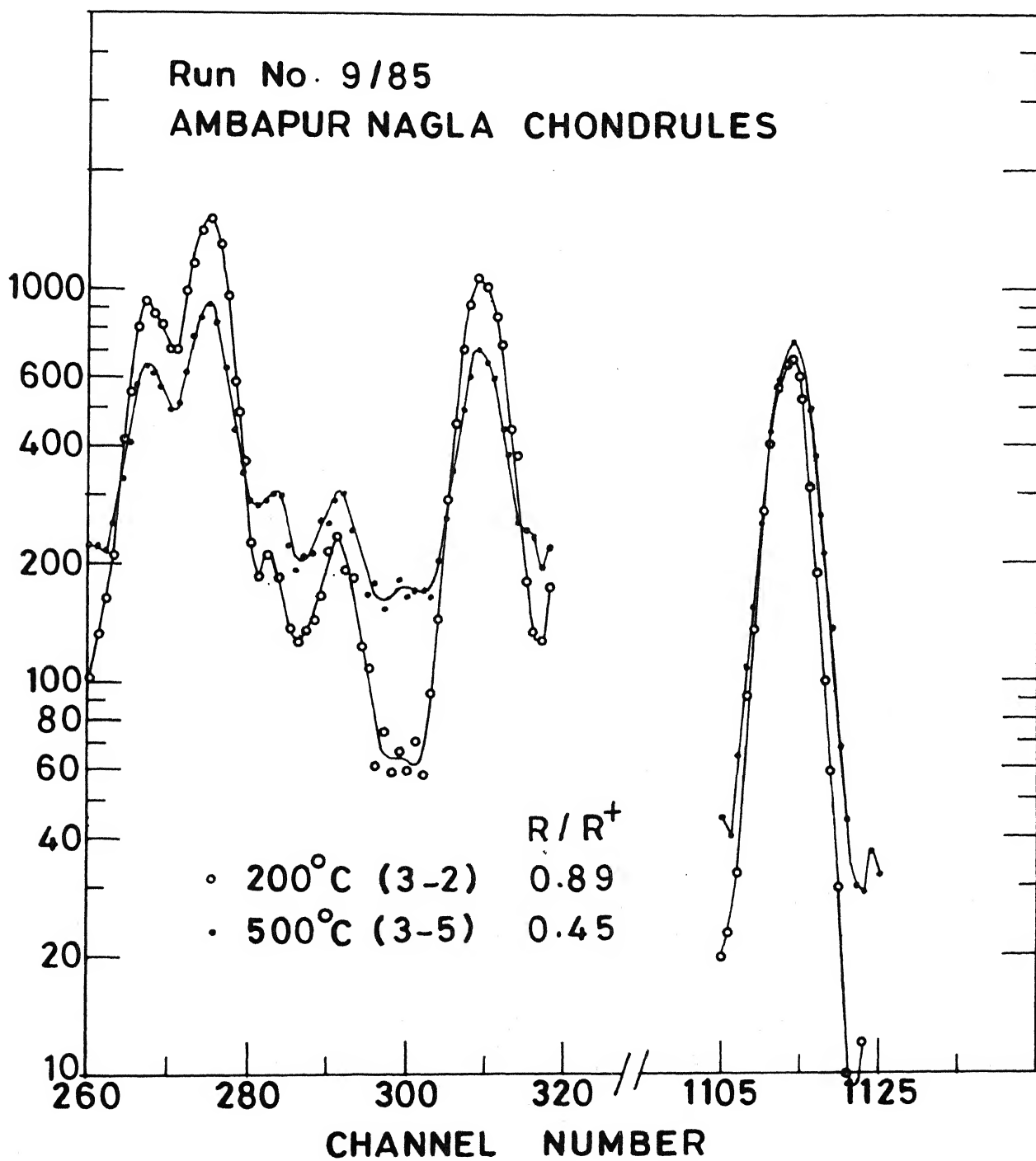


Fig. 3.10 Photon spectra of Hg distilled from Ambapur Nagla Chondrules

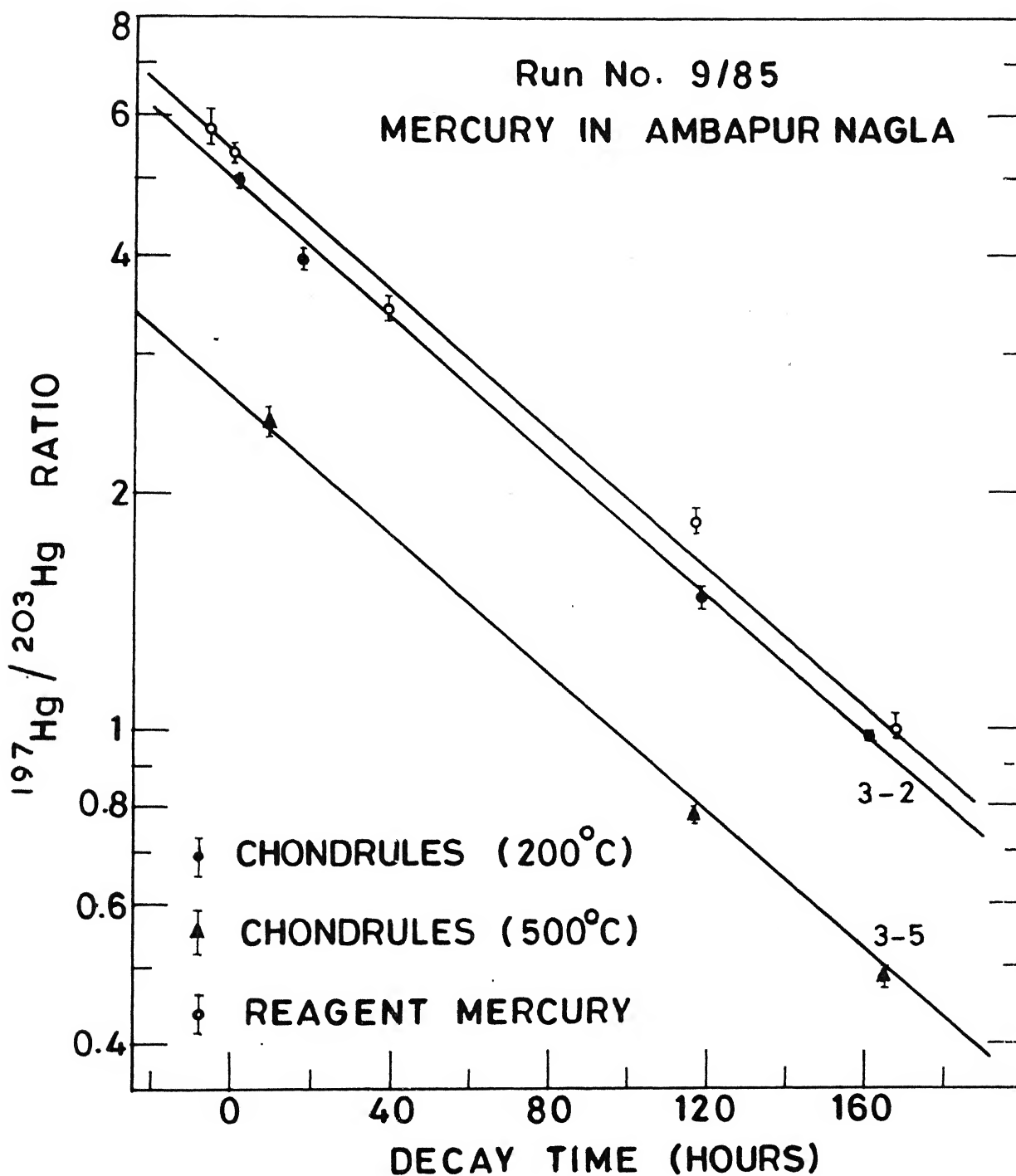


Fig. 3.11 Decay measurements on  $^{197}\text{Hg}/^{203}\text{Hg}$  ratio from some Ambapur Nagla samples

Table 3.12 Calculated gross ratios (Vial No. 9/85)

Sample	Total Hg (ppb)	R/R <sup>+</sup>	
		Ranges	Gross
A.N. Bulk I	74	0.25-0.70	0.44
A.N. Bulk II	3141	0.53-1.09	0.94
A.N. Bulk III	3445	0.71-1.13	1.04
A.N. Magnetic	537	0.54-0.98	0.91
A.N. Chondrules	1609	0.48-0.89	0.80
A.N. Non-Mag.	4755	0.62-0.99	0.96
Rangala Bulk I	2168	0.48-1.00	0.95
Rangala Bulk II	1342	0.38-1.09	1.04



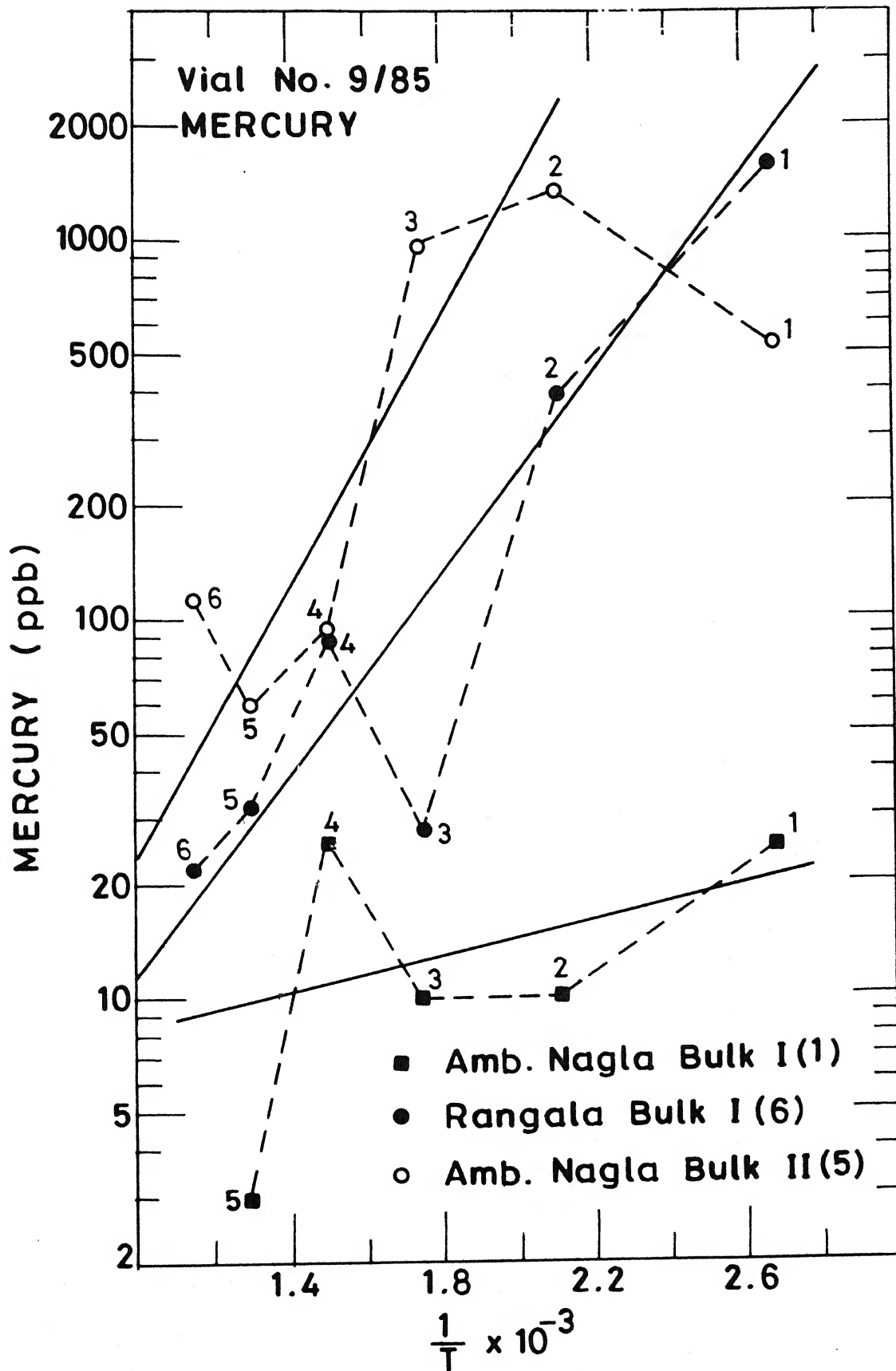


Fig. 3.12 Arrhenius plot for mercury released

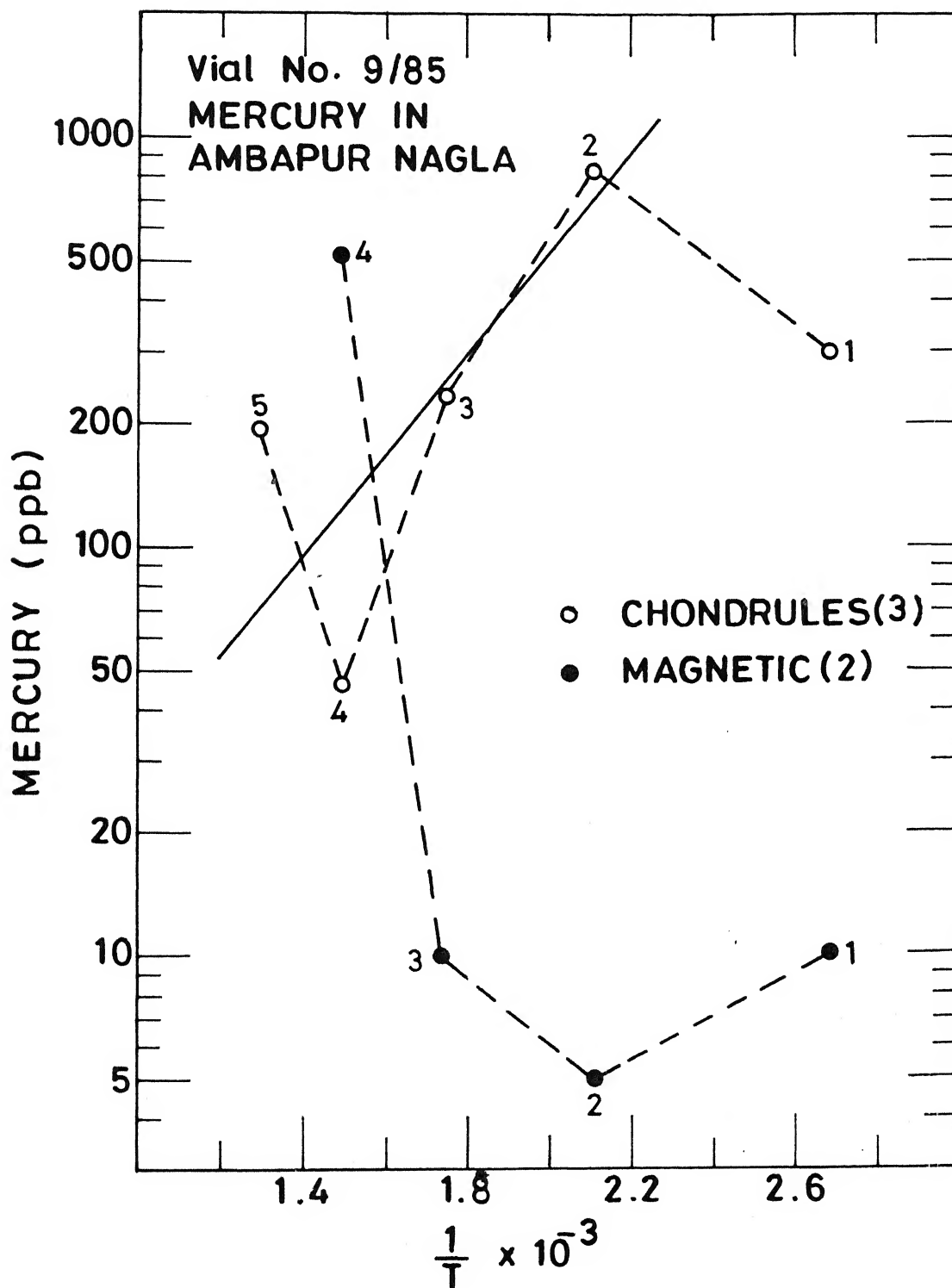


Fig. 3.13 Arrhenius plot for mercury released

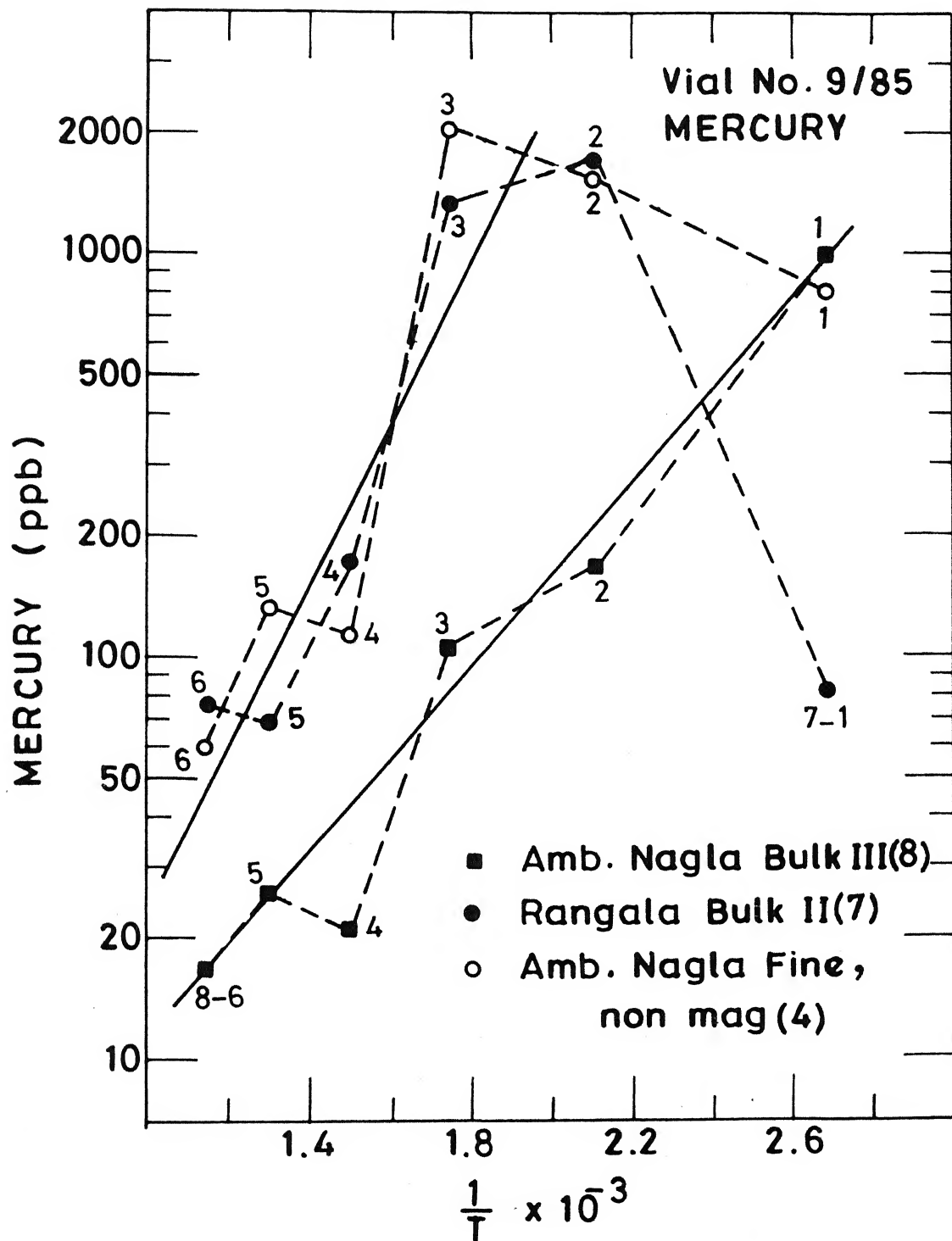
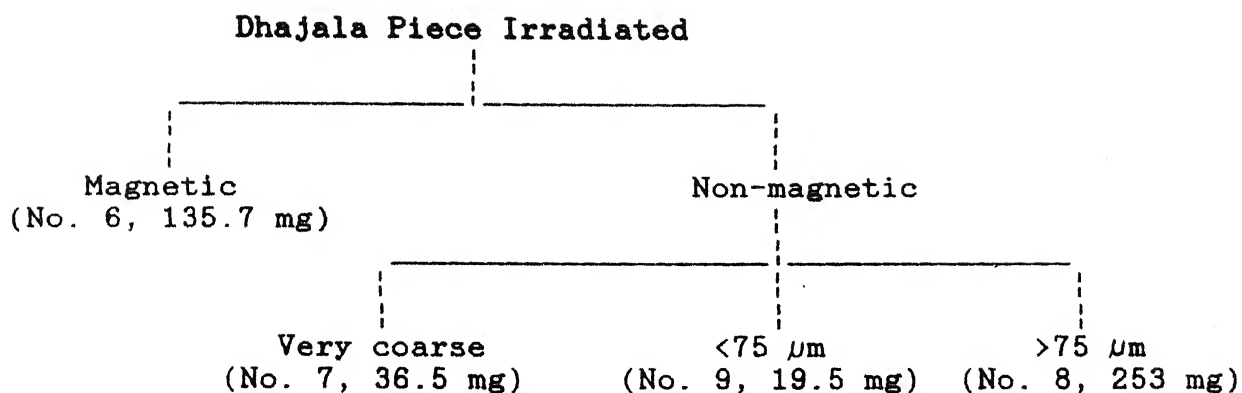


Fig. 3.14 Arrhenius plot for mercury released

Table 3.13 Activation energy of mercury released from Ambapur Nagla and Rangala (Vial No. 9/85)

Sample		$-\Delta H$ (k cal mole <sup>-1</sup> )	Quality
Code	Description		
1	Amb. Nagla Bulk I	1.1	Scatter
2	Amb. Nagla (Mag.)	-	Large Scatter
3	Amb. Nagla Chondrules	5.6	C
4	Amb. Nagla (Non-mag.) Fine	9.2	A
5	Amb. Nagla Bulk II	8.2	B
6	Rangala Bulk I	6.1	B
7	Rangala Bulk II	5.3	A
8	Amb. Nagla Bulk III	9.2	A



The meteorite, after irradiation, was separated according to the above Schemes. Some fine quartz pieces got mixed with the sample and could not be separated. The results are shown in Table 3.14. The accuracy in most cases is very poor. In some cases the ratio is not measurable due to low counting rates. It is not possible to draw any conclusion regarding anomalous isotopic mercury from this vial.

### 3.11 Vial No. 2/86

Samples of acid insoluble residues of iron meteorites, Carbo, Sikhote Alin and Canyon Diablo, packed in aluminium capped quartz tubes and pieces of Elenovka and Cold Bokeveld stone meteorite wrapped in aluminium foils, were bombarded for this vial. After irradiation, both stones were crushed and separated into bulk, coarse, and fine fractions.

The results obtained are shown in Table 3.15. Since there were a large number of samples, only two to three temperature

Sample	Mass (mg)	Temp (°C)	Code	cps/2.5	ppm (Hg)	$^{197}\text{Hg}/^{203}\text{Hg}$ Replicate	Hg Ratio Best**	R/R <sup>+</sup> Reliability
Blank (Heated A.N.)	34.5	400	1	<0.007	-	-	-	-
<u>Dhajala powder</u>								
Magnetic	106.7	200	2-1	0.23	2.85	0.96 ± 0.3, 0.86 ± 0.2	0.9 ± 0.3	1.58(40) B
		400	2-2	-	-	-	-	-
Non-mag. coarse ( >75 μm)	185*	300 600	3-1 3-2	0.17	1.23	1.32 ± 0.4	1.3 ± 0.4	2.31 (81) C
Non-mag. very coarse	167.8	300 600	4-1 4-2	0.05	0.43	<0.037	<0.037	< 0.06 U
Non-mag. fine ( <75 μm)	107.5	300 600	5-1 5-2	0.27	3.27	0.67 ± 0.1, 0.51 ± 0.2	0.7 ± 0.1	1.18 (27) A
				0.06	0.72	0.25 ± 0.3	0.2 ± 0.3	0.35 (52) U

Contd.....

Sample	Mass (mg)	Temp (°C)	Code	cps/2.5 (Hg)	ppm (Hg)	$^{197}\text{Hg}/^{203}\text{Hg}$ Ratio		R/R <sup>+</sup>	Reliability
						Replicate	Best		
<u>Dhajala piece</u>									
Magnetic	135.7	300	6-1	0.11	1.06	0.59 ± 0.2, 0.31 ± 0.1	0.5 ± 0.2	0.88(38)	B
		600	6-2	0.15	1.5	0.69 ± 0.2, 0.66 ± 0.1, 0.62 ± 0.2	0.7 ± 0.1	1.18 (27)	A
Non-mag. very coarse	96.5	300	7-1	0.06	0.77	1.29 ± 0.5	1.3 ± 0.5	2.26 (96)	U
		600	7-2	-	-	-	-	-	-
Non-mag. coarse ( > 75 μm)	253	300	8-1	0.15	0.80	1.17 ± 0.3	1.2 ± 0.3	2.05 (63)	C
		600	8-2	0.24	1.25	0.84 ± 0.1	0.8 ± 0.1	1.47 (31)	C
Non-mag. fine ( < 75 μm)	159.5	300	9-1	0.10	0.83	0.53 ± 0.10, 0.21 ± 0.38	0.5 ± 0.1	0.89 (24)	A
		600	9-2	0.18	1.46	0.04 ± 0.02	0.04±0.02	0.08 (4)	C
Heated Menow + 0.84 μg Hg		400	M-1	0.64	-	0.56 ± 0.1, 0.81 ± 0.2	0.57±0.07	1.00 (13)	A

Samples marked heated were subjected to 1000°C for Hg extraction in a previous experiment; U = Unreliable;  
 \*Corrected mass for quartz pieces that were mixed with sample during grinding; \*\*Values for sample 6-1  
 and 9-1 were taken from graph.

Sample	Mass (mg)	Code	T (°C)	cps/5	ppm (Hg)	$^{197}\text{Hg}/^{203}\text{Hg}$ Ratio		R/R <sup>+</sup>	Reliability
						Replicate	Best		
Carbo, <38 $\mu\text{m}$ , mag.	104	1-1	300	24.7	51.5	4.86, 4.89, 5.05,	5+0.1	1.04	A
		1-2	600	2.66	5.54	5.19, 5.13, 5.05 4.51, 5.04, 4.63	4.7	0.98	A
Carbo, 38-75 $\mu\text{m}$ , mag.	88.5	2-1	300	17.9	43.82	4.96, 5.19, 4.75, 5.13, 4.98, 4.85	5+0.1	1.04	A
		2-2	600	0.81	1.98	4.78	4.8	1.00	A
Carbo, >150 $\mu\text{m}$ , mag.	74.5	3-1	200	10.38	30.19	5.07	5.0	1.04	A
		3-2	400	0.18	0.523	3.93, 4.13, 2.9	4+0.1	0.83	B
Sikhote Alin Inclusion	217.5	3-3	600	0.2	0.582	Os interference	-	-	U
		4-1	200	0.89	0.887	4.26, 4.26, 4.12	4.2+0.1	0.88	A
		4-2	400	0.113	0.113	2.91	2.9	0.60	B
		4-3	600	0.096	0.096	2.66	2.7	0.56	C
Canyon Diablo, >150 $\mu\text{m}$	205.5	5-1	200	0.52	0.548	5.18	5.2	1.08	A
		5-2	400	1.95	2.06	5.94, 5.49	5.5	1.15	A
		5-3	600	0.34	0.358	4.59, 4.67	4.6	0.96	A
Elenovka Bulk	247.3	E-1-1	200	1.74	1.52	4.8, 5.05	5.0	1.04	A
		E-1-2	400	0.16	0.14	3.27, 2.3	3+0.2	0.63	B
		E-1-3	600	Low	-	-	-	-	U
Elenovka Fine	196.0	E-2-1	300	0.31	0.343	4.63	4.6	0.96	A
		E-2-2	600	6.35	7.02	6.09, 5.2, 4.52	5.5	1.15	A



Table 3.15 continued

Sample	Mass (mg)	Code	T (°C)	cps/5	ppm (Hg)	$^{197}\text{Hg}/^{203}\text{Hg}$ Ratio		R/R <sup>+</sup>	Reliability
						Replicate	Best		
Elenovka Coarse	473.5	E-3-1	200	2.56	1.17	4.99	5.0	1.04	A
		E-3-2	400	0.25	0.114	4.87	5.0	1.04	A
		E-3-3	600	0.1	0.046	5.01	5.0	1.04	A
Cold Bokeveld Bulk	163.4	C-1-1	300	21.25	28.18	5.33	5.3	1.10	A
		C-1-2	600	3.57	4.73	4.95	5.0	1.04	A
Cold Bokeveld Fine	166.8	C-2-1	200	16.94	22.0	5.54, 5.0	5.3±0.1	1.10	A
		C-2-2	400	7.01	9.1	4.51	4.5	0.94	A
		C-2-3	600	0.94	1.22	2.26	2.3±0.1	0.48	A
Cold Bokeveld Coarse	278.2	C-3-1	100	2.85	2.22	5.31, 5.59	5.4±0.1	1.13	A
		C-3-2	250	14.5	11.3	4.66, 5.09	4.9±0.1	1.02	A
		C-3-3	400	25.05	19.5	5.08, 5.05	5.0±0.1	1.04	A
		C-3-4	550	0.48	0.374	4.3	4.3	0.90	A
Monitor-Hg	0.078 µg	Mon	-	0.36	-	4.65, 5.21, 4.64	4.8±0.2	1.00	B
Blank				Uncountable					

Samples of Carbo and Canyon Diablo were irradiated in Al-capped quartz capsules. Others were wrapped in Al-foil, which were crushed and sieved after the irradiation.

Errors are less than ±5% unless otherwise stated. U = Unreliable

steps were used to extract mercury. Soon after the distillation of sample No. 3-2 while removing the liquid nitrogen trap, the external connector with stopper exploded probably due to improper annealing. There may be a loss of Hg in this sample.

Sample 3-3 showed osmium peaks, some of these seriously interfering in the lower energy region of  $^{197}\text{Hg}$  making it difficult to measure the isotopic ratio of Hg. Usually a more reasonable value of isotopic ratio was worked out by plotting the spectrum on a linear scale. In some cases (especially when the count-rate is low) statistics is not good and slight shift in channel number of the peak gives a change in the background. Those measurements are ignored or given a poor reliability. Some of the spectra are shown in Figure 3.15 and 3.16. In Figure 3.15 sample C (C-2-1) with +ve is compared with two others (C-2-2 and C-2-3) having a negative (-). In Figure 3.16 sample B (5-1) and D (E-2-2) both are having above normal values on different counting dates. The other two, viz., A (4-2) and C (4-1), have negative anomaly. Decay lines of some interesting samples are given in Figures 3.17, 3.18 and 3.19.

### 3.12 Vial No. 3/86

This vial contained pieces of Allende, four of which were, later, ground individually and termed as bulk (No. I, II, III and IV). The other pieces were mixed and homogenised to make sample Nos. V and VI. A hand magnet could not separate any magnetic fraction from the mixed powder. Four temperature

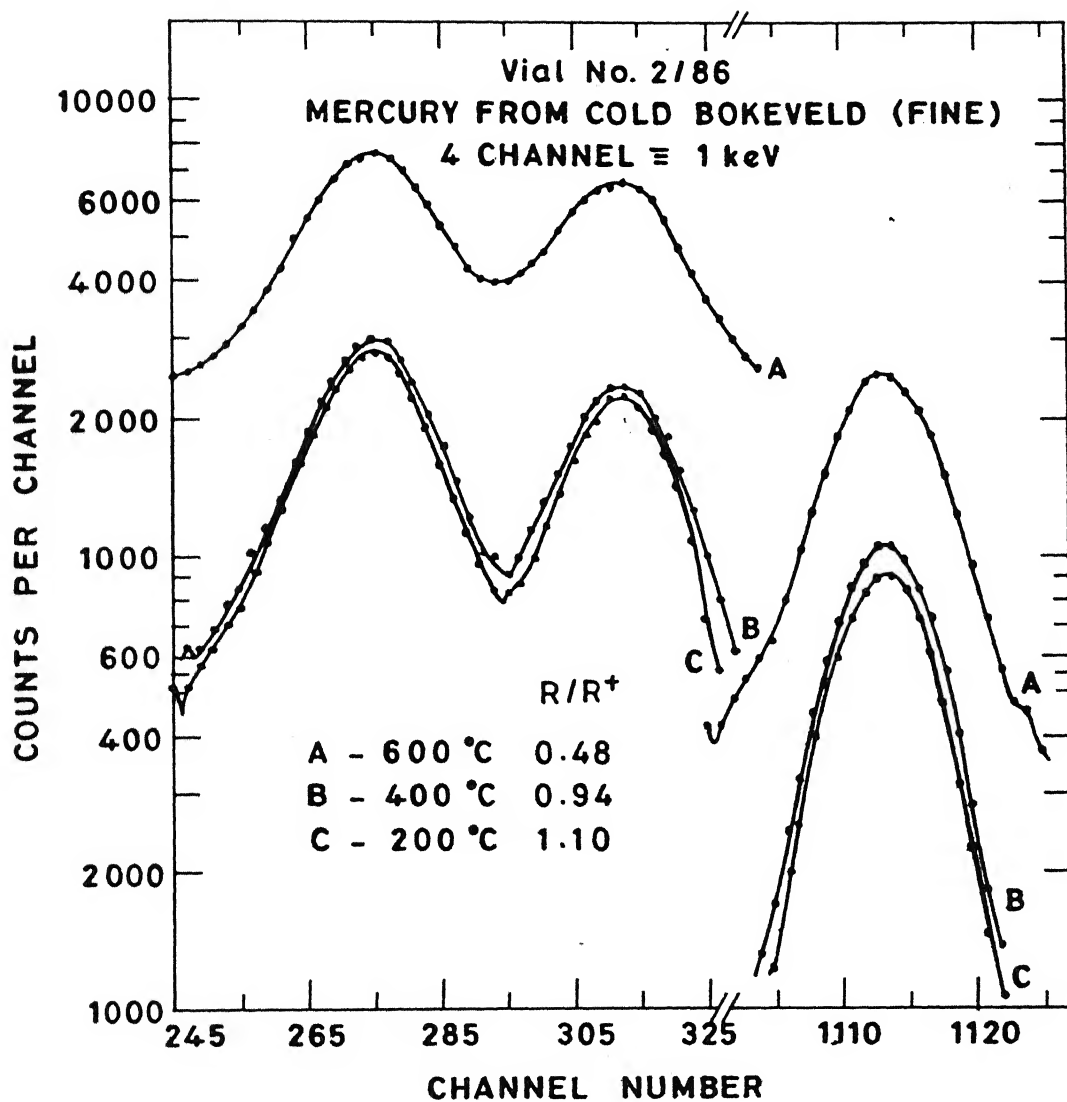


Fig. 3.15 Photon spectra of cold Bokeveld samples

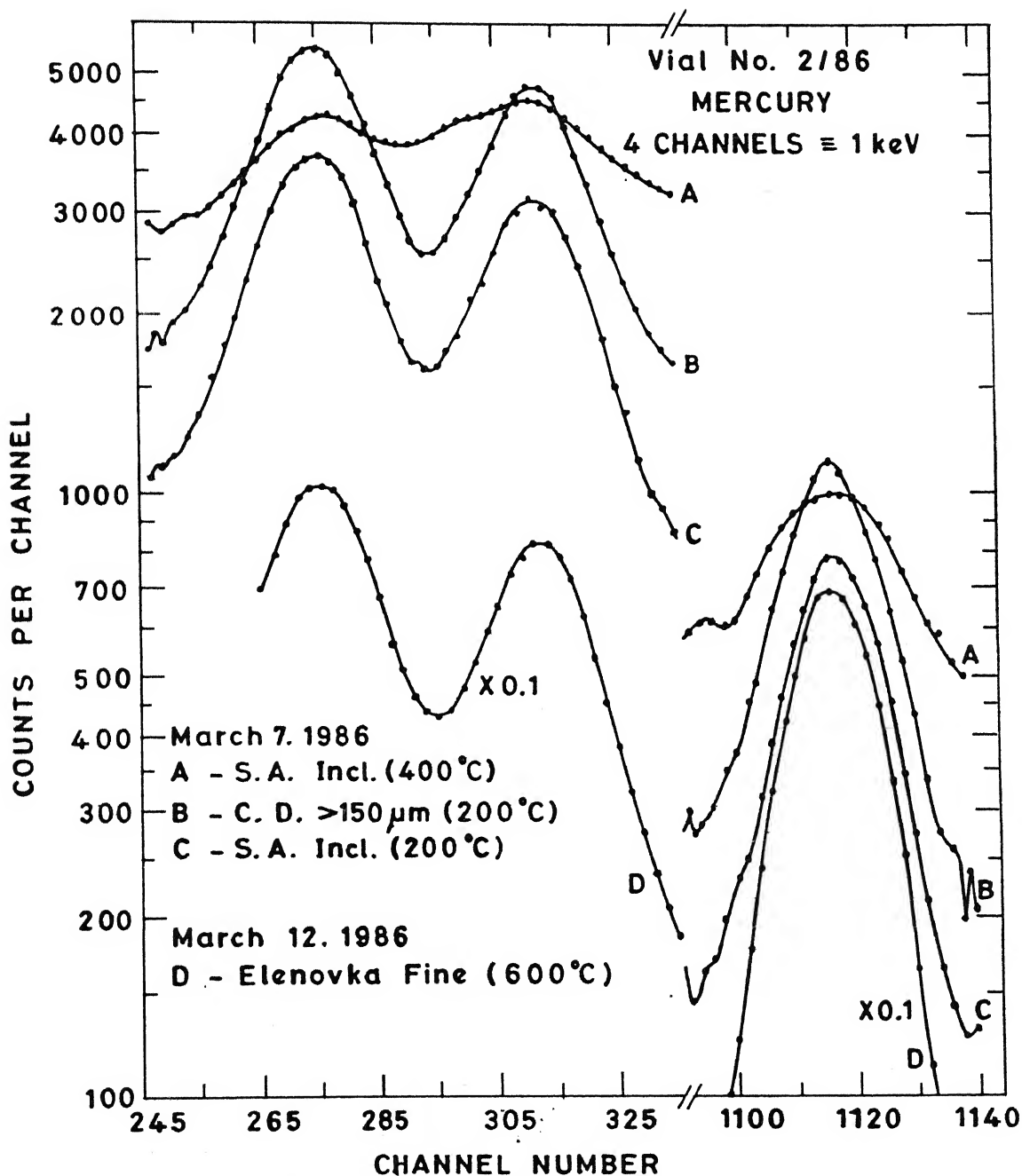


Fig. 3.16 Photon spectra of Hg released from some samples in Vial No.2/86  
sample A is highly anomalous

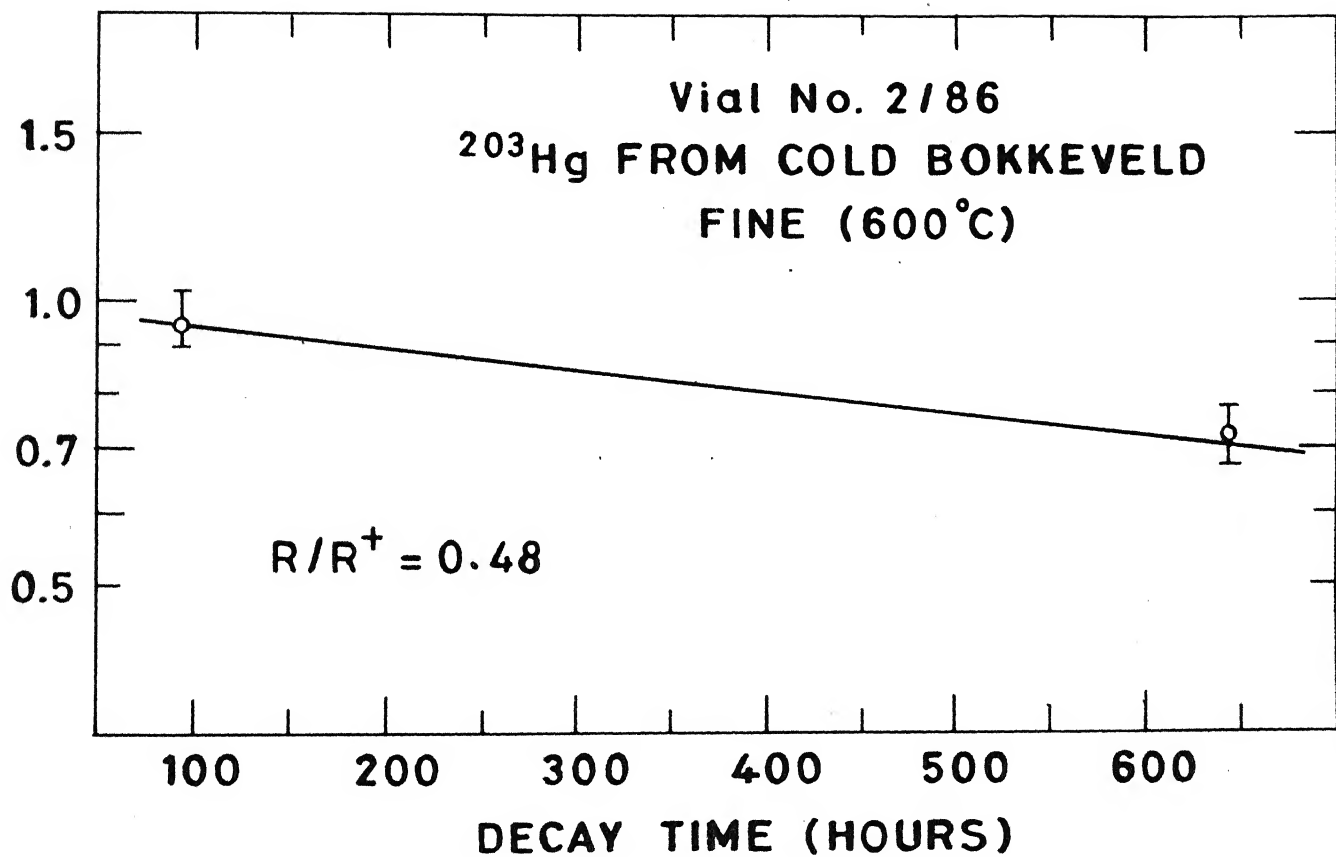


Fig. 3.17 Decay line of  $^{203}\text{Hg}$  from Cold Bokkeveld sample

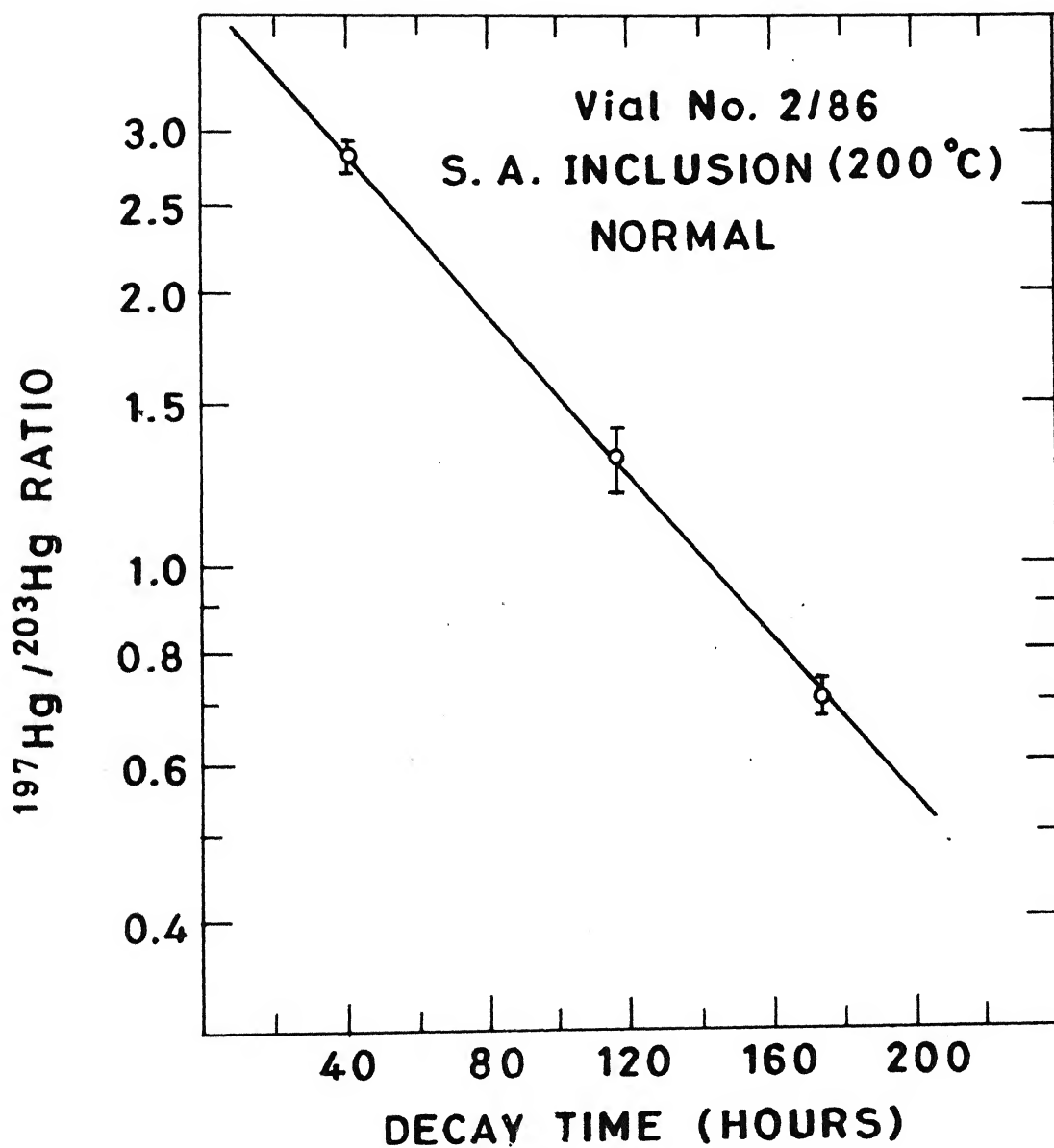


Fig. 3.18 Decay line of activity ratio of Hg isotopes from Sikhote Alin inclusion

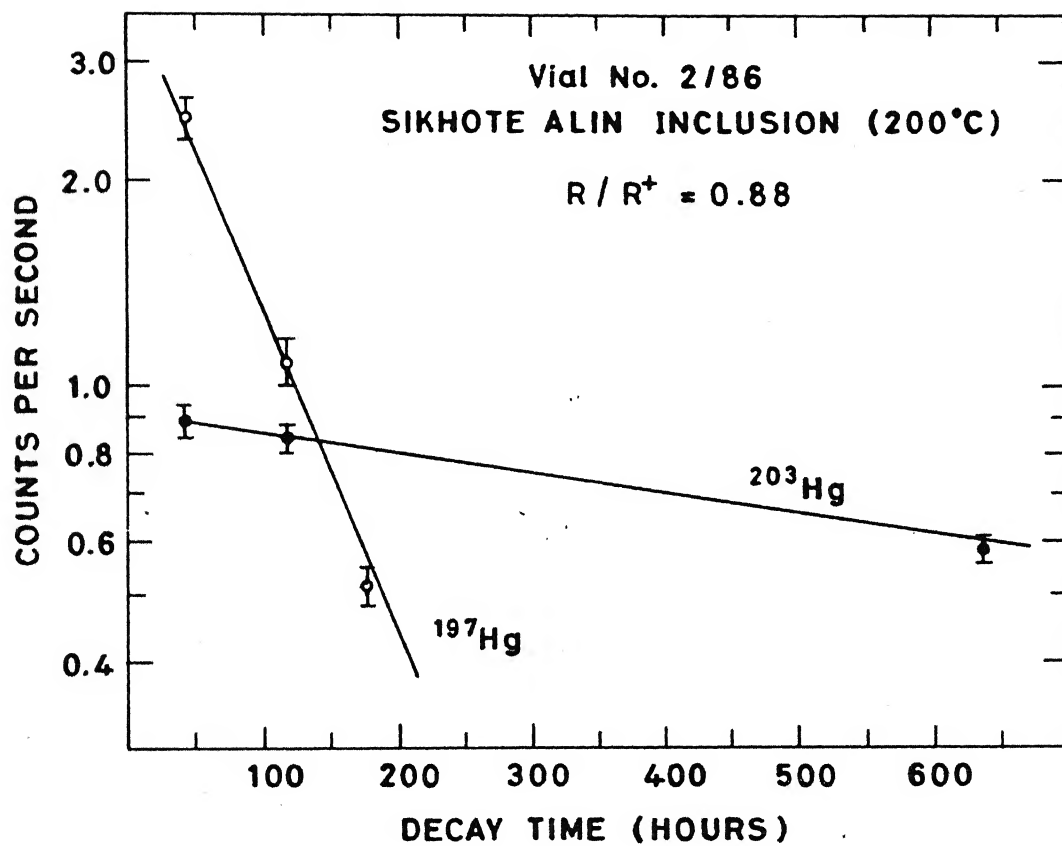


Fig. 3.19 Decay lines of  $^{197}\text{Hg}$  and  $^{203}\text{Hg}$  from Sikhote Alin inclusion

steps were used to extract mercury. Stopcock grease of the line developed some minor leakage that was detected in second sample. During third sample distillation the stopcock broke. As a result some loss of mercury is expected in first three samples. The results of the measurements are presented in Table 3.16. In spite of the problems, stated above, a variation in the isotopic composition of the first three bulk samples is found. The fourth fragment and the other two homogenised samples showed a temperature profile (Figure 3.20), similar to the Ambapur Nagla results. Since the counting rate is low, making the counting errors large, the reliability of the measurements is poor (B class). All the samples were spectrum analysed. Some of the interesting spectra are compared in the next few pages. In Figure 3.21 the photon spectra of the two abnormal samples from bulk I and bulk II are compared with that of a normal sample from bulk III. The spectrum of the standard is compared with a below normal sample (Bulk I, 150°C) and an above normal sample (Bulk V, 250°C) in Figure 3.22. The spectra of a near normal sample (Bulk VI, 350°C) and two abnormal samples (Bulk VI, 150°C and Bulk I, 150°C) are given in Figure 3.23. The photon spectra of the three temperature fraction of a single fragment (Bulk IV) are presented in Figure 3.24. The results were further confirmed by following the decay of ratio as well as of  $^{203}\text{Hg}$ . Some of the decay lines are shown in Figures 3.25, 3.26, 3.27 and 3.28.

### 3.13 Vial No. 4/86

A new furnace was designed with vertical movement and an automatic temperature controller. The advantage of the vertical



Table 3.16 Vial No. 3/86 Mercury from Allende fragments

Sample	Mass (mg)	Code	T(°C)	cps/5	ppb (Hg)	$^{197}\text{Hg}/^{203}\text{Hg}$ Replicate	Best	R/R <sup>+</sup>	Reliability
Bulk I (one piece)	140.7	1-1	150	1.07	976.3	1.1±0.05, 1.04±0.06	1.0±0.06	0.38(2)	A
						0.85±0.05			
		1-2	250	0.03	27.4	-			
		1-3	350	0.06	54.7	-			
		1-4	450	0.18	169.7	0.47±0.15	0.47±0.15	0.18(6)	B
Bulk II (one piece)	183.5	2-1	150	0.43	301.5	1.74±0.03	1.74±0.03	0.67(1)	A
		2-2	250	Low	-	-	-	-	
		2-3	350	0.23	162.3	1.07±0.11	1.07±0.11	0.41(4)	A
		2-4	450	0.04	28	-	-	-	
Bulk III (one piece)	197.0	3-1	150	0.26	173.3	2.71±0.16	2.7±0.1	1.04(4)	A
		3-2	250	Low	-	-	-	-	
		3-3	350	Low	-	-	-	-	
		3-4	450	0.09	63.9	1.0±0.4, <0.6	1.0±0.4	0.38(15)	B
Bulk IV (one piece)	224.5	4-1	150	0.43	249.9	2.38±0.14	2.38±0.14	0.92(5)	A
		4-2	250	0.33	188.7	3.00±0.1	3.00±0.1	1.15(4)	A
		4-3	350	0.13	78.3	1.71±0.03	1.71±0.03	0.66(1)	A
		4-4	450	Low	-	-	-	-	

Contd.....

Table 3.16 continued

Sample	Mass (mg)	Code	T (°C)	cps/5	ppb (Hg)	$^{197}\text{Hg}/^{203}\text{Hg}$		R/R <sup>+</sup>	Reliability
						Replicate	Best		
Bulk V (homogenized)	425.0	5-1	150	0.39	117.8	2.43±0.17	2.43±0.17	0.93(7)	A
		5-2	250	0.62	188.8	4.07±0.2,	4.0±0.2	1.54(8)	A
		5-3	350	0.12	38.1	3.87±0.12	2.4±0.2	0.92(8)	A
		5-4	450	0.05	16.6	2.42±0.24, 2.42±0.24	-	-	-
Bulk VI (homogenized)	309.8	6-1	150	0.21	89.1	3.49±0.3	3.5±0.3	1.35(12)	A
		6-2	250	0.25	106.1	3.14±0.25	3.15±0.25	1.21(10)	A
		6-3	350	0.12	49.7	2.91±0.4	2.9±0.4	1.12(15)	B
		6-4	450	0.06	26.9	1.7±0.4	1.7±0.4	0.65(15)	B
Monitor-Hg (0.038 µg)		Mon	-	0.296	-	2.66±0.3 2.60±0.2	2.6±0.2	1.00(10)	A

Samples I through IV were crushed individually for Hg-extraction, whereas samples V and VI were prepared by crushing several fragments and thorough mixing.

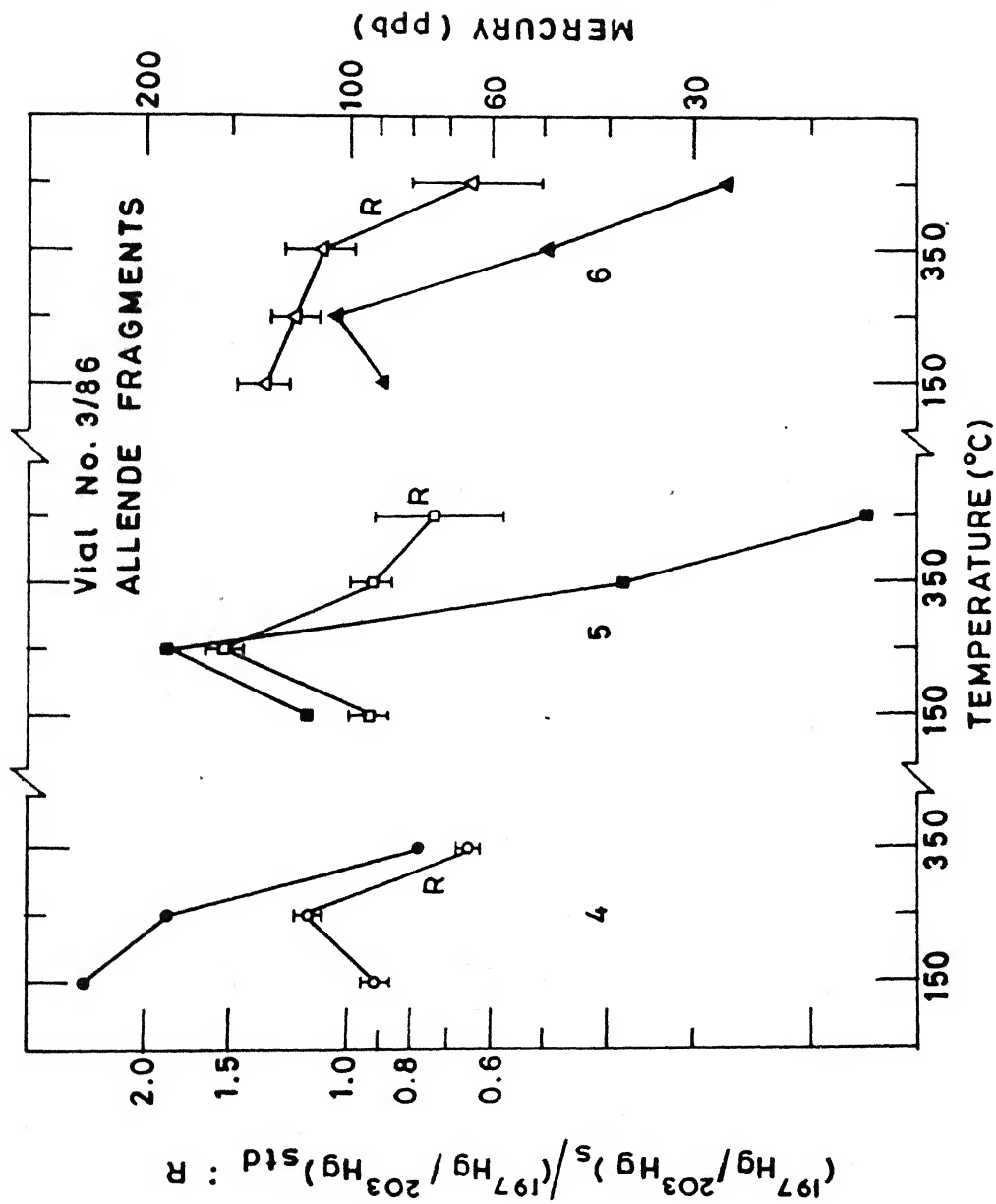


Fig. 3.20 Mercury concentration (right scale) and its isotopic ratios (left scale) measured at different temperatures in samples of Allende

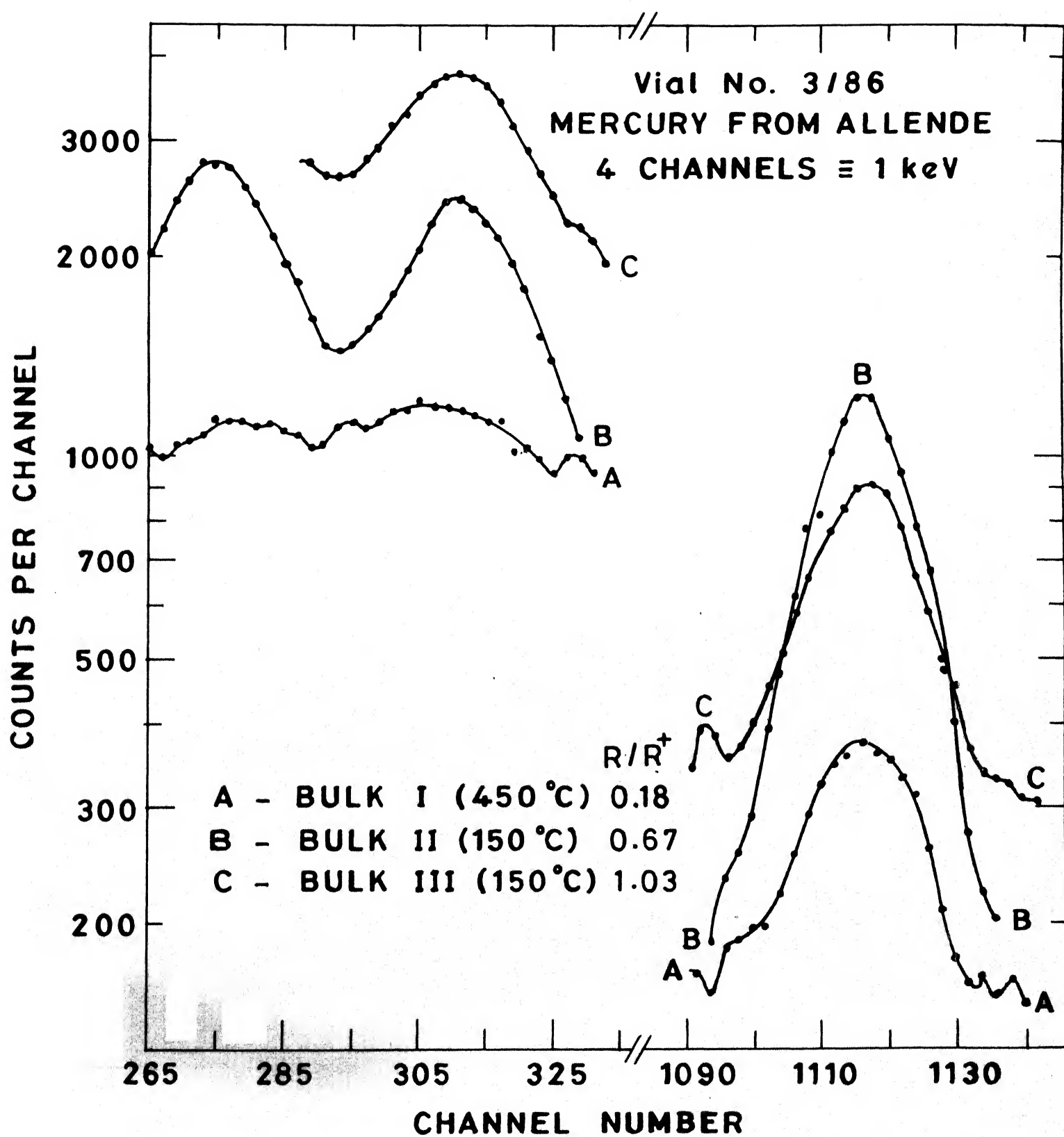


Fig. 3.21 Photon spectra of some Hg distillates from Allende

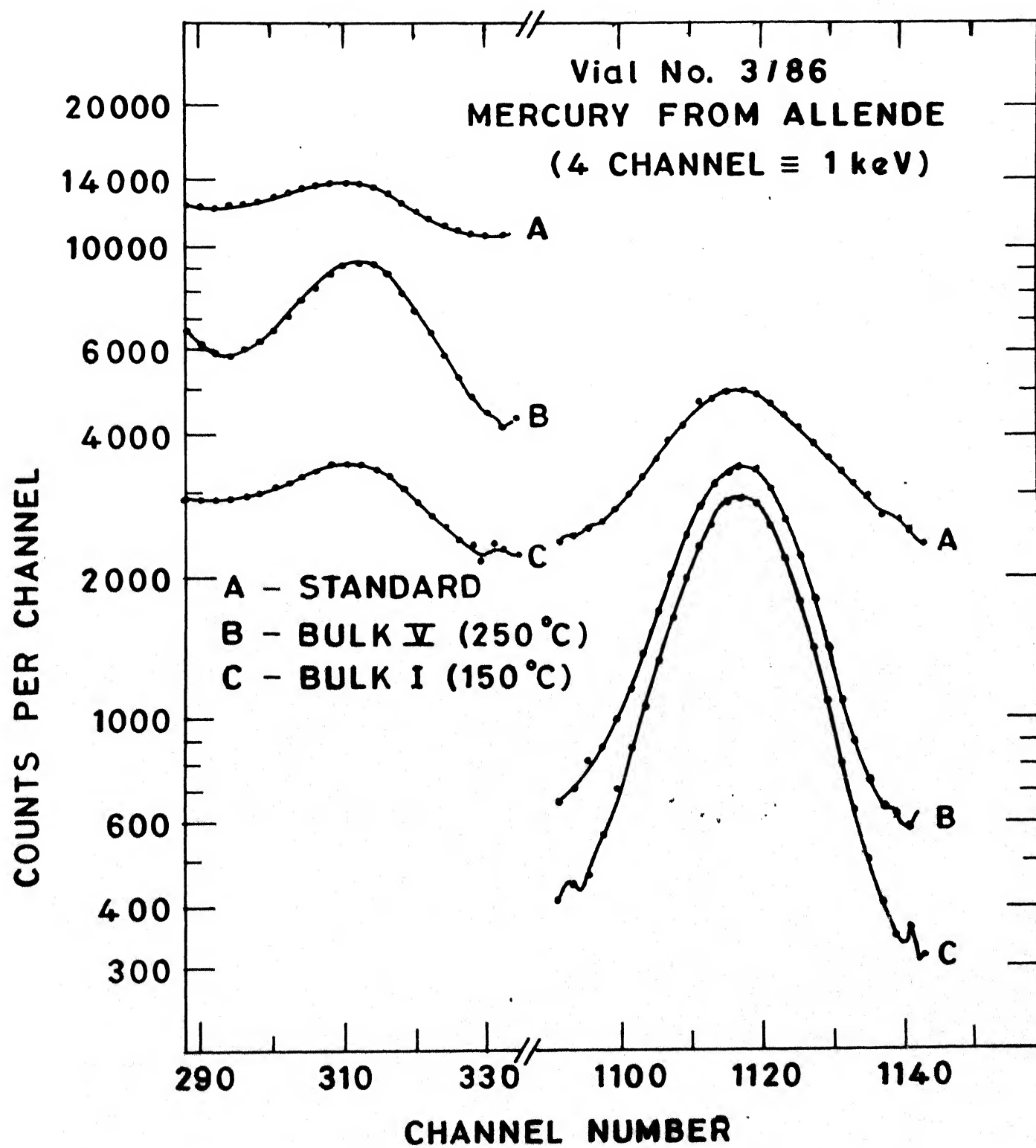


Fig. 3.22 Photon spectra of some Hg samples isolated from Allende

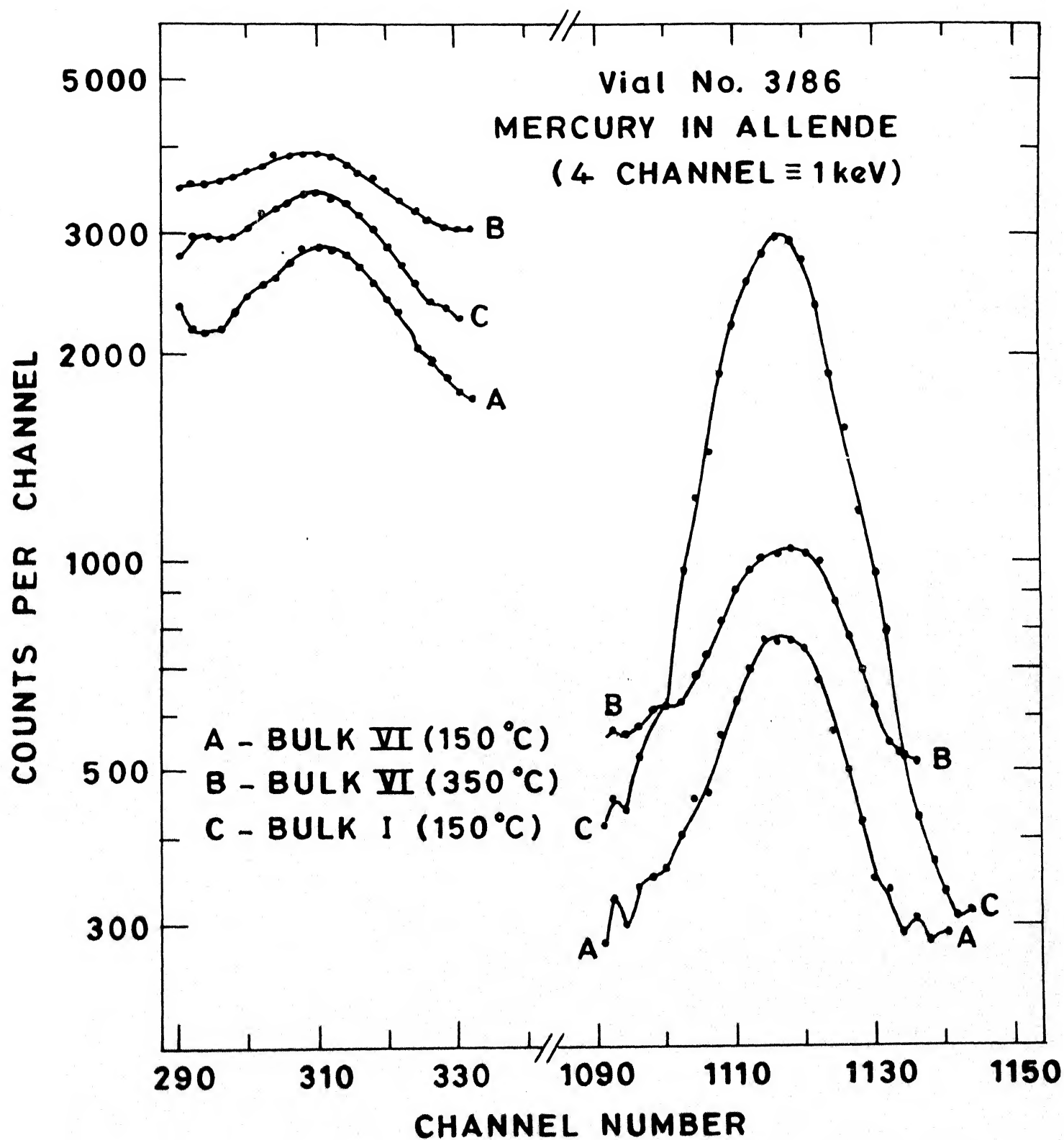


Fig. 3.23 Photon spectra of some Hg samples isolated from Allende

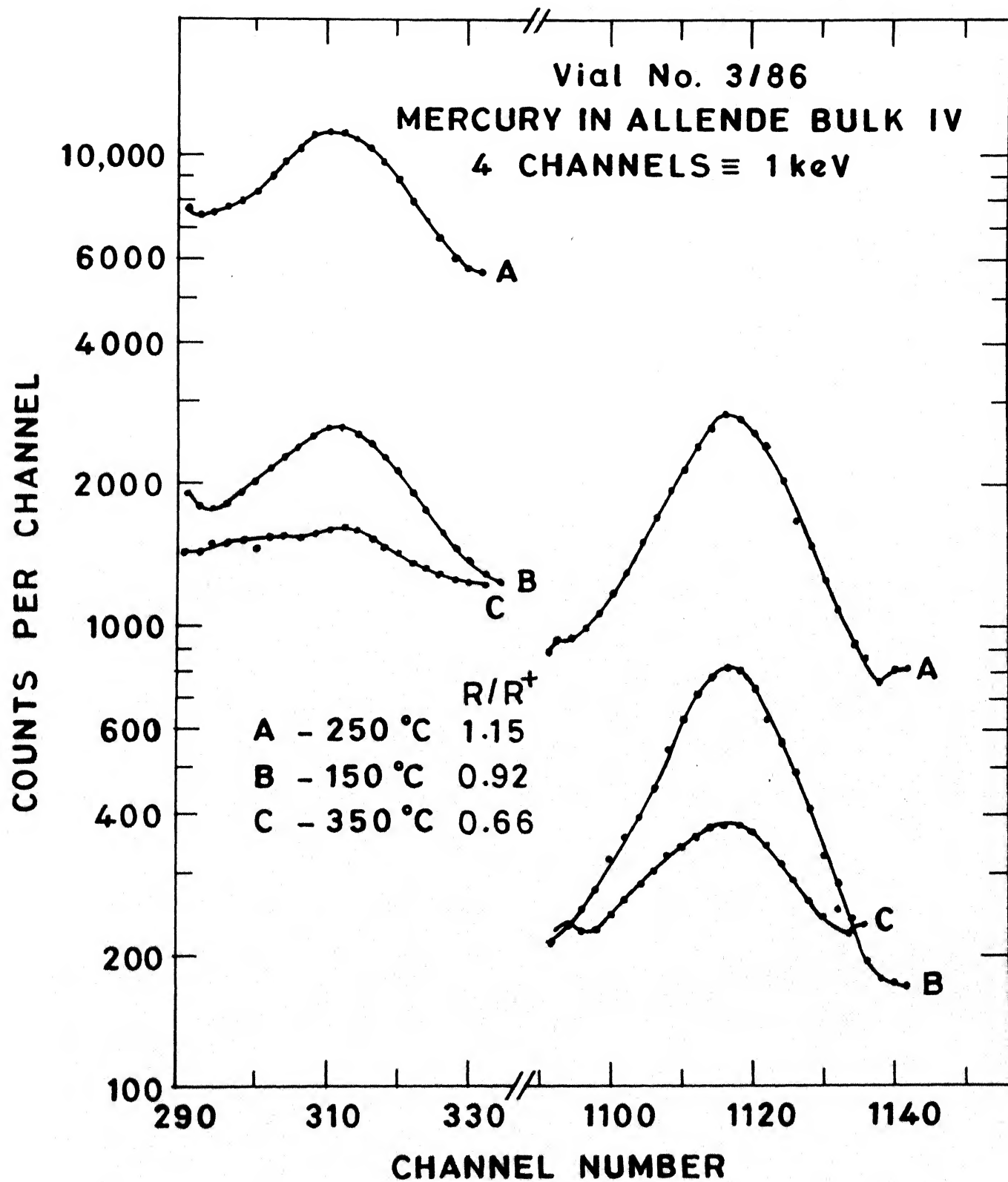


Fig. 3.24 Photon spectra of some Hg samples isolated from Allende

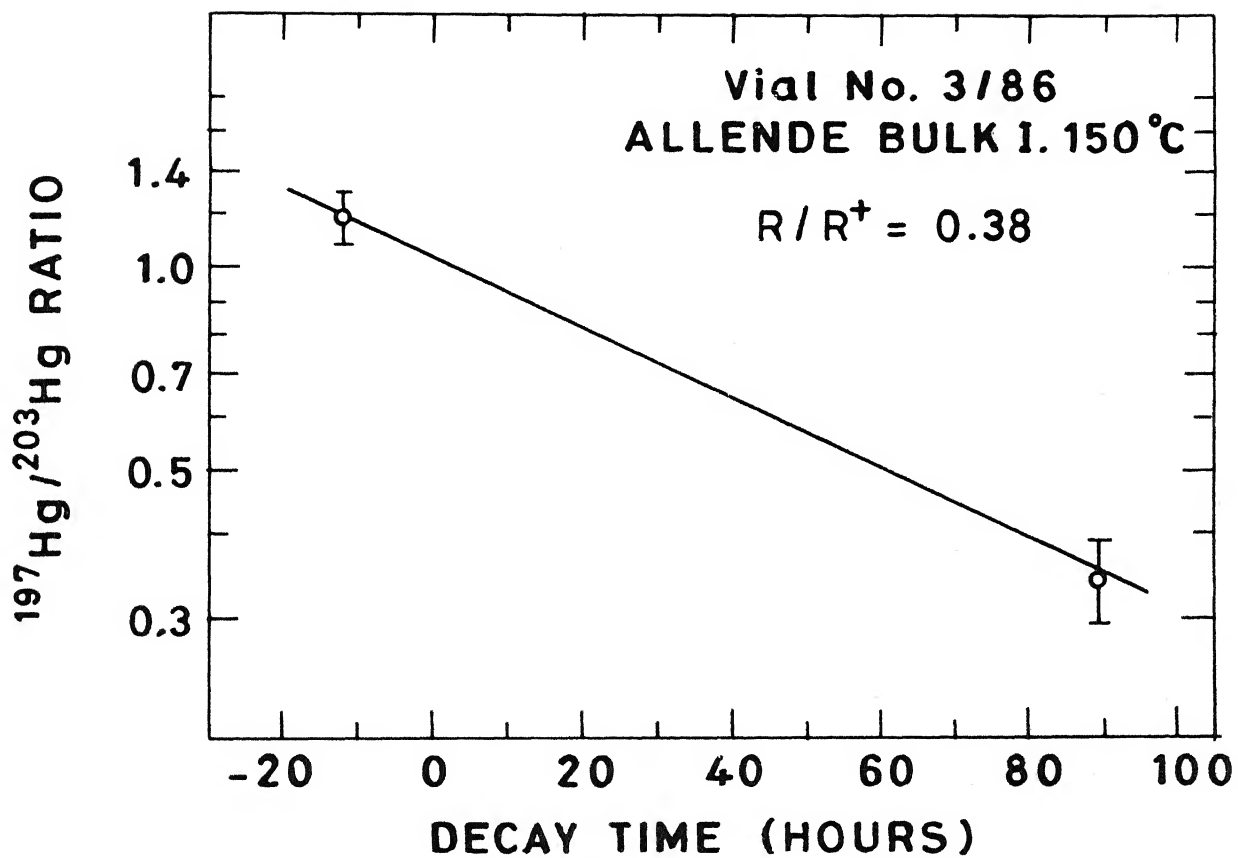


Fig. 3.25 Decay line of activity ratio of Hg isotopes from Allende sample



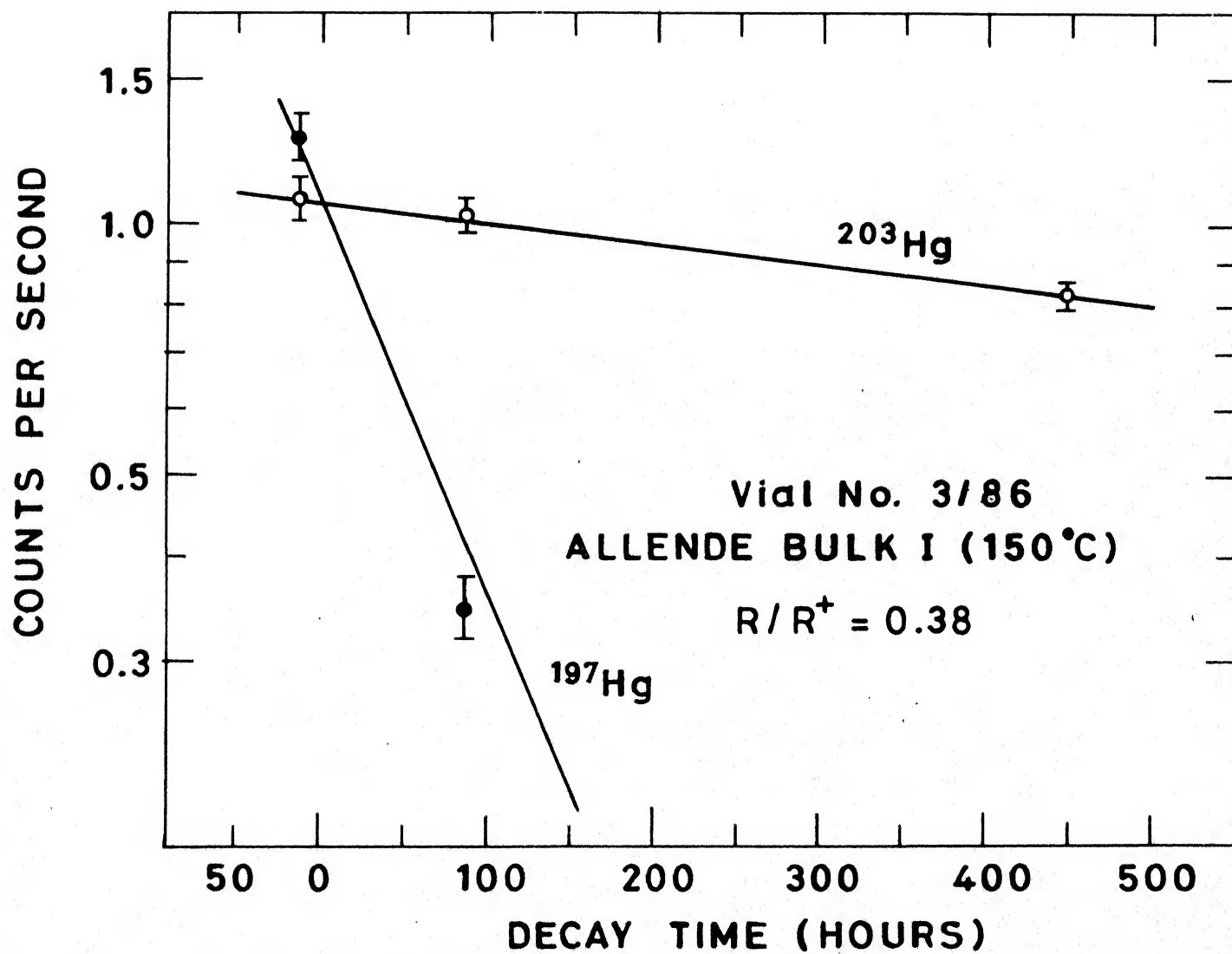


Fig. 3.26 Decay lines of  $^{197}\text{Hg}$  and  $^{203}\text{Hg}$  from Allende sample

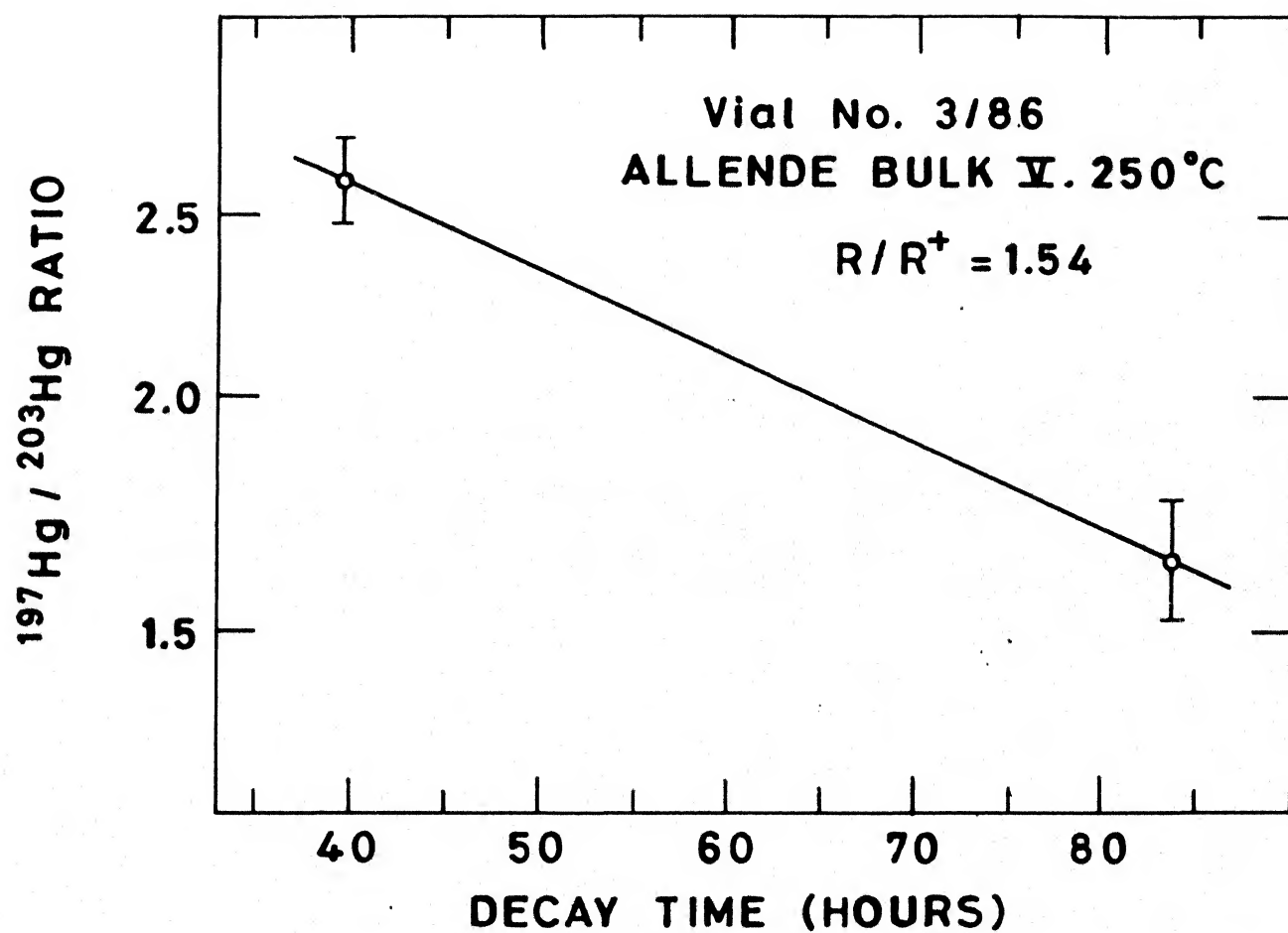


Fig. 3.27 Decay line of activity ratio of Hg isotopes from Allende sample

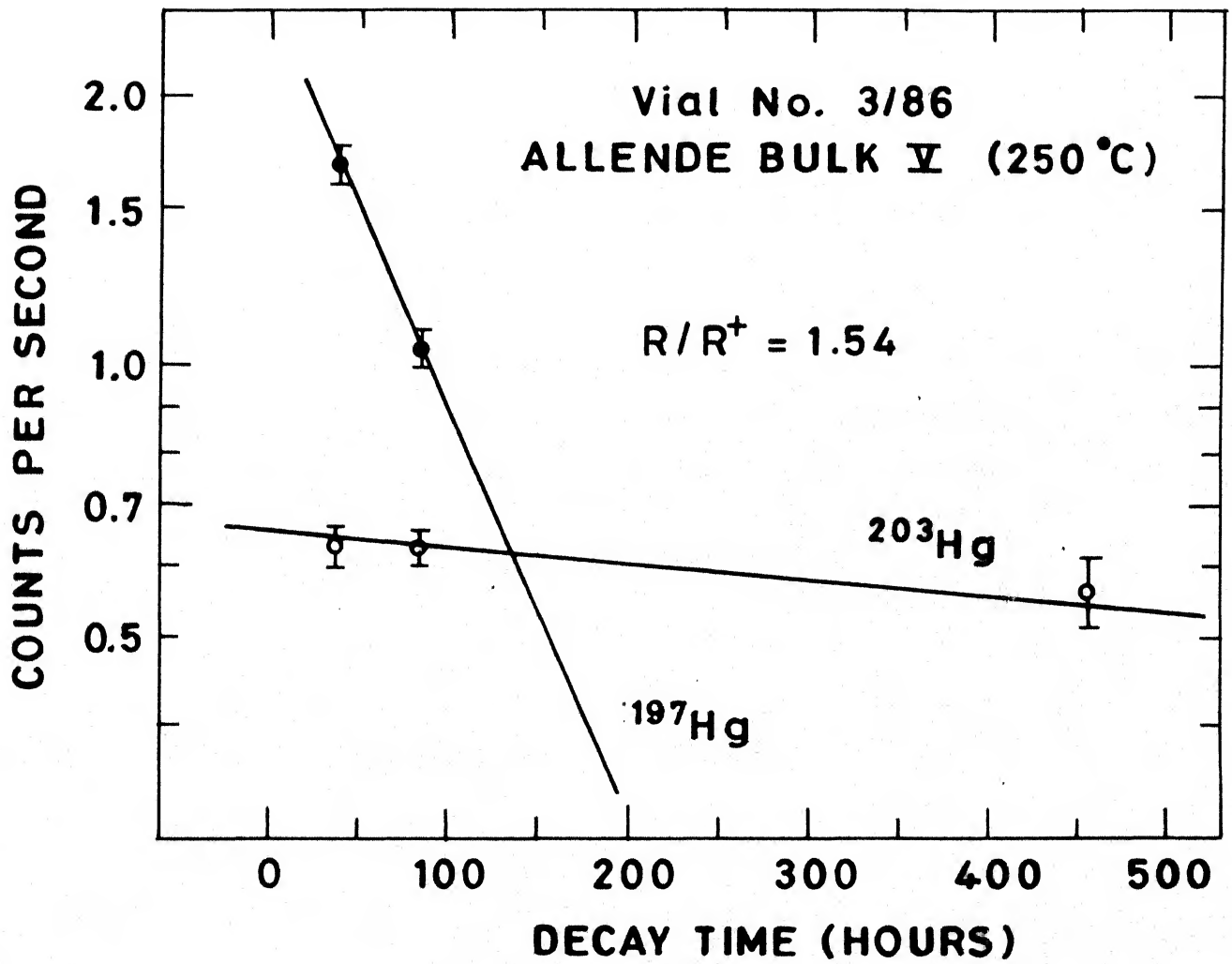


Fig. 3.28 Decay lines of  $^{197}\text{Hg}$  and  $^{203}\text{Hg}$  from Allende sample

movement of the furnace is that it can be lowered after each extraction so that the sample tube can be cooled rapidly, so that the next extraction could be done soon after. Cooling is essential to avoid (or atleast minimise) the pumping loss of Hg. Also we started using a heating tape wrapped around the glass tubes of the distillation line instead of flaming it to ensure uniform heating. The temperature imparted by the tape is  $\sim 250^{\circ}\text{C}$ .

Samples from Ambapur Nagla in aluminium capped quartz capsules as well as fragments of the meteorite were packed. The results on the measurements of Ambapur Nagla samples are presented in Table 3.17 and Figure 3.29. Most of the samples gave values of isotopic ratio similar to the reagent mercury. The table also gives the calculated values of isotopic ratio for each gross sample. This again looks normal within the error limits. Graphs of the photon spectra showed that, due to low counting rate, the data could not be taken with high reliability. Only 7-1, 7-3 and 2-4 seem to be slightly abnormal. In Figure 3.30 spectra of two apparently abnormal samples are compared with that of a normal sample, No. 1-4. The marker positions, shown with the arrows, determine the peak area. It is obvious that slight shift in the marker position may result in a different value of peak area and background. Few more spectra are given in Figure 3.31. The decay of the samples, because of their non-anomalous nature, was not followed.

Sample numbers 4, 5 and 6 were heated samples of Ambapur Nagla (used in a previous vial for Hg distillation prior to

Table 3.17 Vial No. 4/86 : Mercury from Ambapur Nagla

Sample*	Mass (mg)	T(°C)	Code	cps/7.5	ppm (Hg)	$^{197}\text{Hg}/^{203}\text{Hg}$	R/R <sup>+</sup>	Gross ratio
75-106 $\mu\text{m}$ , nm	120.5	100	1-1	0.15	0.39	2.3 $\pm$ 0.2	1.00(9)	
		150	1-2	2.03	5.26	2.6 $\pm$ 0.05	1.13(2)	
		150	1-3	0.75	1.95	2.54 $\pm$ 0.13	1.10(6)	
		200	1-4	1.82	4.72	2.34 $\pm$ 0.05, 2.3	1.02(2)	
		300	1-5	2.11	5.47	2.5 $\pm$ 0.05	1.09(2)	2.5
106-125 $\mu\text{m}$ , nm	119.9	100	2-1	0.58	1.51	2.96 $\pm$ 0.07	1.29(3)	
		150	2-2	1.29	3.36	2.82 $\pm$ 0.08, 2.2	1.23(3)	
		150	2-3	0.30	0.78	2.50 $\pm$ 0.07	1.09(3)	
		200	2-4	1.27	3.31	2.72 $\pm$ 0.05, 2.43	1.18(2)	
		300	2-5	2.20	5.73	2.68 $\pm$ 0.04	1.17(2)	2.5
125-150 $\mu\text{m}$ , nm	112.2	100	3-1	0.22	0.61	2.55 $\pm$ 0.12	1.11(5)	
		150	3-2	1.25	3.48	2.8 $\pm$ 0.1, 2.5	1.22(4)	
		150	3-3	0.25	0.70	2.23 $\pm$ 0.2	0.97(9)	
		200	3-4	0.94	2.62	2.37 $\pm$ 0.12	1.03(5)	
		300	3-5	1.78	4.96	2.32 $\pm$ 0.15, 2.4	1.01(7)	2.5
Bulk I	332.1	100	7-1	0.10	0.09	1.95 $\pm$ 0.26	0.85(11)	
		150	7-2	0.31	0.29	2.18 $\pm$ 0.15	0.95(7)	
		150	7-3	0.22	0.21	1.7 $\pm$ 0.2	0.74(9)	
		200	7-4	2.02	1.90	2.6 $\pm$ 0.05	1.13(2)	
		300	7-5	4.24	3.99	2/7 $\pm$ 0.08	1.17(3)	2.6

Contd.....

Table 3.17 continued

Sample *	Mass (mg)	T(°C)	Code	cps/7.5	ppm (Hg)	$^{197}\text{Hg}/^{203}\text{Hg}$	R/R <sup>+</sup>	Gross ratio
Bulk II	267.5	100	8-1	V. Low				
		150	8-2	0.76	0.89	2.4±0.06	1.04(3)	
		150	8-3	0.39	0.46	2.67±0.2	1.16(9)	
		200	8-4	3.49	4.08	2.65±0.07	1.15(3)	
		300	8-5	10.52	12.29	2.6±0.13	1.13(6)	
		400	8-6	1.32	1.54	2.4±0.07	1.04(3)	2.6
Magnetic	212.2	100	9-1	V. Low				
		150	9-2	2.92	4.30	2.69±0.06	1.17(3)	
		150	9-3	0.55	0.81	2.35±0.1	1.02(4)	
		200	9-4	4.30	6.33	2.55±0.1	1.11(4)	
		300	9-5	7.08	10.43	2.67±0.1	1.16(4)	
		400	9-6	1.05	1.55	2.64±0.2	1.15(9)	2.6
Non-Magnetic	431.0	100	10-1	0.04	0.03	**		
		150	10-2	0.27	0.20	2.7±0.06	1.17(3)	
		150	10-3	2.64	1.91	2.53±0.03	1.10(1)	
		200	10-4	3.99	2.89	2.55±0.08	1.11(3)	
		300	10-5	7.13	5.17	2.65±0.03	1.15(1)	
		400	10-6	1.49	1.08	2.44±0.1	1.06(4)	
Monitor-Hg	0.1 µg	-	Mon	0.75	0.54	2.48±0.1	1.08(4)	2.55
				0.32		2.3±0.2	1.00	

\* Samples 1,2 and 3 were irradiated in Al-capped quartz capsules. Several meteorite pieces were irradiated as wrapped under Al-foil, those were crushed and separated into magnetic and non-magnetic fractions to make samples 7,8,9 and 10.

\*\* Value calculated with the help of spectrum.

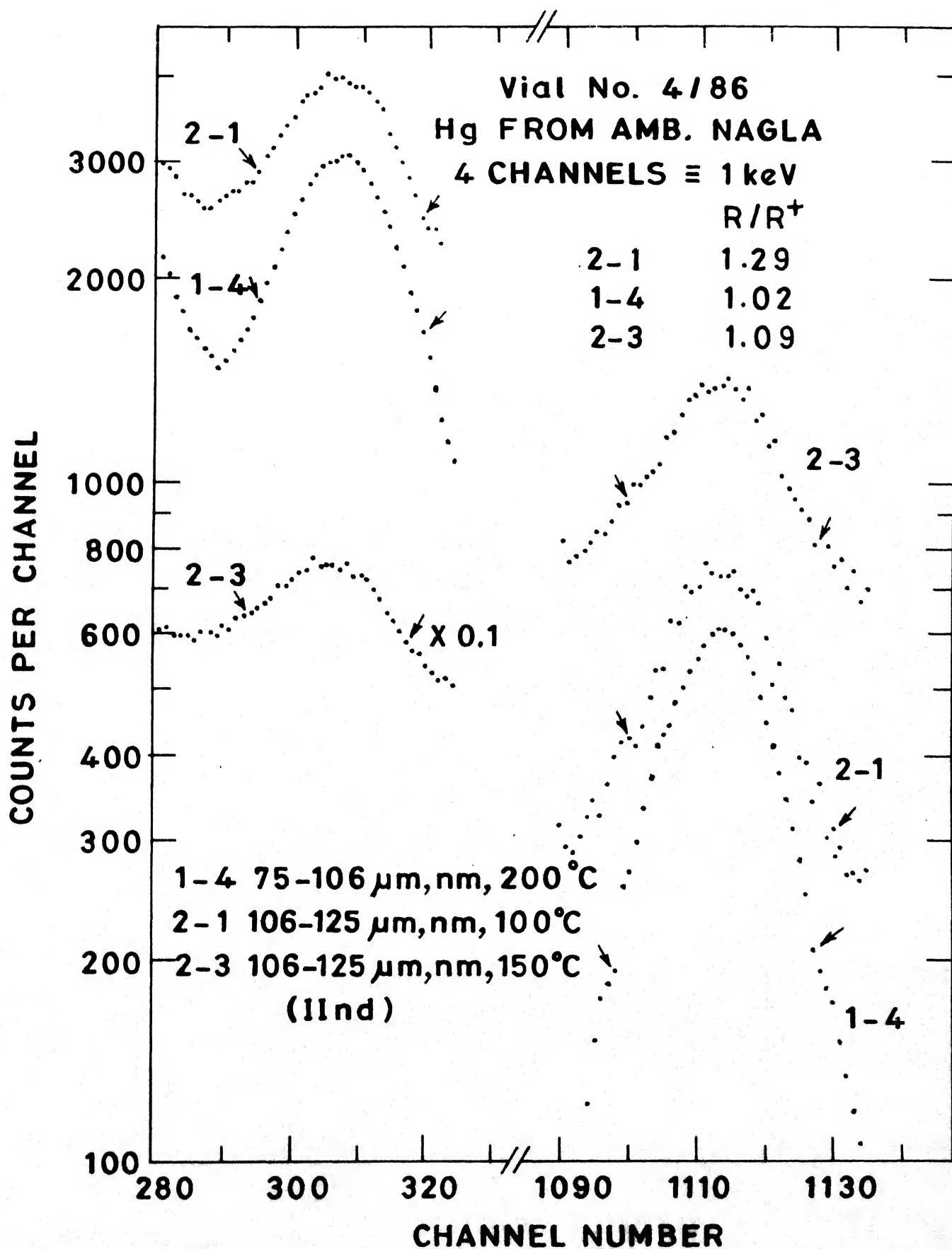


Fig. 3.30 Photon spectra of some Hg samples isolated from Ambapur Nagla

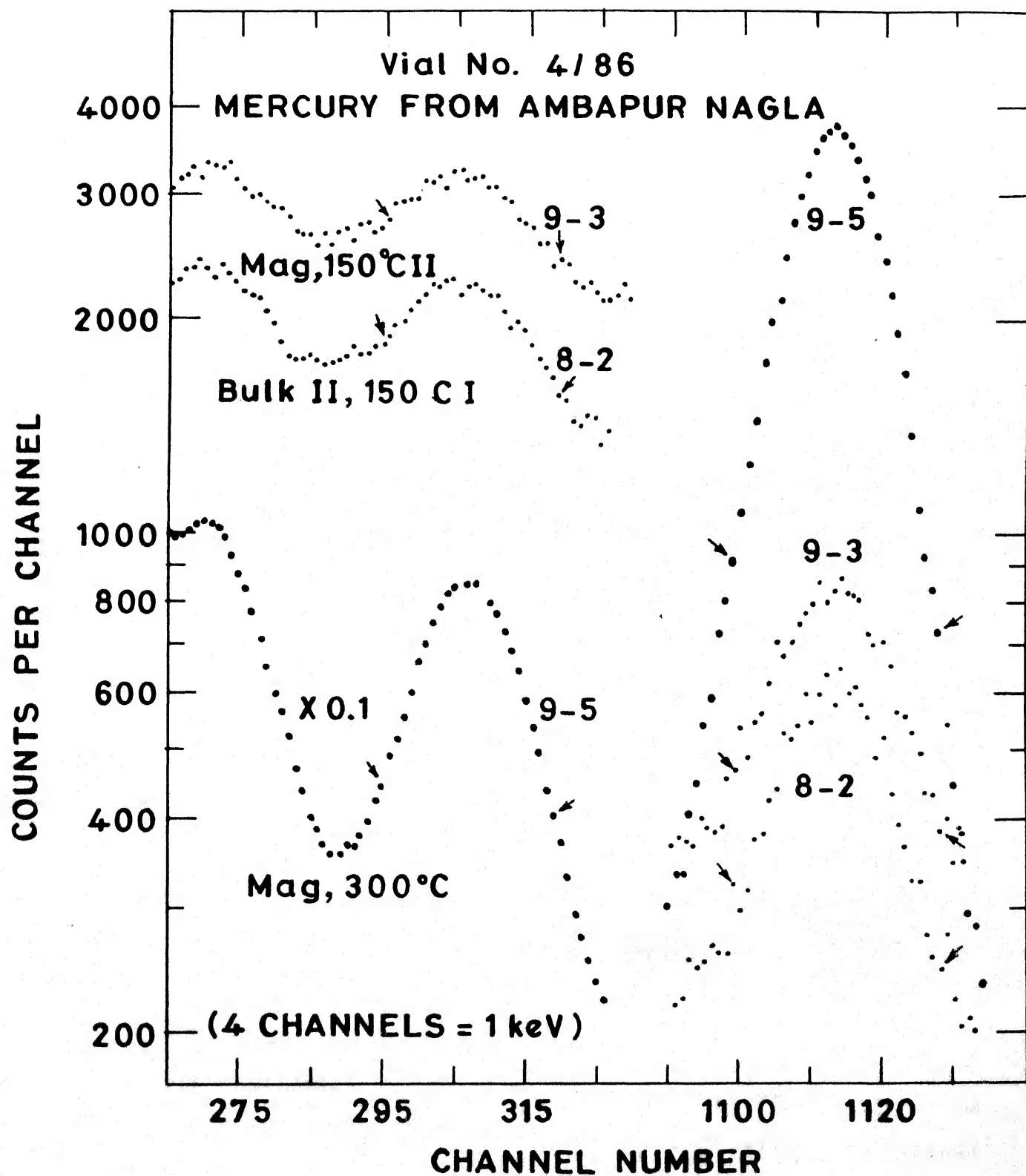


Fig. 3.31 Photon spectra of some Hg samples isolated from Ambapur Nagla



irradiation) meant for blank level determination. Since the activities were very low ( $<0.01$  c/sec with  $2\sigma$  error limit) in these, the results are not included in the table. These shall be discussed in Chapter 5.

### 3.14 Vial No. 5/86

Four stone meteorites-Richardton, Dhajala, Allegan and Allende were studied in this vial. Richardton was separated before irradiation. Dhajala and Allende were irradiated as pieces and Allegan was irradiated in the powder form. During grinding process of Allegan two very small inclusions were seen but not separated. All the powdered samples were packed in the form of tablets with the use of double layer of aluminium foil and stacked over one other in the irradiation can.

The delayed shipment of this vial due to high radiation field resulted in a loss of short lived  $^{197}\text{Hg}$  activity. Thus, in many cases isotopic ratio measurements were not possible. The results are shown in Table 3.18. There is a large variation in the mercury abundance and also in the isotopic ratio (one case only). The largest variation of isotopic ratio can be seen in Richardton nm,  $<32\ \mu\text{m}$  sample (No. 4-5) which is having only 30% (with  $2\sigma$  error) of the terrestrial ratio for reagent mercury. Its spectrum is shown in Figure 3.32. Since the counting rate is poor, its statistics is not good. But the lighter nuclide  $^{197}\text{Hg}$  is certainly depleted. Figures 3.33 and 3.34 give a more clear

Table 3.18 Results from Vial No. 5/86

Sample	Mass (mg)	T(°C)	Code	cps/6.25 ppb (Hg)	$^{197}\text{Hg}/^{203}\text{Hg}$ Ratio	R/R <sup>+</sup>
Allegan	220	150	1-1	6.03	0.91±0.03	1.10(4)
		250	1-2	0.21	-	
		350	1-3	0.026	-	
		450	1-4	0.021	-	
		550	1-5	0.002	-	
<u>Richardton</u>						
Magnetic	416.5	150	2-1	4.21	0.92±0.05	1.11(6) 1.31(24)
		250	2-2	0.41	1.09±0.2	
		350	2-3	0.006	-	
		450	2-4	0.03	-	
		550	2-5	0.04	-	
Chondrules, nm	466.5	150	3-1	2.15	0.90±0.04	1.08(5) 1.51(24)
		250	3-2	0.20	1.25±0.2	
		350	3-3	0.042	-	
		450	3-4	0.025	-	
		550	3-5	0.026	-	
nm, < 32 μm	134.3	150	4-1	17.17	0.94±0.03	1.13(4) 0.99(5) 1.04(2) 0.95(4) <0.4(2 σ)
		250	4-2	3.08	0.82±0.04	
		350	4-3	1.65	0.86±0.02	
		450	4-4	1.53	0.79±0.03	
		550	4-5	0.45	<0.33(2σ)	
nm, >32 μm	547.5	150	5-1	27.8	0.90±0.2, 0.83±0.03	1.00(3) 0.96(3) 1.14(7) 0.87(16) 1.22(30)
		250	5-2	15.9	0.76±0.03, 0.85±0.03	
		350	5-3	1.78	0.95±0.06	
		450	5-4	0.44	0.72±0.13	
		550	5-5	0.23	1.01±0.25	

Contd.....

Table 3.18 continued

Sample	Mass (mg)	T(°C)	Code	cps/6.25	ppb (Hg)	$^{197}\text{Hg}/^{203}\text{Hg}$ Ratio	R/R <sup>+</sup>
<u>Dhajala</u>							
Chondrules, mag.	200.4	150	6-1	0.34	150.0	Large error	
		250	6-2	0.068	30.0	-	
		350	6-3	0.055	24.3	-	
		450	6-4	0.113	49.9	-	
		550	6-5	0.018	8.0	-	
Magnetic, fine	138.5	150	7-1	0.50	319.6	Large error	
		250	7-2	0.086	55.0	-	
		350	7-3	0.03	19.2	-	
		450	7-4	0.005	3.2	-	
		550	7-5	Low	-	-	
Non-Mag., fine	367.5	150	8-1	0.35	84.0	0.65±0.05	0.81(6)
		250	8-2	0.35	84.0	0.73±0.07	0.91(9)
		350	8-3	0.19	46.0	Large error	
		450	8-4	Low	-		
		550	8-5	Low	-		
<u>Allende bulk</u>	653.5	150	9-1	5.6	759.0	1.02±0.05, 0.86±0.05	1.14(11)
		250	9-2	4.2	569.0	0.83±0.04	1.00(10)
		350	9-3	0.37	50.0	0.52±0.10	0.63(13)
		450	9-4	0.16	22.0	1.69±0.18	2.04(24)
		550	9-5	0.08	11.0	1.37±0.30	1.65(40)
Monitor-Hg	0.71 µg			8.02		0.88±0.04, 0.83±0.02, 1.00(4)	
						0.80±0.04, 0.72±0.08	

Richardton was separated prior to irradiation whereas the pieces of Dhajala were separated after irradiation. Allegan was irradiated in the powdered form. Allende was irradiated as pieces and was grinded later. This vial was delayed by BARC because of high radiation field thus repeat counting was not possible.

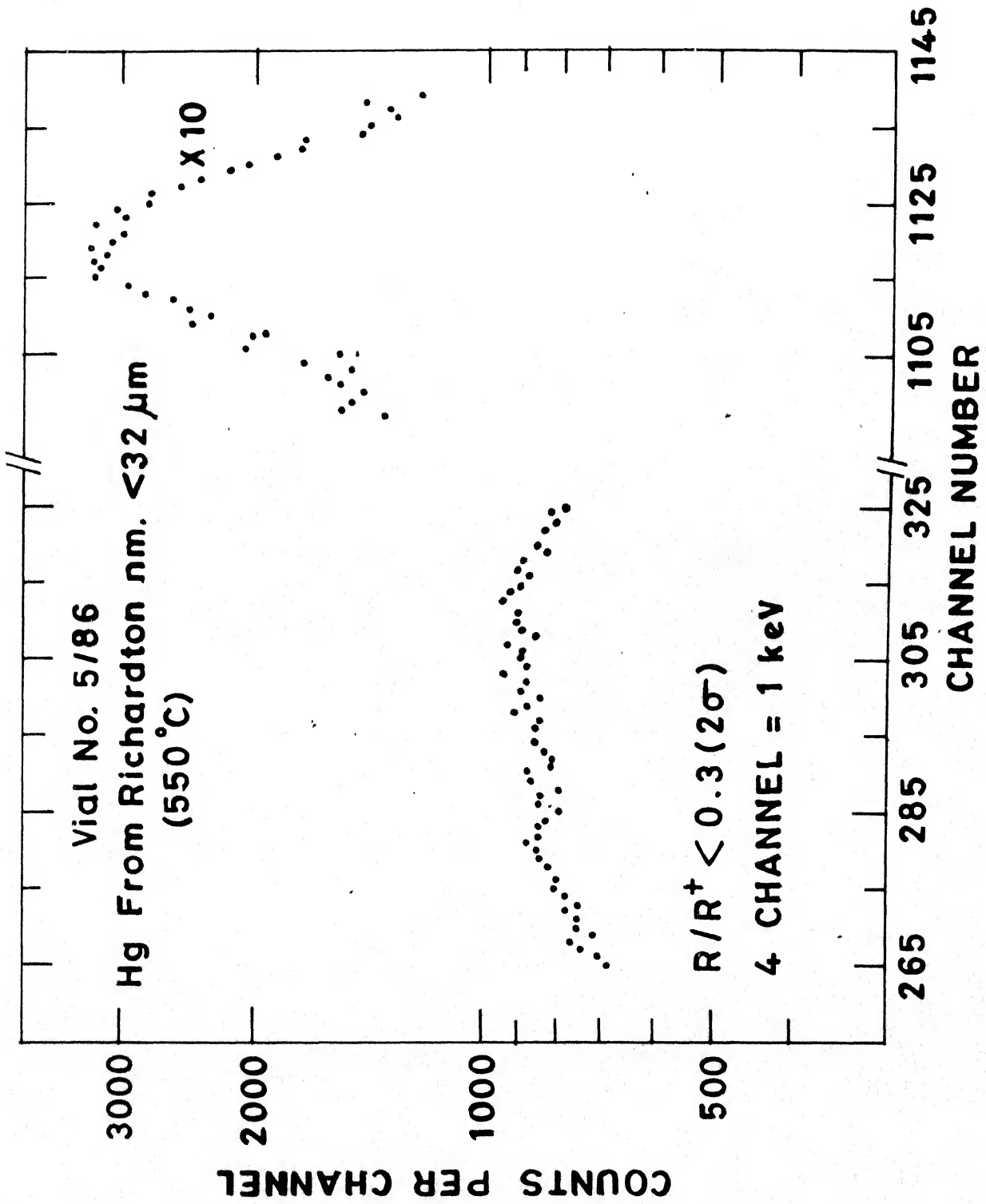


Fig. 3.32 Photon spectrum of an anomalous sample of Richardton

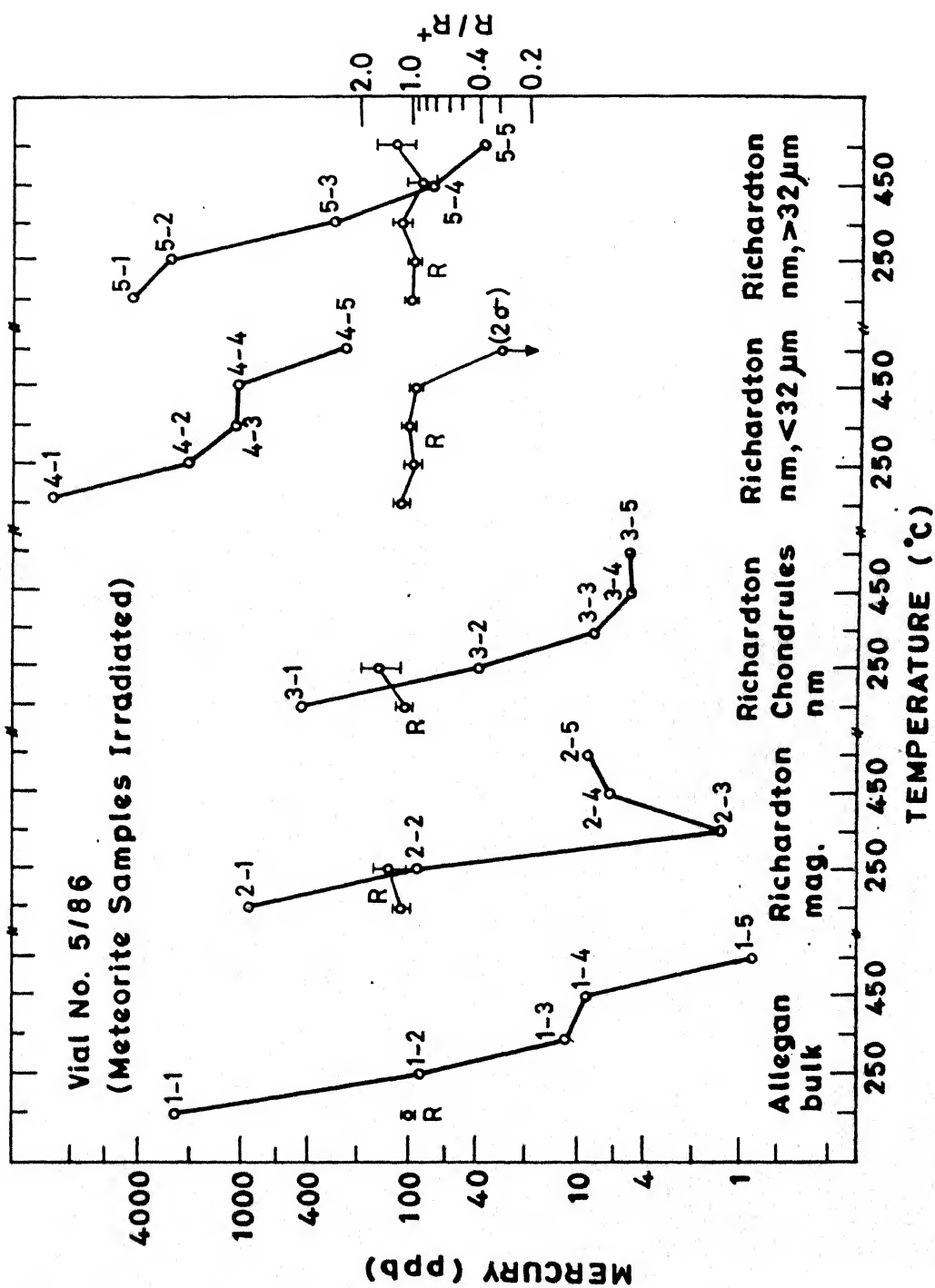


Fig. 3.33 Mercury concentration (left scale) and its isotopic ratios (right scale) measured at different temperatures in samples of Allegan and Richardton

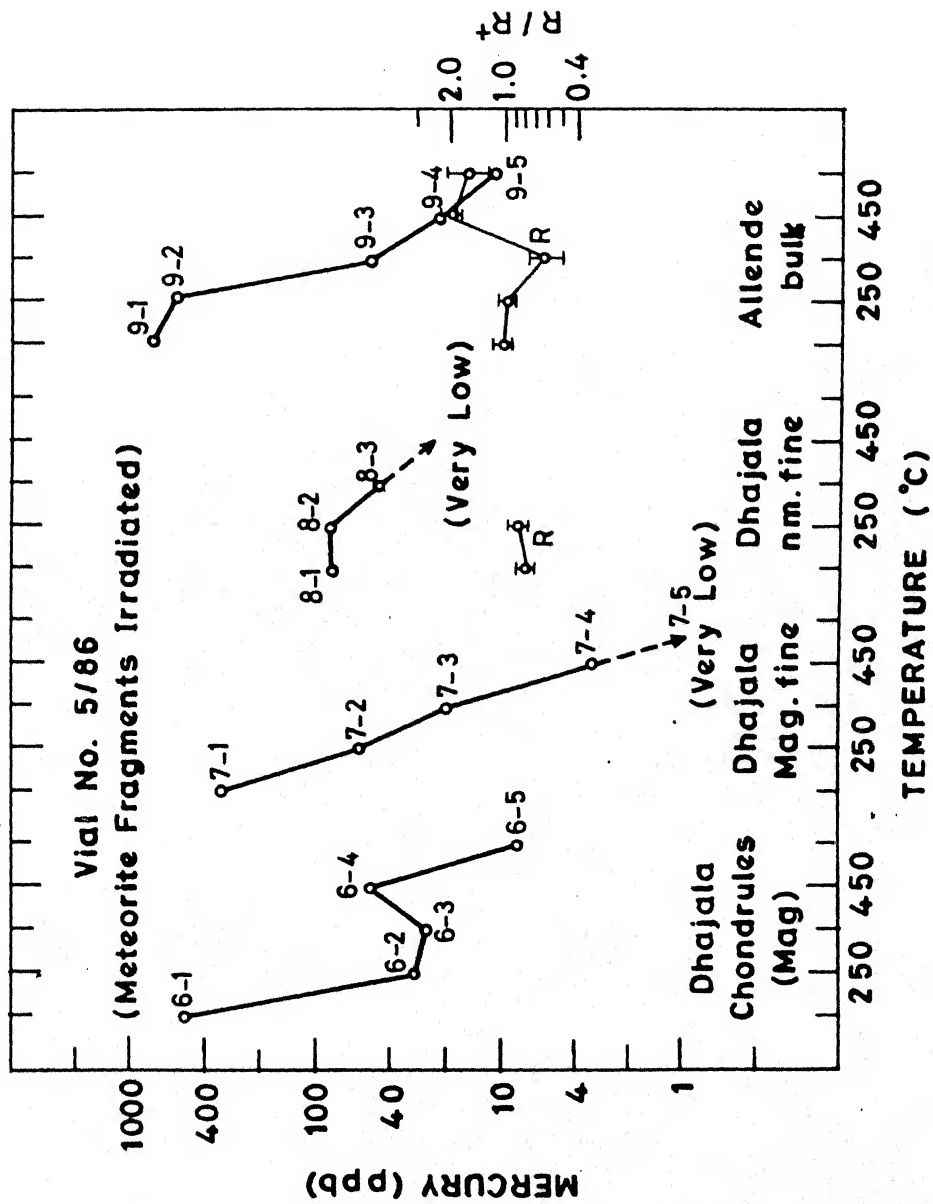


Fig. 3.34 Mercury concentration (left scale) and its isotopic ratios (right scale) measured at different temperatures in samples of Dhajala and Allende

picture of the measurements made. The Hg abundances in general decrease with temperature. The ratios normalised to the terrestrial value ( $R/R^+$ ) are unity except the above discussed sample 4-5 which is below normal. Sample 9-4 may also be slightly higher than normal. Unfortunately only one measurement could be made on Allegan, which may be a very interesting meteorite. It is important to note that Javanovic and Reed (1976) reported huge anomaly of Hg isotopic ratio in the 300°C fraction released from Allegan chondrules; their measured ratio of ( $^{197}\text{Hg}/^{203}\text{Hg}$ ) relative to the terrestrial value being  $0.044 \pm 0.007$ .

### 3.15 Vial No. 6/86

Samples from Carbo and Elga acid residues were packed in this vial. Carbo residue was freshly prepared. Elga acid insoluble residue was benzene-washed to study organic compounds (for an earlier experiment). Sample preparation was done by sieving, hand picking (flakes, silicates) and magnetic characterisation. Five temperature steps were used to extract Hg from an irradiated sample.

The results from this vial are reported in Table 3.19 and Figure 3.35. The two monitors used (located in central and outer part of the Al-irradiation can) were radiochemically purified after the irradiation. There is a very good consistency between the two results with respect to their isotopic ratios as well as mercury abundance (through counts per second). This

Table 3.19 Vial No. 6/86 Mercury from Iron Meteorite Residues

Sample	Mass (mg)	T(°C)	Code	cps/6.25	ppm (Hg)	$^{197}\text{Hg}/^{203}\text{Hg}$		R/R <sup>+</sup>
						Replicate	Best	
Elga Silicate Incl. v.w. mag.	120.0	150	1-1	2.16	1.11	2.5, 2.8	2.8	0.97(5)
		250	1-2	0.91	0.47	2.36, 2.29, 2.4	2.36	0.81(4)
		350	1-3	0.13	0.07	2.8	2.8	0.97(5)
		450	1-4	0.05	0.03	-	-	-
		550	1-5	-	-	-	-	-
Magnetic Flakes	53.0	150	2-1	1.93	2.25	2.98, 2.66	2.98	1.03(5)
		250	2-2	0.58	0.68	2.35, 2.68	2.35	0.81(4)
		350	2-3	0.06	0.07	3.21, 3.21	3.21	1.11(8)
		450	2-4	-	-	-	-	-
		550	2-5	-	-	-	-	-
Magnetic Fine	176.2	150	3-1	3.10	1.09	3.1	3.1	1.07(5)
		250	3-2	3.96	1.39	2.68, 2.52	2.6	0.90(5)
		350	3-3	0.25	1.09	2.96	2.96	1.02(5)
		450	3-4	0.11	0.04	-	-	-
		550	3-5	-	-	-	-	-
Carbo > 150 $\mu\text{m}$ , mag.	86.5	150	4-1	6.86	4.90	3.15	3.15	1.09(5)
		250	4-2	8.60	6.14	2.78, 2.71	2.7	0.93(5)
		350	4-3	0.28	0.20	-	-	-
		450	4-4	0.12	0.09	-	-	-
		550	4-5	-	-	-	-	-
75-125 $\mu\text{m}$ , mag.	91.2	150	5-1	27.67	18.74	2.7	2.7	0.93(5)
		200	5-2	5.85	3.96	2.62	2.6	0.90(5)
		250	5-3	0.80	0.54	2.4, 2.6	2.6	0.90(5)
		350	5-4	0.40	0.27	2.6	2.6	0.90(5)

134

Contd.....



Table 3.19 continued

Sample	Mass (mg)	T(°C)	Code	cps/6.25	ppm (Hg)	$^{197}\text{Hg}/^{203}\text{Hg}$		R/R <sup>+</sup>
						Replicate	Best	
Carbo 38-75 $\mu\text{m}$ , mag.	146.1	100	6-1	0.19	0.08	-		
		150	6-2	1.10	0.47	2.84	2.84	0.98(5)
		200	6-3	24.61	10.41	2.82	2.82	0.97(5)
		350	6-4	8.79	3.72	2.54	2.54	0.87(5)
<38 $\mu\text{m}$ , mag.	121.0	100	7-1	0.28	0.14	-		
		150	7-2	0.56	0.29	2.56	2.56	0.88(4)
		200	7-3	25.98	13.26	2.8	2.8	0.97(5)
		250	7-4	7.33	3.74	2.8	2.8	0.97(5)
		400	7-5	0.87	0.44	2.52	2.52	0.87(5)
Hg-Monitor-A, Central	0.85 $\mu\text{g}$		Mon-A	13.76		2.9, 2.8, 2.7, 2.96, 2.69, 2.85	2.9	1.00(3)
Hg-Monitor-B, Outer	0.83 $\mu\text{g}$		Mon-B	13.38		2.90	2.9	1.00(3)

Errors in the ratios are less than  $\pm 5\%$ .

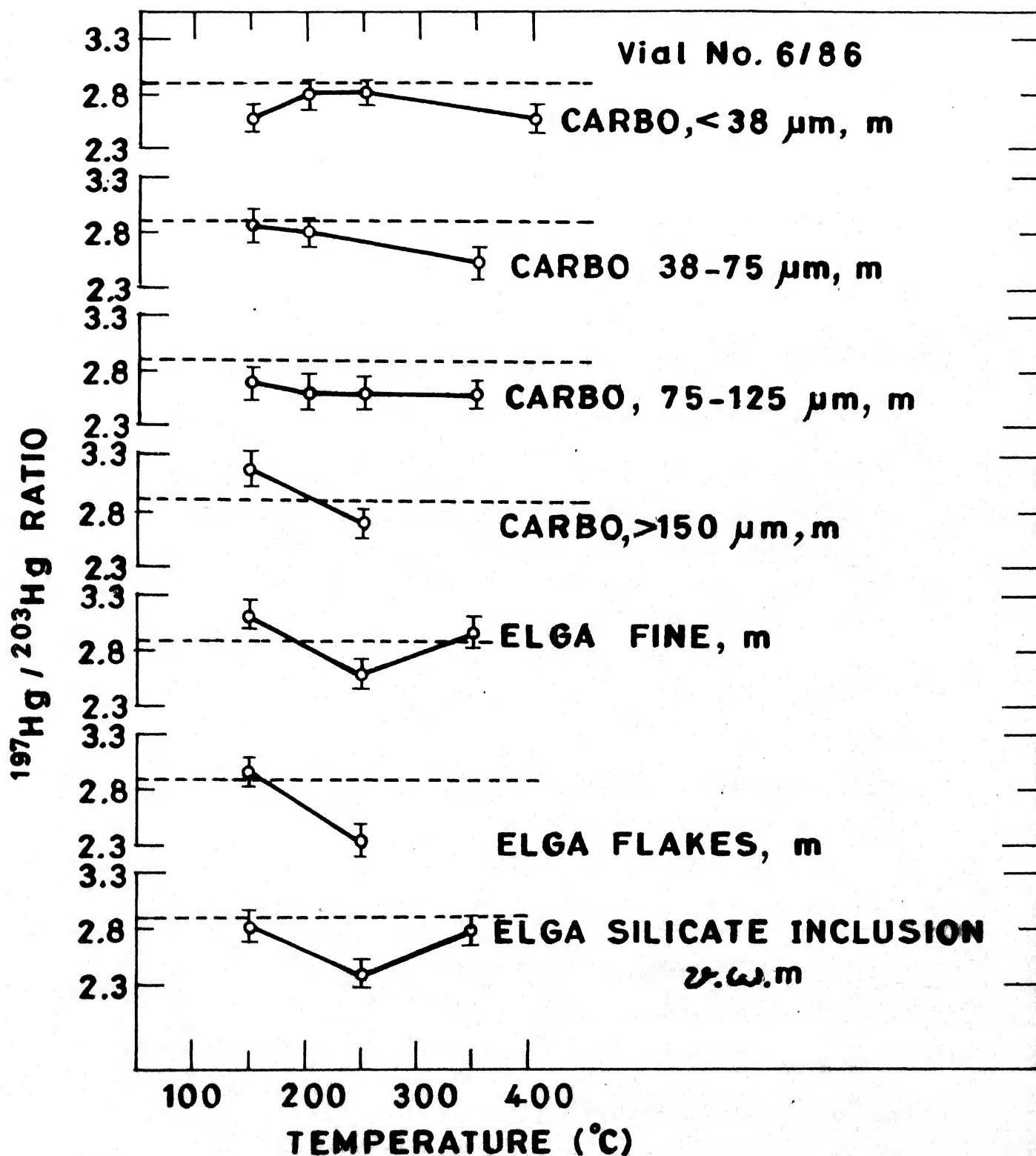


Fig. 3.35 The isotopic ratio data from Vial No. 6/86

result shows the absence of neutron self shielding effect from other samples for the size of our irradiation can.

Results of iron meteorite residues showed a isotopic ratio variation from 3.1 to 2.35 for Elga and from 3.15 to 2.52 for Carbo, whereas the reagent value was 2.9. The spectra of two Elga samples are shown in Figure 3.36. Mercury abundance pattern in case of Elga shows a maximum at lower temperature fraction that decreases sharply with temperature. For Carbo the maximum occurs at a mid temperature fraction with decreasing values on both sides, except for the 75-125  $\mu\text{m}$  size when the maximum is located at the lower temperature (150°C) site.

### 3.16 Vial No. 7/86

Freshly prepared  $\text{H}_2\text{SO}_4$  acid insoluble residue samples from Sikhote Alin, iron meteorite, were packed in aluminium capped quartz tubes for this vial. Post-irradiation distillation steps varied from four to six.

In this vial we found highly isotopically anomalous Hg. The results are presented in Table 3.20. In the spectrum of sample No. 6-3 the 77 keV peak cannot be seen, only the hump due to the 73 keV photon from  $^{203}\text{Hg}$  is observed (Figure 3.37). Sample No. 6-5 is also anomalous but in this case the 77 keV peak is definitely there. Because of its lower abundance it is overshadowed by the 73 keV peak. The same is the case with 7-2 and 7-4. Surprisingly 7-3 is a normal sample. The spectrum of 7-3 is compared with that of 7-2 in Figure 3.38. Other anomalous

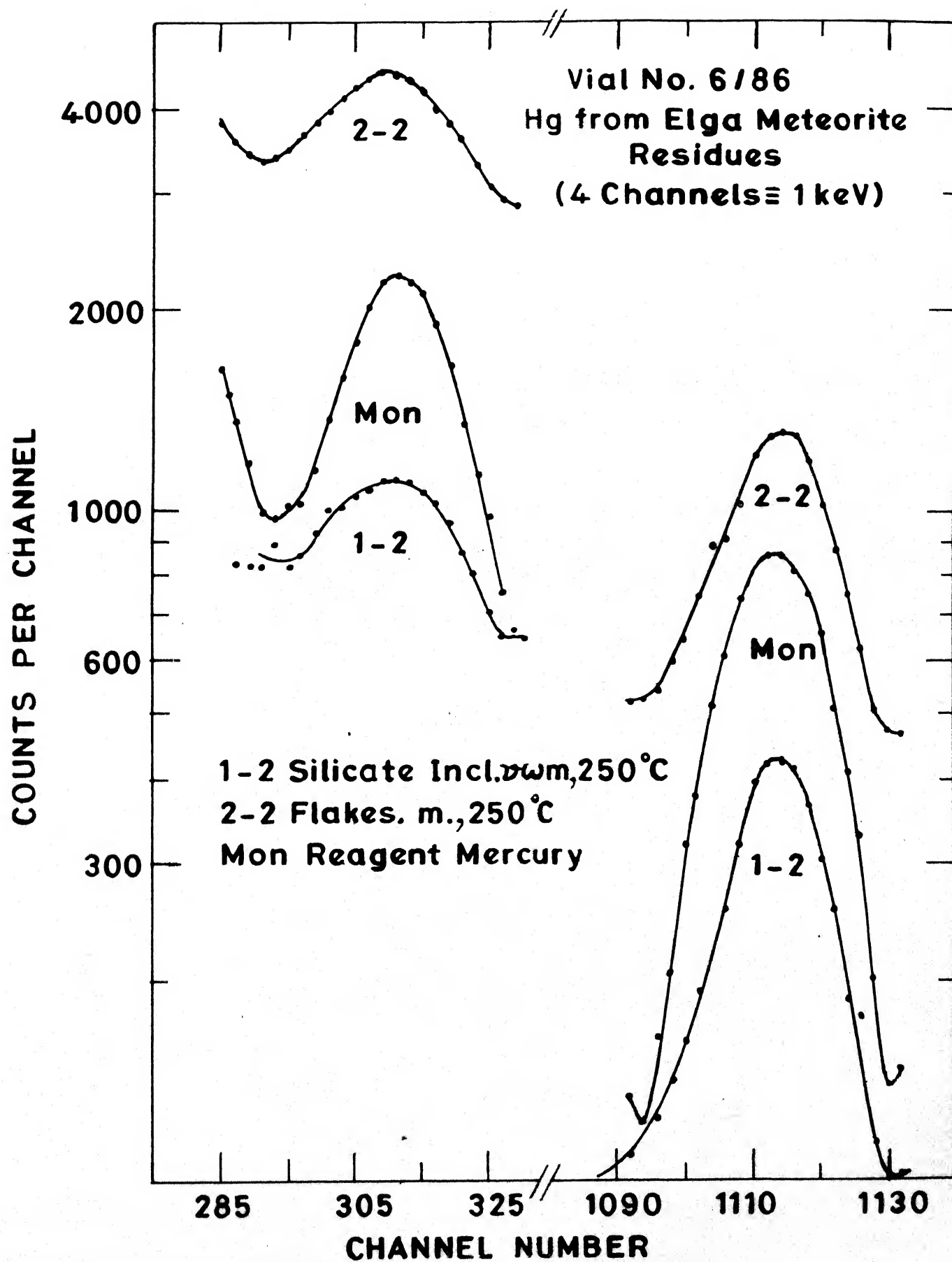


Table 3.20 Vial No. 7/86 Mercury from Sikhote Alin Residues

Sample	Mass (mg)	T (°C)	Code	cps/10	ppm (Hg)	$^{197}\text{Hg}/^{203}\text{Hg}$	R/R <sup>+</sup>
Inclusion	332.5	150	1-1	0.25	0.09	1.25±0.1	0.86(7)
		175	1-2	0.06	0.02	-	
		200	1-3	0.12	0.04	-	
		225	1-4	Low	-		
		250	1-5	Low	-		
		300	1-6	Low	-		
<u>Non Magnetic</u>							
150-300 $\mu\text{m}$	25.4	150	2-1	4.89	21.82	1.56, 1.65	1.10(6)
		200	2-2	1.52	6.78	1.61, 1.28±0.1	1.10(6)
		250	2-3	0.31	1.38	1.29±0.2	0.89(12)
		300	2-4	0.27	1.20	1.32±0.1	0.91(7)
		400	2-5	Low	-		
< 150 $\mu\text{m}$	39.6	150	3-1	Low	-		
		200	3-2	3.62	10.36	1.36	0.94(5)
		250	3-3	0.55	1.57	1.24±0.1, 1.32±0.2	0.90(5)
		300	3-4	0.29	0.83	-	
		400	3-5	Low	-		
<u>Magnetic</u>							
<38 $\mu\text{m}$	84.8	150	4-1	4.10	5.48	1.61, 1.51	1.10(5)
		200	4-2	18.75	25.06	1.63	1.12(5)
		250	4-3	4.20	5.61	1.34, 1.59	0.97(5)
		300	4-4	1.95	2.61	1.46, 1.47	1.01(6)

Contd.....

Table 3.20 continued

Sample	Mass (mg)	T(°C)	Code	cps/10	ppm (Hg)	$^{197}\text{Hg}/^{203}\text{Hg}$	R/R <sup>+</sup>
<u>Magnetic</u>							
38-45 $\mu\text{m}$	82.2	150	5-1	0.05	0.07	-	
		200	5-2	0.60	0.83	-	
		250	5-3	2.02	2.79	1.44±0.1	0.99(7)
		300	5-4	1.59	2.19	1.64	1.13(6)
45-75 $\mu\text{m}$	75.2	150	6-1	Low	-		
		200	6-2	Low	-		
		250	6-3	7.33	11.05	<0.017, <0.05	<0.01(2 $\sigma$ )
		300	6-4	0.15	0.23	-	
		400	6-5	0.36	0.54	1.06±0.1	0.73(7)
75-106 $\mu\text{m}$	64.0	200	7-1	Low	-		
		250	7-2	1.02	1.81	0.27±0.02	0.19(1)
		300	7-3	4.67	8.27	1.49±0.01, 1.74±0.1	1.03(5)
		400	7-4	0.43	0.76	<0.59, <0.30	<0.41(2 $\sigma$ )
106-125 $\mu\text{m}$	95.5	200	8-1	8.45	10.03	1.51	1.04(5)
		250	8-2	2.68	3.18	1.40±0.1	0.97(7)
		300	8-3	1.22	1.44	1.02±0.2, 1.37±0.1	0.94(7)
		400	8-4	1.14	1.36	1.64	1.13(6)
Monitor-Hg	0.34 $\mu\text{g}$		Mon.	3.00		1.44, 1.49, 1.45, 1.37, 1.39, 1.50	1.00(4)

Powdered Samples irradiated in Al-capped quartz tubes. Errors are usually less than  $\pm 5\%$  unless otherwise stated.

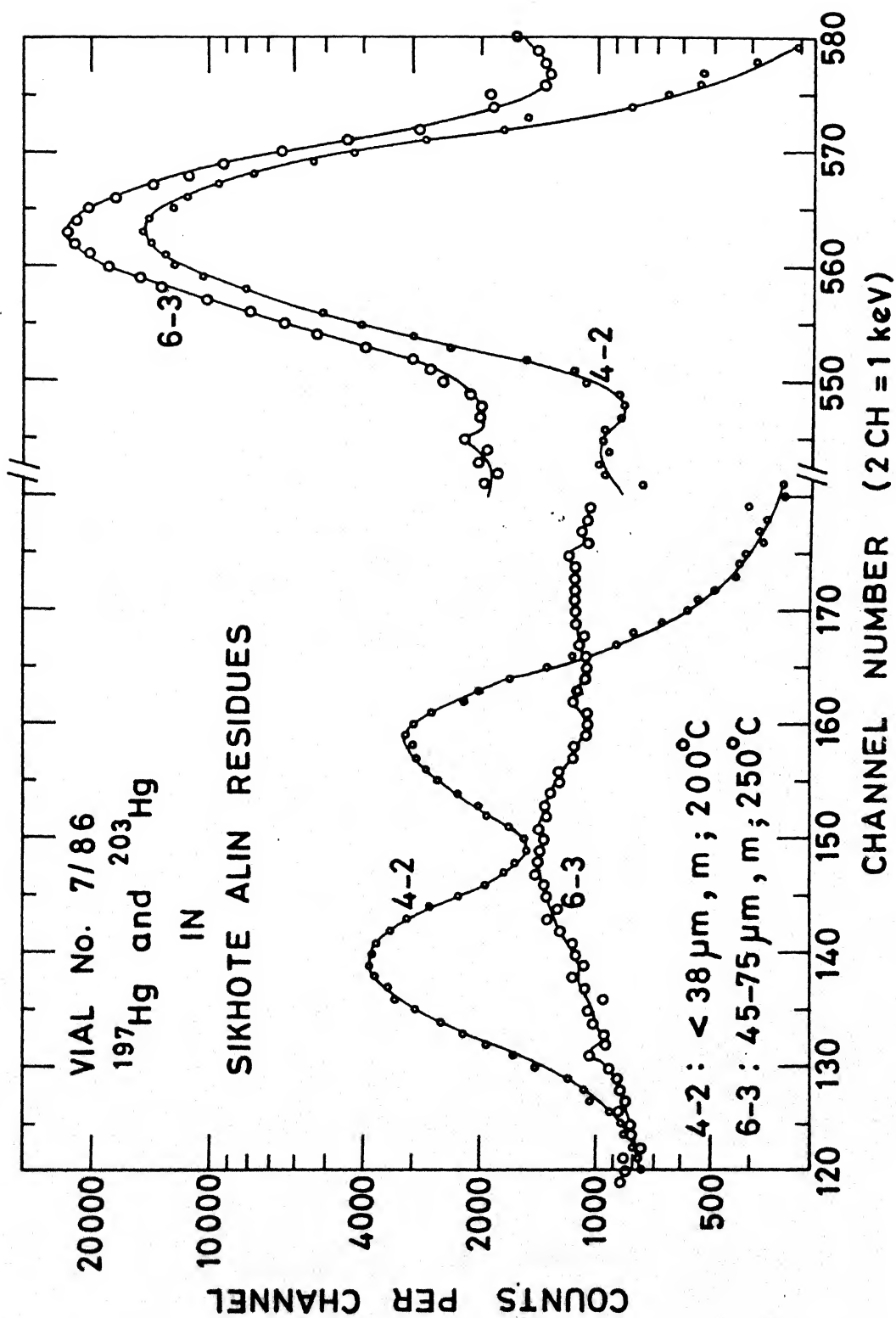


Fig. 3.37 Photon spectra of normal and anomalous samples of Sikhote Alin residue

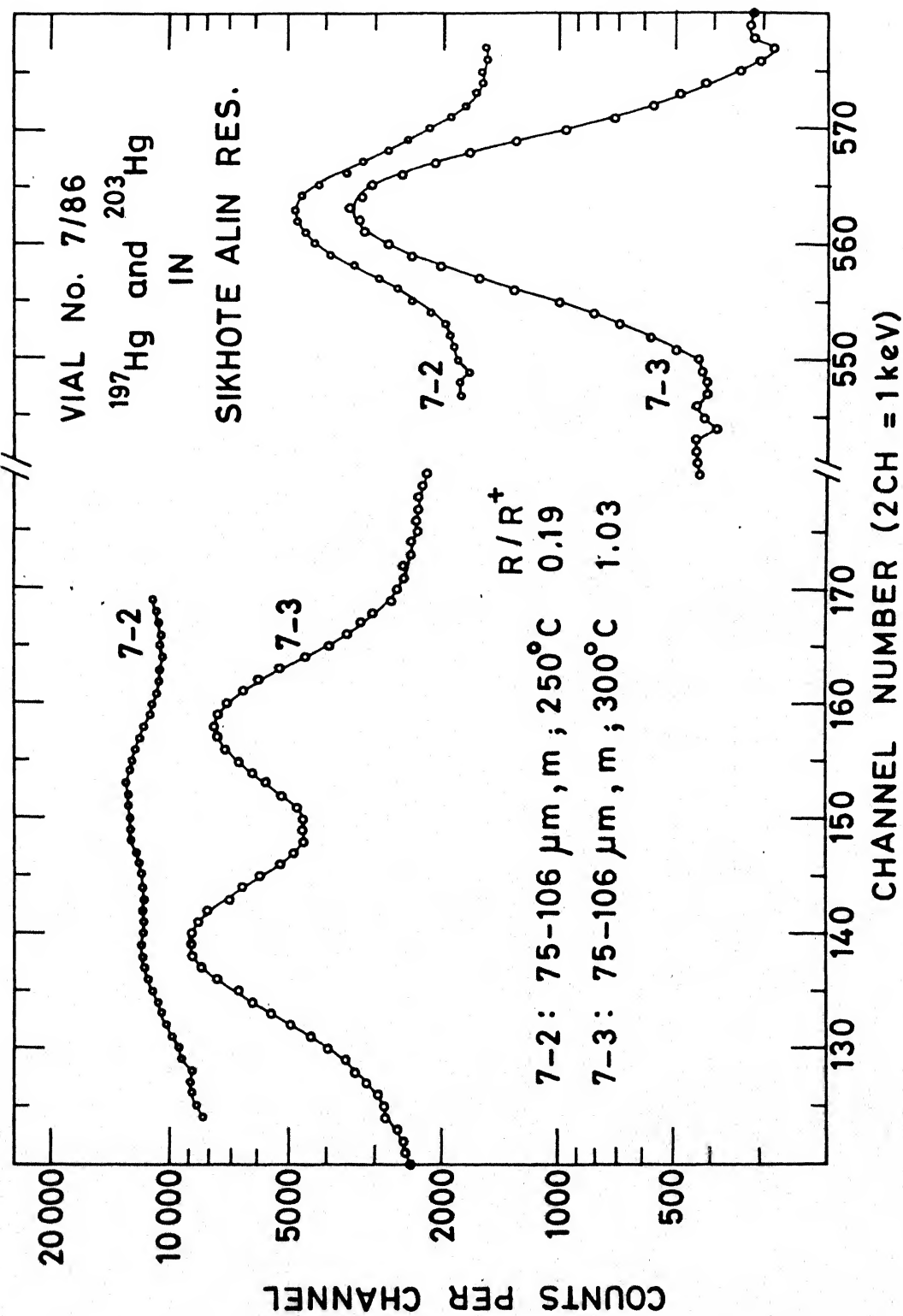


Fig. 3.38 Photon spectra of some samples of Sikhote Alin residue



samples 7-4 and 6-5 are compared with the normal sample 8-3 in Figure 3.39.

We followed the decay lines of the anomalous samples along with the other normal samples. In the case of the anomalous samples, since the short lived species is missing, only the long lived  $^{203}\text{Hg}$  could be followed. The decay points for more than two half lives of  $^{203}\text{Hg}$  are shown in Figures 3.40 and 3.41. All points lie on the theoretical line.

It was decided to preserve the samples for reirradiation and/or mass spectrometric studies to verify the results further. Our distillation process involved the use of mercury manometer in the vacuum line exposing the sample to the mercury vapour that might be present in the line. The presence of this inert mercury might dilute the original inherent mercury of the sample which may in turn cause isotopic dilution. Moreover, carrier Hg was used to purify the monitor. It was thus decided not to use mercury manometer for pressure measurement in the vacuum line. Instead a thermoionic vacuum gauge was used. Also the chemistry of monitor was modified by avoiding the use of carrier and a number of steps to minimise contamination. Repeat measurements on some of the aliquots of these residues were done by fresh bombardment in vial No. 9/86.

### 3.17 Vial No. 8/86

About one gram Ambapur Nagla fragments and two pieces of gold coated mylar films were irradiated. After activation one

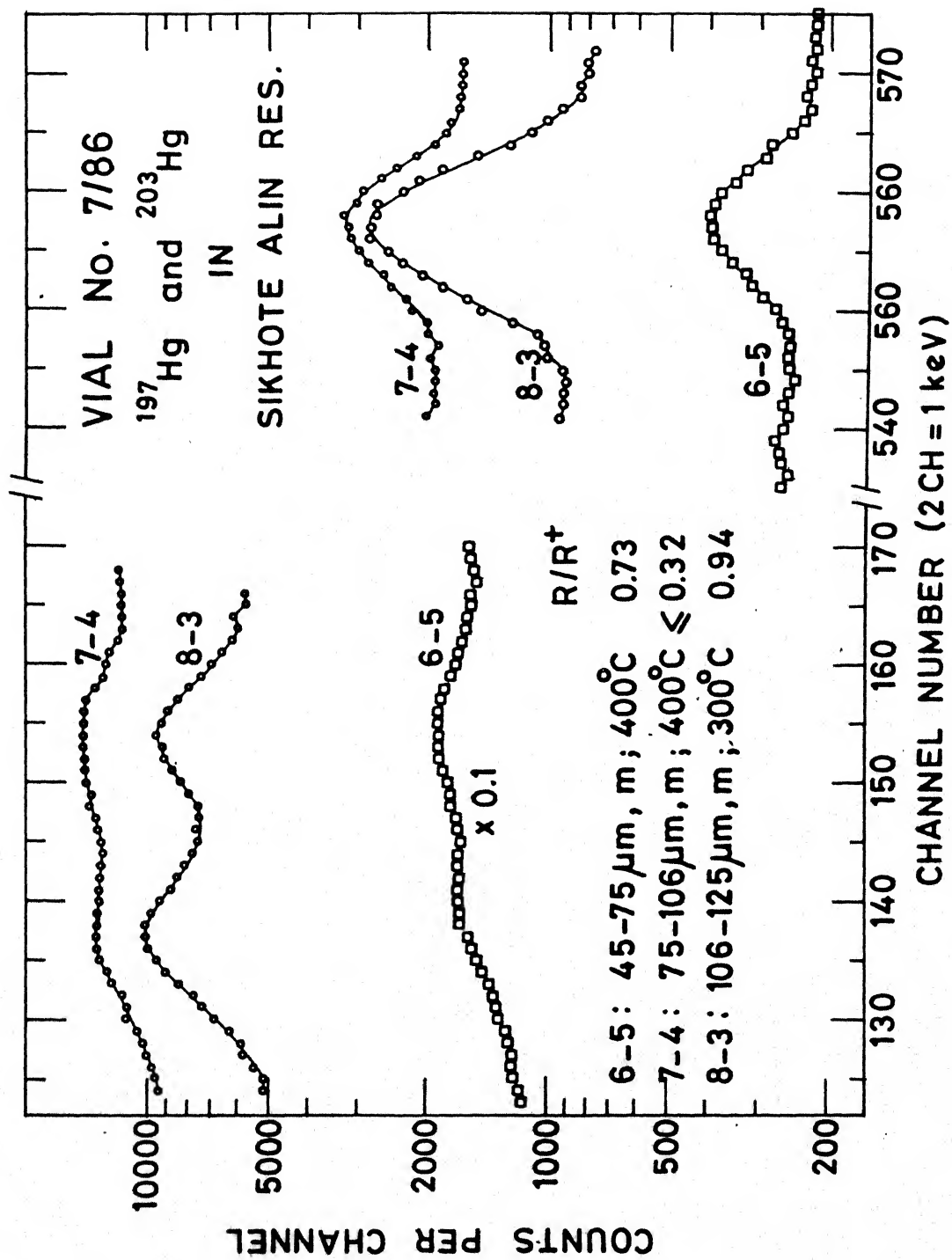


Fig. 3.39 Photon spectra of some samples of Sikhote Alin residue

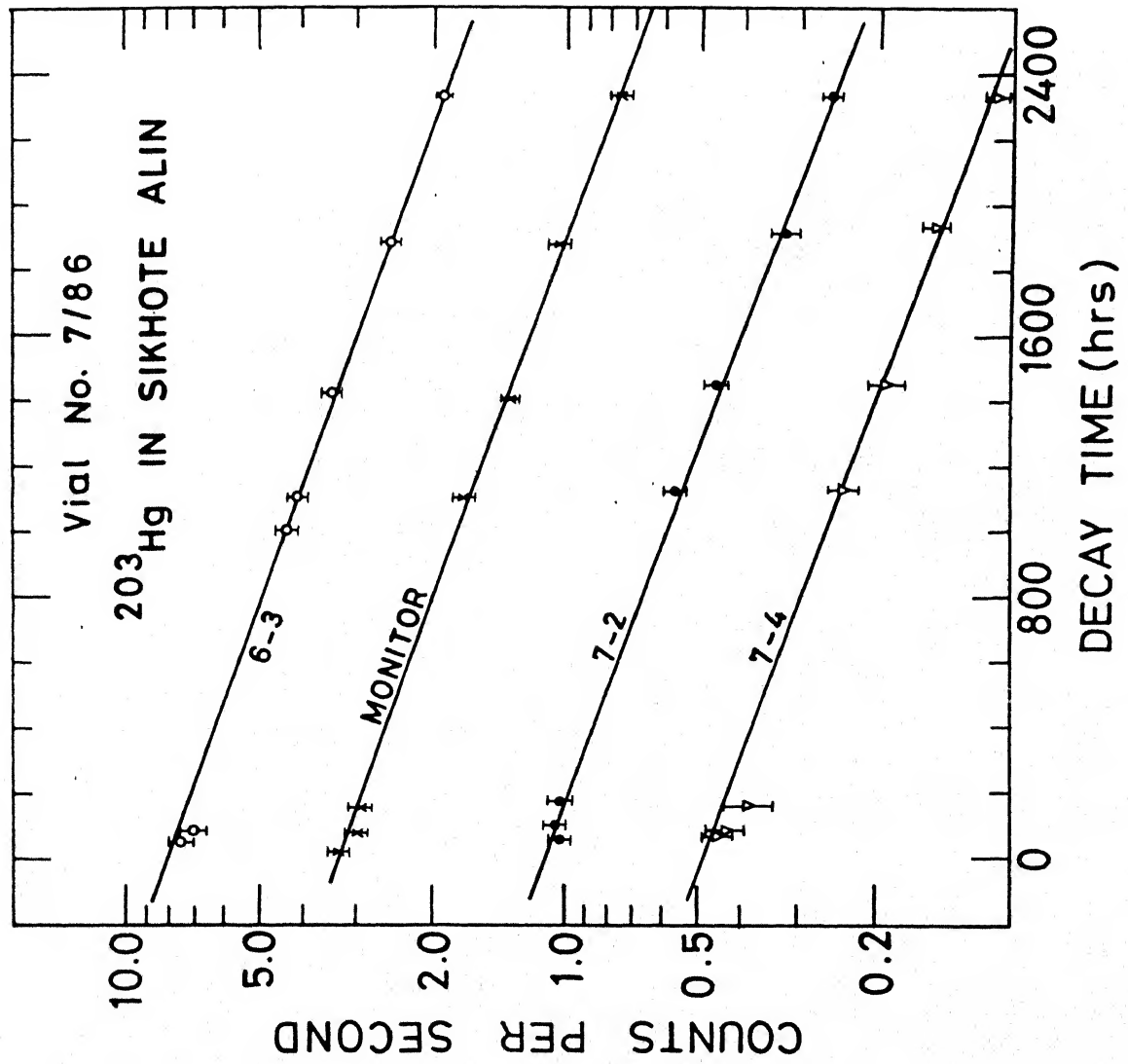


Fig. 3.40 Decay lines of  $^{203}\text{Hg}$  from samples of Sikhote Alin residue

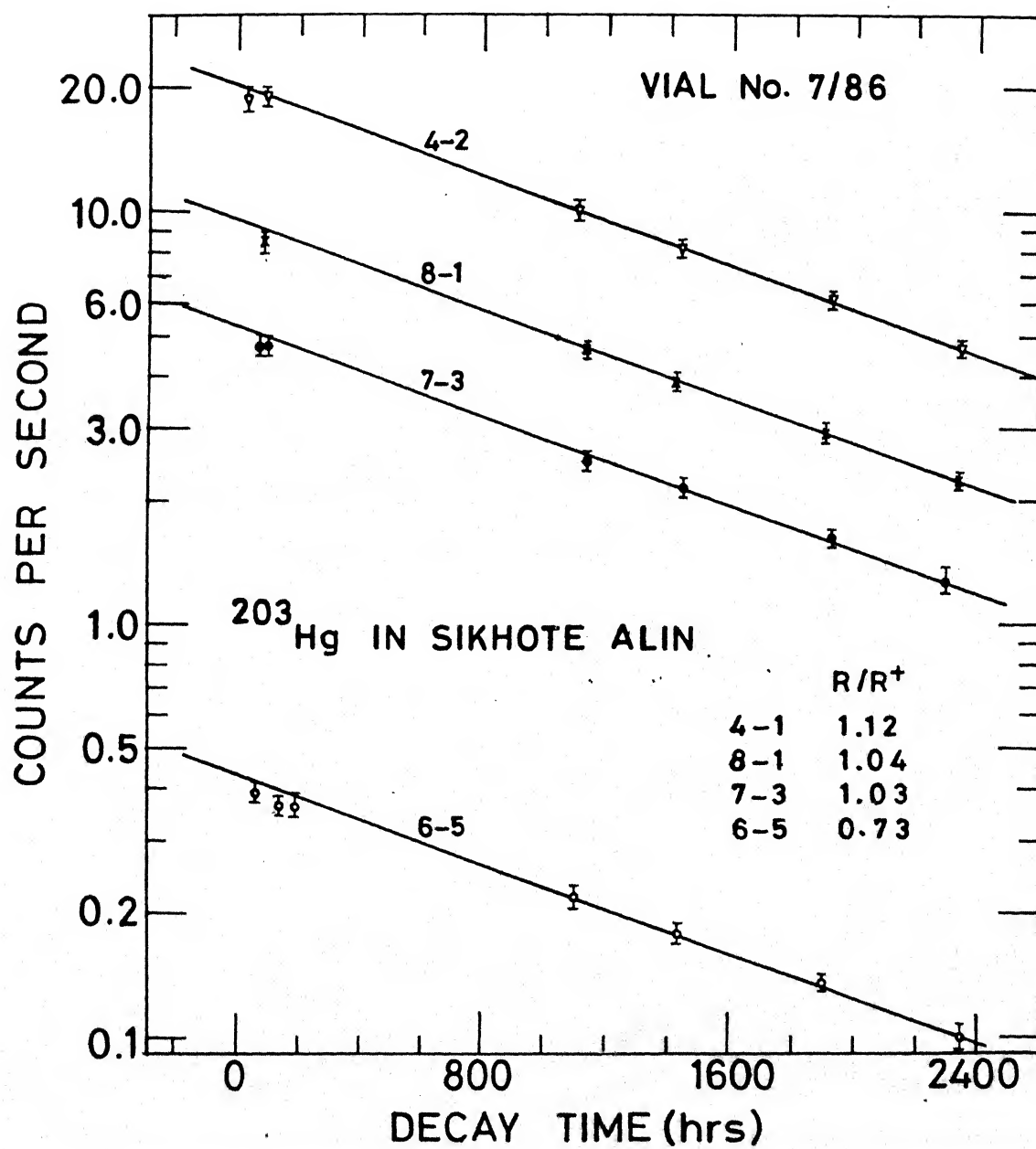


Fig. 3.41 Decay lines of  $^{203}\text{Hg}$  from samples of Sikhote Alin residue

fragment was powdered to make bulk sample. Other fragments were crushed, mixed and separated into, coarse (mostly chondrules) magnetic and non-magnetic samples. All these samples were heated in six temperature steps to extract Hg. A major modification that was made from this vial onwards was the closing of mercury manometer part of the vacuum line. Also no Hg carrier was used in the radiochemical purification <sup>9</sup> if the monitor. All this was to avoid the addition of reagent mercury to a sample, so that it could be reirradiated for further verification, if desired.

The trend of the anomaly found is of similar nature as in the earlier cases of Ambapur Nagla (Figures 3.42 and 3.43), viz., lower than normal, above normal, normal, and again lower than normal with the increase of temperature. The results are given in Table 3.21. Sample 3-1, having good counting rate, is clearly anomalous. The short lived species is almost absent. Its spectrum is given in Figure 3.44 where it is compared with another abnormal sample 3-2 and the spectrum of the reagent Hg. Sometimes the errors are large for two reasons: (i) the counting rate was poor and (ii) previous samples took longer times of counting so that the short-lived species decayed off. These measurements are rated to fall in category B or C in terms of their reliabilities. The chondrule sample, 1-1 is below normal and 1-2 is slightly above normal. The spectra of samples 1-1 and 1-2 are compared with that of the standard in Figure 3.45. Spectra of the other less abnormal samples are given in

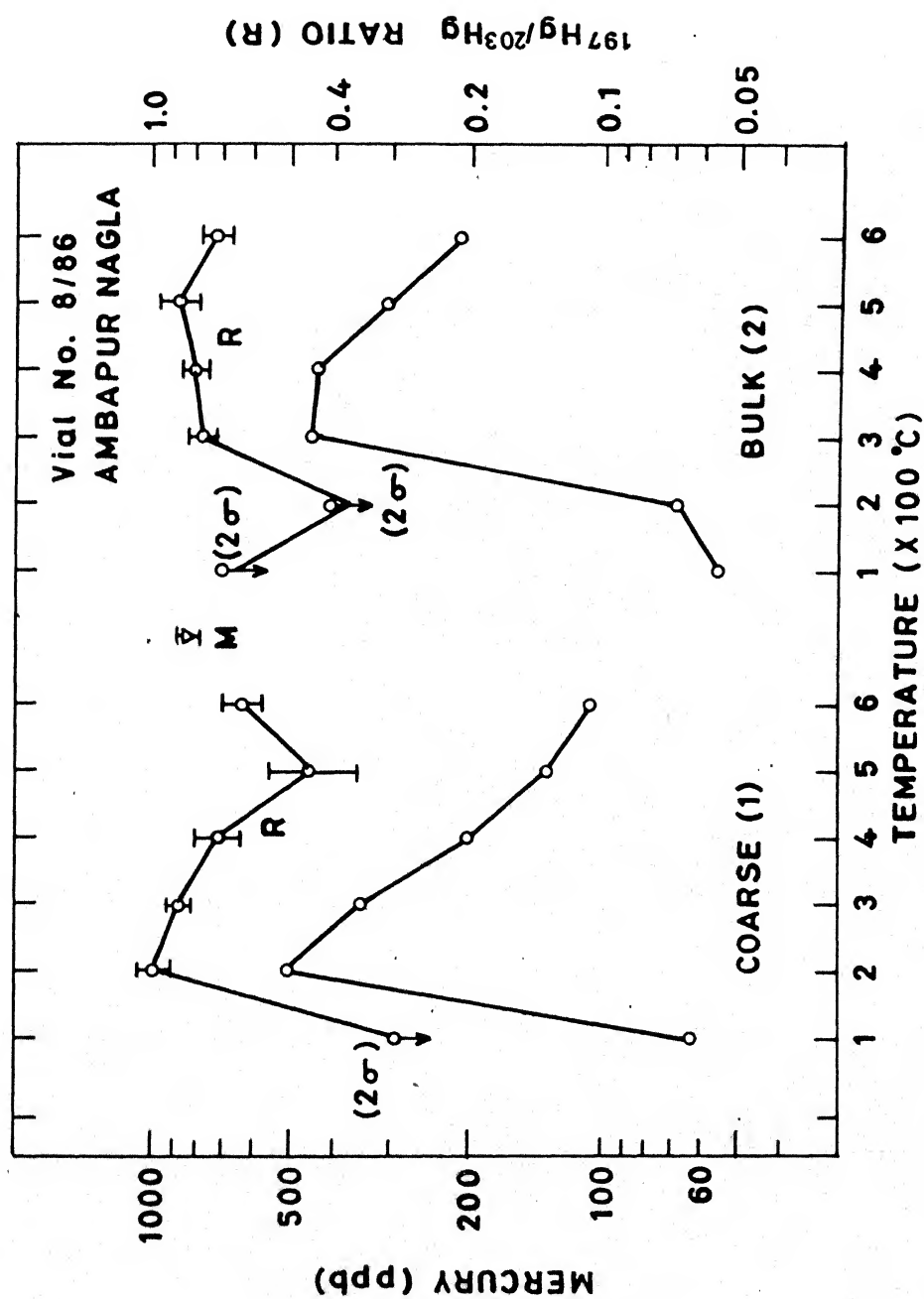


Fig. 3.42 Mercury concentration (left scale) and its isotopic ratios (right scale) measured at different temperatures in samples of Ambapur Nagla

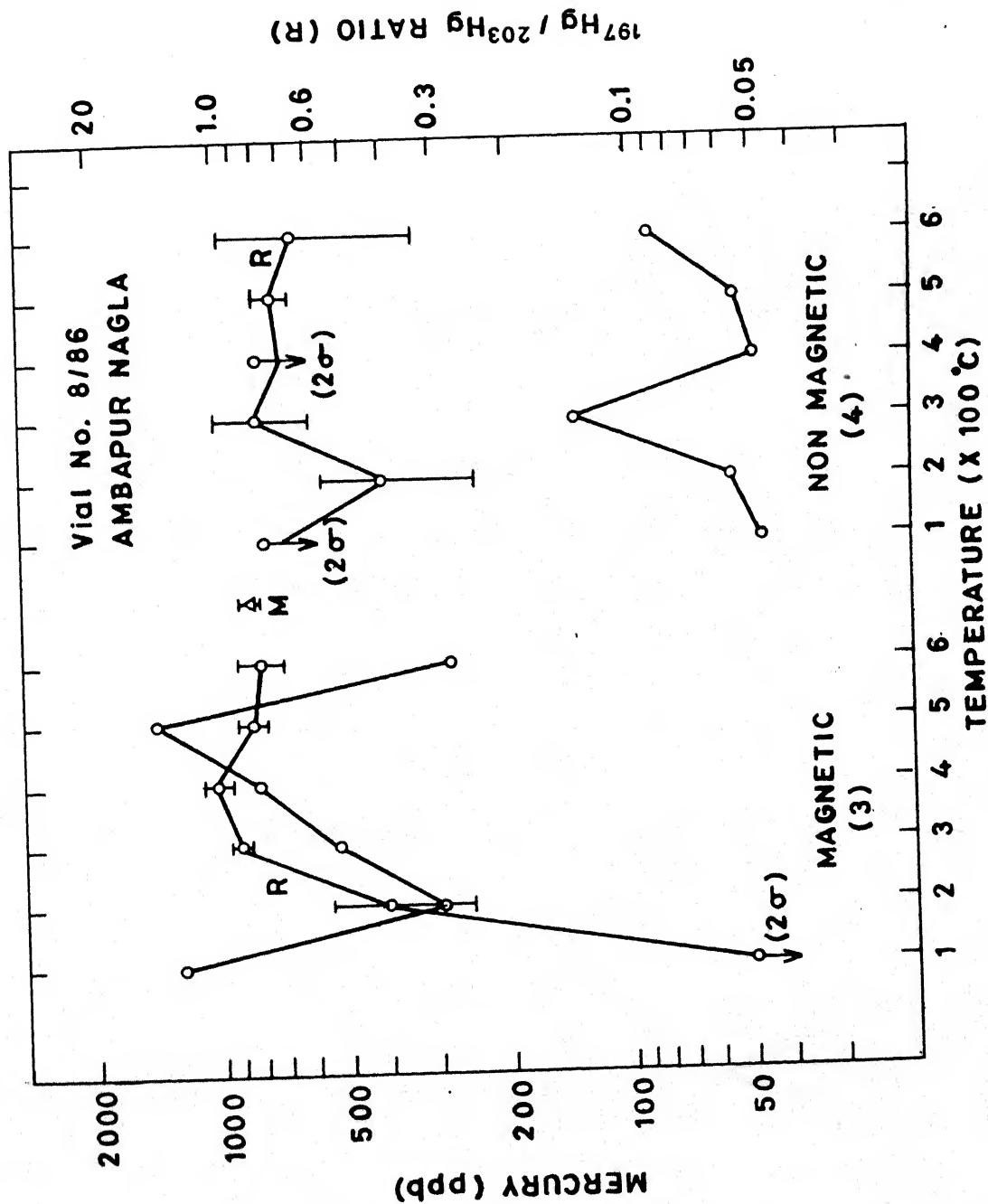
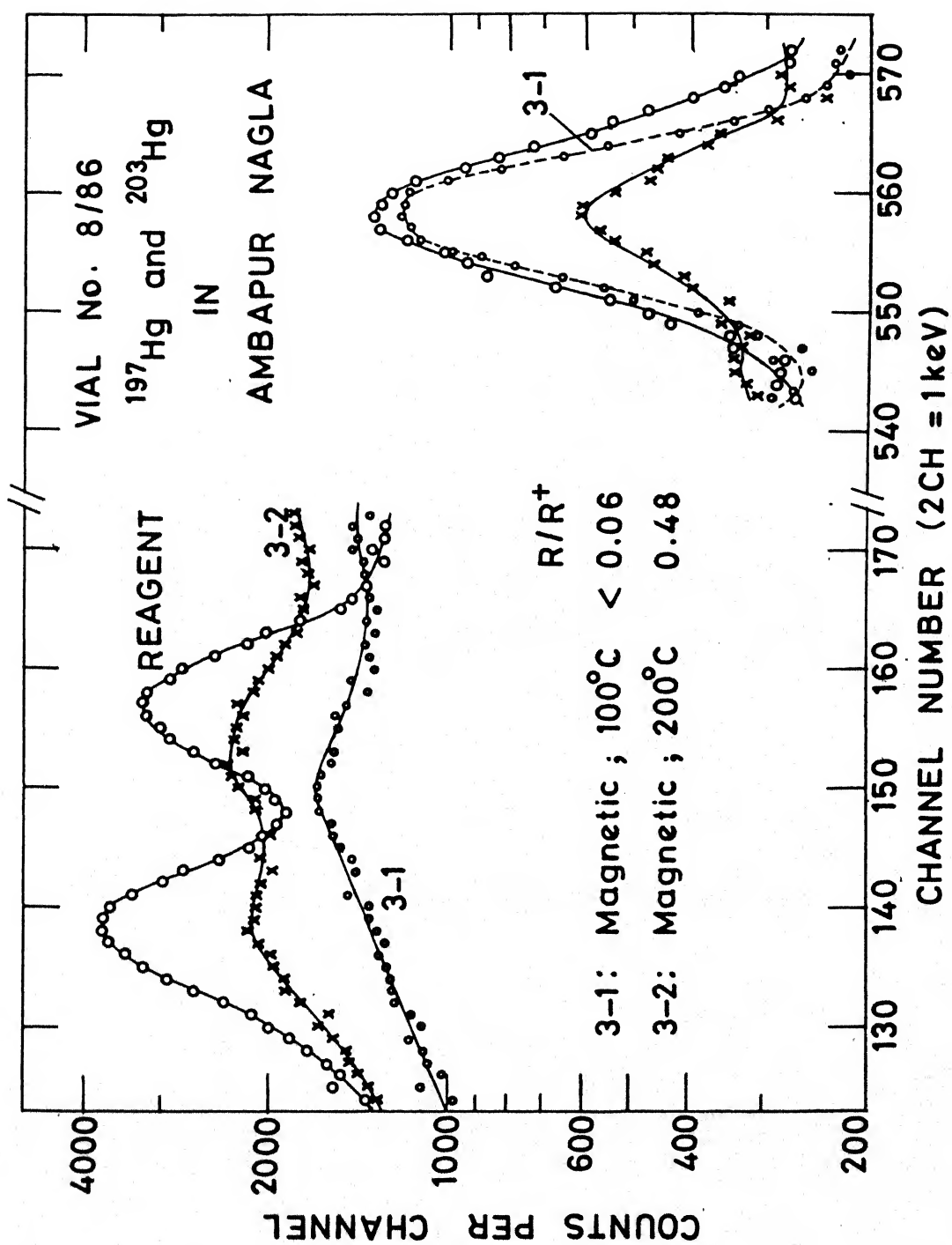


Fig. 3.43 Mercury concentration (left scale) and its isotopic ratios (right scale) measured at different temperatures in samples of Ambapur Nagla

Table 3.21 Vial No. 8/86 Mercury from Ambapur Nagla fragments

Sample	Mass (mg)	T(°C)	Code	cps/10	ppb (Hg)	$^{197}\text{Hg}/^{203}\text{Hg}$ Ratio	R/R <sup>+</sup>
Coarse, Mag. (mostly Chondrules)	304.0	100	1-1	0.16	62.8	<0.29(2 $\sigma$ ), <0.2(2 $\sigma$ )	<0.3(2 $\sigma$ )
		200	1-2	1.28	501.5	0.99 $\pm$ 0.06, 0.94 $\pm$ 0.04	1.13(7)
		300	1-3	0.88	345.6	0.87 $\pm$ 0.04	1.05(5)
		400	1-4	0.51	200.7	0.72 $\pm$ 0.08	0.87(9)
		500	1-5	0.34	133.1	0.50 $\pm$ 0.10, 0.4 $\pm$ 0.1	0.60(10)
		600	1-6	0.28	108.0	0.63 $\pm$ 0.06	0.76(7)
Bulk (one fragment)	216.0	100	2-1	0.10	55.3	<0.7(2 $\sigma$ )	<0.84(2 $\sigma$ )
		200	2-2	0.12	68.0	<0.4(2 $\sigma$ )	<0.48(2 $\sigma$ )
		300	2-3	0.81	449.9	0.77 $\pm$ 0.05	0.93(6)
		400	2-4	0.79	437.2	0.80 $\pm$ 0.05	0.96(6)
		500	2-5	0.55	305.1	0.87 $\pm$ 0.09	1.05(10)
		600	2-6	0.38	212.2	0.72 $\pm$ 0.05	0.87(6)
Fine (Magnetic)	153.6	100	3-1	1.65	1282.3	<0.05(2 $\sigma$ )	<0.06(2 $\sigma$ )
		200	3-2	0.38	296.1	0.4 $\pm$ 0.15	0.48(18)
		300	3-3	0.68	526.2	0.91 $\pm$ 0.03	1.10(4)
		400	3-4	1.05	816.0	1.02 $\pm$ 0.08	1.23(10)
		500	3-5	1.82	1412.1	0.84 $\pm$ 0.06	1.01(7)
		600	3-6	0.35	272.0	0.8 $\pm$ 0.1	0.96(12)
Fine (Non.Mag.)	292.1	100	4-1	0.11	46.2	<0.65(2 $\sigma$ )	<0.78(2 $\sigma$ )
		200	4-2	0.14	55.6	0.4 $\pm$ 0.16	0.48(19)
		300	4-3	0.33	134.9	0.8 $\pm$ 0.2	0.96(24)
		400	4-4	0.09	39.6	<0.8(2 $\sigma$ )	<0.96(2 $\sigma$ )
		500	4-5	0.13	53.9	0.74 $\pm$ 0.07	0.89(8)
		600	4-6	0.22	87.9	0.65 $\pm$ 0.32	0.78(38)
Monitor-Hg	0.96 $\mu\text{g}$	-	Mon.	8.00	-	0.83 $\pm$ 0.03	1.00(4)





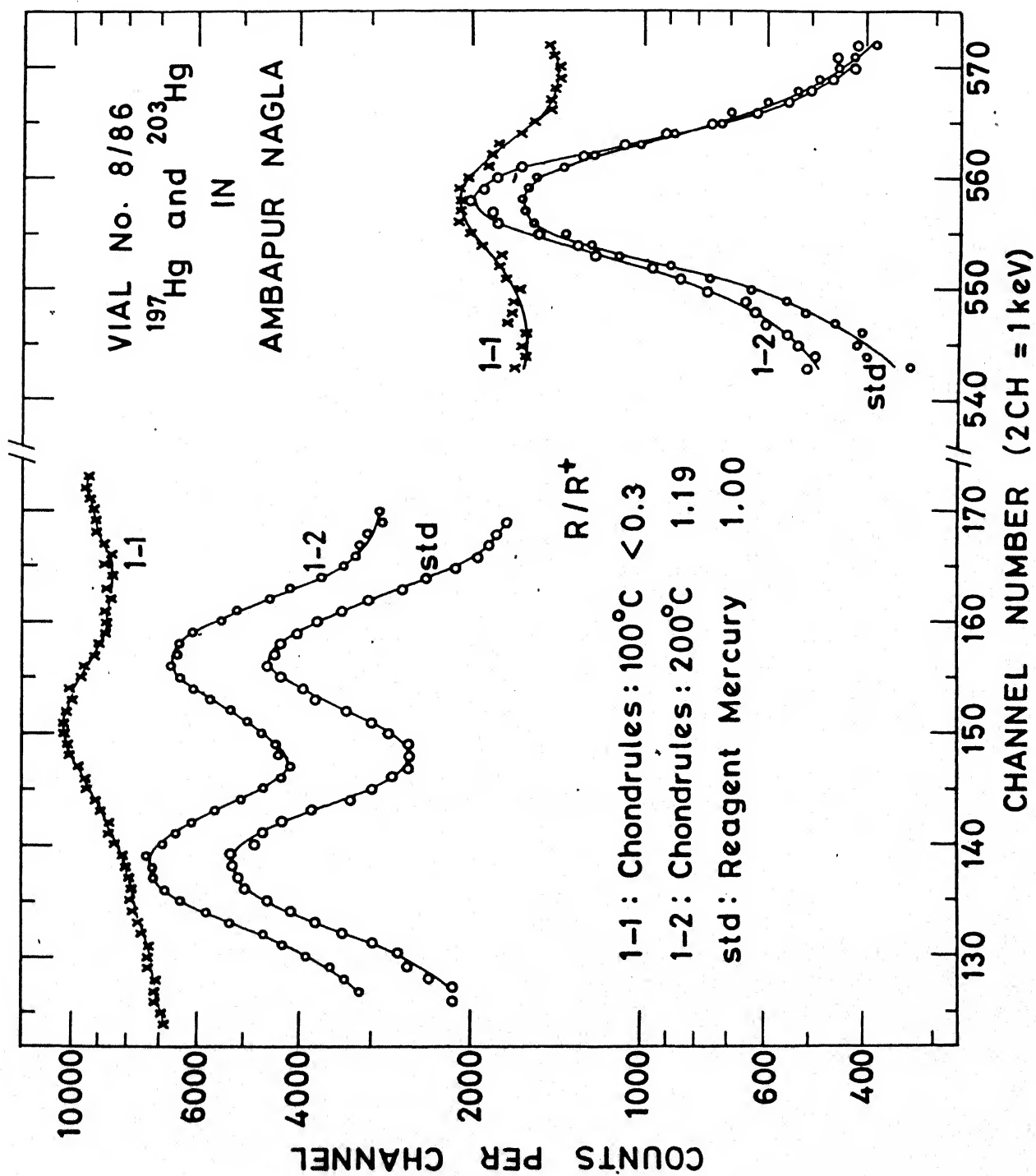


Fig. 3.45 Photon spectra of some samples of Ambapur Nagla

Figures 3.46 and 3.47. The Arrhenious plot of mercury released is shown in Figures 3.48 and 3.49. It looks more complicated than it was in vial No. 9/85. Presumably there are several activation energies involved in the process of the distillation of Hg.

Photon spectra of all samples were recorded. Their decays were also followed. The decay of ratios followed for some samples are given in Figure 3.50. The decay lines of  $^{203}\text{Hg}$  were followed upto more than two half lives and are given in Figures 3.51 and 3.52.

Gold foil upon distillation gave huge counting rate for  $^{203}\text{Hg}$  as well as  $^{198}\text{Au}$  (typically more than 1000 counts per second). This forced us to drop the idea of using gold foil (available with us) for transplanting the Hg samples and to get it reirradiated. The aluminium foils showed negligible amount of Hg activity.

### 3.18 Vial No. 9/86

This run was undertaken with the prime objective to repeat the measurements of vial No. 7/86 that gave anomalous isotopic ratios. Other aliquots of sample No. 6 (45-75  $\mu\text{m}$ , mag.) and 7 (75-106  $\mu\text{m}$ , mag.) of 7/86 were packed in aluminium capped quartz tubes. The first sample (45-75  $\mu\text{m}$ , mag.) was distilled at seven temperature steps and the spectra were found to be clean. In the second sample the spectra of first three distillates showed

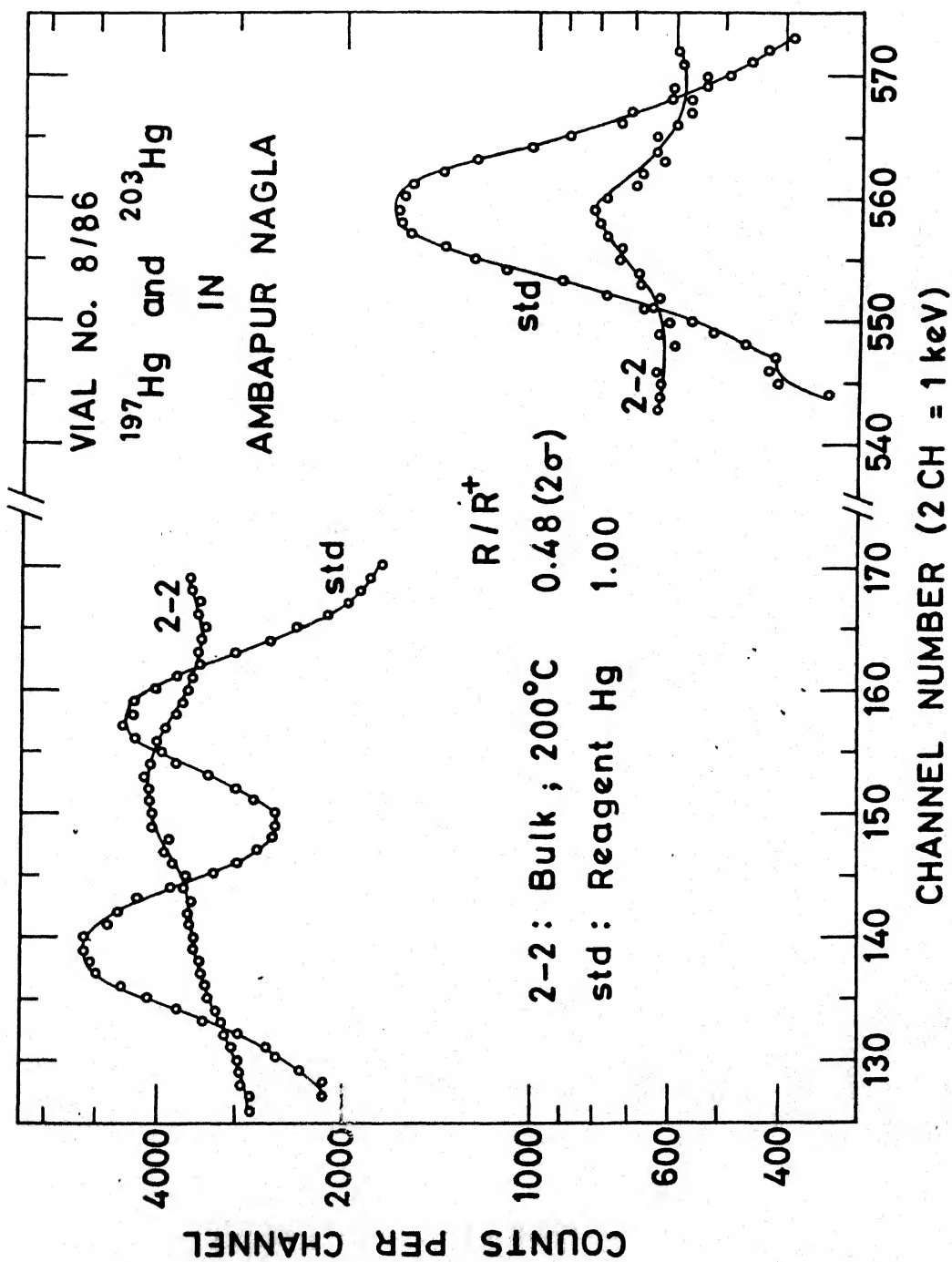


**Fig. 3.46** Photon spectra of some samples of Ambapur Nagla

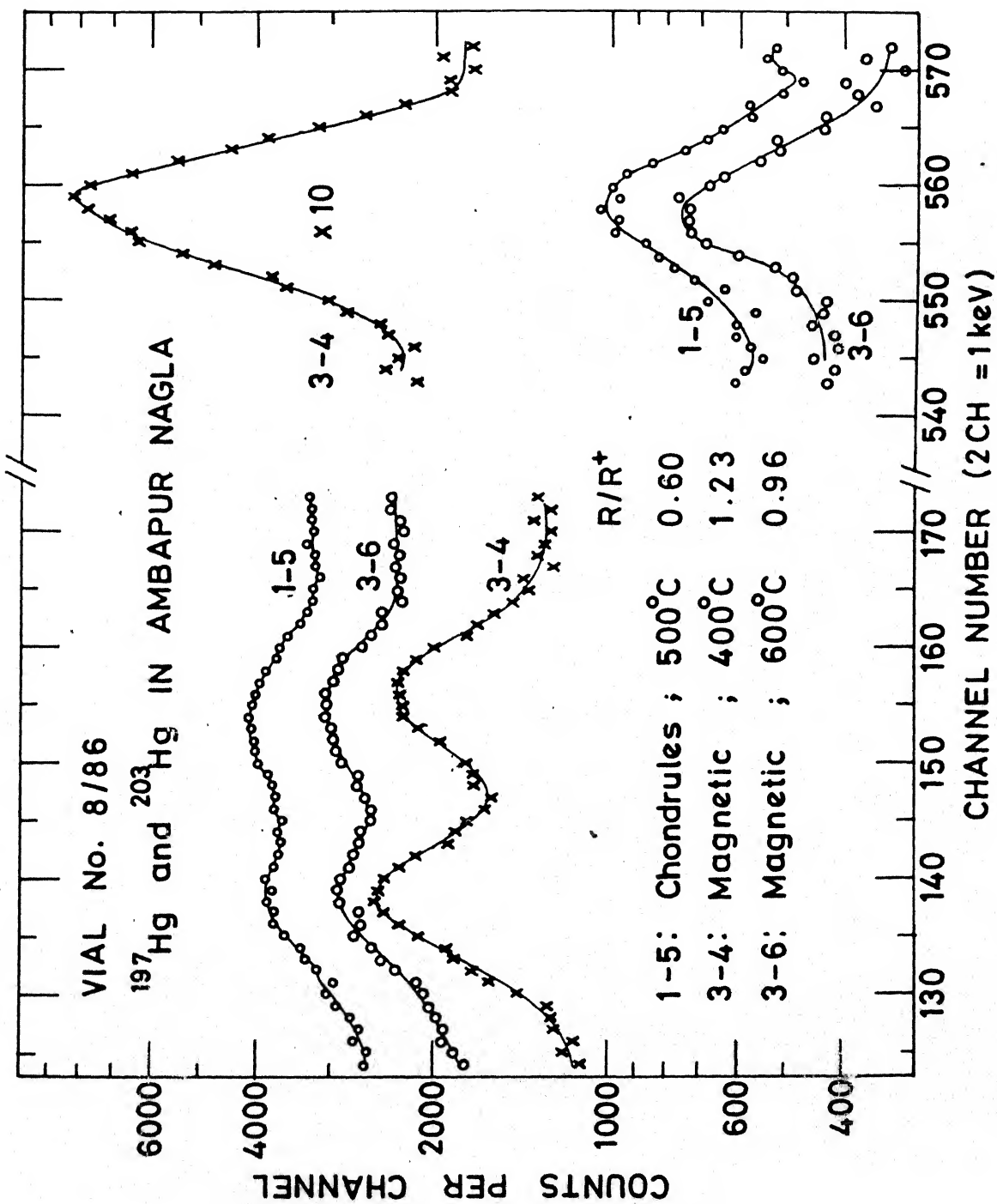


Fig. 3.47 Photon spectra of some samples of Ambapur Nagla

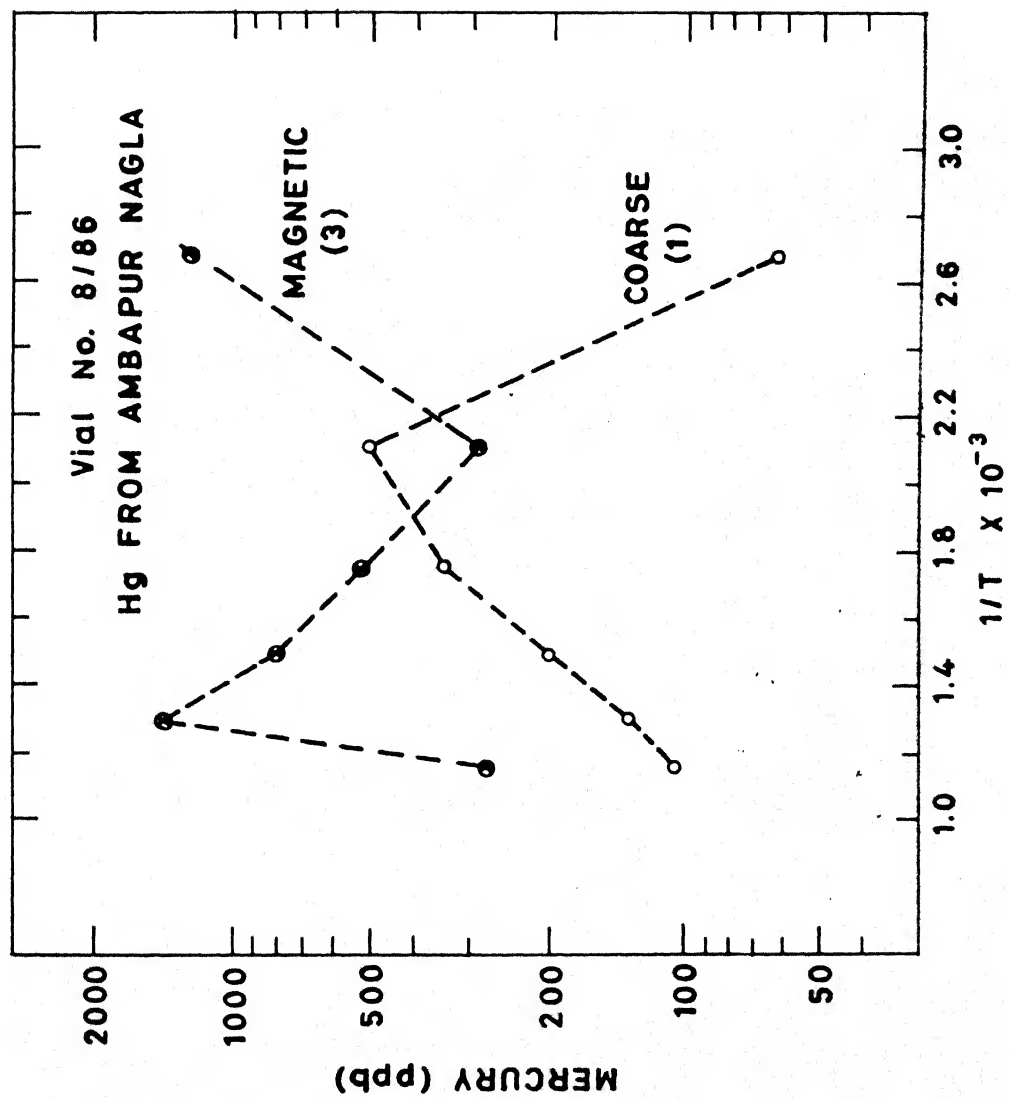


Fig. 3.48 Arrhenius plot for mercury released

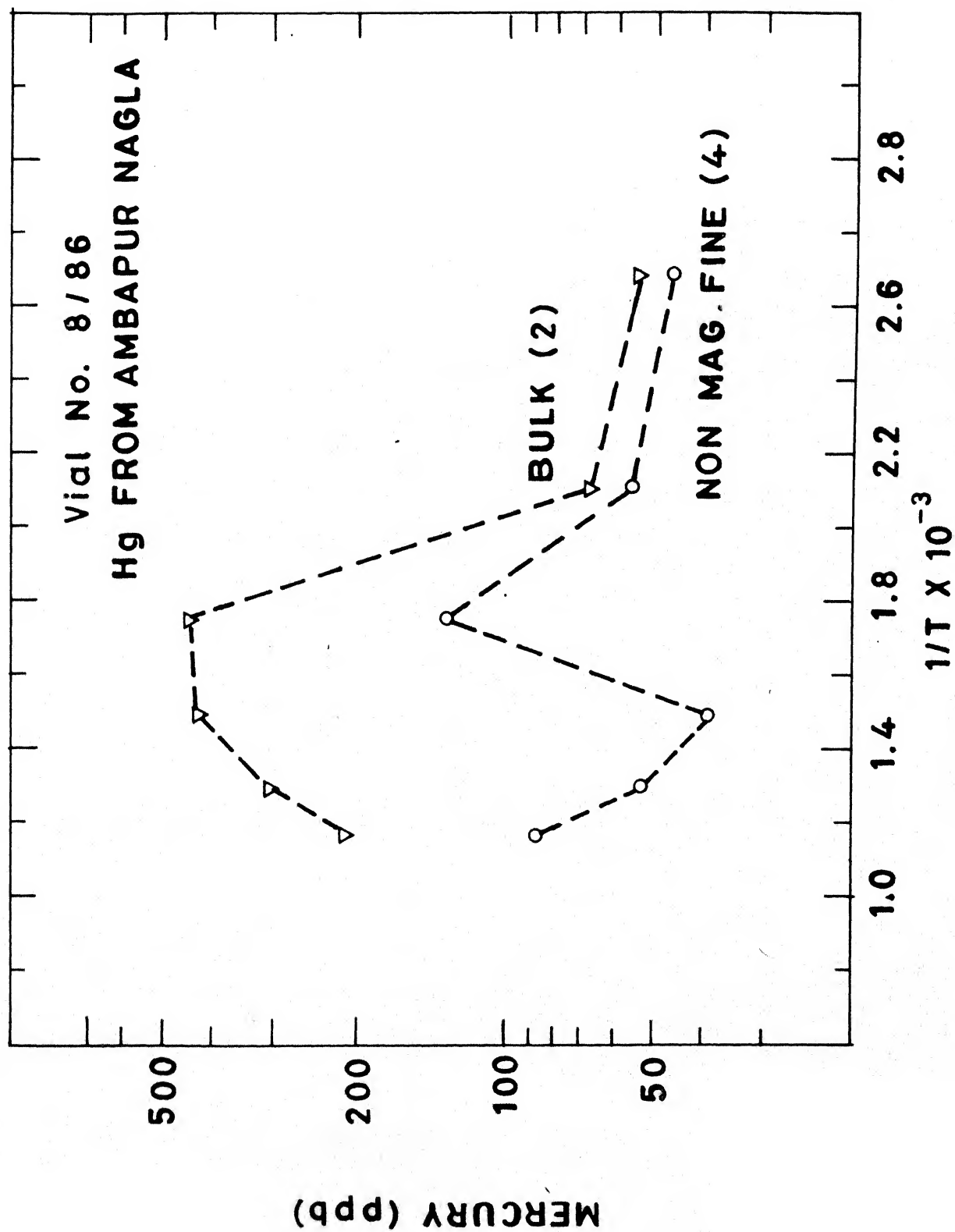


Fig. 3.49 Arrhenius plot for mercury released

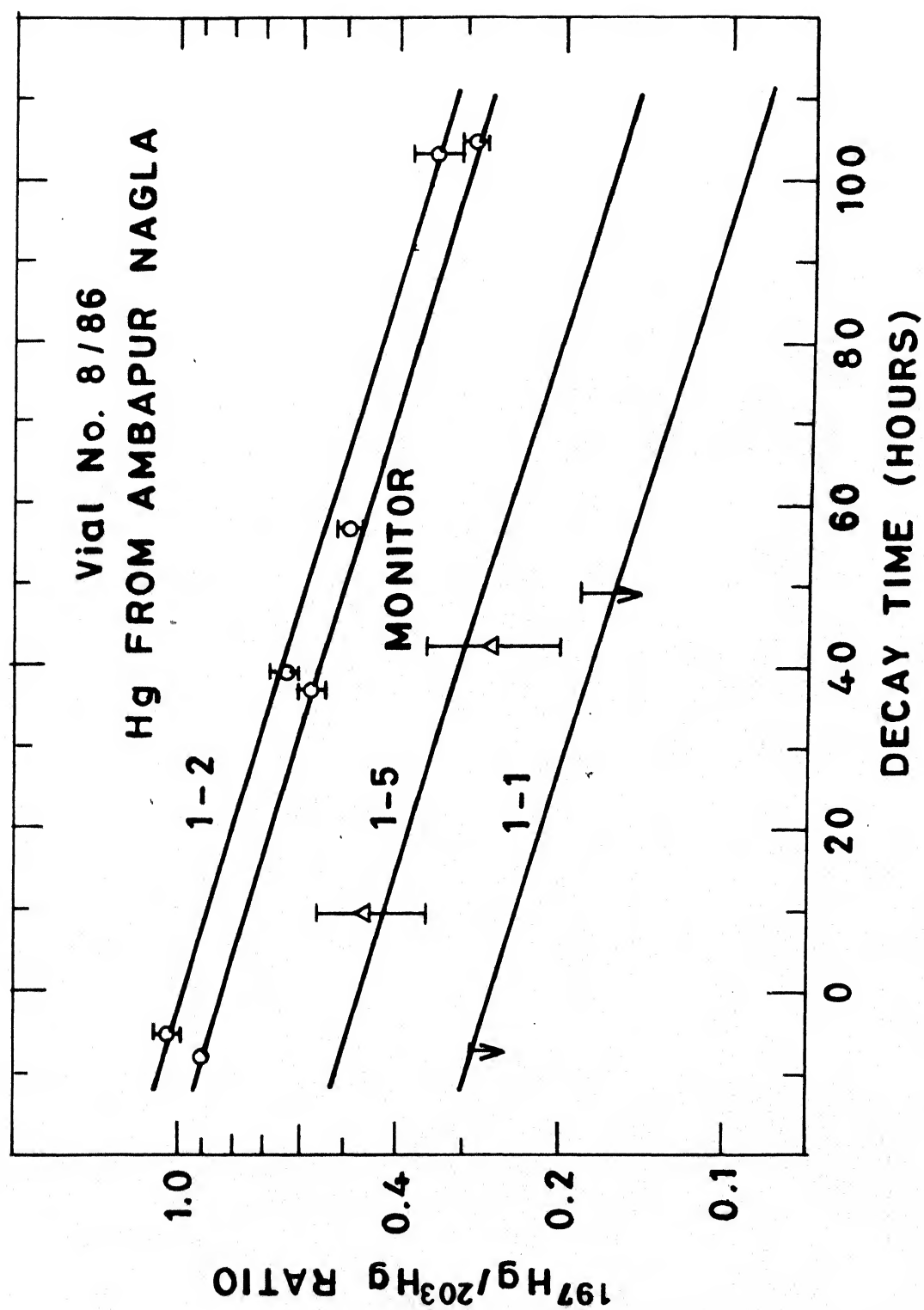


Fig. 3.50 Decay lines of activity ratios of Hg in some samples from Ambapur Nagla



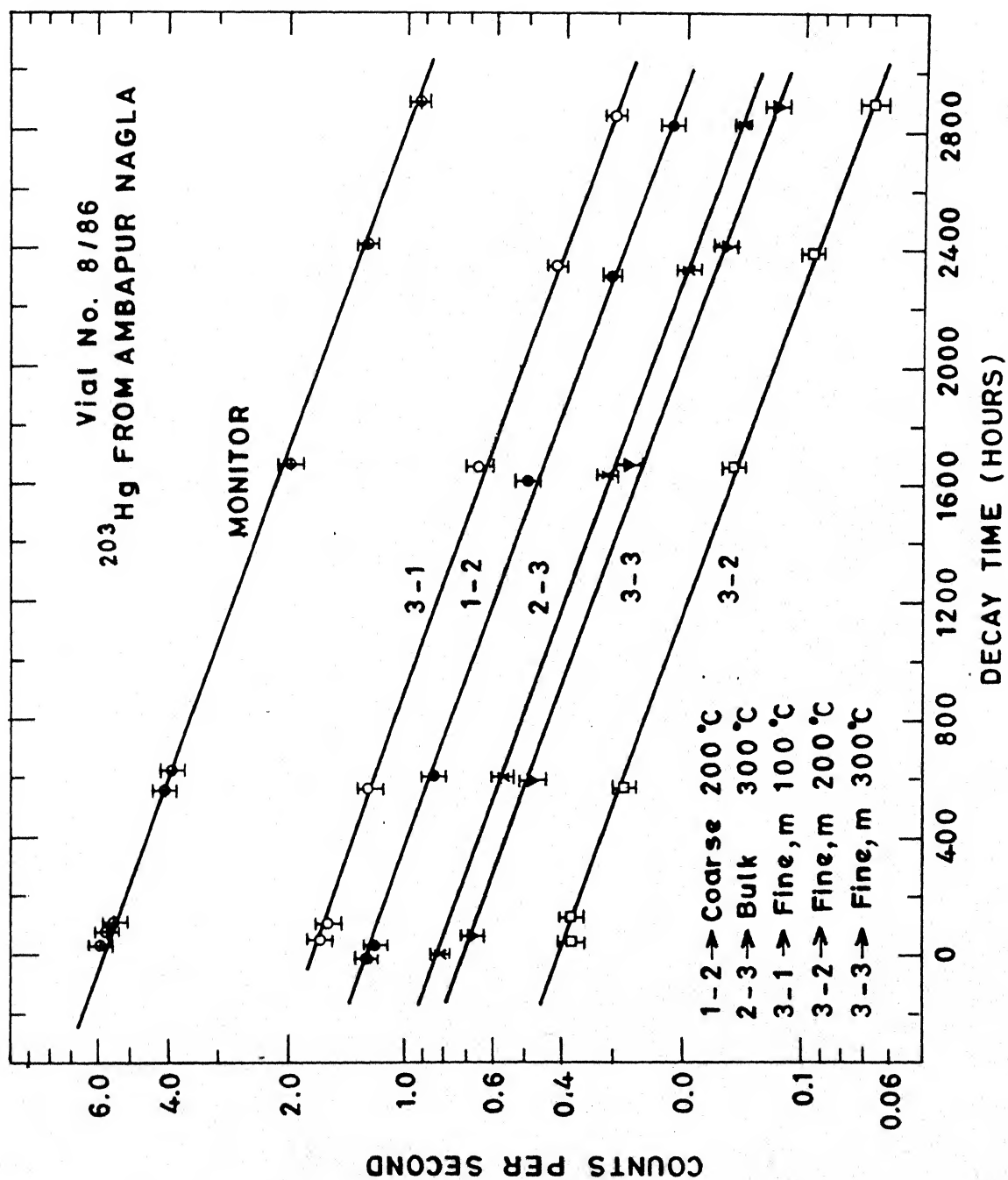


Fig. 3.51 Decay line of  $^{203}\text{Hg}$  from some samples of Ambapur Nagla

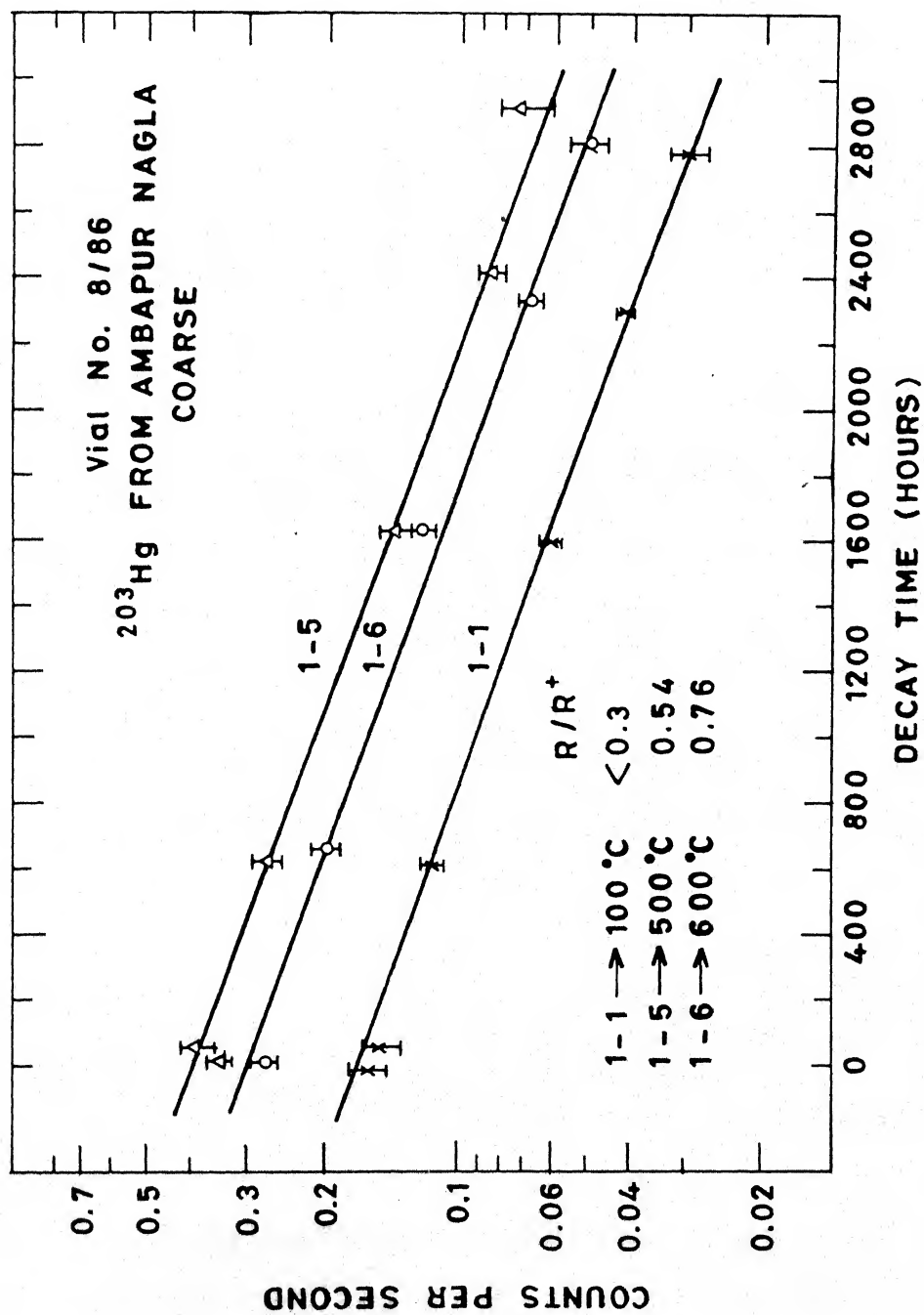


Fig. 3.52 Decay line of  $^{203}\text{Hg}$  from a sample of Ambapur Nagla

interferences. Particularly the X-rays from other contaminating nuclides were affecting the 77 keV peak of  $^{197}\text{Hg}$ . Further purification was, therefore, necessary. The samples were nearly dried under infrared heat lamp to a drop which was transferred to a fresh combustion tube and dried completely at room temperature, by reducing the pressure. During this drying process the distillates were collected at liquid nitrogen temperature and were labelled as No. 2-1-D, 2-2-D and 2-3-AD. The residues when redistilled at  $400^{\circ}\text{C}$  each, were called 2-1-R, 2-2-R and 2-3-AR. Since the third temperature step was discontinued in between, the former part was termed as 2-3-A and accordingly 2-3-AR and 2-3-AD after purification. The line was later cleaned thoroughly and again third fraction (sample No. 2-3) was collected. The results are reported in Table 3.22. It is found that the first sample is either normal or slightly above normal. The second sample shows negative anomaly for all temperature steps. Since the counting rate became poor, the 7th step was ignored in the case of the 2nd sample. Sample No. 2-3-A (before drying and redistillation as discussed above) contained osmium peaks as well. The spectrum of one of the anomalous samples, 2-3, is given in Figure 3.53 and is compared with that of the monitor. The decay points for the ratio upto ~200 hours are given in Figure 3.54. The decay lines of  $^{197}\text{Hg}$  from two abnormal samples and the standard are given in Figure 3.55. The long-lived species  $^{203}\text{Hg}$  was followed for three half lives, as shown in Figures 3.56 and 3.57. In all cases the theoretical lines fit very well with the experimental points. Sample No. 2-2-D was

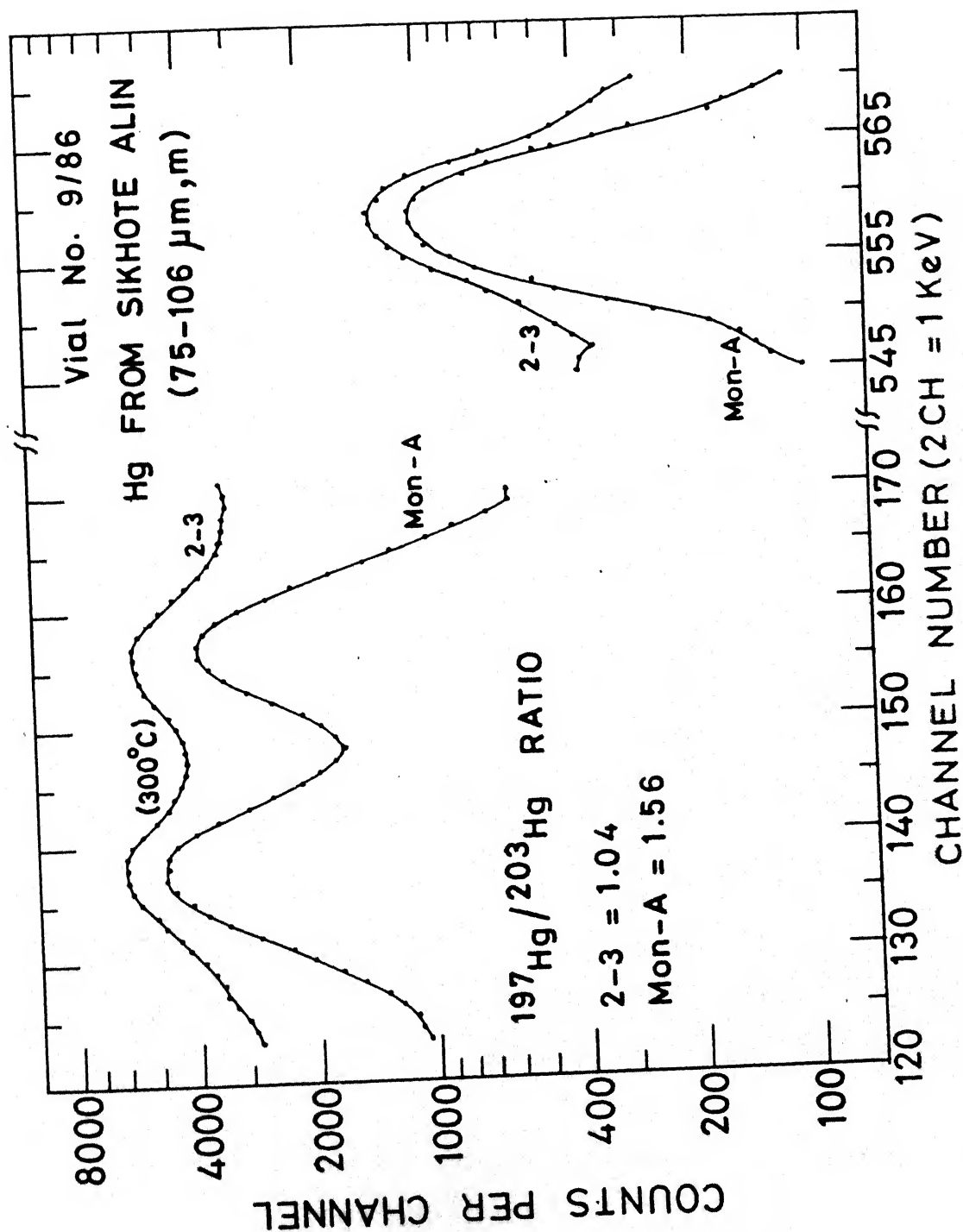


Fig. 3.53 Photon spectra of an anomalous sample of Sikhote Alin residue

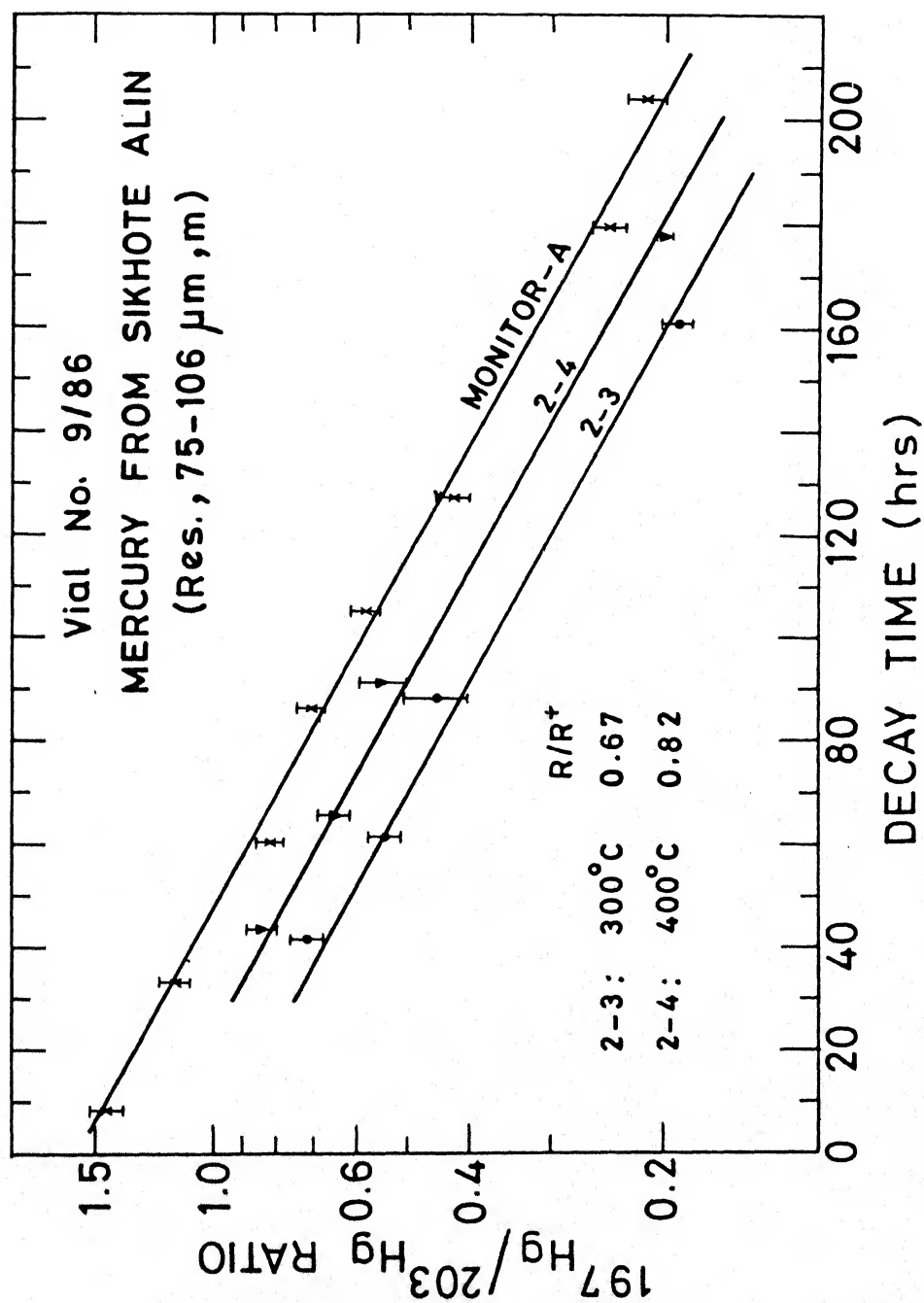


Fig. 3.54 Decay lines of activity ratio of Hg from samples of Sikhote Alin residue

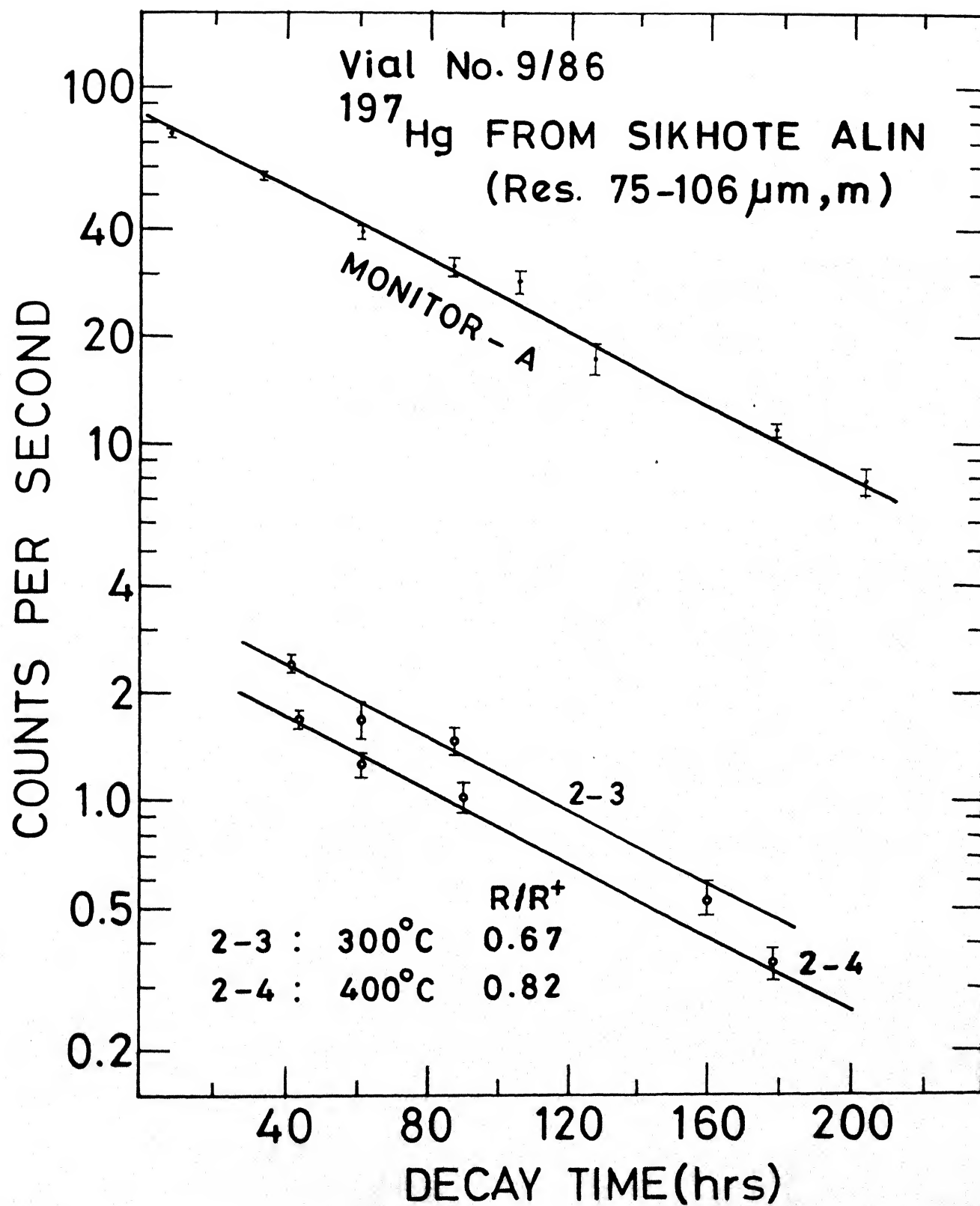


Fig. 3.55 Decay lines of  $^{197}\text{Hg}$  from samples of Sikhote Alin residue

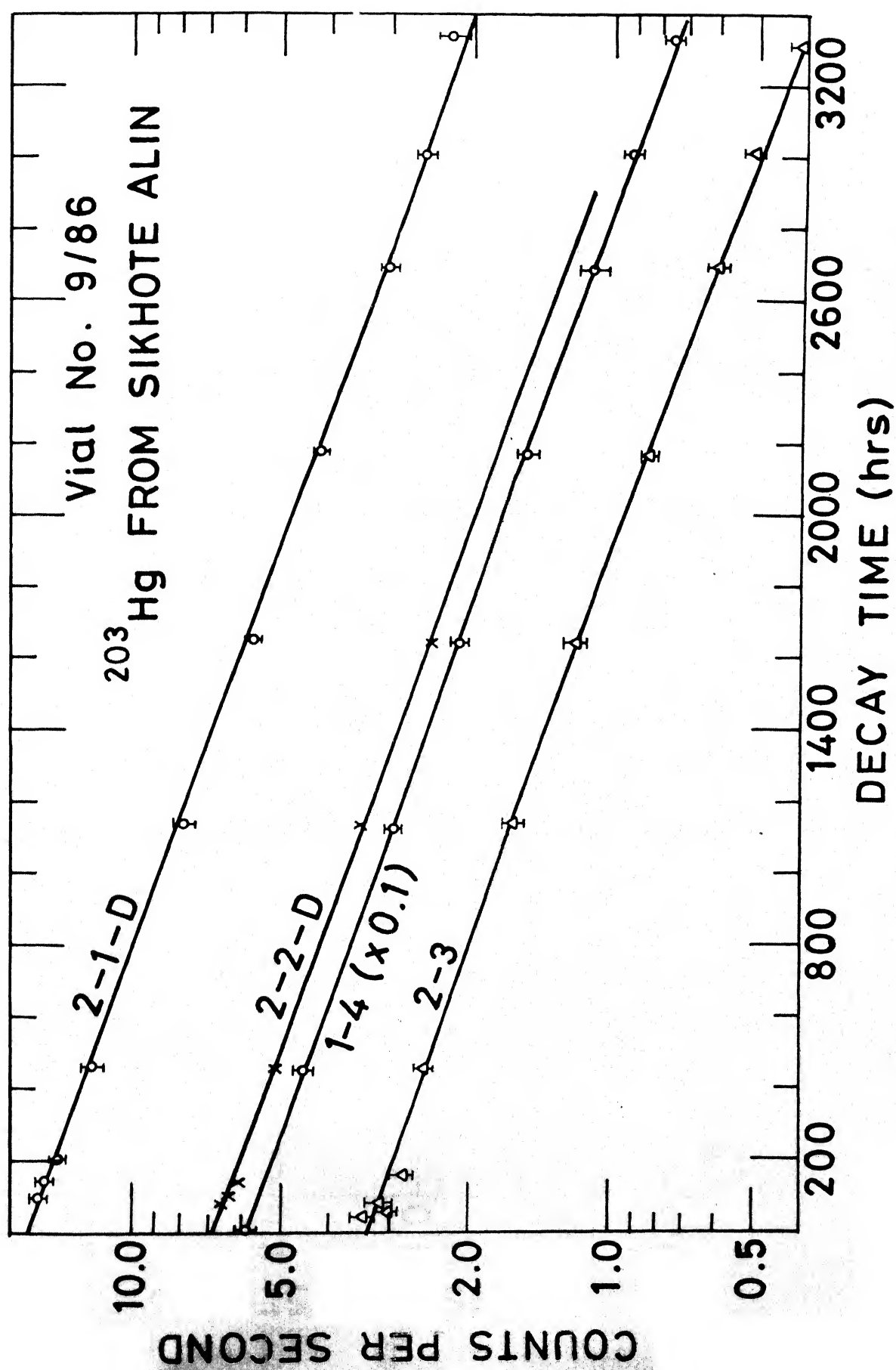


Fig. 3.56 Decay lines of  $^{203}\text{Hg}$  from some samples of Sikhote Alin residue

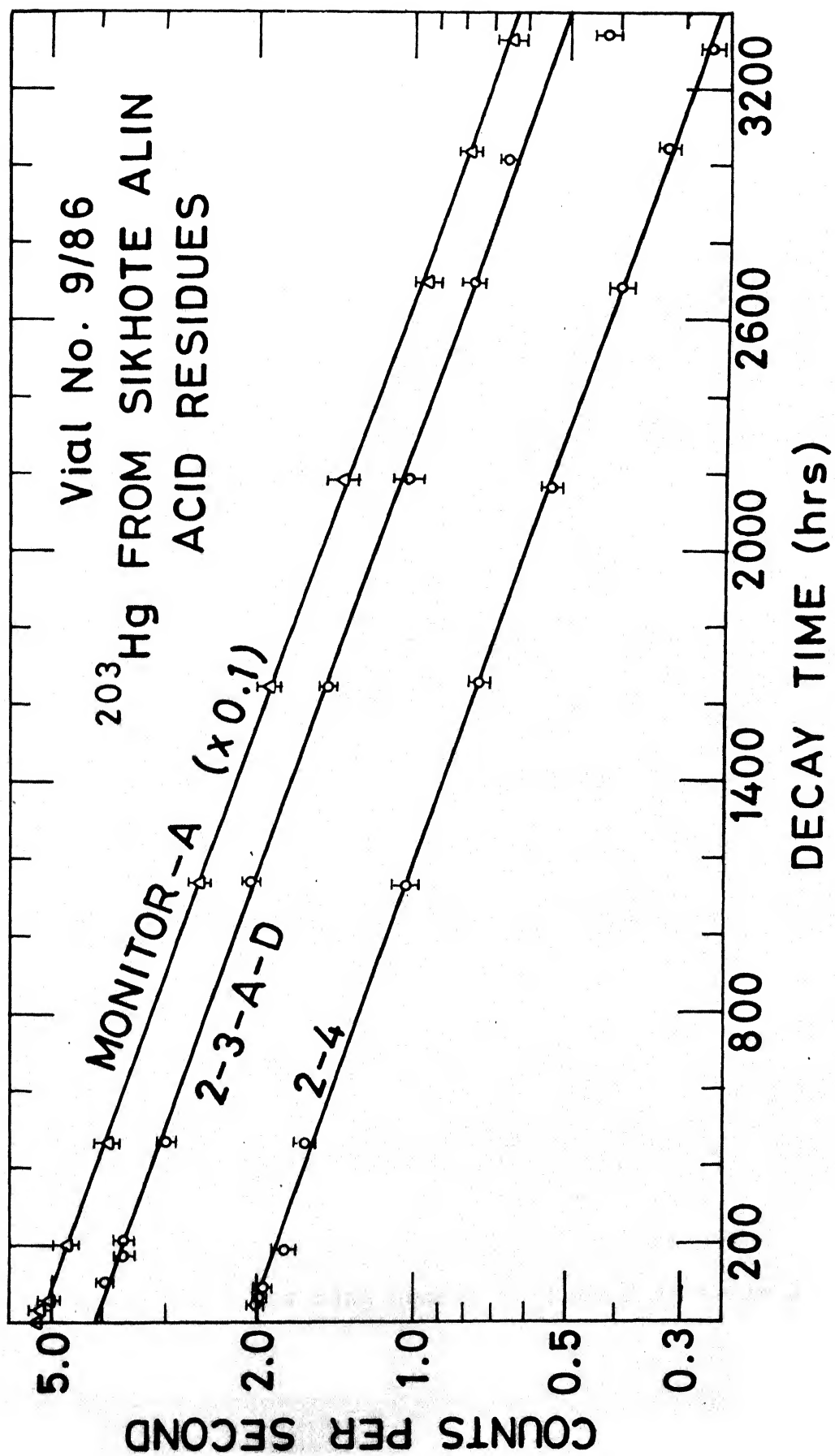


Fig. 3.57 Decay lines of  $^{203}\text{Hg}$  from some samples of Sikhote Alin residue



packed for a reirradiation experiment and therefore its decay could not be followed for a longer period. Some of the samples got dried during the long time for following the decay. It is possible that some loss of mercury might have caused a shift in the points towards a lower value. The two monitors analysed gave a consistent value of the isotopic ratio.

### 3.19 Vial No. 10/86

This vial, having fragments of Karkh and Rangala, got stuck in the reactor and got delayed in reaching the laboratory. Short-lived  $^{197}\text{Hg}$  isotope had already decayed and it was not possible to measure the  $^{197}\text{Hg}/^{203}\text{Hg}$  ratio. It was decided to distill Hg according to our previous procedures with a modification to wash the collector tube with the extracting reagent (sodium diethyl dithioarbamate in carbon tetrachloride, discussed in Section 2.6). The lower end of the collector tube was provided with a bulb for the convenience of shaking (Figure 2.2). The extract and another wash with a few drops of  $\text{CCl}_4$  was nearly dried over a watch glass, the tiny drop pipetted to small quartz irradiation capsules, dried completely and counted. These counting data were helpful to get a feeling for the Hg abundance, and are given in Table 3.23. The distilled samples of Karkh were then sent for reirradiation (except 3-1 and 3-4 which had very low counting rate) in the vial No. 4/87. Samples from Rangala were not sent because this meteorite was earlier studied in vial No. 1/87.

Table 3.23 Vial No. 10/86 Mercury from Karkh and Rangala

Sample	Mass (mg)	T(°C)	Code	cps/10	ppb-Hg
Karkh Bulk (one piece)	184	100	1-1	1.60	317.6
		200	1-2	0.55	109.2
		300	1-3	0.34	67.5
		450	1-4	0.68	135.0
Rangala Bulk (one piece)	227	100	2-1	3.70	595.4
		200	2-2	8.78	1412.9
		300	2-3	0.66	106.2
		450	2-4	1.00	160.9
Karkh Bulk	185	100	3-1	0.02	3.9
		200	3-2	0.97	586.4
		300	3-3	0.23	45.4
		450	3-4	0.09	17.8
Monitor-Hg	0.8 µg	-	Mon	2.19	

First sample of Karkh contained a small metallic inclusion that was seen upon grinding. All samples were counted after the transfer and drying of the extract in small Quartz irradiation tubes, thus the ppb values are approximate.

### 3.20 Vial No. 1/87

This vial contained residues of Chinge iron meteorite and pieces of Rangala stone meteorite. The results are shown in Tables 3.24 and 3.25. Rangala shows no variation in isotopic composition except two samples, No. R-1-4 and R-2-4 at high temperatures. But the counting rate is poor and the points on spectrum are not very smooth. Chinge showed more variations, again, with low counting rates. Sample C-1-3 had osmium peaks interfering with the mercury ratio measurements. All the three temperature fractions, C-1-1, C-1-2 and C-1-3 appear to be anomalous. To further confirm this result four samples from this vial (Nos. C-1-1, C-2-1, C-3-3 and C-4-1) were packed for reirradiation in vial No. 5/87. The results from reirradiation experiments confirmed that these anomalies are real (see Chapter 4).

From this vial onwards the monitor chemistry was modified as follows. The MgO matrix is dissolved in very dilute  $\text{HNO}_3$  and  $\text{AgNO}_3$  solution is added as scavenger.  $\text{AgCl}$  is precipitated out. The pH is increased to  $\sim 10$  by the addition of  $\text{NH}_3$  and mercury is extracted using the NaDDTC reagent.

Sample No. R-1-1 and R-1-2 was washed twice with 0.5 ml of NaDDTC solution to see whether the extraction is complete in one shaking or not. The second wash showed negligible counting rate. Thus, it was decided to carry out one washing only

Table 3.24 Vial No. 1/87 Mercury from Rangala

Fragment	Mass (mg)	T(°C)	Code	cps/10	ppb (Hg)	$^{197}\text{Hg}/^{203}\text{Hg}$ Ratio	Best Ratio	R/R <sup>+</sup>
One piece	226.0	100	R-1-1	15.9	114.6	1.64, 1.53, 1.59	1.6	1.00 (5)
		200	R-1-2	23.3	168.1	1.60, 1.7, 1.51	1.6	1.00 (5)
		300	R-1-3	0.7	5.0	1.7, 1.4	1.6	1.00 (5)
		400	R-1-4	0.32	2.3	1.25, 1.28	1.28	0.80 (4)
One piece	209.1	100	R-2-1	15.15	118.1	1.55, 1.61, 1.63	1.61	1.00 (5)
		200	R-2-2	19.6	152.9	1.64, 1.65, 1.63	1.64	1.03 (5)
		300	R-2-3	1.6	12.4	1.43, 1.50	1.45	0.91 (5)
		400	R-2-4	0.87	6.8	1.23, 1.48, 1.27	1.3	0.81 (4)
One piece	237.5	100	R-3-1	9.82	67.4	1.55	1.55	0.97 (5)
		200	R-3-2	9.44	64.8	1.73	1.73	1.08 (5)
		300	R-3-3	1.31	8.9	1.50	1.50	0.94 (5)
		400	R-3-4	0.52	3.6	1.51	1.51	0.94 (5)
Monitor	1 $\mu\text{g}$	-	Mon	64.3		1.44, 1.58, 1.60, 1.5	1.60	1.00 (2)

Table 3.25 Vial No. 1/87 Mercury from Chinga residues

Residue <sup>*</sup>	Mass (mg)	T(°C)	Code	cps/10	ppb (Hg)	$^{197}\text{Hg}/^{203}\text{Hg}$ Ratio	R/R <sup>+</sup>
Fourth fraction (1.5)	15.4	100 200 300	C-1-1 C-1-2 C-1-3	0.25 0.21 0.45	26.6 22.1 47.0	1.12 1.2 Os interference	0.72 (3) 0.77 (4) -
Second fraction (2.8)	64.5	100 200 300	C-2-1 C-2-2 C-2-3	8.5 3.9 1.34	213.9 98.6 33.9	1.71 1.66 1.47	1.10 (5) 1.10 (5) 0.95 (5)
Third fraction (1.8)	42.5	100 200 300	C-3-1 C-3-2 C-3-2	4.82 21.82 6.05	185.0 837.4 232.2	1.59 1.55 1.41	1.03 (5) 1.00 (5) 0.91 (5)
First fraction (3.1)	32.5	100 200 300	C-4-1 C-4-2 C-4-3	25.8 11.07 1.76	1295.4 555.7 88.3	1.5 1.57 1.75	0.97 (5) 1.01 (5) 1.13 (5)
Monitor-Hg	1 µg	-	Mon	61.3	-	1.44, 1.58, 1.60, 1.5	1.00 (2)

\*Numbers in parentheses are mass(mg) per mm of column length in the packing capsule.

At the time of Chinge dissolution the residues were separated from the undissolved meteorite before each addition of fresh acid. This is how the first to fourth fractions are termed.

### 3.21 Vial No. 2/87

It contained three samples of acid residues of Campo del Cielo, prepared by dissolving separate aliquotes of the meteorite, packed in aluminium capped quartz capsules. A single fragment of Holbrook stone meteorite, wrapped in aluminium foil was also kept in this vial. Table 3.26 shows the results on the measurements done. Holbrook contains very little Hg compared to the other chondrites. It was not possible to measure the isotopic ratio for temperature steps of 300°C and higher. CdC residue samples show positive as well as negative anomaly. The replicate measurements on C-1-1, C-1-2, C-3-1, C-3-2 and monitor are presented in Table 3.27. Although the extent of isotopic anomaly is small, both types of anomalies are evidently real as is indicated through its consistency of decay points (Figure 3.58).

### 3.22 Vial No. 3/87

A fragment of Ambapur Nagla weighing 200 mg was distilled at five temperatures of 100-, 150-, 200-, 250-, and 300°C. The distillate, washed with NaDDTC/ $\text{CCl}_4$  reagent, was transferred and dried in small quartz irradiation tube. Aluminium capped ampules were sent for neutron bombardment along with other reirradiation samples. After activation the samples again were distilled at

Table 3.26 Vial No. 2/87 Mercury from Holbrook and CdC residues

Sample	Mass (mg)	T (°C)	Code	cps/10	ppm (Hg)	$^{197}\text{Hg}/^{203}\text{Hg}$ Ratio	R/R <sup>+</sup>
Holbrook bulk	282.5	100	H-1	0.52	0.060	0.97	1.02 (5)
		200	H-2	1.36	0.157	0.92	0.97 (4)
		300	H-3	0.12	0.014	-	-
		400	H-4	0.13	0.015	-	-
		500	H-5	Low	-	-	-
CdC residue	127.7	100	C-1-1	2.61	0.67	1.04	1.10 (6)
		200	C-1-2	31.21	7.99	0.84	0.94 (5)
		300	C-1-3	1.80	0.46	0.92	0.97 (5)
		400	C-1-4	0.95	0.24	0.96	1.01 (5)
		500	C-1-5	0.32	0.08	0.46 ± 0.15	0.49 (15)
CdC residue	83.8	100	C-2-1	6.11	2.38	1.05	1.11 (6)
		200	C-2-2	25.59	9.98	1.06	1.12 (6)
		300	C-2-3	2.59	1.01	0.98	1.03 (5)
		400	C-2-4	1.62	0.63	1.12	1.18 (6)
		500	C-2-5	1.13	0.44	0.94	0.99 (5)
CdC residue	65.8	100	C-3-1	4.73	2.35	1.19	1.26 (6)
		200	C-3-2	11.16	5.54	0.88	0.93 (4)
		300	C-3-3	1.21	0.60	0.95	1.00 (5)
		400	C-3-4	1.13	0.56	1.09	1.15 (6)
		500	C-3-5	0.74	0.37	1.10 ± 0.13	1.16 (14)
Monitor (0.99 µg Hg)	-	-	Mon	30.6	-	0.95 ± 0.02	1.00 (2)
Quartz Blank	-	400	Q-6	Very low	-	-	-

All the residues of CdC were prepared by dissolving separate aliquotes of the meteorite.

Table 3.27 Vial No. 2/87 Mercury from CdC residues (supplementary data)

Sample	Code	cps/10	$^{197}\text{Hg}/^{203}\text{Hg}$ Ratio	
			Replicate	Best
CdC residue	C-1-1	2.61	1.041±0.05 1.148±0.08 1.00±0.06 0.975±0.12	1.04±0.05
	C-1-2	31.2	0.839±0.01 0.84±0.04 0.89±0.02	0.84±0.01
CdC residue	C-3-1	4.73	1.272±0.04 1.11±0.05 0.963±0.02	1.12±0.05
	C-3-2	11.16	0.876±0.04 0.88±0.05 0.83±0.03	0.88±0.04
Monitor-Hg	Mon	30.6	0.947±0.02 0.883±0.03 0.996±0.02 0.950±0.03 0.936±0.02 0.898±0.04	0.95±0.02



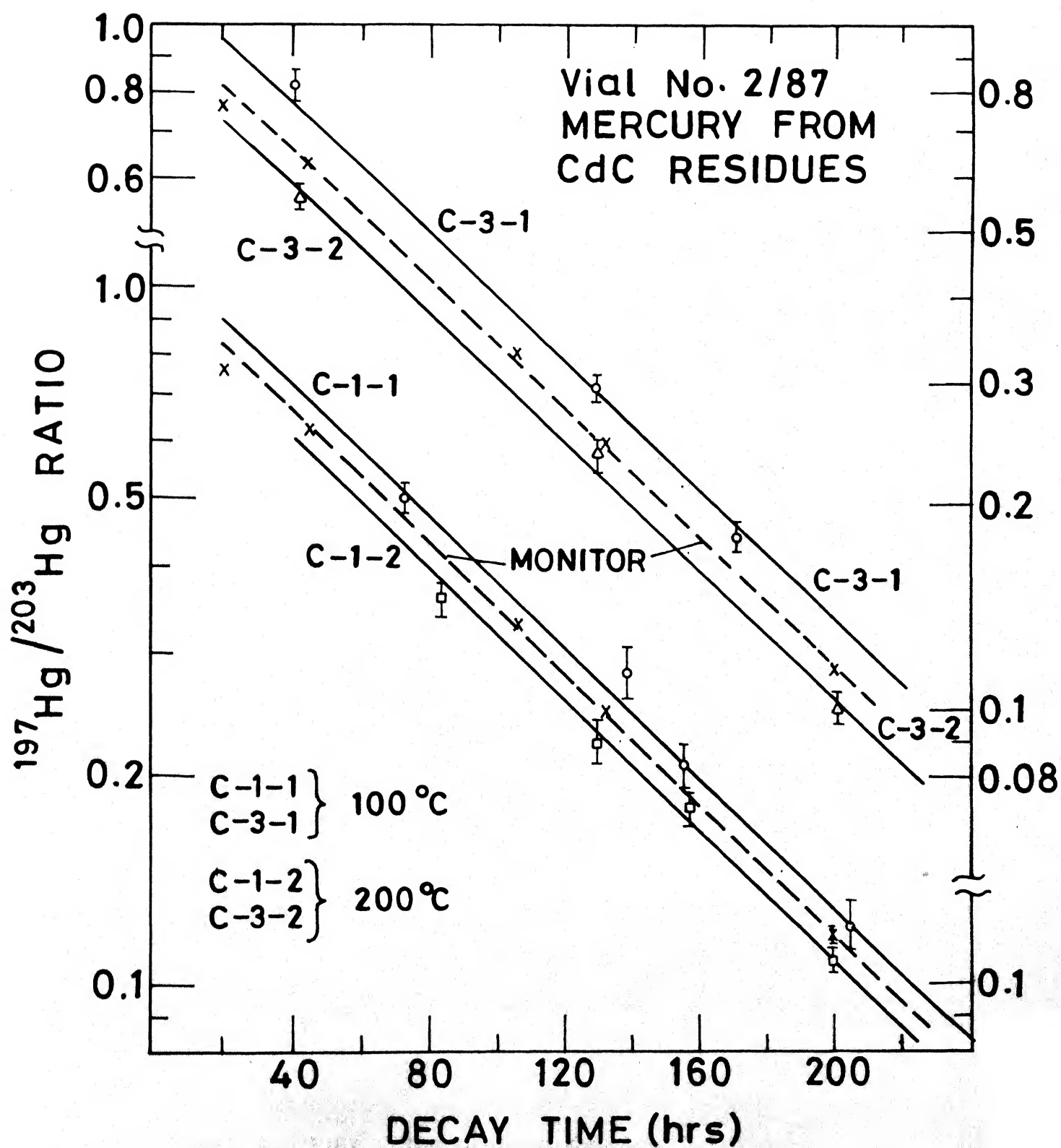


Fig. 3.58 Decay lines of activity ratios of Hg isotopes from Campo del Cielo residue samples

400°C for one hour each. All samples gave indistinguishable values of isotopic ratios, within error limits, compared to the reagent monitor. The data are given in Table 3.28.

### 3.23 Vial No. 4/87

This vial had distilled Hg samples of Karkh from vial No. 10/86 that could not be analysed at that time because of the mechanical fault during its irradiation in the reactor and subsequent delay in its arrival in the laboratory. The results are given in Table 3.29. There are very little variation which cannot be taken seriously. The values of Hg abundances from both the vials should not be compared because the geometry of counting differs drastically.

### 3.24 Vial No. 6/87

There was no meteorite sample present in vial No. 5/87. In vial No. 6/87, heavier part of  $\text{HNO}_3$  treated acid insoluble residue of Odessa was irradiated. After irradiation this was divided in two parts and each distilled at five temperatures. The results are given in Table 3.30. Because of the lower counting rates, longer counting time was required for each sample, hence replicate counting could not be done on all samples.

### 3.25 Vial No. 7/87 : The Organic Extract

There is a possibility that the isotopically anomalous mercury in meteorites might be present in the form of organic

Table 3.28 Vial No. 3/87 Results from Ambapur Nagla bulk (200 mg)

Code	T(°C)	cps/10	Hg ( $\mu$ g)	$\frac{^{197}\text{Hg}}{^{203}\text{Hg}}$ Ratio	
				Replicate *	Average
5	100	1.84	0.03	1.08, 1.10, 1.026, 1.074 $\pm$ 0.1	1.1
6	150	2.44	0.038	1.277, 1.291, 1.17, 0.992 $\pm$ 0.06	1.2
7	200	4.043	0.062	1.235, 1.248, 1.18, 1.045 $\pm$ 0.1	1.2
8	250	2.71	0.042	1.237, 1.223, 1.17, 0.933 $\pm$ 0.04	1.2
9	350	0.994	0.015	1.132, 1.098, 1.043, 0.986 $\pm$ 0.16	1.1
Monitor	-	10.15	0.156	1.10, 1.205, 1.132, 1.174, 1.31, 1.046 $\pm$ 0.05 1.235	1.2

Distillates from the meteorite irradiated in NaDDTC complexed form and, the activated samples, again distilled at 400°C for one hour each.

\*Errors are less than  $\pm$  5% unless otherwise stated.

Table 3.29 Vial No. 4/87 Irradiation of Hg distilled from Karkh fragments \*

Sample	Mass (mg)	T(°C)	Code	c/sec**	Hg (µg)	$^{197}\text{Hg}/^{203}\text{Hg}$ Ratio	R/R <sup>+</sup>
Bulk I	184	100	5	11.73	0.601	$1.38 \pm 0.05$	1.10 (4)
		200	6	9.18	0.470	$1.27 \pm 0.02$	1.02 (2)
		300	7	4.58	0.235	$1.22 \pm 0.04$	0.98 (3)
		450	8	5.11	0.262	$1.23 \pm 0.04$	0.98 (3)
Bulk II	185	200	9	3.59	0.184	$1.19 \pm 0.03$	0.95 (2)
		300	10	2.01	0.103	$1.24 \pm 0.04$	0.99 (3)
Monitor -Hg	-	-	11	15.06	0.772	$1.25 \pm 0.02$	1.00 (2)

\* Samples were irradiated at a lower neutron flux for vial No. 10/86, some of the distilled Hg samples were repacked for this vial.

\*\* c/sec/10 keV, 279 keV (20 Ch).

Table 3.30 Vial No. 6/87 Mercury from Odessa Residues (HNO<sub>3</sub> heavy)

Mass (mg)	Temp. (°C)	Code	cps/10	ppm (Hg)	$\frac{^{197}\text{Hg}/^{203}\text{Hg}}{\text{Replicate}}$	$\frac{\text{Hg Ratio}}{\text{Best/average}}$	R/R <sup>+</sup>
71.9	100	0-1-1	0.94	0.57	3.14, 3.24±0.39	3.14	1.10
	200	0-1-2	1.71	1.03	2.38, 2.50	2.44	0.85
	300	0-1-3	0.89	0.53	2.29, 2.19±0.13	2.29	0.80
	400	0-1-4	0.39	0.24	Unmeasurable	-	-
	500	0-1-5	0.03	0.02	Unmeasurable	-	-
78.8	100	0-2-1	0.26	0.14	2.94, 3.07±0.30	2.94	1.03
	200	0-2-2	1.39	0.77	2.15, 3.0±0.4	2.15	0.75
	300	0-2-3	0.52	0.29	2.12, 1.5±0.2	2.12	0.74
	400	0-2-4	0.03	0.02	Unmeasurable	-	-
	500	0-2-5	0.04	0.02	Unmeasurable	-	-
Reagent Hg (0.33 µg)		Mon	7.60	-	2.91, 2.88, 2.80	2.86	1.0

\* Errors are less than ± 5% unless otherwise stated.

compounds. This is because mercury forms a large number of organometallic compounds, many of which are very stable and may survive in the presolar conditions. We performed a set of extraction experiments to isolate organic compounds using different solvents.

Four meteorites, Allende, Murchison, Forest City and Millbillillie, in finally ground form, were taken in the amounts of about 200 mg. Three solvents benzene, carbon tetrachloride and dichloromethane were used in sequence for extraction. The shaking period was approximately twelve hours each. The drying procedure was similar to that for the NaDDTC/ $\text{CCl}_4$  reagent extractions. All the samples were aluminium capped and were packed along with a mercury monitor. All these samples showed near blank Hg-activities. Maximum Hg-abundance found ( $0.03 \mu\text{g}$ ) was from the  $\text{CCl}_4$  extract of Millbillillie (Table 3.31). The isotopic ratio measurements were not possible. Further investigation using other organic solvents is under progress.

Table 3.31 Vial No. 7/87 : Solvent Extraction Experiment

Solvent	Meteorite	Mass (mg)	Code	c/s/20 keV (279 keV)	Hg (ppb)
$C_6H_6$	Allende	210.3	B-1	$0.10 \pm 0.02$	14
	Murchison	199.7	B-2	$<0.08 (2\sigma)$	$<11$
	Forest City	231.8	B-3	$0.09 \pm 0.02$	11
	Millbillillie	222.4	B-4	$<0.01 (2\sigma)$	$<1$
$CCl_4$	Allende	210.3	C-1	$0.011 \pm 0.005$	1
	Murchison	199.7	C-2	$<0.04 (2\sigma)$	$<5$
	Forest City	231.8	C-3	$0.07 \pm 0.01$	9
	Millbillillie	222.4	C-4	$1.3 \pm 0.07$	174
$CH_2Cl_2$	Allende	210.3	D-1	$<0.08 (2\sigma)$	$<11$
	Murchison	199.7	D-2	$0.06 \pm 0.02$	8
	Forest City	231.8	D-3	$0.11 \pm 0.02$	14
	Millbillillie	222.4	D-4	$<0.06 (2\sigma)$	$<8$
Hg-Monitor (0.43 $\mu$ g)		-	Mon	$14.4 \pm 0.2$	-

## Chapter 4

### RESULTS FROM RE-IRRADIATION EXPERIMENTS

Some of the distilled radioactive condensates of Hg from several runs were re-irradiated. This was to verify that any artifacts introduced during meteorite irradiations due to such causes as neutron energy spectrum variation, interference from the matrix element, self shielding effects, etc., are not responsible for the observed isotopic variations. In these re-irradiation experiments, a set of Hg samples (monitor, normal, anomalous, isotopically diluted and blank) were in identical chemical forms and were bombarded under similar conditions. Sample preparations were done as follows. Concentrated ammonia was added to increase the pH of a sample, that was in acid medium, to about 10 and the sample was taken into a micro shaking flask (Figure 4.1). It was shaken vigorously with 0.5 ml of extracting reagent, NaDDTC/ $\text{CCl}_4$ , as discussed in section 2.6. The lower (organic) layer was separated. The aqueous layer was washed once with 0.5 ml of carbon tetrachloride; the washings being combined with the organic extract which was allowed to evaporate at room temperature on a watch glass. The final drop was pipetted into a small quartz irradiation tube and was allowed to dry by itself at room temperature (it took 4-5 hours). The aluminium capped capsules were irradiated as usual. The results are described for each re-irradiation experiments.

#### 4.1 Vial No. 1/87

The purpose of this run was to see the level of contamination incurred in the procedure. The samples were chosen such that their count-



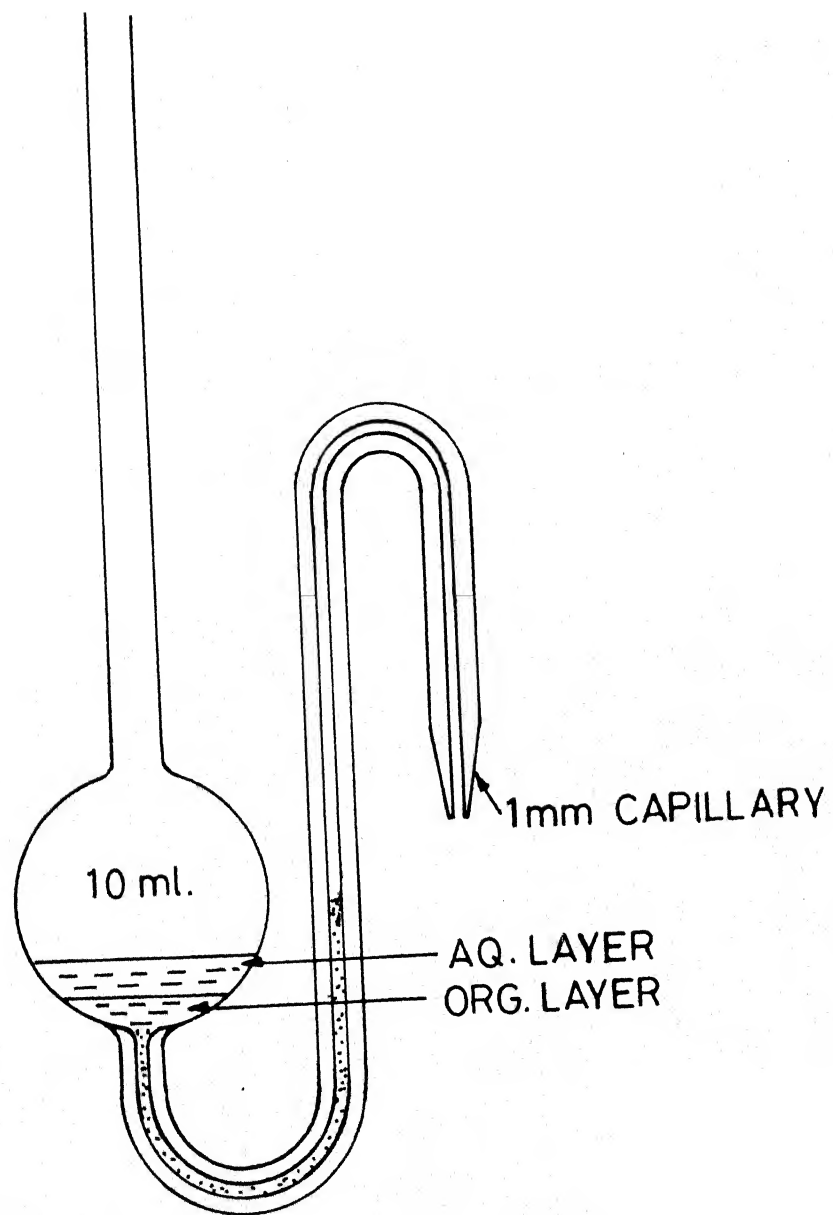


FIG. 4.1 MICRO SHAKING FLASK

ing rates varied over two orders of magnitude but the  $^{197}\text{Hg}/^{203}\text{Hg}$  was normal. Of the five samples given in Table 4.1, two (No.7 and No.8) were prepared as follows. A high activity sample from Au-foil was extracted and dried after dividing into two unequal parts. The fifth sample was a blank run sample from vial No. 9/86 that was distilled in between two meteorite samples. All the procedures of extraction, drying, etc., were followed in an identical manner. The other two samples (No.5 and No.6) were those obtained in the normal way from vial No. 9/86 and from which Hg was extracted by the extracting reagent. After re-irradiation, samples 5,6,7 and 9 were heated at  $400^{\circ}\text{C}$  to distill Hg and washed/ extracted with the NaDDTC reagent. Sample No.8 was washed only and counted. Since the later sample was counted after long delay the ratio could not be measured. The results are presented in Figures 4.2 and 4.3. On the basis of consistency of  $^{197}\text{Hg}/^{203}\text{Hg}$  ratios measured and the ratio of the counting rates among the samples, apparently no contamination of stable Hg from reagents is visible.

#### 4.2 Vial No. 2/87

This vial contained five extracted samples, out of which two had anomalous Hg. The data are given in Table 4.2. It seems that all the samples are contaminated, in addition to the handling loss, to a variable extent. By looking at the counting rates of the re-irradiated samples, No.5 is contaminated to the highest level while No.4 has the lowest contamination. Sample numbers 1 and 2 may be accounted for by some loss during sample transfer before drying into the quartz irradiation tube (it was transferred using a disposable needle and syringe).

Table 4.1 Vial No. 1/87 Re-irradiation Control Experiment

Sample		c/sec/10 keV, 279 keV (20 ch)*			$^{199}\text{Hg}/^{203}\text{Hg}$
Code	Source	Before drying	After drying	After Re-irradiation	Ratio
5	1-6 of 9/86	2.8	2.2	3.1	1.27
6	1-5 of 9/86	19.0	17.14	23.5	1.39
7	6 of 9/86	-	49.6	43.3	1.27
8	6 of 9/86	-	130.04	138.5	not measured
9	Blank of 9/86	No activity	-	No activity	No activity

\* There is a difference in the geometry of countings given in columns 4 and 5.

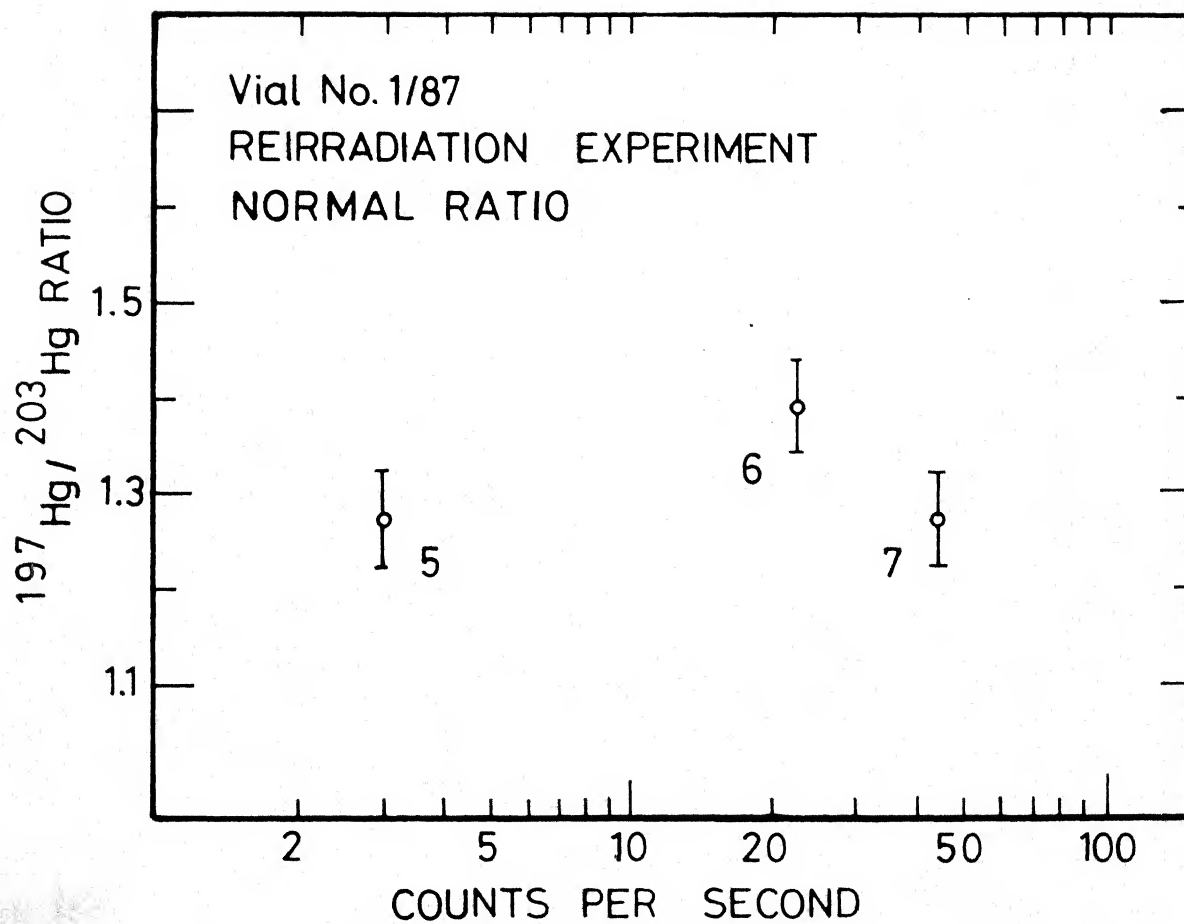


Fig. 4.2 Ratio vs. count-rate of re-irradiated normal samples (1/87)

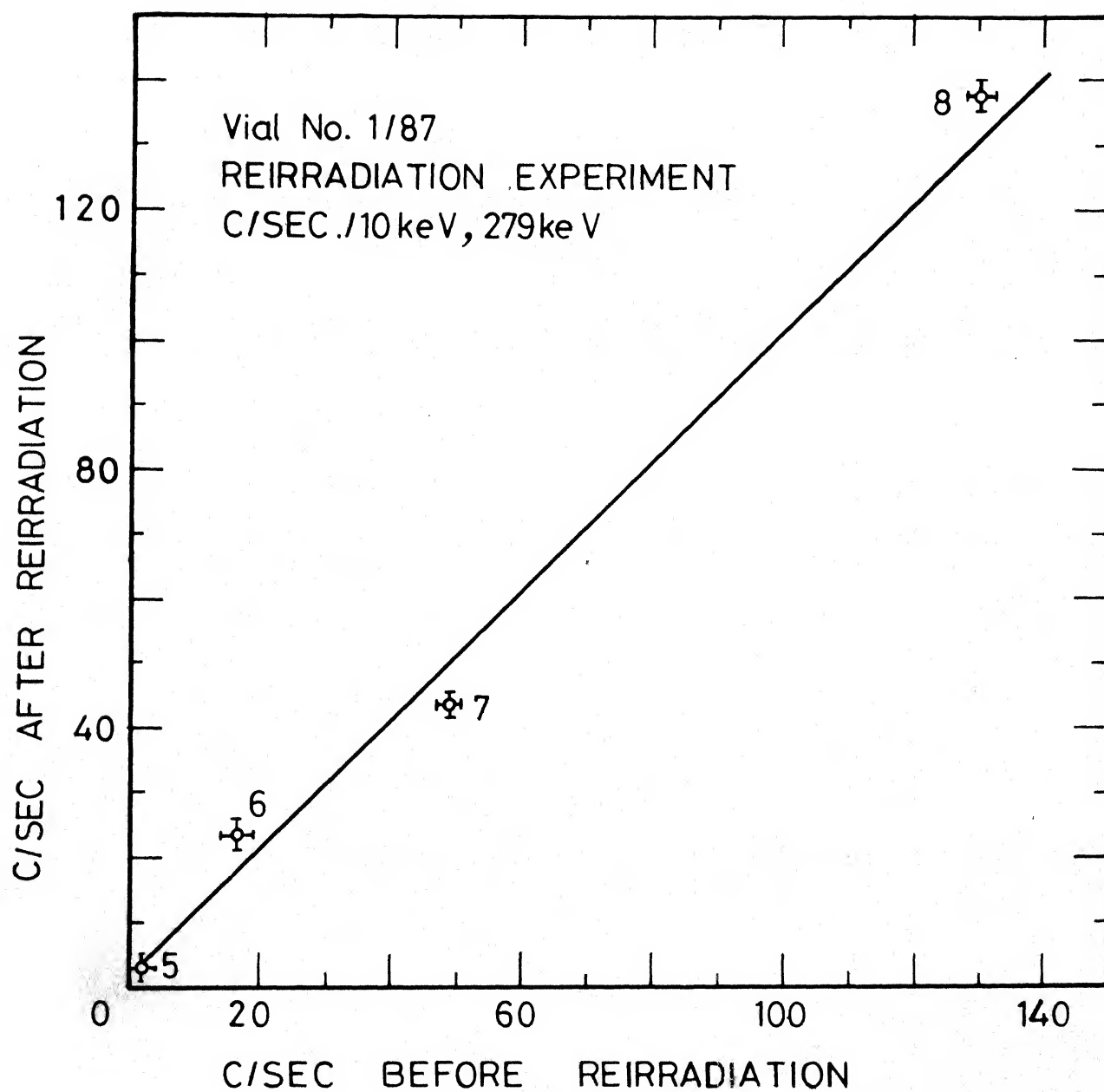


Fig. 4.3 Count-rate before re-irradiation vs. count-rate after re-irradiation (1/87)

Table 4.2  $^{197}\text{Hg}/^{203}\text{Hg}$  Ratio in Acid Insoluble Residues (magnetic) of Sikhote Alin Iron Meteorite

Sample description	Irradiation of Meteorite acid residues				Re-irradiation of Distilled Hg			
	Vial No. 9/86				Vial No. 2/87			
	Code No.	Mass (mg)	Hg ( $\mu\text{g}$ )	R/R <sup>+</sup>	Code No.	Hg* ( $\mu\text{g}$ )	Ratio Replicate      Best	R/R <sup>+</sup>
45-75 $\mu\text{m}$ , 200°C	1-1	81.1	3.9	1.089	1	0.476	1.07, 1.025	1.07
45-75 $\mu\text{m}$ , 600°C	1-7	81.1	0.096	0.974	3	0.281	0.93, 0.94 0.93	0.93
75-106 $\mu\text{m}$ , 300°C	2-2-D	76.6	0.088	0.743	5	0.679	0.98, 1.00 0.94, 0.96	0.98
75-106 $\mu\text{m}$ , 600°C	2-6	76.6	0.013	0.647	4	0.120	0.81, 0.88 0.91, 0.84	0.89
Monitor-Hg	Mon-B	-	2.64	1.000	2	0.388	0.80, 0.83 0.87, 0.79	0.84

\* Some Hg contamination from laboratory is probably present.

Some of the samples from this set were counted intact without breaking the ampule and chemistry. Mercury peaks could be seen. But at lower energies, X-rays of interfering nature were seen. It was decided that chemistry should essentially be done to purify the re-irradiated mercury. Blank quartz tube gave almost negligible counting rate in the high energy region (279 keV).

Samples No. 1 and 2 had originally high mercury content and the isotopic ratios differed by about 10 %. This information is retained even after the contamination. But in case of the other samples (Nos. 3, 4 and 5) contamination created more trouble. All the samples were having relatively lower content of mercury (c/sec). Since the ratio of sample No. 4 was very much off, it still retains the memory to some extent even after dilution from inert mercury. Sample No. 5 was not much off. Thus was diluted to give a normal value of isotopic ratio after contamination. Sample No. 3 was already normal.

#### 4.3 Vial No. 3/87

For re-irradiation purpose, a set of samples was prepared from anomalous and normal samples of Sikhote Alin from vial No. 7/86. The highly anomalous sample 6-3 upon extraction was divided into two parts. One part was spiked with the extract of a normal sample No. 7-3 having similar counting rate; another part was transferred and dried as such in the irradiation tube. A portion of a high activity sample No. 4-2, with normal isotopic composition, was extracted and packed. This set also contained a dried extract from a sample of a very low counting rate, meant for blank level monitoring. The results obtained are shown in

Table 4.3. Apparently there is some loss of Hg but the contamination level is extremely low as judged from the blank sample. The maximum loss is shown by the spiked sample where the measured value is almost 50 % of the expected one. There is a very good agreement between the expected and measured values of the isotopic ratios. The highly anomalous sample (No.6-3) maintained the anomaly. Similar is the case with normal and spiked samples. All the samples were spectrum analysed (Figure 4.4). The decay points of the activity ratios and the short lived nuclide  $^{197}\text{Hg}$ , followed upto 200 hours are shown in Figure 4.5 and Figure 4.6 respectively.

#### 4.4 Vial No. 4/87

Anomalous and normal samples of Ambapur Nagla from vial No. 8/86 were packed in this vial. Sample Nos. 1-2 and 3-5 are normal and are to be compared with the clearly anomalous sample, No. 3-1, whereas No. 4-4 was chosen for blank. The results are given in Table 4.4 and Figure 4.7. There was a little loss of mercury after second irradiation but the contamination is negligible as could be seen from the blank sample (code No. 4). The highly anomalous sample (code No.2) remained as such. Its photon spectra is compared with that of the monitor and is given in Figure 4.8. There is no peak due to  $^{197}\text{Hg}$  at all, in the anomalous sample.

#### 4.5 Vial No. 5/87

This vial had two sets for re-irradiation investigation. One set of Sikhote Alin, prepared from vial No. 7/86, had isotopic ratios varying between 0.27 to 1.63 and a blank sample, No. 1-6. The other set consisted of four Chinge samples and a monitor from vial No. 1/87 having variations in isotopic ratios from 1.1 to 1.7. A fresh monitor of mercury was also



Table 4.3  $^{197}\text{Hg}/^{203}\text{Hg}$  Ratio in Sikhote Alin Magnetic Residues

Sample fraction	Irradiation of Meteorite acid-residues Vial No. 7/86			
	Code No.	Mass (mg)	Hg ( $\mu\text{g}$ )	R/R <sup>+</sup>
< 38 $\mu\text{m}$ , 200°C	4-2	85	2.12	1.1
45-75 $\mu\text{m}$ , 250°C	6-3	75	0.82	<0.01 <sup>*</sup>
75-106 $\mu\text{m}$ , 300°C	7-3	64	0.53	1.0
75-106 $\mu\text{m}$ , 200°C	7-1	64	< 0.06	U

---

Sample fraction	Code No.	Re-irradiation of Distilled Hg Vial No. 3/87			
		Expected		Measured	
		Hg ( $\mu\text{g}$ )	R/R <sup>+</sup>	Hg ( $\mu\text{g}$ )	R/R <sup>+</sup>
<38 $\mu\text{m}$ , 200°C	1	0.22	1.1	0.2	1.1
45-75 $\mu\text{m}$ , 250°C	2	0.50	< 0.01	0.33	< 0.003 <sup>*</sup>
45-75 $\mu\text{m}$ , 250°C	3	0.30	0.60	0.34	0.42
75-106 $\mu\text{m}$ , 300°C		0.40			
75-106 $\mu\text{m}$ , 200°C	4	<0.06	-	< 0.07	U

$$R/R^+ = (^{196}\text{Hg}/^{202}\text{Hg})_s / (^{196}\text{Hg}/^{202}\text{Hg})_{\text{std.}}$$

\* = 2  $\sigma$  limit

U = Unmeasurable

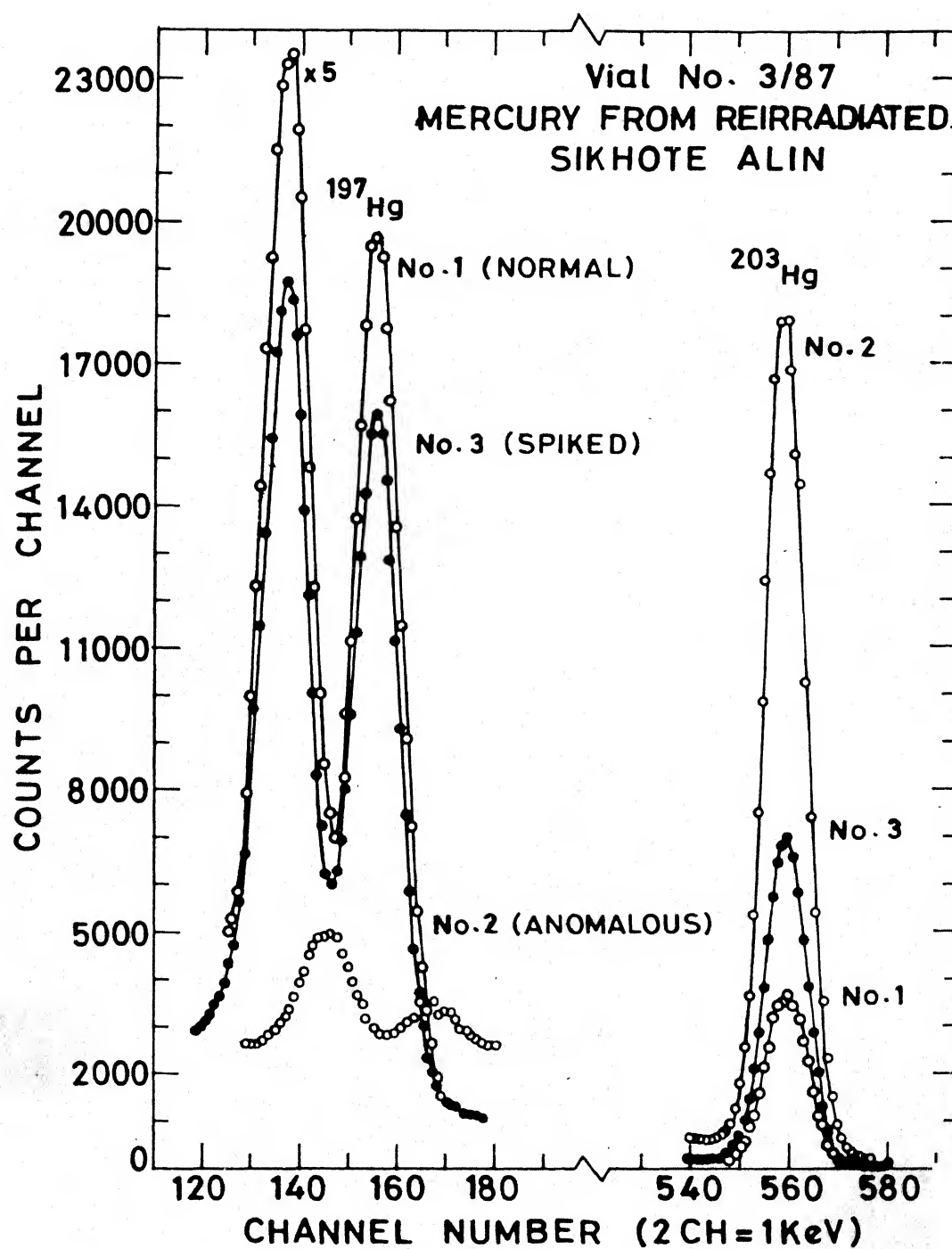


Fig. 4.4 Photon spectra of re-irradiated samples of Sikhote Alin (3/87)

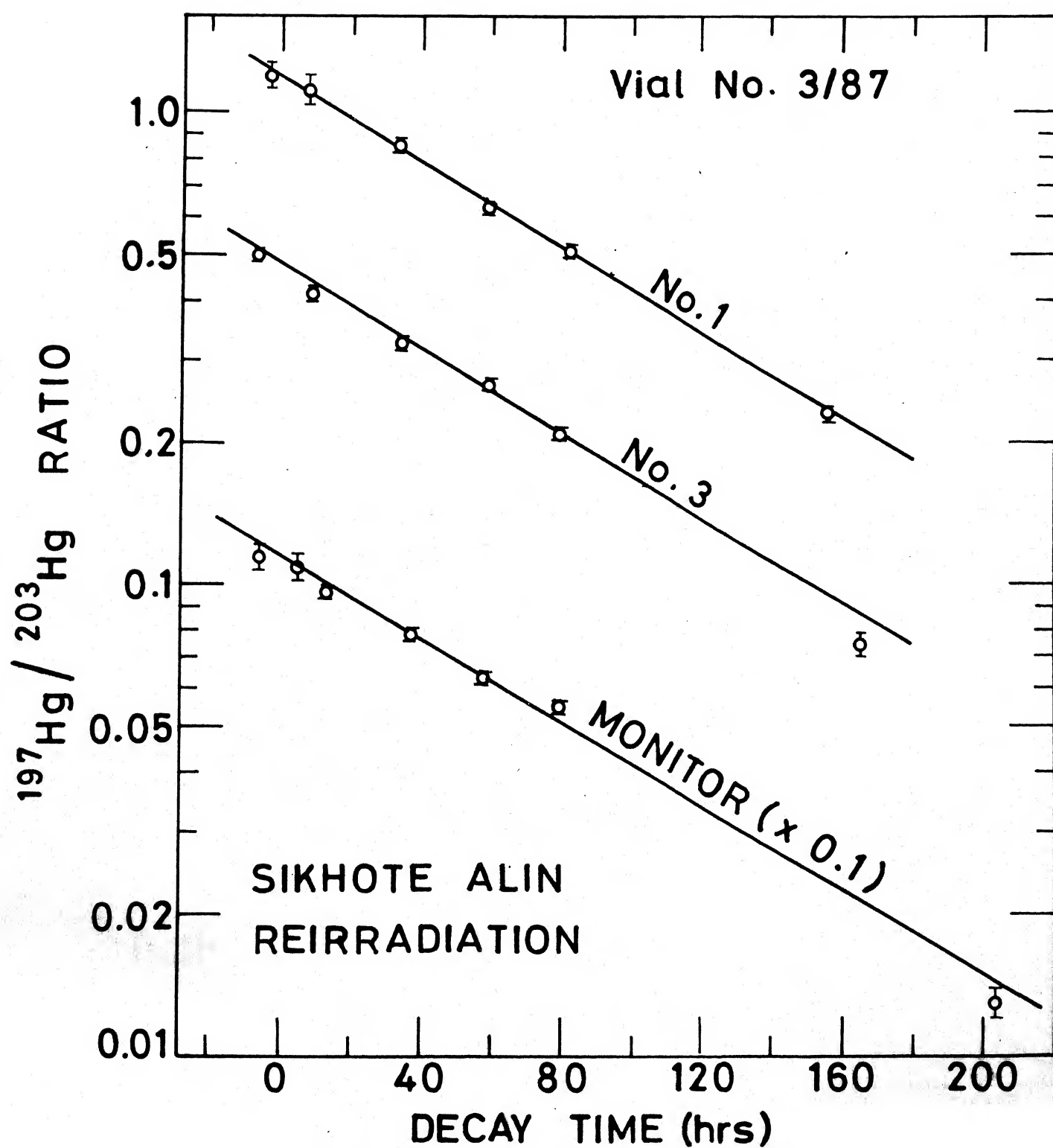


Fig. 4.5 Decay lines of ratio of re-irradiated samples (3/87)

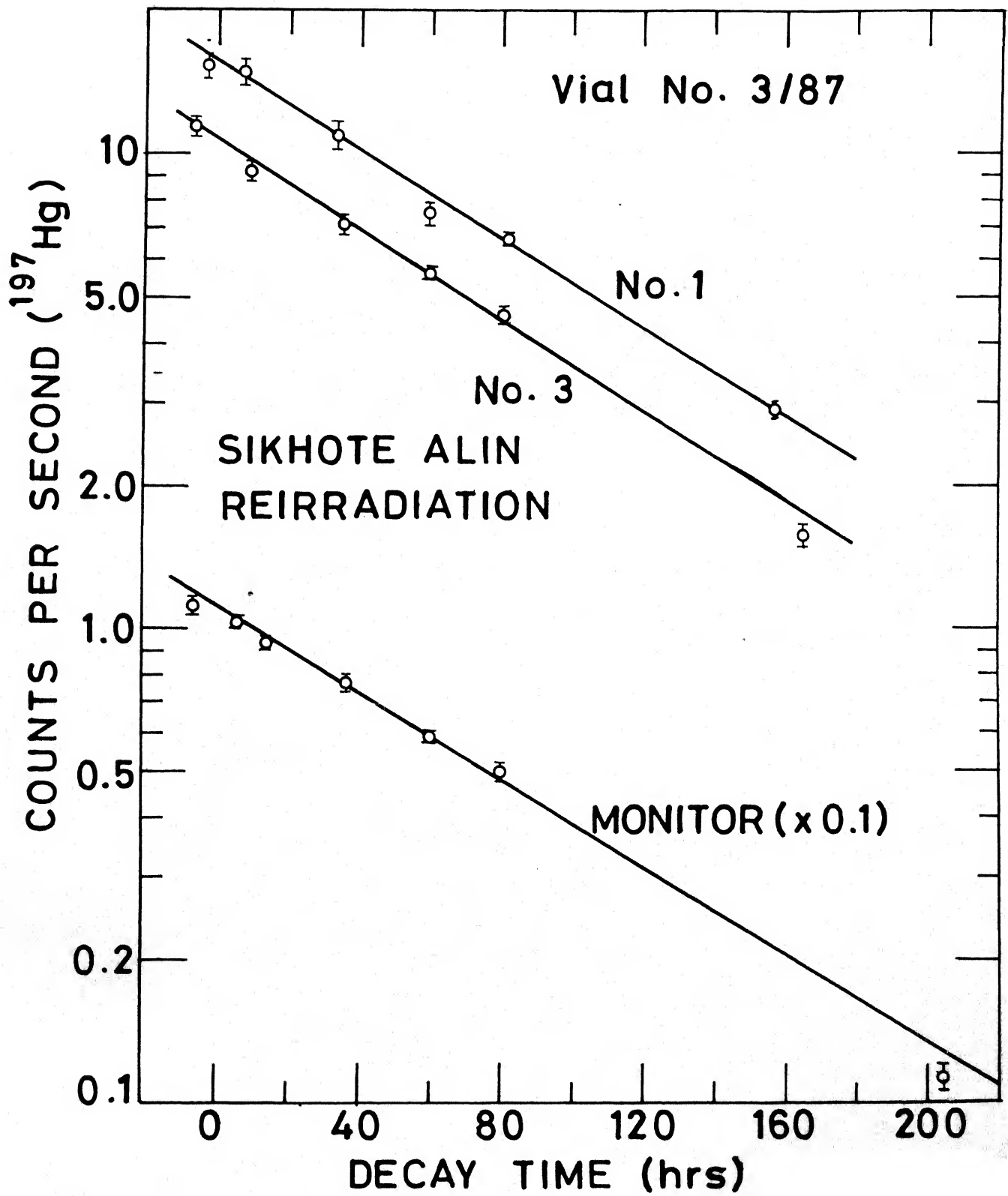


Fig. 4.6 Decay lines of  $^{197}\text{Hg}$  of re-irradiated samples (3/87)

Table 4.4  $^{197}\text{Hg}/^{203}\text{Hg}$  Ratio in Ambapur Nagla

Sample	Irradiation of Meteorite Sample Vial No. 8/86			
	Code No.	Mass (mg)	Hg ( $\mu\text{g}$ )	R/R <sup>+</sup>
Chondrules, m, 200°C	1-2	304.0	0.152	1.13
Fine, m, 100°C	3-1	153.6	0.197	< 0.06*
Fine, m, 500°C	3-5	153.6	0.217	1.01
Fine, nm, 400°C	4-4	292.1	0.01	0.96
Reagent Hg	Mon	-	0.955	1.00
<hr/>				
Sample	Re-irradiation of Distilled Hg Vial No. 4/87			
	Code No.		Hg ( $\mu\text{g}$ )	R/R <sup>+</sup>
Chondrules, m, 200°C	1		0.123	1.08
Fine, m, 100°C	2		0.159	<0.02*
Fine, m, 500°C	3		0.174	1.04
Fine, nm, 400°C	4		<0.006	U
Reagent Hg	11		0.772	1.00

\* = 2  $\sigma$  limit; U = Unmeasurable

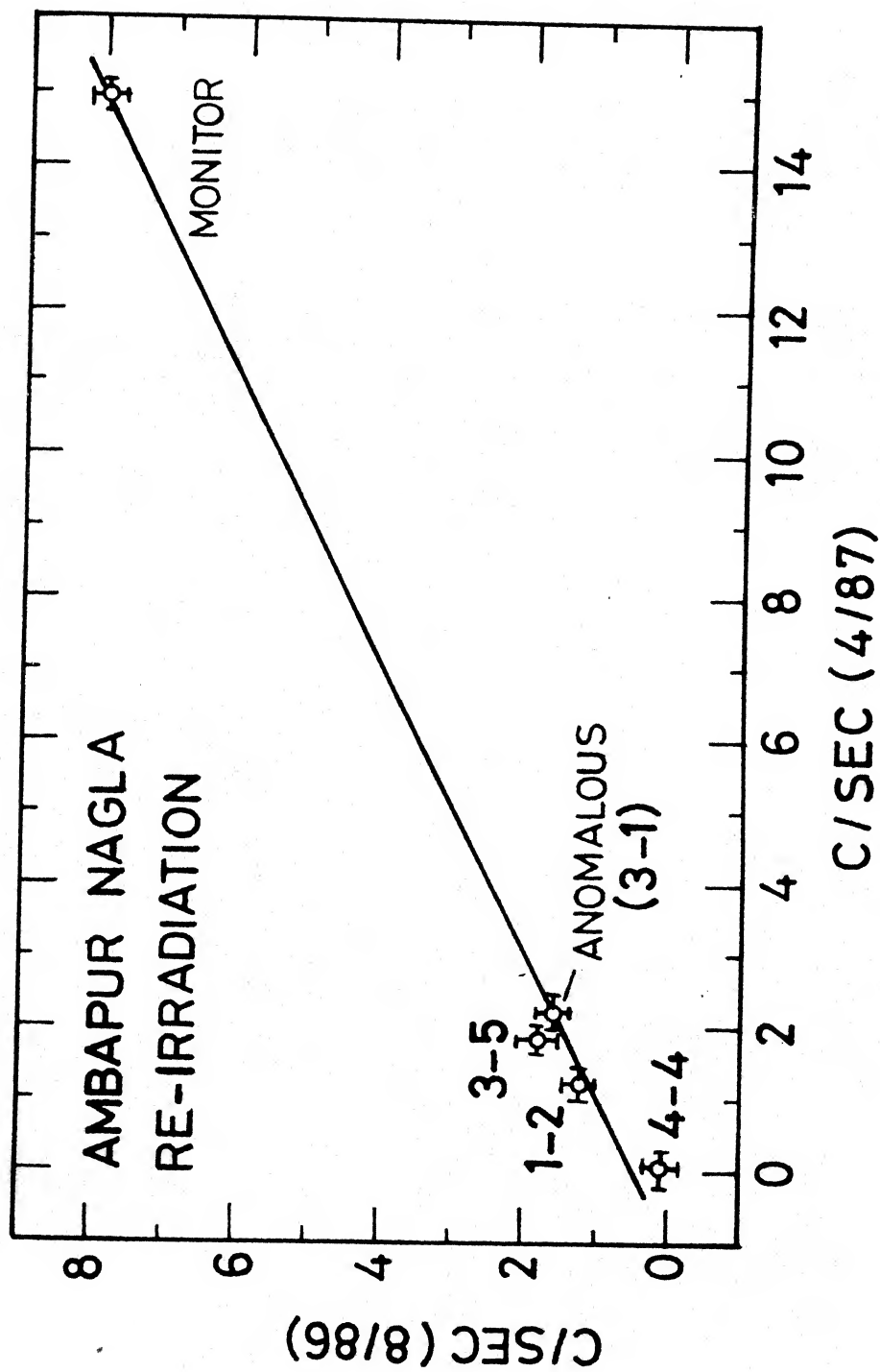


Fig. 4.7 Count-rate in Vial No. 8/86 vs. count-rate in Vial No. 4/87 of Ambapur Nagla samples

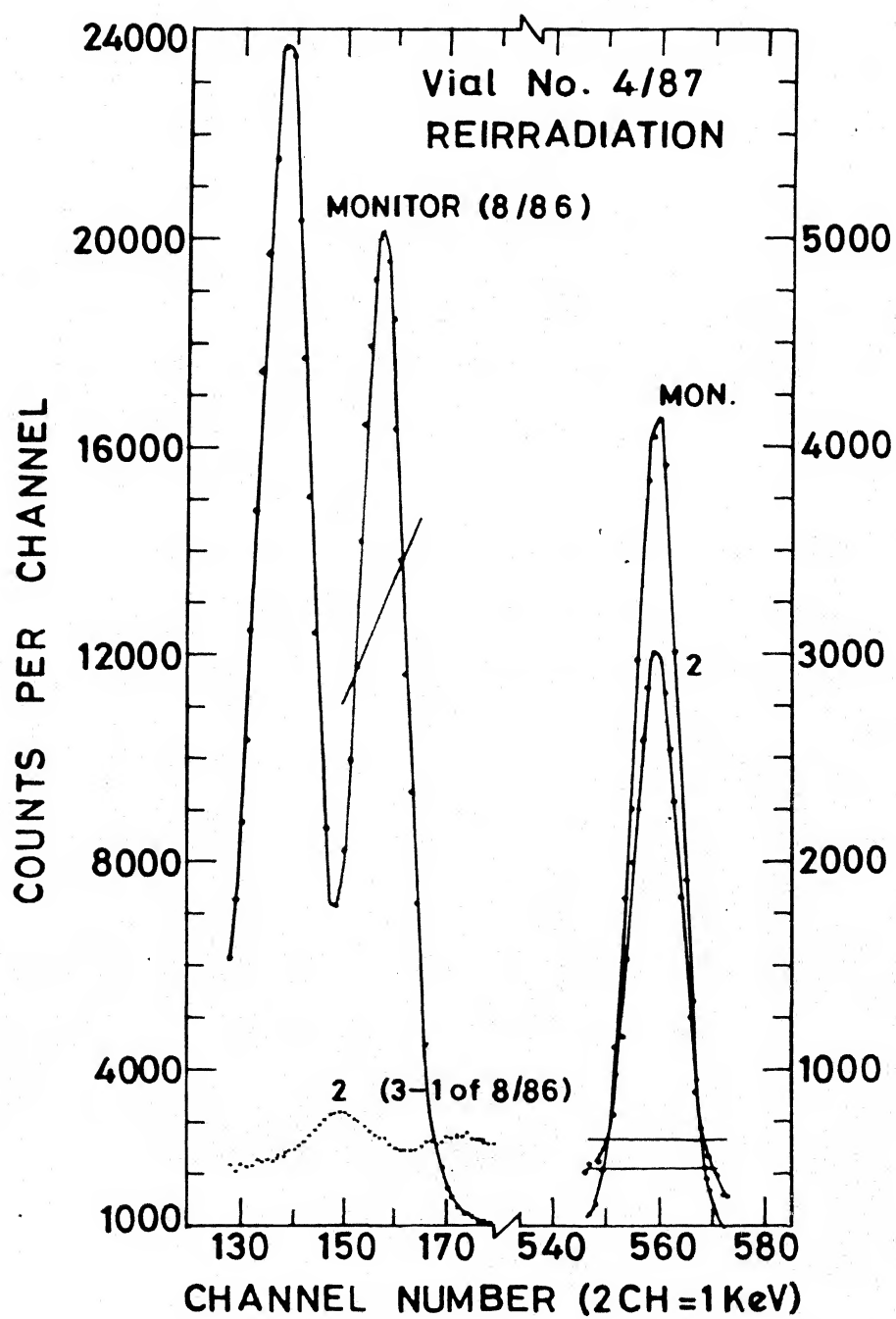


Fig. 4.8 Photon spectra of re-irradiated anomalous sample of Ambapur Nagla and monitor (4/87)

kept alongwith those mentioned above. Re-irradiated samples were distilled at 400°C for one hour each and washed with the NaDDTC/ $\text{CCl}_4$  reagent as usual. The results from the replicate measurements are given in Table 4.5. The average values obtained are compared to the meteorite results in the ~~next two~~ <sup>4.7 and 4.8</sup> tables. The results from Chinge re-irradiation are shown in Table 4.6 and Figure 4.9. It seems that the 23 % negative anomaly in the first sample C-1-1 is real. All others may be just normal. Sikhote Alin re-irradiation results are given in Table 4.7 and Figure 4.10. The blank sample did not show any appreciable counting rate, but sample No. 7-2 may be a bit contaminated. Other isotopic ratios show good agreement from previous results of vial No. 7/86.

#### 4.6 Vial No. 6/87

A set of extracted dried samples of Sikhote Alin from vial No. 9/86 was packed for re-irradiation. It consisted of a normal sample, No. 1-3, a terrestrial standard, and the anomalous samples, Nos. 2-1-D, 2-3-AD, 2-3-AR, 2-3, 2-4 and 2-5. This time the Hg content of some of the anomalous samples were very low. The results are shown in Table 4.8 and 4.9. There are losses in the recovered mercury. Ratios of samples having lower Hg-contents could not be measured because of large errors associated with the countings. Very long countings do not help since background peaks from natural radioactivities interfere around the low energy peak. The high activity samples showed good correlation of the recovered Hg (Figure 4.11) as well as of the ratios (Table 4.9). This measurement probably reflects the limit of detection using this extraction technique.



Table 4.6  $^{197}\text{Hg}/^{203}\text{Hg}$  Ratio in Chinge Residues

Code	Irradiation of Meteorite Sample				Re-irradiation of Distilled Hg	
	Description	Mass (mg)	Hg ( $\mu\text{g}$ )	$\text{R/R}^+$	Hg ( $\mu\text{g}$ )	$\text{R/R}^+$
C-1-1	4th fraction 100°C	15.4	0.004	0.75	0.02	0.77
C-2-1	2nd fraction 100°C	64.5	0.14	1.14	0.14	1.1
C-3-3	3rd fraction 300°C	42.5	0.10	0.94	0.14	1.0
C-4-1	1st fraction 100°C	32.5	0.42	1.0	0.42	1.0
Mon	Reagent Hg	-	1.0	1.0	1.0	1.0

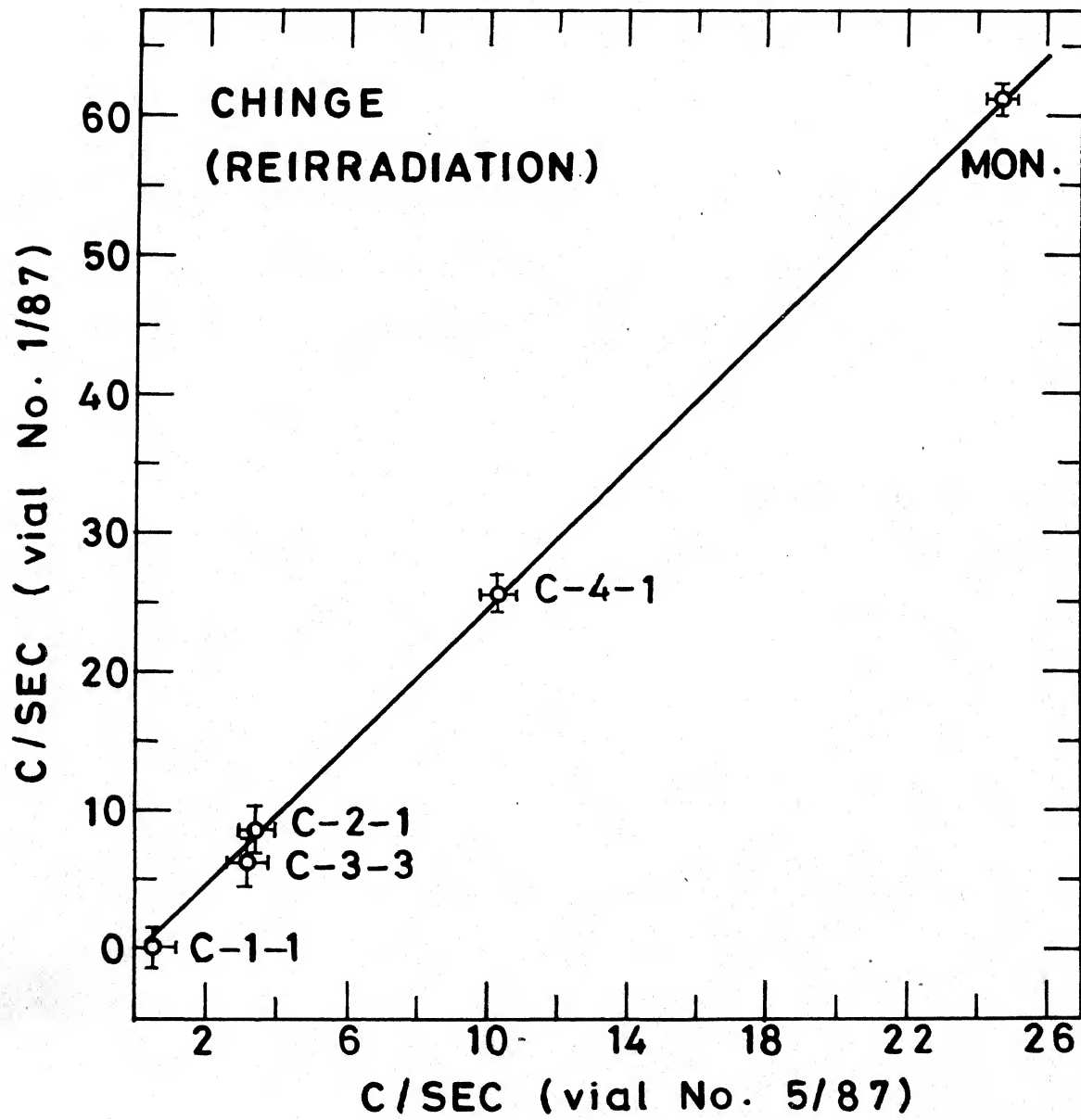


Fig. 4.9 Count-rate in Vial No. 1/87 vs. count-rate in Vial No. 5/87 of Chinge samples

Table 4.7  $^{197}\text{Hg}/^{203}\text{Hg}$  Ratio in Sikhote Alin Residues

Code	Irradiation of Meteorite Samples Vial No. 7/86				Re-irradiation of Distilled Hg; Vial No. 5/87	
	Description	Mass (mg)	Hg ( $\mu\text{g}$ )	R/R <sup>+</sup>	Hg ( $\mu\text{g}$ )	R/R <sup>+</sup>
4-2	< 38 $\mu\text{m}$ , m 200°C (part)	84.8	1.87	1.12(5)	1.88	1.15(2)
6-5	45-75 $\mu\text{m}$ , m 400°C	75.2	0.04	0.73(7)	0.05	0.67(2)
7-2	75-106 $\mu\text{m}$ , m 250°C	64.0	0.115	0.19(2)	0.156	0.80(1)
7-4	75-106 $\mu\text{m}$ , m 400°C	64.0	0.05	$\leq 0.41$	0.05	0.50(2)
1-6	Inclusion 300°C	332.5	Blank	U	<0.002	U
Mon	Reagent Hg	-	-	-	0.90	1.00(2)

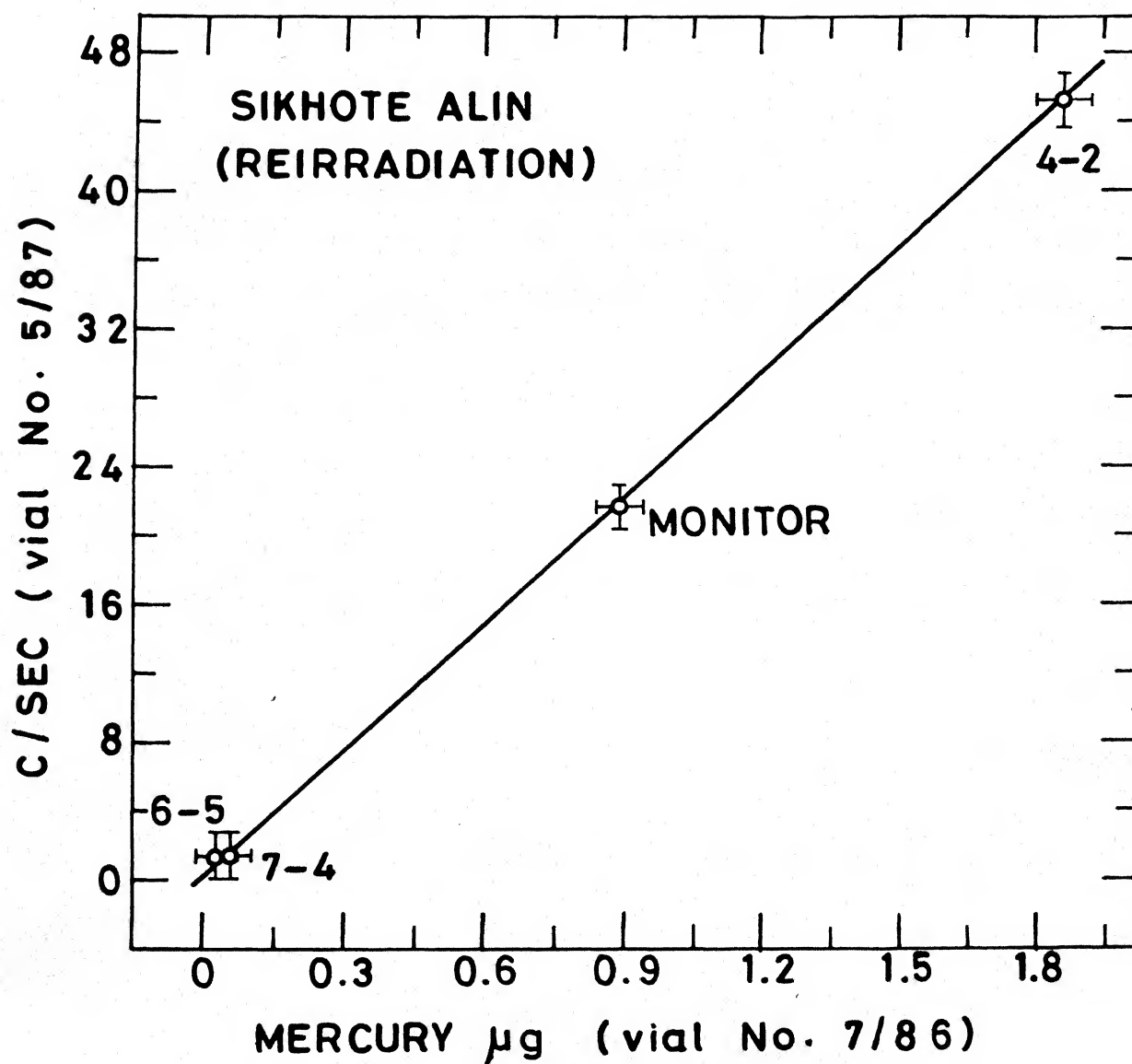


Fig. 4.10 Mercury  $\mu$ g in Vial No. 7/86 vs. count-rate in Vial No. 5/87 of Sikhote Alin samples

Table 4.8 Vial No. 6/87 Reirradiation of Hg Distilled from Sikhote Alin

Sample fraction	Code	cps/10	$\frac{{}^{197}\text{Hg}/{}^{203}\text{Hg} \text{ Ratio}}{\text{Replicate}^*}$		R/R <sup>+</sup>
				Average	
45-75 $\mu\text{m}$ , 81.1 mg 300°C	1-3	30.99	2.89, 2.89, 2.8	2.86	1.0
75-106 $\mu\text{m}$ , 76.6 mg					
200°C	2-1 D	5.42	1.88, 1.89, 1.8	1.86	0.7
300°C	2-3 AD	0.31	Unmeasurable	-	-
300°C	2-3 AR	0.08	Unmeasurable	-	-
300°C	2-3	0.17	Unmeasurable	-	-
400°C	2-4	0.18	2.24±0.3	2.2±0.3	0.8
500°C	2-5	0.11	Unmeasurable	-	-
Reagent Hg (0.7 $\mu\text{g}$ )	Mon I	15.9	2.89, 2.91, 2.89	2.9	1.0
Fresh Monitor (0.33 $\mu\text{g}$ Hg)	Mon	7.6	2.91, 2.88, 2.8	2.9	1.0

\* Errors are less than  $\pm$  5% unless otherwise stated.

Table 4.9  $^{197}\text{Hg}/^{203}\text{Hg}$  Ratio in Sikhote Alin Magnetic Residues

Sample fraction	Code	Irradiation of Meteorite acid residues Vial No. 9/86		Reirradiation of distilled Hg Vial No.6/87	
		Hg (μ g)	R/R <sup>+</sup>	Hg (μ g)	R/R <sup>+</sup>
45-75 μm, 81.1 mg					
300°C	1-3	1.43	1.08	1.39	1.0
75-106 μm, 76.6 mg					
200°C	2-1 D	0.21	0.73	0.21	0.7
300°C	2-3 AD	0.05	0.64	0.01	U
300°C	2-3 AR	0.008	0.65	0.003	U
300°C	2-3	0.04	0.67	0.007	U
400°C	2-4	0.03	0.82	0.01	0.8
500°C	2-5	0.012	0.77	0.004	U
Reagent Hg	Mon	0.70	1.00	0.69	1.0

U = unmeasurable

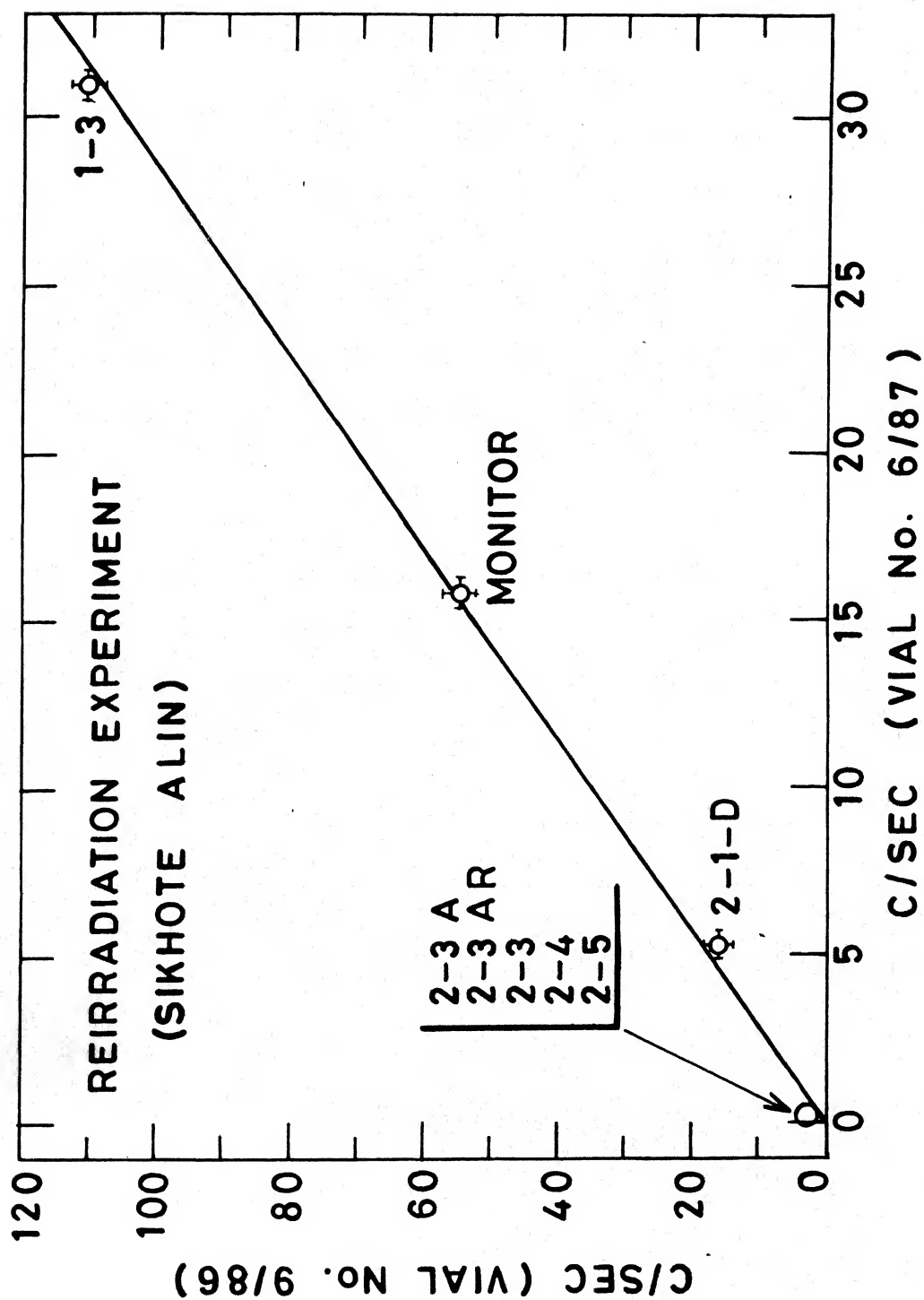


Fig. 4.11 Count-rate in Vial No. 9/86 vs. count-rate in Vial No. 6/87 of Sikhote Alin samples

## Chapter 5

### DISCUSSION

In almost all meteorites, stones as well as irons, in some phase and at some temperature, anomalous  $^{197}\text{Hg}/^{203}\text{Hg}$  ratio is found. The observed deviations are both positive and negative compared to the isotopic ratio of the reagent mercury. The anomalous component appears to be heterogeneously distributed in meteoritic sites or in minerals, apparently having different thermal retentivities and chemical nature. The results obtained from several re-irradiation experiments demonstrate that the anomalies must be real. Also several control experiments rule out the possibility of any experimental artifacts responsible for the observed mercury isotopic variations. The results obtained from the measurements on different meteorites are being given here. Many of the experiments were of exploratory nature. Also sometimes due to incomplete extraction of mercury or due to other experimental difficulties the reliabilities of the results obtained were poor (refer Chapter-3). Those results are not emphasized in this chapter but were given earlier for the sake of completeness.

#### 5.1 Absence of experimental artifacts

In view of the profound implications of the existence of isotopic anomalies of the kind found in meteorites, (Goel and Murty, 1983) it is necessary that a thorough scrutiny of various steps involved in the experiments is carried out to ensure that the observed abnormal activity ratios that we have sporadically found are not due to experimental artifacts which might have arisen either during irradiation or during the subsequent radiochemical purification and counting stages. It may be plausible that the anomaly arises



during irradiation due to causes such as (i) variation in the composition of samples, (ii) modification of neutron energy spectra at different sample sites and (iii) generation of secondary neutrons at some specific sites. These are interrelated factors and, if present, would be responsible for significant self shielding effects. The high absorption cross section for  $^{196}\text{Hg}$  implies a low-lying resonance level for this nuclide. Its activation may therefore be prone to local fluctuations in the neutron energy spectrum. It must be clearly demonstrated that the matrix effects are absent in the relative activation of  $^{196}\text{Hg}$  and  $^{202}\text{Hg}$  during neutron irradiation.

#### 5.1.1 Matrix effects

The influence of elements in the matrix with high neutron absorption cross section was studied in the following experiment. Some meteorite samples were heated to  $1000^{\circ}\text{C}$  in vacuum to extract mercury. The heated powders were mixed with boric acid or cadmium sulphate, and were spiked with reagent mercury (Table 5.1). These homogenised samples were irradiated alongwith the other meteorite samples in sealed quartz capsules in Vial No. 1/86, as usual. The activated samples were heated at  $400^{\circ}\text{C}$  for two hours each to extract mercury. The isotopic ratios were found to be invariable within the limits of error. This result shows that the presence of neutron absorbers like Cd and B do not affect the Hg-activity ratio.

#### 5.1.2 Sample position in a Vial

Two different monitor samples placed at different places in a vial, one at the central and the other at the outer region showed indistinguishable  $^{197}\text{Hg}/^{203}\text{Hg}$  ratio ( $2.9 \pm 0.1$  each) upon activation (see Vial No. 6/86, Table 3.19). Counting rates were also in good agreement, 13.76 and

Table 5.1 Results of Isotopic Ratio of Hg Loaded on Different Matrices

Matrices <sup>*</sup>	Code	cps/2.5	Hg ( $\mu$ g)	$^{197}\text{Hg}/^{203}\text{Hg}$ Ratio
Menow + 0.84 $\mu$ g Hg	M-1	0.64	0.84	$0.57 \pm 0.07$
Menow + 2.5 mg $\text{H}_3\text{BO}_3$ + 0.15 $\mu$ g Hg	M-2	0.08	0.11	U **
Menow + 2 mg $\text{CdSO}_4$ + 1.68 $\mu$ g Hg	M-3	1.26	1.65	$0.51 \pm 0.08$
Amb. Nagla + 2 mg $\text{H}_3\text{BO}_3$ + 0.85 $\mu$ g Hg	M-4	0.64	0.84	$0.59 \pm 0.06$
Amb. Nagla + 1.9 mg $\text{CdSO}_4$ + 2.15 $\mu$ g Hg	M-5	1.63	2.13	$0.60 \pm 0.06$

\* Menow and Ambapur Nagla (~35 mg each) had been already heated earlier at 1000°C in vacuum to extract mercury.

\*\* U means unmeasurable.

13.38 c/s for 0.85 and 0.83  $\mu\text{g}$  Hg respectively. These results show that, within a vial, the neutron energy spectrum in a normal packing does not get modified in a significant way to give any difference in the relative activation of  $^{196}\text{Hg}$  and  $^{202}\text{Hg}$  in the same packing.

### 5.1.3 Counting geometry and sample volume

During sample counting, errors may arise from : (i) a variation in counting geometry, (ii) a variation in counting rate, (iii) the presence of peaks near any of the gamma lines due to contamination and (iv) a drift in instrument gain. Sufficient checks have been made, as given below, to ensure that none of these are responsible for the observed mercury isotopic anomalies.

In order to investigate the effect of geometry on the ratio four equal aliquotes from a high activity mercury monitor were taken and diluted to volumes ranging from 0.20 ml to 1.5 ml. The measured activity ratios are shown in Figure 5.1. In spite of large changes in the counting volume, the ratios remain unchanged. In practice we did not allow the counting volume to change by more than  $\pm 0.1$  ml and kept it generally as 1.0 ml.

### 5.1.4 Dependence of ratio on counting rates

Since the mercury contents of samples in some vials varied by several orders of magnitude, the counting rates were also widely different. Even though the resolution of the detector becomes poor at very high counting rates, it was experimentally demonstrated (Figure 5.2) that the value of ratio did not change. However, the monitor samples of very high counting rates were diluted to maintain good resolution. Diluted aliquotes are labelled as M1, M2, M3 etc.

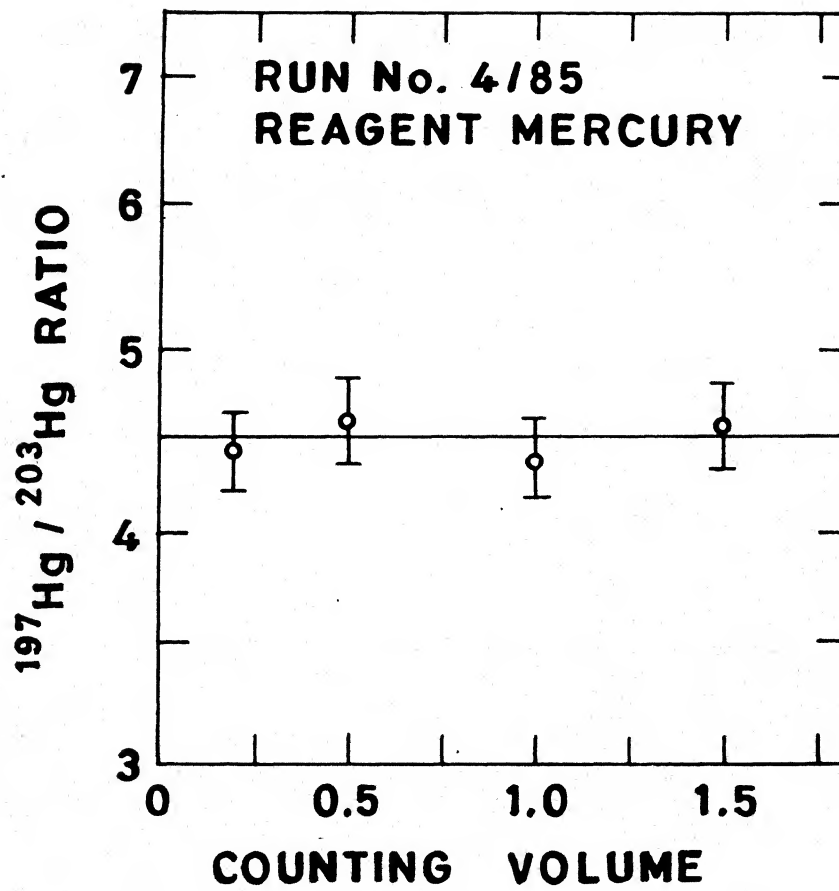


Fig. 5.1  $^{197}\text{Hg}/^{203}\text{Hg}$  ratio vs. counting volume in reagent mercury

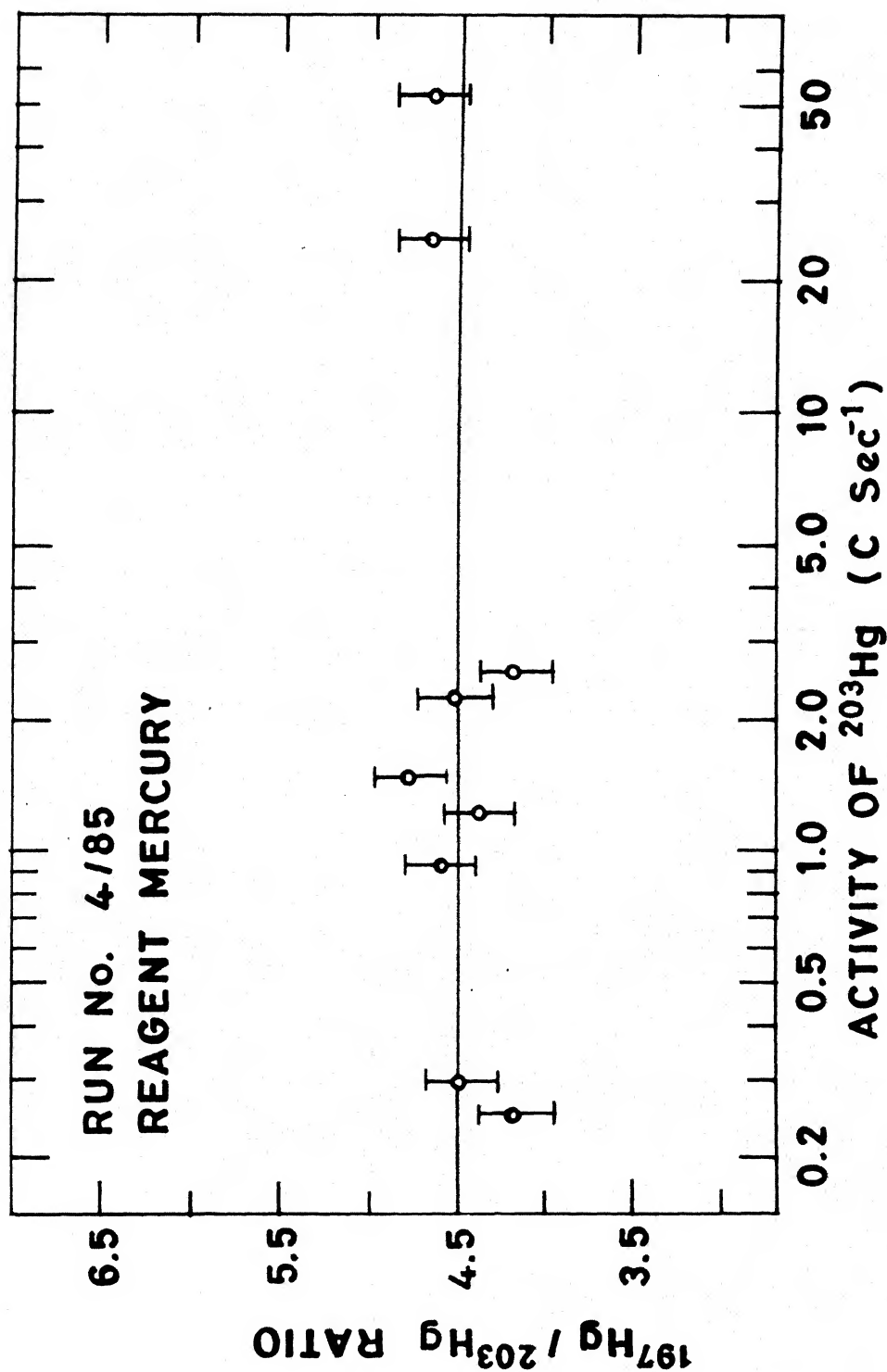


Fig. 5.2  $^{197}\text{Hg}/^{203}\text{Hg}$  ratio vs. activity of  $^{203}\text{Hg}$  in reagent mercury

### 5.1.5 Interferences from other gamma lines

Isotopic ratios of  $^{202}\text{Hg}$  to  $^{196}\text{Hg}$  measured in samples of Vial No. 1/85 on the basis of 279.2 to (77.3 + 77.9) keV photons and 279.2 to (67.0 + 68.8) keV photons are shown in Figure 5.3. This is a case of a set of normal samples and the values are identical within  $\pm 2\%$ . All the isotopic ratio measurements were based on photons of 279.2 keV for  $^{203}\text{Hg}$  and (77.3 + 77.9) keV for  $^{197}\text{Hg}$ . The (67.0 + 68.8) keV photon energies were not used mainly because of the peak being broader. The area under this peak was, however, always recorded to provide a double check on the R values.

In most cases we have verified that the activities decayed with the half lives of the two isotopes. This ensures the absence of contaminants in the vicinity of their photon peaks, and also freedom from line drift and gain shift etc. Other possible factors influencing the measurement of isotopic ratios, such as the differences in the attenuation due to possible variations in the thickness of the counting vials were also found to be unimportant. For example, in the dilution experiment stated above the vials are changed without affecting the isotopic ratios. Several samples and their aliquotes counted over long period give constant ratio.

Several types of blanks, including the meteorite blanks (a heated meteorite sample) showed extremely low mercury level. This shows an absence of contaminants as well as non-interference from mercury from the previous run.

### 5.1.6 Mass fractionation during distillation

For heavy elements like Hg the isotopic fractionation during distillation or any other chemical operation is not expected to be appreciable.

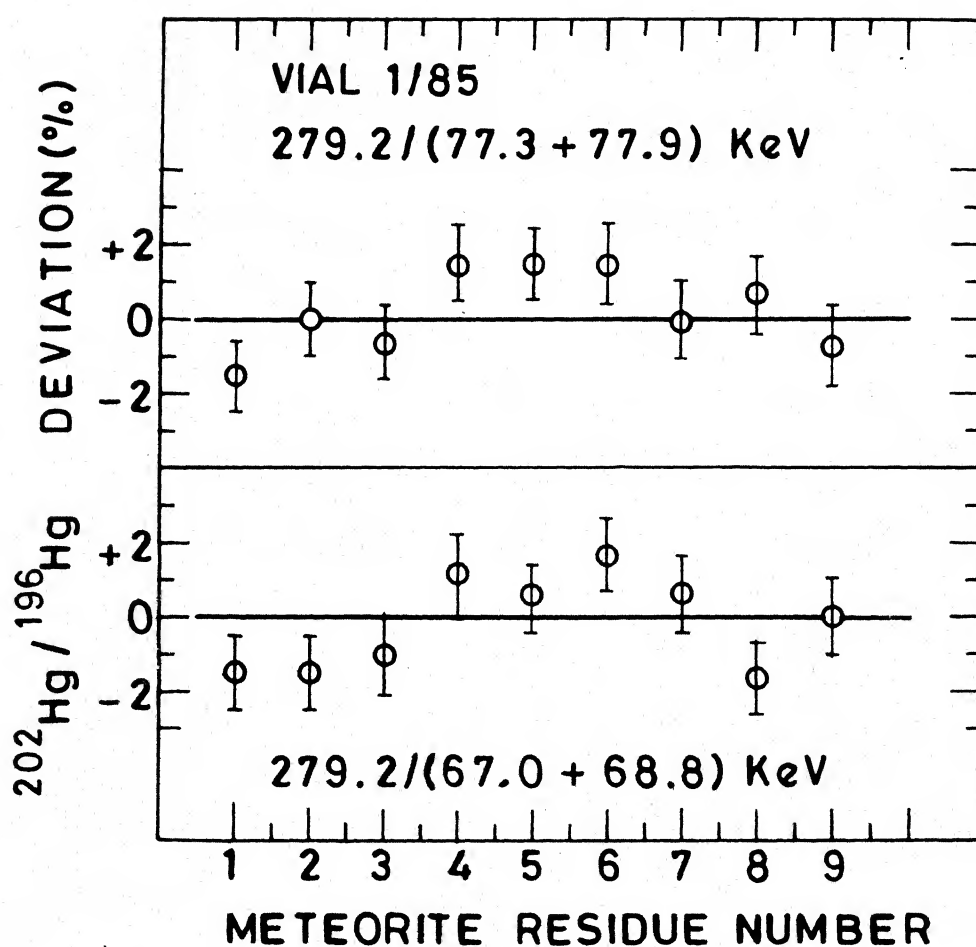


Fig. 5.3 Ratio deviation (%) based on 77 keV and 68 keV photons (from  $^{197}\text{Hg}$ ) and 279 keV gamma energy (from  $^{203}\text{Hg}$ ) in iron meteorite residues

Suitable experiments to verify this for Hg isotopes could not be performed due to the short half life of  $^{197}\text{Hg}$ . However, it has been shown that the mass fractionation of Os isotopes during the distillation of osmium as osmic acid is insignificant (Goel, 1987). The same must be true for Hg isotopes.

### 5.1.7 Re-irradiation experiments

The most convincing evidence against the presence of experimental artifacts during neutron irradiation, chemical processing and counting comes from the results of our re-irradiation experiments as described in Chapter 4. As discussed earlier, it is possible to distill Hg from meteorites with essentially no chemical contamination from the environmental Hg. Several such samples (isolated from meteorites) with known  $^{196}\text{Hg}/^{202}\text{Hg}$  ratios (normal as well as anomalous) were packed under identical chemical forms as well as with comparable contents of Hg and were irradiated again in the reactor. In all cases the pattern of the re-determined  $^{196}\text{Hg}/^{202}\text{Hg}$  ratio remained as in the previous irradiation. The anomalous samples remained anomalous to the same extent. A photon spectrum of an anomalous Hg sample is compared with another samples that has been isotopically diluted in Figure 5.4, both having been irradiated again.

## 5.2 Anomalies in stone meteorites

Samples from twelve stone meteorites have been studied. The measurements on Ambapur Nagla were repeated several times. The extreme values of isotopic ratios,  $(R/R^+)$ , normalised to terrestrial values were  $< 0.06$  ( $2\sigma$ ) to 1.5 in Ambapur Nagla and Allende respectively. Often we noticed a pattern in isotopic ratio variation with the temperature.



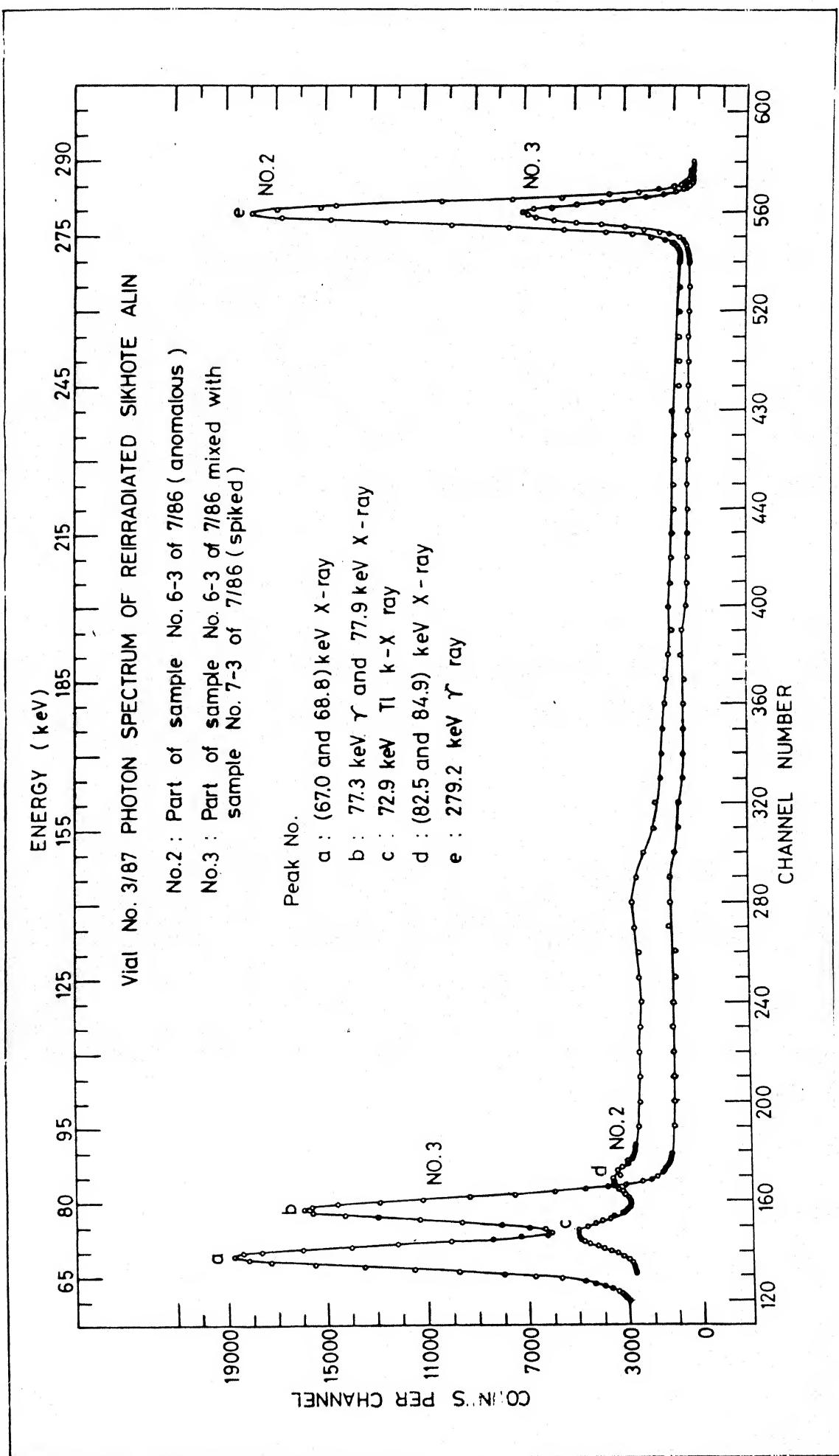


Fig. 5.4 Photon spectra of re-irradiated samples of Sikhote Alin residue

### 5.2.1 Allegan (H5)

One bulk sample of Allegan meteorite was studied in Vial - No.5/86. The isotopic ratio measured in the 100°C temperature released fraction was slightly above normal (~10%). The total mercury content of the bulk was 2.5 ppm.

### 5.2.2 Allende (CV3)

A vial full of Allende fragments alone (3/86) was analysed. The  $R/R^+$  values varied from 0.41 to 1.54. Two bulk samples (Nos. IV and V) showed a similar profile of isotopic ratio with respect to temperature. The lower temperature fraction has isotopic ratio lower than normal. The ratios of next higher temperature fractions go to above the normal and again drop down to lower than the normal. Bulk VI has, unlike others, a high ratio at the lowest temperature. The Hg abundances measured in three bulk samples (Nos. IV, V and VI) range from 0.27 to 0.51 ppm.

In Table 5.2 are given those data on Allende meteorite samples where the  $R/R^+$  values deviate from the normal value (unity) by more than  $\pm 10\%$ . All data for Allende samples are shown schematically in Figures 5.5 and 5.6. The Hg distilled at 150°C shows a wider variation in having both positive and negative deviations. The 250°C fraction has, like the other higher temperature fractions, a lower Hg abundance. However  $R/R^+$  is higher than normal in all the cases at 250°C while the same is lower than normal in the other higher temperature distillates.

### 5.2.3 Ambapur Nagla (H5)

Samples of this meteorite have been analysed in ten different vials. While many samples and their temperature fractions were normal,

Table 5.2 Anomalies in Allende (Vial No. 3/86): the summary

Sample	Mass (mg)	Code	T(°C)	ppb (Hg)	R / R <sup>+</sup>
Bulk I	140.7	1-1	150	976	0.38 (2)
		1-4	450	170	0.18 (6)
Bulk II	183.5	2-1	150	302	0.67 (1)
		2-3	350	162	0.41 (4)
Bulk IV	224.5	4-2	250	189	1.15 (4)
		4-3	350	78	0.66 (1)
Bulk V	425.0	5-2	250	189	1.54 (8)
Bulk VI	309.8	6-1	150	89	1.35 (12)
		6-2	250	106	1.21 (10)
		6-4	450	27	0.65 (15)

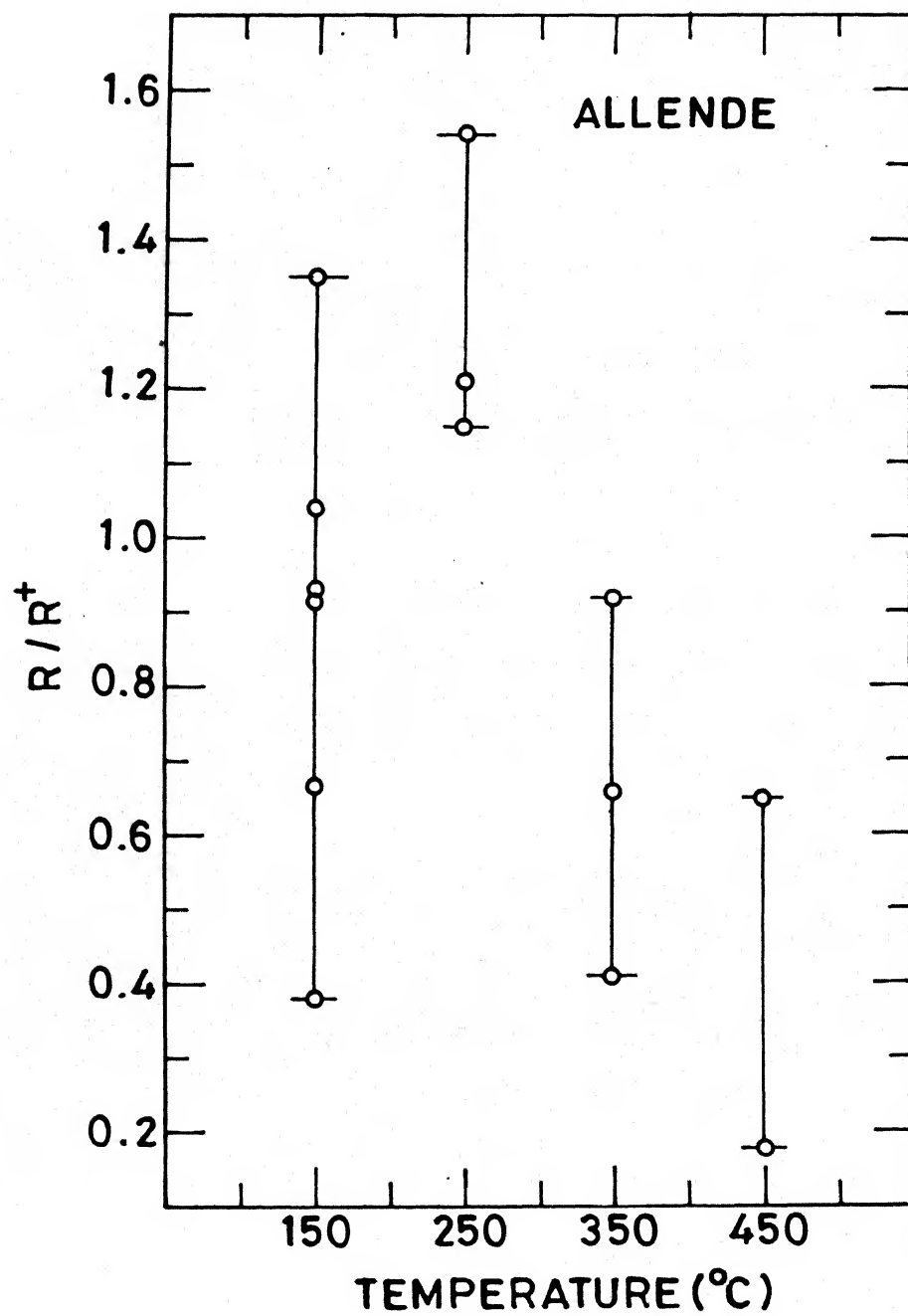


Fig.5.5  $R/R^+$  vs. temperature in Allende.

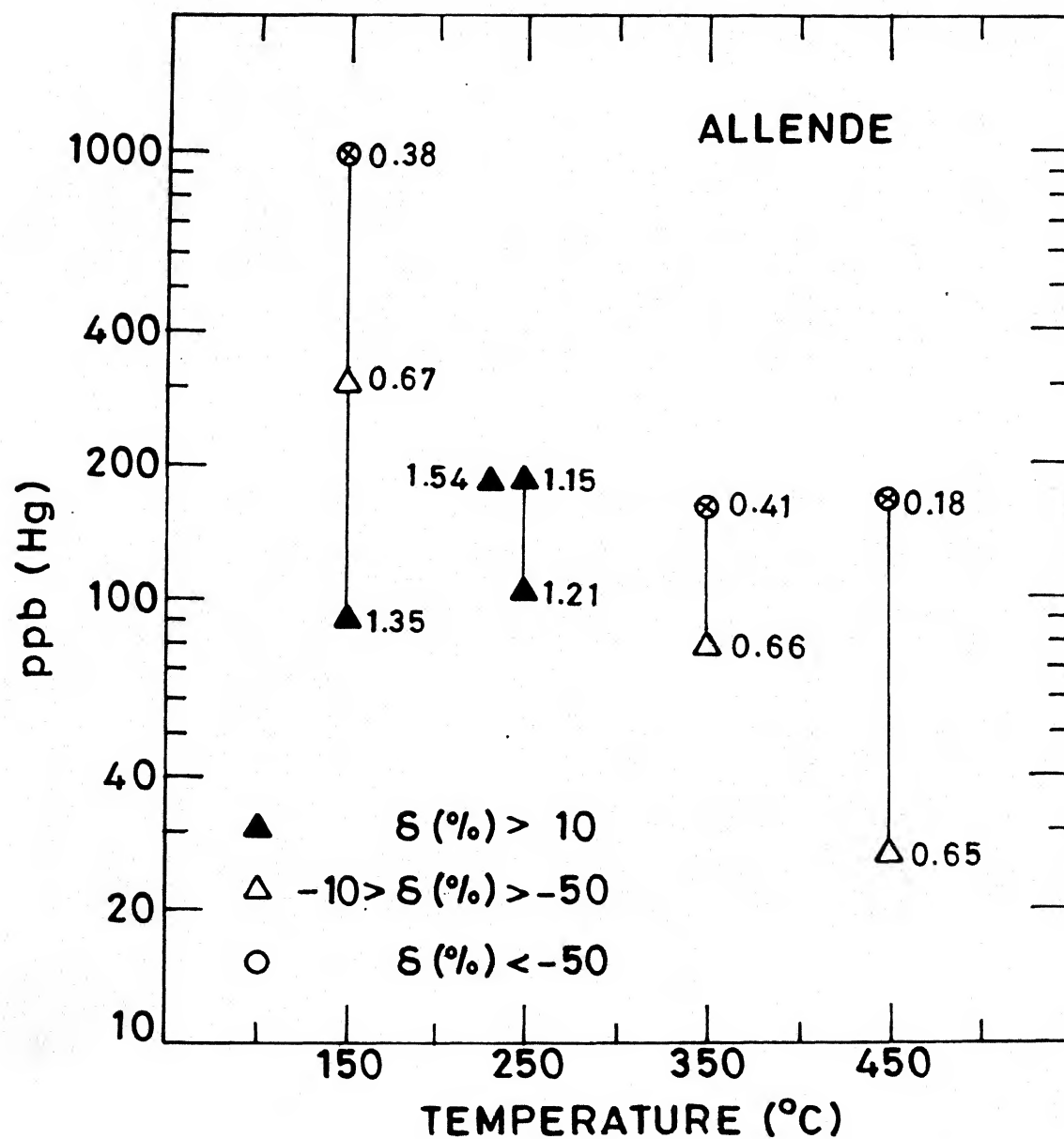


Fig.5.6 ppb-Hg vs. temperature in Allende.

often some showed mercury isotopic variations. The extreme values of  $R/R^+$  were  $<0.06$  ( $2\sigma$ ) and 1.18. Several times the following temperature profile of isotopic ratio variation was observed : lower than normal, above normal (or sometimes just normal), normal and again lower than normal with the increase of temperature. Usually the mercury contents of the anomalous fractions were low. Fortunately the most anomalous sample, No. 3-1 of 8/86, had a reasonably high Hg-concentration (1.3 ppm). In the spectrum of this sample the photons of the lighter nuclide,  $^{197}\text{Hg}$  were completely missing.

The calculations of gross ratios (page ) show that due to the generally lower abundances of the anomalous components, if one were to isolate total mercury from all temperature sites, one would get, in most cases, a normal value of the isotopic ratio. Total mercury contents of different samples vary significantly (from 74 ppb to 234 ppm).

The calculated ratios,  $R/R^+$ , for all the analysed samples are given in Table 5.3. In 9 cases out of 20 we note a variation in  $R/R^+$  which is greater than 10% of the normal value. In Table 5.4 are summarized the data on the samples of Ambapur Nagla where the anomalies are greater than 10%. There does not seem to be any preponderance of anomalous data in any particular kind of sample like chondrules, magnetic, non-magnetic fractions, etc. Some trend is however seen in the variation of the isotopic ratio with the temperature of distillation. This is seen more clearly in Figure 5.7. Low temperature distillates have a tendency to give low  $R/R^+$  which goes to the above-normal value at 200 - 300°C. Finally both, the concentration, and  $R/R^+$ , values drop down at high temperature (Figure 5.8).

Table 5.3 Gross values of  $R/R^+$  and Hg contents in Ambapur Nagla

Sample	Mass (mg)	Vial No.	Gross	
			ppb (Hg)	$R/R^+$
Bulk	201.5	9/85	74	0.47
	83.0	9/85	3445	1.04
	145.0	9/85	3141	0.95
	332.1	4/86	6481	1.13
	267.5	4/86	19253	1.12
	216.0	8/86	1527	0.93
Chondrules	217.7	9/85	1609	0.80
	304.0	8/86	1353	0.95
Bulk, mag.	183.3	9/85	537	0.91
	212.2	4/86	23413	1.14
Bulk, non-mag.	431.0	4/86	11822	1.12
<75 $\mu\text{m}$ , mag.	153.6	8/86	4604	$\geq 0.76$
<75 $\mu\text{m}$ , non-mag.	340.5	9/85	4755	0.96
	292.1	8/86	419	0.83
<38 $\mu\text{m}$ , non-mag.	227.9	8/85	2536	1.05
>38 $\mu\text{m}$ , non-mag.	243.2	8/85	516	0.82
>38 $\mu\text{m}$ , mag.	62.9	8/85	746	1.05
	89.5	8/85	411	1.07
75-106 $\mu\text{m}$ , non-mag.	120.5	4/86	17788	1.08
125-150 $\mu\text{m}$ , non-mag.	112.2	4/86	12364	1.08

Table 5.4 Summary of Anomalous Isotopic Ratios in Ambapur Nagla

Sample	Mass (mg)	Vial No.	Code	T(°C)	ppb (Hg)	R/R <sup>+</sup>
Bulk	201.5	9/85	1-1	100	25	0.25 (2)
			1-2	200	10	0.39 (5)
			1-4	400	26	0.66 (7)
Bulk	83.0	9/85	8-1	100	83	0.71 (7)
			8-5	500	69	0.77 (7)
			8-6	600	76	0.79 (5)
Bulk	145.0	9/85	5-4	400	95	0.77 (5)
			5-5	500	60	0.55 (4)
			5-6	600	115	0.54 (4)
Bulk	332.1	4/86	7-4	200	1900	1.13 (2)
			7-5	300	3989	1.17 (3)
Bulk	267.5	4/86	8-4	200	4077	1.15 (3)
			8-5	300	12289	1.13 (6)
Bulk	216.0	8/86	2-2	200	68	<0.48 (2 $\sigma$ )
Chondrules	304.0	8/86	1-1	100	63	<0.30 (2 $\sigma$ )
			1-5	500	133	0.60 (10)
			1-6	600	108	0.76 (7)
Chondrules	217.7	9/85	3-1	100	300	0.77 (4)
			3-2	200	830	0.89 (2)
			3-3	300	236	0.79 (2)
			3-4	400	47	0.70 (2)
			3-5	500	196	0.48 (1)

Contd.....



Table 5A continued

Sample	Mass (mg)	Vial No.	Code	T(°C)	ppb (Hg)	R/R <sup>+</sup>
<38 $\mu$ m, mag.	13.0	4/85	6	400	2000	0.78 (7)
<38 $\mu$ m, nm	4.0	4/85	3	400	5300	0.56 (5)
38-75 $\mu$ m, nm	34.0	4/85	5	400	1700	0.62 (5)
>38 $\mu$ m, nm	89.2	8/85	4	500	142	0.55 (8)
	243.2	8/85	14	600	25	0.64 (7)
>38 $\mu$ m, mag.	62.9	8/85	10	500	11	0.39 (6)
106-125 $\mu$ m, nm	119.9	4/86	2-4	200	3310	1.18 (2)
			2-5	300	5733	1.17 (2)
<75 $\mu$ m, mag.	153.6	8/86	3-1	100	1282	<0.06 (2 $\sigma$ )
<75 $\mu$ m, nm	292.1	8/86	4-1	100	46	<0.78 (2 $\sigma$ )
	340.5	9/85	4-5	500	131	0.66 (4)
			4-6	600	60	0.63 (5)
Bulk, mag.	183.3	9/85	2-3	300	10	0.54 (7)
	212.2	4/86	9-2	150	4300	1.17 (3)
			9-5	300	10426	1.16 (4)
Bulk, non-mag.	431.0	4/86	10-5	300	5169	1.15 (1)

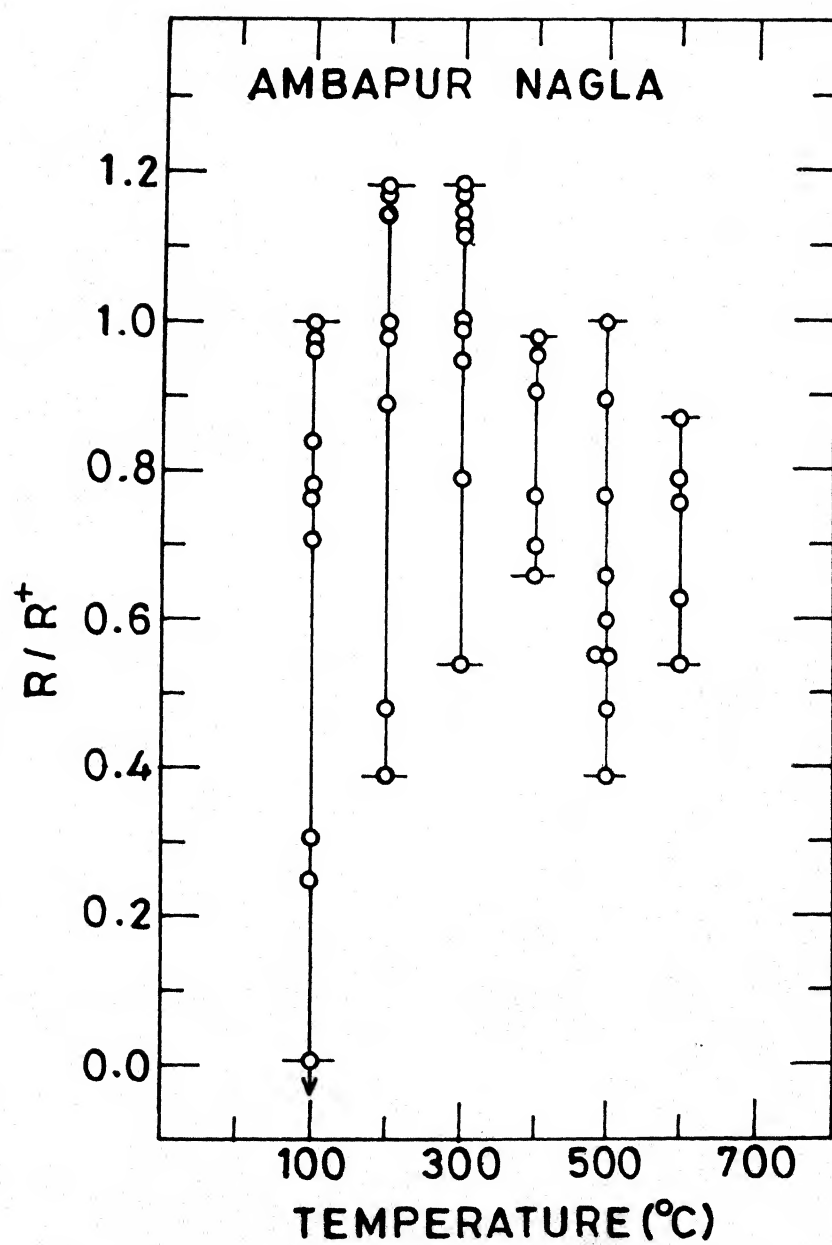


Fig.5.7  $R/R^+$  vs. temperature in Ambapur Nagla.

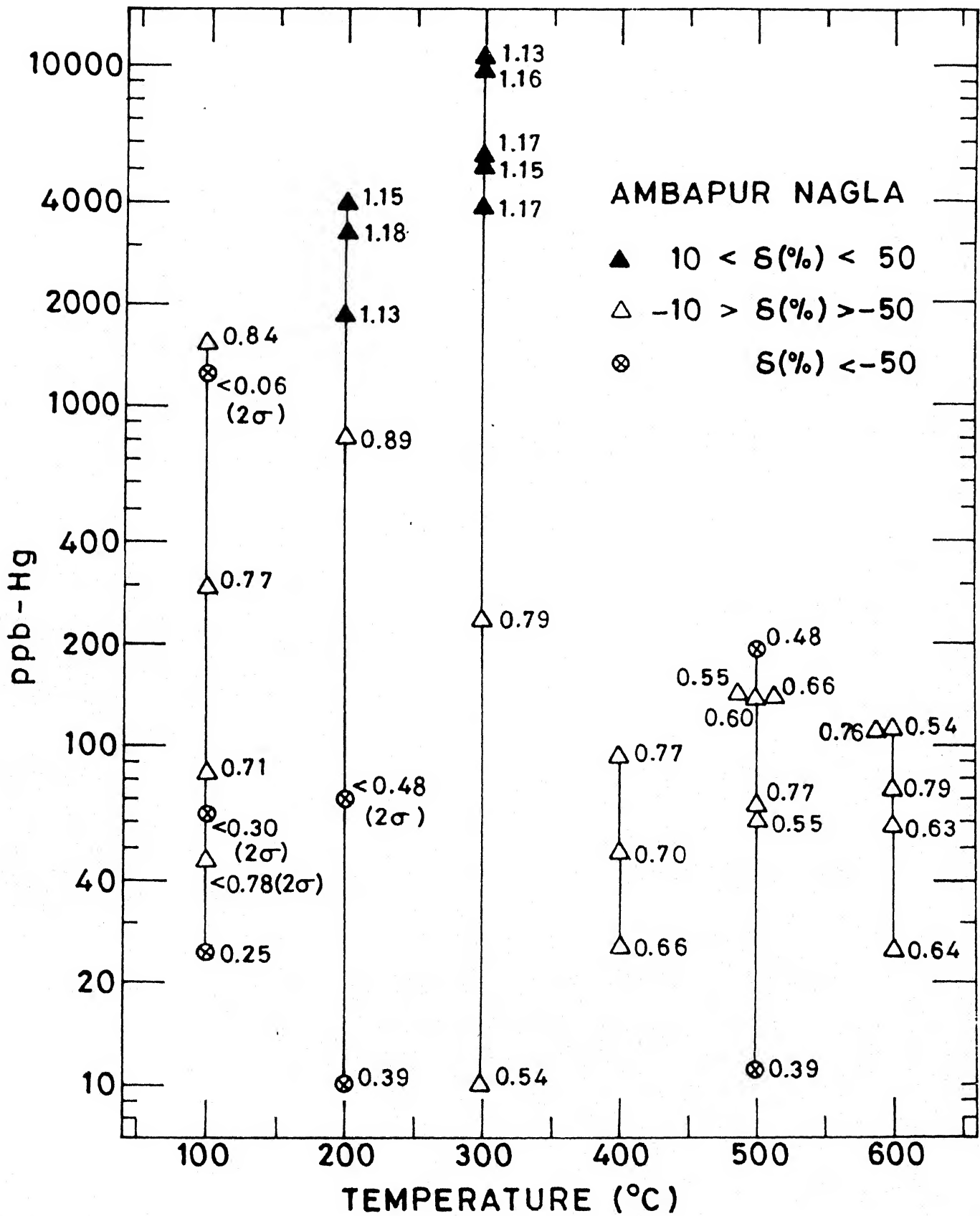


Fig.5.8 ppb-Hg vs. temperature in Ambapur Nagla.

#### 5.2.4 Cold Bokeveld (CM2)

Three samples of this meteorites, analysed, in Vial No. 2/86, gave  $R/R^+$  values from 0.5 to 1.13. There is no regularity in the temperature profile. The Hg-abundances are remarkably high in these samples. All three samples viz., bulk, fine and coarse showed a very similar total mercury contents of 32.9, 32.3 and 33.3 ppm respectively.

#### 5.2.5 Dhajala (H3-4)

Although Dhajala samples were studied in three different vials (Nos. 3/85, 1/86 and 5/86), most of the measurements were unsatisfactory. The results, with large errors, indicate that some of the samples from this meteorite might have a high positive anomaly in addition to the negative anomaly.

#### 5.2.6 Elenovka (L5)

Three samples of Elenovka (bulk, fine and coarse) were analysed in Vial No. 2/86. The  $R/R^+$  values vary between 0.48 to 1.15. There is no regular pattern with respect to temperature. The total Hg-concentrations are 1.66, 7.36 and 1.33 for bulk, fine and coarse samples respectively. A summary of anomalous isotopic ratios in Cold Bokeveld, Dhajala and Elenovka are given in Table 5.5.

#### 5.2.7 Forest Vale (H4)

Two samples of this meteorite were studied in Vial Nos. 5/85 and 7/85. Both of them were found to have a normal isotopic composition of mercury.

Table 5.5 Anomalies in Cold Bokeveld, Dhajala and Elenovka: the summary

Sample	Mass (mg)	Vial No.	Code	T(°C)	ppm (Hg)	R/R <sup>+</sup>
Cold Bokeveld						
Fine	166.8	2/86	C-2-3	600	1.22	0.48 (2)
Coarse	278.2	2/86	C-3-1	100	2.22	1.13 (2)
Dhajala						
< 75 $\mu$ m, nm	107.5	1/86	5-1	300	3.27	1.18 (27)
	367.5	5/86	8-1	150	-	0.81 (6)
> 75 $\mu$ m, nm	185.0	1/86	3-1	300	1.23	2.31 (81)
Olivines, 75-210 $\mu$ m	488.5	3/85	12	500	0.72	4.30 (87)
Elenovka						
Bulk	247.3	2/86	E-1-2	400	0.14	0.48 (3)
Fine	196.0	2/86	E-2-2	600	7.02	1.15 (2)

### 5.2.8 Holbrook (L6)

A single fragment of Holbrook was studied at four temperature steps in Vial No. 2/87. The first two temperature (100- and 200°C) steps released mercury that was close to normal. The ratios in the next two temperature (300- and 400°C) fractions could not be measured because of very poor counting rate.

### 5.2.9 Karkh (L6)

Two irradiated fragments of Karkh were distilled at four temperature steps for Vial No. 10/86. Since the ratios could not be measured, some of the distillates (with good Hg-concentrations) were re-irradiated for Vial No. 4/87. All samples were found to be close to normal within a conservative error of  $\pm 10\%$ .

### 5.2.10 Menow (H4)

Only one sample of Menow was studied in Vial No. 5/85. The Hg released at 500°C was 0.17 ppm with a normal composition of the isotopic ratio.

### 5.2.11 Rangala (L6)

Five bulk samples studied in two different Vials (Nos. 9/85 and 1/87) rendered total Hg-concentrations between 0.14 to 2.1 ppm. The  $R/R^+$  variations, measured in different temperature fractions of Hg released, are from 0.38 to unity. The profile of isotopic ratio variations with temperature is similar to the Ambapur Nagla results. A summary of results is given in Table 5.6.

Table 5.6 Anomalies in Rangala and Richardton: the summary

Sample	Mass (mg)	Vial No.	Code	T(°C)	ppb (Hg)	R/R <sup>+</sup>
Rangala						
Bulk	180.1	9/85	6-4	400	89	0.54 (2)
			6-5	500	32	0.55 (2)
			6-6	600	22	0.48 (4)
Bulk	154.0	9/85	7-2	200	170	0.86 (5)
			7-4	400	21	0.73 (9)
			7-5	500	26	0.54 (5)
			7-6	600	17	0.38 (5)
Bulk	226.0	1/87	R-1-4	400	2	0.80 (4)
Bulk	209.1	1/87	R-2-4	400	7	0.81 (4)
Richardton						
Chondrules,nm	466.5	5/86	3-2	250	38	1.51 (24)
<32 $\mu$ m, nm	134.3	5/86	4-5	550	297	<0.4 (2 $\sigma$ )

### 5.2.12 Richardton (H5)

Four samples of this meteorite showed highly variable Hg-concentrations (0.46 to 15.74 ppm). Mercury isotopic anomalies were also found. The  $R/R^+$  values range from  $<0.4$  ( $2\sigma$ ) to  $1.51 \pm 0.24$ . Any clear pattern of isotopic ratio variation with temperature was not seen.

A comparison of mercury abundances in stone meteorites measured in this work to those of the literature values is presented in Table 5.7. In general there is a good agreement (within a factor to two) except in the case of carbonaceous chondrite Type II. It would be interesting to study other meteorites of this class.

## 5.3 Anomalies in Iron meteorite residues

Samples from  $H_2SO_4$  acid-insoluble residues of nine iron meteorites have been studied. More extensive investigations were carried out on residues from Sikhote Alin. Isotopic anomalies have been found in many of these measurements. The extreme values of  $^{197}Hg/^{203}Hg$  ratio, normalised to the monitor, ( $R/R^+$  values) are  $<0.003$  ( $2\sigma$ ) and 1.3. No bulk sample of iron meteorite was analysed because of the radiation hazard problems. There does not appear to be any regular pattern of isotopic anomaly with respect to temperature. Iron meteorites also seem to have a sporadic behaviour in the variations of the Hg isotopic ratios, as noted for stones.

### 5.3.1 Bear Creek (III B)

Three samples obtained from this meteorite were studied in Vial No. 1/85. There was no mercury monitor present. All the samples gave the same isotopic ratio, which is assumed to be normal.



Table 5.7 Mercury from Chondrites

Meteorite Classification	No. of Meteorites	Concentration Range (ppm)	
		This work	Literature*
In Bulk			
L-Group	4	0.25 - 8.52	0.02 - 5.99
H-Group	7	0.07 - 19.25	0.07 - 13.90
Carbonaceous II	1	32.9	1.57 , 6.82
Carbonaceous III	1	0.27 - 1.2	0.009 - 7.3
In Chondrules	5	0.23 - 1.6	0.91 - 2.01

\* Compiled from Reed et al., 1960; Ehman and Lovering, 1967; and Reed, 1971. Carbonaceous II value for this work is from Cold Bokveld whereas the literature value is from Murray and Mighei.

### 5.3.2. Campo del Cielo (1A)

Samples of residues obtained from Campo del Cielo were analysed in five different vials (Nos. 1/85, 3/85, 5/85, 6/85 and 2/87). Most of the measurements showed a normal isotopic composition of mercury. Results from Vial No. 2/87 showed variations in  $R/R^+$  values from 0.5 to 1.3 (Table 5.8), in bulk residues. The total mercury concentrations in three bulk samples were 9.44, 14.44, 9.42 ppm.

### 5.3.3 Canyon Diablo (1A)

Hg-isotopic ratio in the samples of Canyon Diablo residues were measured in three different vials (Nos. 3/85, 5/85 and 2/86). The  $R/R^+$  values varied from 0.63 to 1.15.

### 5.3.4 Carbo (IID)

Carbo samples were irradiated in three different vials (Nos. 7/85, 2/86 and 6/86). Measurements from one of the vials (No. 6/86) gave all normal values within  $\pm 10\%$ . The  $R/R^+$  variations observed from the other two vials range from 0.36 to 1.04. Hg abundances of different samples vary from 11.3 to 57.04 ppm.

### 5.3.5 Chinga (IV B ANOM)

The extreme  $R/R^+$  values observed in Chinga are 0.72 and 1.13 (Table 5.9). A correlation of isotopic ratio variation is not found with the densities of the residues or with the temperature steps. The Hg abundances vary from 1.9 ppm to 96 ppb.

Table 5.8 Summary of Anomalous Isotopic Ratios in Campo del Cielo, Canyon Diablo and Carbo residues

Sample	Mass (mg)	Vial No.	Code	T(°C)	ppm (Hg)	R/R <sup>+</sup>
Campo del Cielo						
Bulk	127.7	2/87	C-1-5	500	0.08	0.49 (15)
Bulk	65.8	2/87	C-3-1	100	2.35	1.26 (6)
Canyon Diablo						
75-105 $\mu\text{m}$ , m	23.9	3/85	5	500	0.65	0.63 (8)
> 150 $\mu\text{m}$ , m	205.5	2/86	5-2	400	2.06	1.15 (7)
Carbo						
< 38 $\mu\text{m}$ , m	38.2	7/85	13	500	-	0.54 (3)
38-75 $\mu\text{m}$ , m	37.2	7/85	14	200	-	0.36 (6)
			15	500	-	0.49 (8)
> 150 $\mu\text{m}$ , m	74.5	2/86	3-2	400	0.52	0.83 (2)

Table 5.9 Summary of Anomalous Isotopic Ratios in Chinga, Elga and Odessa residues

Sample	Mass (mg)	Vial No.	Code	T(°C)	ppm (Hg)	R/R <sup>+</sup>
Chinga						
4th Fraction	15.4	1/87	C-1-1	100	0.027	0.72 (3)
			C-1-2	200	0.022	0.77 (4)
1st Fraction	32.5	1/87	C-4-3	300	0.088	1.13 (5)
Elga						
Bulk magnetic	13.9	3/85	7	500	0.79	0.43 (8)
Silicate Incl. (vwm)	120.0	6/86	1-2	250	0.47	0.81 (4)
Flakes, mag.	53.0	6/86	2-2	250	0.68	0.81 (4)
			2-3	350	0.07	1.11 (8)
Odessa						
Bulk	71.9	6/87	0-1-1	100	0.57	1.10 (5)
			0-1-2	200	1.03	0.85 (4)
			0-1-3	300	0.53	0.80 (4)
Bulk	78.8	6/87	0-2-2	200	0.77	0.75 (3)
			0-2-3	300	0.29	0.74 (3)

### 5.3.6 Elga (II E)

From the measurements made in two vials (Nos. 3/85 and 6/86), the normalised Hg-isotopic ratio is seen to vary from 0.43 to 1.11. The abundance of Hg are from 0.79 to 4.18 ppm.

### 5.3.7 Odessa (IA)

The mercury isotopic ratios in two bulk samples of Odessa residues were measured in Vial No. 6/87. Out of the five distillation steps for each, the isotopic ratio could be measured only in the first three temperature fractions. The  $R/R^+$  values ranged between 0.74 and 1.1. The mercury abundance of the two samples were 2.39 and 1.24 ppm.

### 5.3.8 Sikhote Alin (IIB)

This meteorite has shown the largest anomalies in the isotopic ratios of Hg and also of Os (Goel, 1987). Samples of Sikhote Alin iron meteorite were analyzed in five separate vials (Nos. 2/85, 3/85, 2/86, 7/86 and 9/86). The overall variations in the  $R/R^-$  values were from  $<0.01$  ( $2\sigma$ ) to 1.13. Out of the five inclusion samples (Vial No. 2/85), three were anomalous. Another inclusion sample (Vial No. 2/86) showed isotopic anomalies in all three released fractions of Hg (Figure 5.9). In Vial No. 7/86 huge isotopic anomaly was found in the Hg released at 250°C from the 45-75  $\mu\text{m}$  magnetic sample (Code No. 6-3, Figure 5.10). The spectrum of this sample (Figure 5.11) did not show any photon peak due to  $^{197}\text{Hg}$ . Another sieve size sample (75-106  $\mu\text{m}$ , mag.) also showed the anomaly. Other aliquotes of these two samples (45-75  $\mu\text{m}$ , mag. and 75-106  $\mu\text{m}$ , mag.) were packed in Vial No. 9/86. This time the first sample was almost normal while the other one

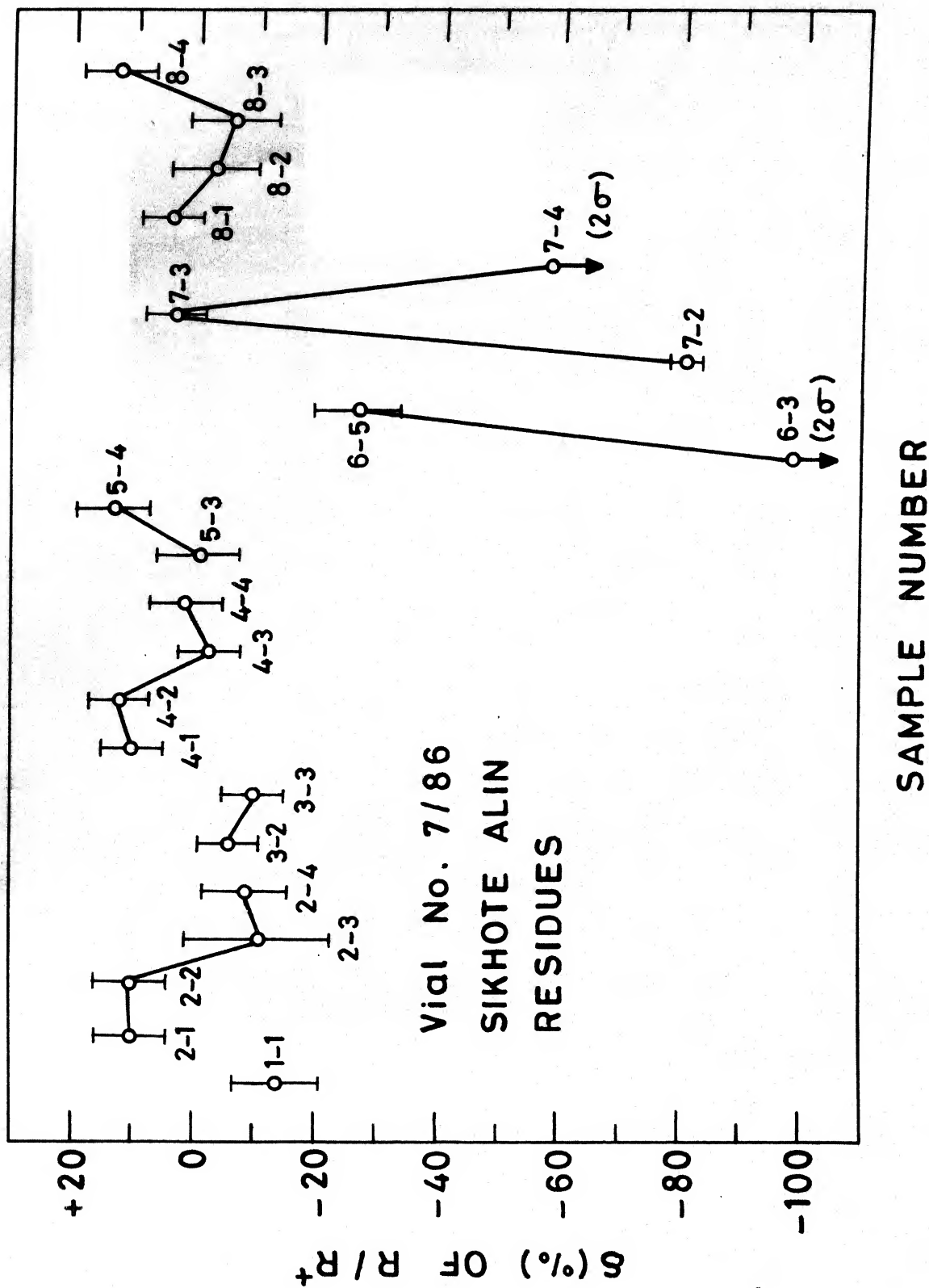


Fig. 5.10  $R/R^+$  variation in Sikhote Alin residue samples

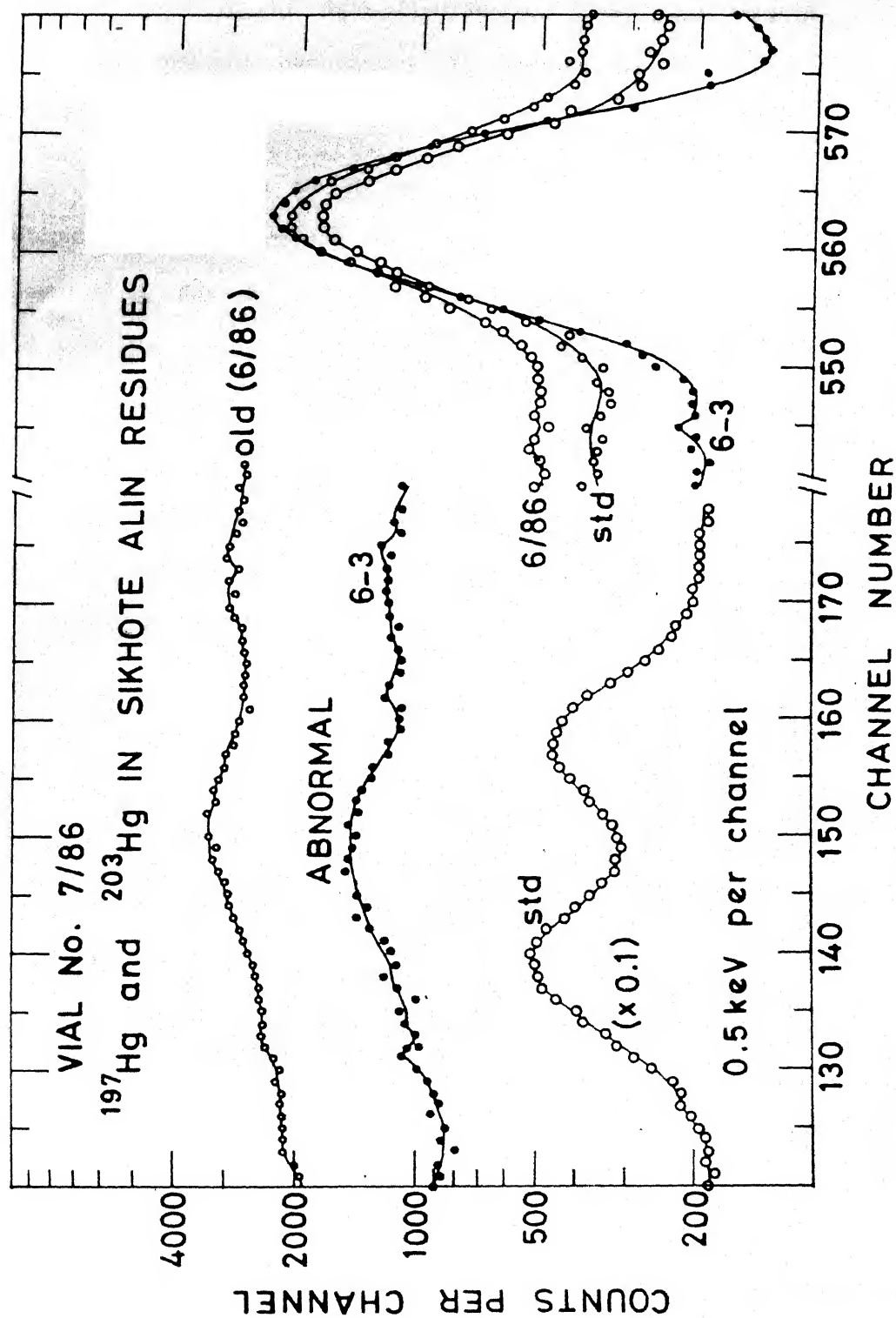


Fig. 5.11 Photon spectra of anomalous and normal samples of Sikhote Alin

was anomalous at all temperatures (Figure 5.12). Most of the interesting samples of Sikhote Alin were re-irradiated to establish that these anomalies were real. Mercury abundances of different samples varied widely; from 0.15 ppm to 129 ppm.

The data on all samples of Sikhote Alin with anomalous Hg isotopic ratios are summarized in Table 5.10. Though one often sees positive values of  $\delta$ , the negative  $\delta$  values are more pronounced and glaring. We find generally negative  $\delta$  values at high temperatures as in the case of Ambapur Nagla stone meteorite. The lowest value is seen at 250°C contrasted with the 100°C value for Ambapur Nagla (see Figure 5.13). The anomalous Hg is often present in relatively high concentrations as seen from Figure 5.14. The calculated gross values of  $R/R^+$  and Hg contents in all samples of Sikhote Alin are given in Table 5.11.

#### 5.3.9 Toluca (1A)

Three residues of this meteorite were analyzed in Vial No. 2/85. Since the ratios were uniform and no monitor was present for comparison the values have been assumed to be normal.

There do not appear any reported Hg abundance measurements in iron meteorites. The reported values of Hg abundances in troilite samples are compared with acid residues values of this work in Table 5.12. The low concentration of Hg found in troilite from iron meteorites appear to eliminate this mineral as the site of most of the Hg found in meteorites (Reed, 1971).



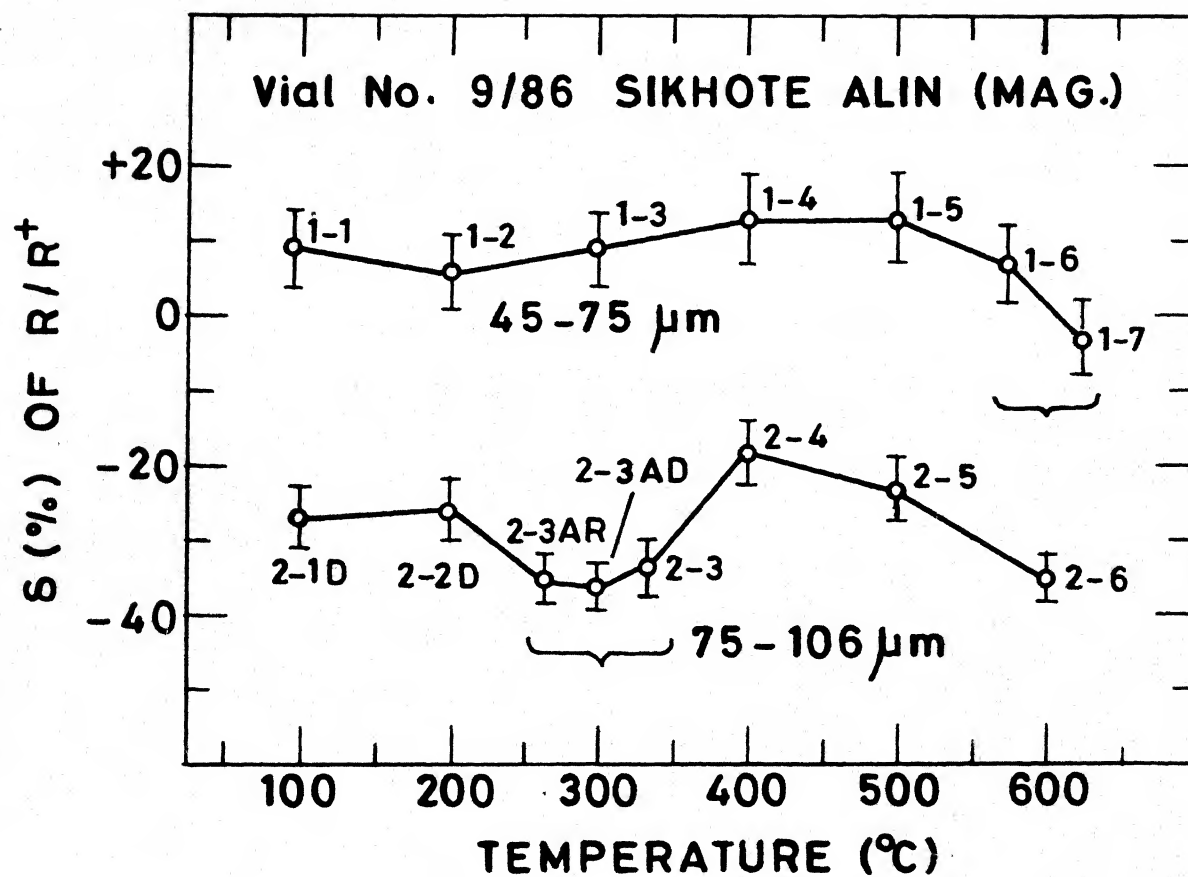
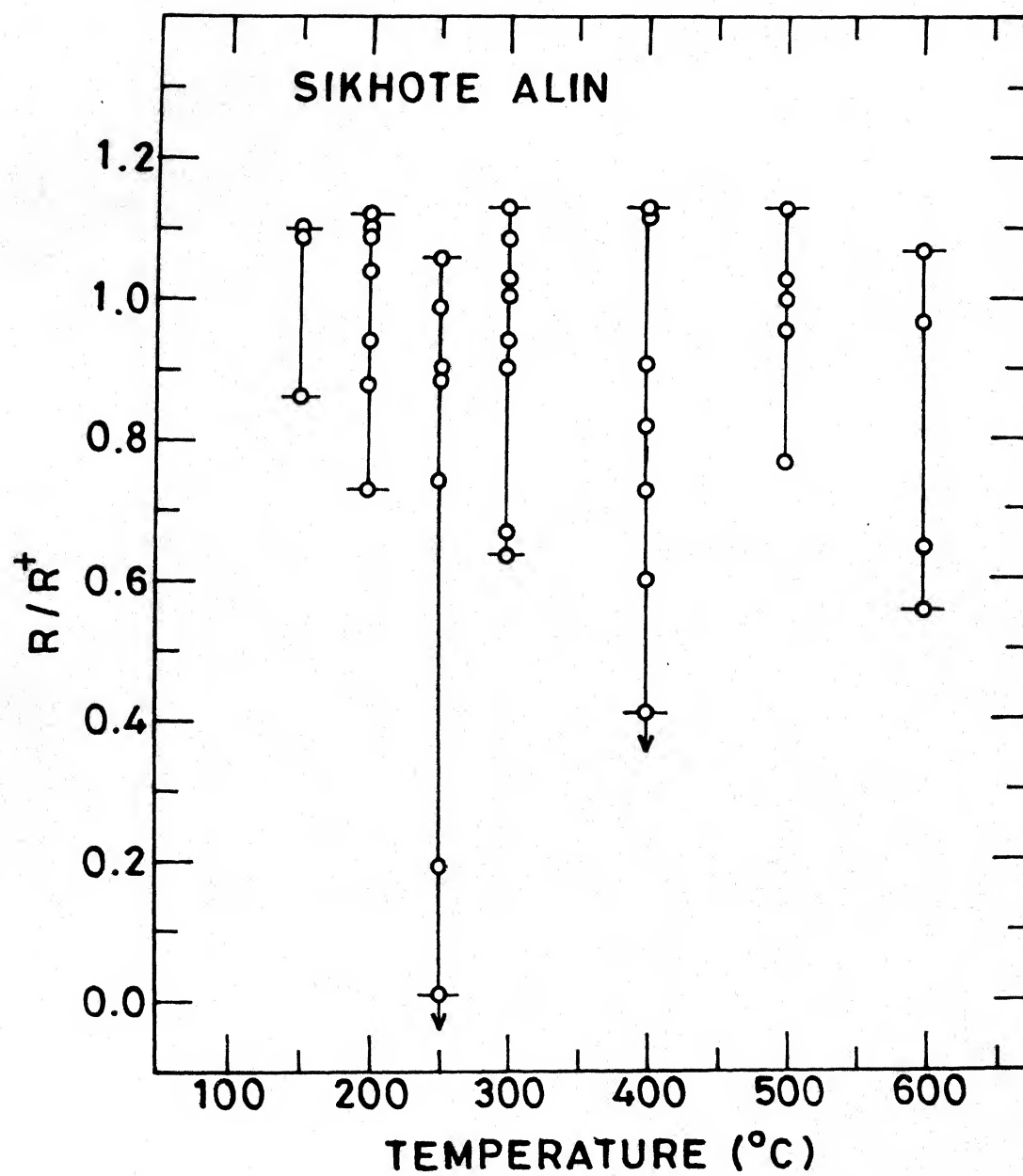


Fig. 5.12 Variation of  $R/R^+$  vs. temperature in Sikhote Alin

Table 5.10 Summary of Anomalous Isotopic Ratios in Sikhote Alin Residues

Sample	Mass (mg)	Vial No.	Code	T(°C)	ppm (Hg)	R/R <sup>+</sup>
Inclusion	155.0	2/85	4	400	0.08	0.58 (6)
	7.0	2/85	4A	400	0.19	0.44 (11)
	8.0	2/85	9A	400	1.14	0.53 (12)
	217.7	2/86	4-1	200	0.89	0.88 (2)
			4-2	400	0.11	0.60 (6)
			4-3	600	0.09	0.56 (5)
	332.5	7/86	1-1	150	0.09	0.86 (7)
<38 $\mu$ m, mag.	84.8	7/86	4-2	200	18.75	1.12 (5)
38-45 $\mu$ m, mag.	82.2	7/86	5-4	300	2.19	1.13 (6)
45-75 $\mu$ m, mag.	75.2	7/86	6-3	250	11.04	< 0.01 (2 $\sigma$ )
			6-5	400	0.54	0.73 (7)
	81.1	9/86	1-4	400	9.45	1.13 (6)
			1-5	500	3.95	1.13 (6)
75-106 $\mu$ m, mag.	64.0	7/86	7-2	250	1.81	0.19 (1)
			7-4	400	0.76	< 0.41 (2 $\sigma$ )
	76.6	9/86	2-1-D	200	2.70	0.73 (4)
			2-2-D	250	1.15	0.74 (4)
			2-3-AD	300	0.67	0.64 (3)
			2-3	300	0.58	0.67 (3)
			2-4	400	0.35	0.82 (4)
			2-5	500	0.16	0.77 (4)
			2-6	600	0.17	0.65 (3)
106-125 $\mu$ m, mag.	95.5	7/86	8-4	400	1.35	1.13 (6)



**Fig. 5.13**  $R/R^+$  vs. temperature in Sikhote Alin .

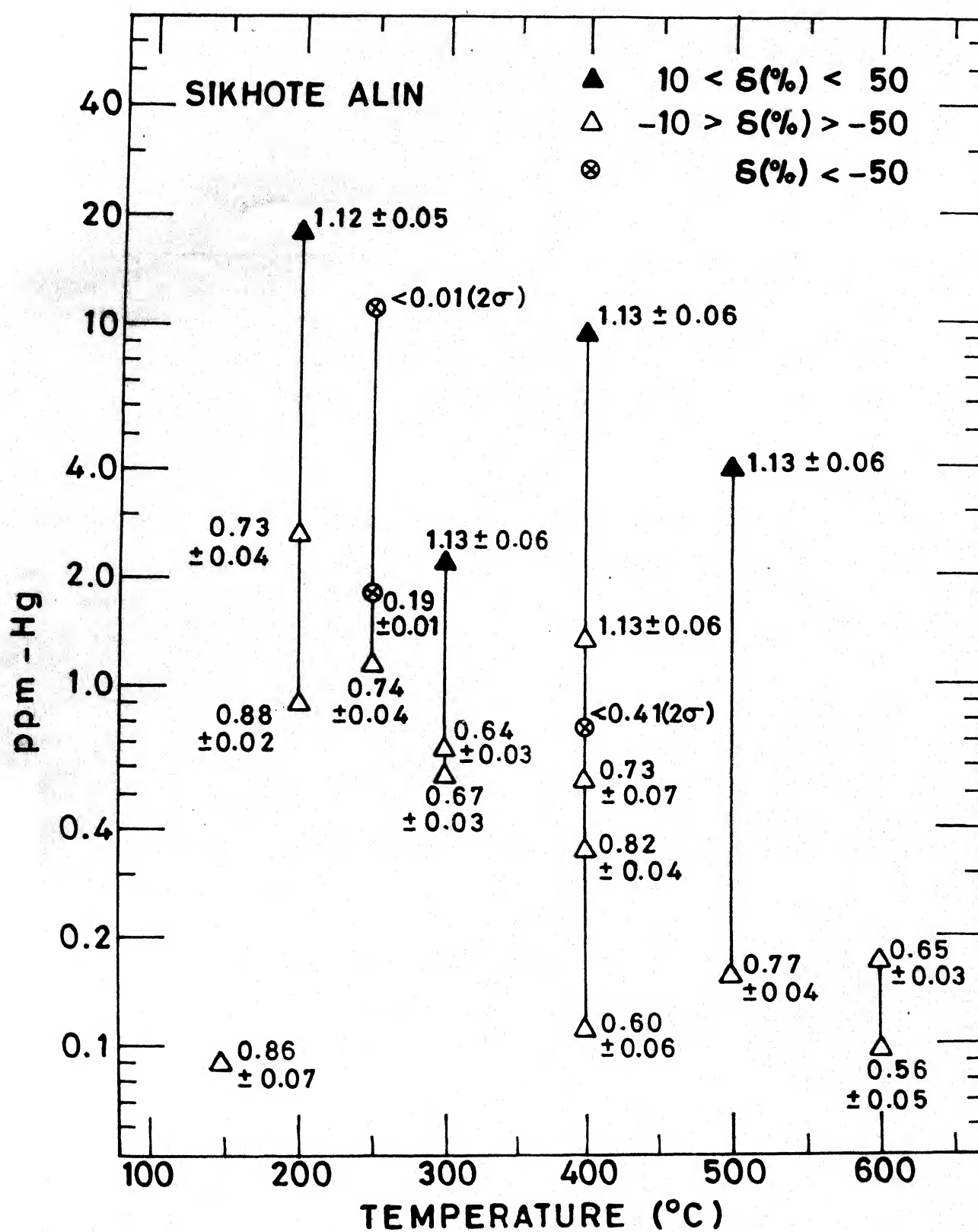


Fig. 5.14 ppm-Hg vs. temperature in Sikhote Alin.

Table 5.11 Gross Values of  $R/R^+$  and Hg contents in Sikhote Alin

Sample	Mass (mg)	Vial No.	Gross	
			ppm (Hg)	$R/R^+$
Inclusion	217.5	2/86	1.10	0.82
	155.0	2/85	0.08*	0.58
	7.0	2/85	0.19*	0.44
	8.0	2/85	1.14*	0.53
<30 $\mu\text{m}$ , mag.	84.8	7/86	29.00	1.09
>30 $\mu\text{m}$ , mag.	54.0	2/85	13.86*	0.91
<30 $\mu\text{m}$ , nm	11.0	2/85	221.93*	0.91
	6.5	2/85	220.34*	0.91
>30 $\mu\text{m}$ , nm	29.0	2/85	214.38*	0.91
45-75 $\mu\text{m}$ , mag.	75.2	7/86	11.81	>0.06
				<0.81
75-106 $\mu\text{m}$ , mag.	81.1	9/86	128.93	1.08
	64.0	7/86	10.84	<0.85
				>0.80
	76.6	9/86	6.22	0.71
106-125 $\mu\text{m}$ , mag.	95.5	7/86	16.01	1.02
150-300 $\mu\text{m}$ , mag.	25.4	7/86	31.18	1.08

\* The Hg contents are estimated values since no monitor was present.

Table 5.12 Mercury Concentration Ranges in different Iron Meteorite Samples

Group	No. of Meteorites	Concentration Range (ppm)	
		In Acid Residues This work	In Troilite Literature *
I	4	9.42 - 14.44	0.70 - 2.2
II	3	4.97 - 66.7	0.09 - 0.5
IV	1	3.64	

\* Compiled from Reed et al., 1960 and Reed, 1971.

#### 5.4 Constrains on the Origin of Meteorites

Extensive measurements on the isotopic composition of Hg from samples of Allende have been recently reported by Nier and Schlutter (1986). They found the isotopic composition of Hg to be normal for all isotopes of Hg and for all temperature steps. To some extent their normal value may be due to the averaging effect of both the positive and the negative anomalies that can be seen only when the sample size is small. We also failed to observe any anomaly in Allende samples of 800 mg sizes (see Table 3.5, Chapter 3). Only when the sample analysed is small can one see the anomaly.

The Hg content of Allende, as inferred from the data given in the table of Nier and Schlutter is about an order of magnitude smaller than our values. It is possible that in their work most of the Hg is pumped off below 250°C. The anomalous component is generally expected to be, according to our results, more pronounced at 100- and 200°C. It is most unfortunate that Nier and Schlutter (1986) pumped off this valuable fraction and hence failed to observe significant isotopic variations that might be present in their samples. Absence of anomaly in samples extracted at high temperatures must be attributed to the averaging effects, memory, and probably some contamination due to out-gassing of the system at high temperature.

The extent of anomalies that we have found in Hg is seen only in hydrogen and nitrogen isotopes. Perhaps the carrier of these anomalies is a volatile phase (gaseous) which gets deposited on solid grains in the solar nebula just prior to its accumulation. This would mean that the anomalies

are due to nuclear causes rather than due to ion-molecular reactions in the interstellar medium.

While a plausible set of events can be postulated to explain the anomalies in stone meteorites, it is far more challenging to extend this to the case of iron meteorites. Clearly iron meteorites must not have been produced by a magmatic differentiation process. Alternative processes for the formation of iron meteorites have been discussed by Goel et al. (Murty et al. 1983, Goel, 1987). One would also have to say that the formation of the Widmanstätten pattern could be due to diffusion of Fe in Fe-Ni over long periods of time but at low temperature. Recent report by Jovanovic and Reed (1987) on the presence of anomalous Hg in the so-called differentiated meteorites (achondrites) suggests that some member of the solar system (may be comets as suggested by Jovanovic and Reed, 1987) contain highly anomalous Hg.

The fact that the most widely variable of the meteorite classes, from carbonaceous chondrites to the irons, show variations in the Hg isotopic ratios suggests that there is no simple relation between  $\delta$  values and meteorite classes. Either mercury from some phases of the meteorites was fractionated relative to the average nebular reservoirs or its isotopic ratio varied in the primitive nebula due to incomplete mixing between the gas and dust grains of various kinds. The same region of the nebulae had difference in the isotopic composition in Hg in various phases.

If one were to attribute the anomalies solely due to possible implantations of material from comets as suggested by Jovanovic and Reed (1987) for lunar and achondritic objects such a process should occur for all



kinds of parent bodies of meteorites. While it may not be difficult to introduce cometary material into the regolith of the stony objects (parent bodies of chondrites and achondrites), it would need some unusual processes and conditions to incorporate cometary matter into the bodies of iron meteorites. Perhaps the gaseous matter may get sucked into the veins and pores of irons and get deposited along the grain boundaries. This would be consistent with the fact that the anomalies are more easily noted in micro-inclusions. However, no independent proof is as yet available supporting the above hypothesis.

It would be a significant step forward to identify the phase which contains the anomalous Hg. Further work in this direction is currently underway in our laboratory.

## REFERENCES

- Abrashkin S. (1985) *Int. J. Appl. Radiat. Isot.* **36** (5), 385-388.
- Adler I. (1986) in *Chemical Analysis*, John Wiley, New York, **81**, 31-36.
- Alaerts L., R.S. Lewis, J.I. Matsuda and E. Anders (1980) *Geochim. Cosmochim. Acta* **44**, 189-209.
- Alfven H. and G. Arrhenius (1974) in *Structure and Evolutionary history of the Solar system* (Reidel), 202-217.
- Alian A. and B. Sansoni (1980) *Z. fur Chem. Anal.* ISSN 0343-7639, 1-46.
- Alian A. and B. Sansoni (1985) in *Inst. Multi-element Analysis*, Verlag Chemie, Eds. B. Sansoni, Weinheim.
- Alian A., R.G. Djingova, B. Kroner and B. Sansoni (1984) *Z. Anal. Chem.* **319**, 47-53.
- Aller L.H. and J.E. Ross (1967) in *the magnetic and related stars*, Ed. R.C. Cameron, Baltimore 339-343.
- Anders E. (1964) *Space Sci. Rev.* **3**, 583-714.
- Anders E. (1971) *Ann. Rev. Astron. Astrophys.* **9**, 1-34.
- Anders E. (1981) *Proc. R. Soc. Lond.*, **A374**, 207-238.
- Anders E. and R. Hayatsu (1981) in *Topics in curr. Chem.*, Ed. F.L. Boschke, Springer Verlag, **99**, 1-37.
- Anders E. and M. Ebihara (1982) *Geochim. Cosmochim. Acta* **46**, 2363-2380.
- Anicich V.G. and W.T. Huntress Jr. (1986) *Astrophys. J.* **62**, 553-672.
- Arnold J.R. and H.E. Suess (1969) *Ann. Rev. Phys. Chem.* **20**, 293-314.
- Arnould M. (1976) *Astron. Astrophys.* **46**, 117-125.
- Arrhenius G. and H. Alfven (1971) *Earth. Planet. Sci. Lett.* **10**, 253-267.
- Ashworth J.R. (1979) *Minerlog. Mag.* **43**, 335-338.
- Ashworth J.R. (1980) *Earth Planet. Sci. Lett.* **46**, 167-177.
- Ashworth J.R., L.G. Mallinson, R. Hutchison and G.M. Biggar (1984) *Nature* **308**, 259-261.

- Audouze J. (1970) *Astron. Astrophys.* **8**, 436-457.
- Audouze J. (1984) *Comments in Astrophysics*, Preprint.
- Audouze J. (1985) *Astrophys. J.* **293**, L53-L57.
- Audouze J. and J.W. Truran (1975) *Astrophys. J.* **202**, 204-213.
- Audouze J. and S. Vauclair (1980) in *Geophys. Astrophys. monograph*. D. Reidel Dordrecht, 128-136.
- Ballad R.V., L.L. Oliver, R.G. Downing and O.K. Manuel (1979) *Nature* **277**, 615-620.
- Bally J. and W.D. Langer (1982) *Astrophys. J.* **255**, 143-148.
- Barber D.J. (1985) *Clay Minerals* **20**, 415-454.
- Becker R.H. and S. Epstein (1981) *Proc. Lunar Planet. Sci. Conf.* **12th**, 1198-1989.
- Becker R.H. and S. Epstein (1982) *Geochim. Cosmochim. Acta* **46**, 97-103.
- Becker R.H. and R.O. Pepin (1984) *Earth Planet. Sci. Lett.* **70**, 1-10.
- Beer H. and R.L. Macklin (1985) *Phys. Rev. C* **32**, 738-755.
- Begemann F. (1980) *Rep. Prog. Phys.* **43**, 1309-1356.
- Begemann F. (1986) in *the Early Universe and its Evolution*, Ed. A. Faessler, *Prog. Part. Nucl. Phys.* **17**, 349-364.
- Behrmann C.J., R.J. Drozd and C.M. Hohenberg (1973) *Earth Planet. Sci. Lett.* **17**, 446-453.
- Bernatowicz T.J. and A.J. Fahey (1986) *Geochim. Cosmochim. Acta* **50**, 445-452.
- Bernatowicz T.J. and F.A. Podosek (1986) *Geochim. Cosmochim. Acta* **50**, 1503-1507.
- Bernatowicz T.J. and B.E. Hagee (1987) *Geochim. Cosmochim. Acta* **51**, 1599-1611.
- Bidelman W.P. (1968) in *Origin and distribution of the Elements*, Ed. L.H. Ahrens, Oxford, 225.
- Biever P. De. and I.L. Barnes (1985) *Intl. J. Mass. Spect. Ion Proc.* **65**, 211-230.
- Birck J.L. and C.J. Allegre (1984) *Geophys. Res. Lett.* **11**, 943-946.
- Birck J.L. and C.J. Allegre (1985) *Meteoritics* **20**, 609.

- Black D.C. (1972) *Geochim. Cosmochim. Acta* **36**, 347-375.
- Black D.C. and R.O. Pepin (1969) *Earth Planet. Sci. Lett.* **6**, 345-394.
- Boato G. (1954) *Geochim. Cosmochim. Acta* **6**, 209-220.
- Bode H. (1954) *Z. Anal. Chem.* **142**, 414-423.
- Bode H. and F. Newman (1959) *Z. Anal. Chem.* **169**, 410-416.
- Bogard D.D. (1983) *Geophys. Res. Lett.* **10**, 773-837.
- Bogard D.D. and P. Johnson (1983 a) *Geophys. Res. Lett.* **10**, 801-803.
- Bogard D.D. and P. Johnson (1983 b) *Science* **221**, 651-654.
- Briggs M.H. (1963) *Nature* **197**, 1290.
- Burbidge E.M., G.R. Burbidge, W.A. Fowler, and F. Hoyle (1957) *Rev. Mod. Phys.* **29**, 547-650.
- Burgess D.D. and P. Hayumbu (1984) *Anal. Chem.* **56**, 1440-1443.
- Byrne A.R., M. Dermelj, L. Kosta, and M. Tusek-Znidaric (1984) *Mikrochimica Acta* **1**, 119-126.
- Cameron A.G.W. (1963) in *Nuclear Astrophys. lecture notes*, Yale University.
- Cameron A.G.W. (1973) *Space Sci. Rev.* **15**, 121-146.
- Cameron A.G.W. (1983) in *Essay in nuclear and astrophysics*, Ed. C.A. Barnes, Cambridge Univ. Press, 23-43.
- Cameron A.G.W. and J.W. Truran (1977) *Icarus* **30**, 447-461.
- Cameron A.G.W. and J.W. Truran (1978) *Icarus* **30**, 497.
- Cameron A.G.W., J.J. Cowan and J.W. Truran (1978) *Lunar Planet. Sci.* **IX**, 146-148.
- Carol M.V., T.K. Mayeda, R.N. Clayton (1986) *Geochim. Cosmochim. Acta* **50**, 2719-2726.
- Carr L.P., M.M. Grady, I.P. Wright, C.T. Pillinger and A.E. Fallick (1983) *Meteoritics* **18**, 276.
- Chen J.H. and G.J. Wasserburg (1981) *Earth Planet. Sci. Lett.* **52**, 1-15.
- Chen J.H. and G.J. Wasserburg (1985) *Lunar Planet. Sci.* **XVI**, 119-120.
- Chevalier R.A. and R.P. Kirshner (1978) *Astrophys. J.* **219**, 931.

- Clayton D.D. (1975) *Astrophys. J.* **199**, 765-769.
- Clayton D.D. (1977 a) *Icarus* **32**, 255-269.
- Clayton D.D. (1977 b) *Earth Planet. Sci. Lett.* **35**, 398-410.
- Clayton D.D. (1978) in *Moon and Planets.* **19**, 109-137.
- Clayton D.D. (1979) *Space Sci. Revs.* **24**, 147-226.
- Clayton D.D. (1981) *Proc. Lunar Planet. Sci.* **12B**, 1781-1802.
- Clayton D.D. (1982) *Q. J. R. Astron.* **23**, 174-212.
- Clayton D.D. (1986) *Astrophys. J.* **310**, 490-498.
- Clayton D.D. and A.W. Fowler (1961) *Ann. Phys. (N.Y.)* **16**, 51-68.
- Clayton D.D. and M.D. Leising (1987) *Phys. Reports* **144**, 1-50.
- Clayton D.D., E. Dwek and S.E. Woosley (1977) *Ap.J.* **214**, 300-315.
- Clayton R.N. (1978) *Ann. Rev. Nucl. Part. Sci.* **28**, 501-522.
- Clayton R.N. and T.K. Mayeda (1977) *Geophys. Res. Lett.* **4**, 295-298.
- Clayton R.N. and T.K. Mayeda (1978) *Earth Planet. Sci. Lett.* **40**, 168-174.
- Clayton R.N. and T.K. Mayeda (1984) *Earth Planet. Sci. Lett.* **67**, 151-161.
- Clayton R.N., L. Grossman and T. Mayeda (1973) *Science* **182**, 485-488.
- Clayton R.N., N. Onuma and T.K. Mayeda (1976) *Earth Planet. Sci. Lett.* **30**, 10-18.
- Clayton R.N., N. Onuma, L. Grossman and T.K. Mayeda (1977 a) *Earth Planet. Sci. Lett.* **34**, 209-224.
- Clayton R.N., L. Grossman, T.K. Mayeda and N. Onuma (1977 b) in the *Soviet-Amer. Conf. Geochem. Moon Planet. NASA-SB370*, 781-785.
- Clayton R.N., T.K. Mayeda and S. Epstein (1978) *Proc. Lunar Planet. Sci. Conf. 9th*, 1267-1278.
- Clayton R.N., T.K. Mayeda, and K. Yanai (1984) in *Mem. Nat. Inst. Polar. Res.* **35**, 267-271.
- Cornelis R. (1985) *Trends in analytical chemistry*, **4**, 237-241.
- Cowley C. and M.E. Aller (1971) *Astrophys. J.* **9**, 159.
- Cowley C.R. and G.C.L. Aikman (1975) *Publ. Astr. Soc. Pacif.* **87**, 513-519.

- Crozaz G. (1985) in 10th Symp. Antarc. Met. Nat. Inst. Pol. Res., 110.
- Dodd R.T. (1986) in Thunderstones and Shooting Stars, Harvard Univ. Press, 147-170.
- Drake M.J. (1979) in Asteroids, Ed. T. Gehrels, 765-782.
- Drozd R.J., B.M. Kennedy, C.J. Morgan, F.A. Podosek, and G.J. Taylor (1976) Proc. Lunar Sci. Conf. 7th, 599-623.
- Dumarcy R., R. Heindryckx and R. Dams (1980) Anal. Chim. Acta 116, 111-117.
- Dusan B., S. Kristiansson, A. Lundberg, I.L. Skardin, J. Werner and G. Osterdahl (1984) in Proc. Trace Element Anal. in biolog. Tiss., Stockholm, 1-19.
- Dworetsky M.M., A.H. Vaughan and R.E. White (1970) Astrophys. J. 181, 811-823.
- Dybczynski R. (1985) Chemia. Analityczna 30, 749-769.
- Dyer P., G.C. Baldwin, C. Kittrell, D.G. Imre, and E. Abramson (1983) Appl. Phys. Lett. 42, 311-313.
- Dziczkaniec M., G. Lumpkin, K. Donohoe and S. Chang (1981) Lunar Planet. Sci. XII, 246-248.
- Eberhardt P. 1978, Proc. Lunar Planet. Sci. Conf. IX, 1027-1051.
- Eberhardt P. (1979) Lunar Planet. Sci. X, 341-343.
- Eberhardt P., M.H.A. Jungck, F.O. Meier and F.R. Niederer (1981) Geochim. Cosmochim. Acta 45, 1515-1528.
- Ehmann W.D. and J.R. Huizenga (1959) Geochim. Cosmochim. Acta 17, 125-135.
- Ehmann W.D., and J.F. Lovering (1967) Geochim. Cosmochim. Acta 31, 357-376.
- Ehmann W.D. and S.W. Yates (1986) Anal. Chem. 58, 49R-64R.
- Epstein S., R.V. Krishnamurthy, J.R. Cronin, S. Pizzarello, and G.U. Yuen (1987) Nature 326, 477-479.
- Esat T.M., R.H. Spear and S.R. Taylor (1986) Nature 319, 576-578.
- Eugster O., J. Geiss, U. Krahenbuhl and S. Niedermann (1986) Earth Planet. Sci. Lett. 78, 139-147.
- Fowler W.A. (1984) Science 226, 922-935.
- Fowler W.A. (1985) Rev. Mod. Phys., 56, 149-186.
- Franchi I.A., I.P. Wright and C.T. Pillinger (1986) Nature 323, 138-140.

- Francoise M. and R. Jacques (1987) in *Topics Curr. Chem.*, Springer-Verlag, 85-117.
- Frick U. (1977) *Proc. Lunar Sci. Conf.*, 8th, 273-277.
- Frick U. and R.O. Pepin (1981) *Earth Planet. Sci. Lett.* 56, 45-63.
- Gaffey M.J. (1986) *Icarus* 66, 468-486.
- Geiss J. and H. Reeves (1981) *Astron. Astrophys.* 93, 189-199.
- Geiss J. and P. Bochsler (1982) *Geochim. Cosmochim. Acta* 46, 529-548.
- Gijbels R. (1967) *Anal. Chim. Acta* 39, 132-135.
- Gobel R., F. Begemann and U. Ott (1982) *Geochim. Cosmochim. Acta* 46, 1777-1792.
- Goel P.S. (1986) *I.A.U. Symp. Goa India (Abstract)*, 495.
- Goel P.S. (1987) *Proc. Indian Acad. Sci. (Earth Planet. Sci.)* 96, 81-102.
- Goel P.S. and S.V.S. Murty (1983) *Adv. Space Res.* 2, 13-18.
- Goel P.S. and A.N. Thakur (1987) Presented at the 50th Annual Meeting of the Meteoritical Society at NewCastle Upon Tyne, 68.
- Gold T. (1984) *Phil. Trans. R. Soc. Lond.* A313, 39-45.
- Greenland L. and J.F. Lovering (1965) *Geochim. Cosmochim. Acta* 29, 821-858.
- Guthrie B.N.G. (1972) *Astrophys. Space Sci.* 15, 214.
- Guthrie B.N.G. (1984) *Mon. Not. R. Astr. Soc.* 206, 85-107.
- Gyorgy P., G. Sandor and P. Erno (1985) *Anal. Chim. Acta* 167, 193-202.
- Hakkila E.A. and G.R. Waterburg (1960) *Anal. Chem.* 32, 1340-1342.
- Halbout J.F.R. and M. Joroy (1986) *Geochim. Cosmochim. Acta* 50, 1599-1609.
- Halbout J., F. Robest and M. Jaroy (1986) *Geochim. Cosmochim. Acta* 50, 1599-1609.
- Halbout J., T.K. Mayeda and R.N. Clayton (1986) *Earth Planet. Sci. Lett.* 80, 1-18.
- Hanan B.B., G.R. Tilton (1985) *Earth Planet. Sci. Lett.* 74, 209-219.
- Hayatsu R. E. Anders (1981) in *Topics Curr. Chem.* 99, Springer-Verlag, 1.
- Heidenreich III J.E. and M.H. Thiemens (1983) *Meteoritics*, 18, 310.

- Heidenreich III J.E. and M.H. Thiemens (1985) *Lunar Planet. Sci.* XVI, 335-336.
- Heidenreich III J.E. and M.H. Thiemens (1986) *J. Chem. Phys.* 84, 2129-2136.
- Heimbürger R., F. Livardjani and M.J.F. Leroy (1986) *Analisis*, 14, 173-180.
- Hertogen J., M.J. Janssens, H. Takahashi, J.W. Morgan, and E. Anders (1983) *Geochim. Cosmochim. Acta* 47, 2241-2255.
- Heydorn K. (1985) *J. Trace Microprobe Techniques*, 3, (3), 197-220.
- Heymann D. (1982) *Proc. Lunar Planet. Sci. Conf.* 12th, 1803-1807.
- Heymann D. and K. Liffman (1986) *Meteoritics* 21, 95-108.
- Hintenberger H. and H. Wanke (1964), *Z. Naturf.* 19a, 210-218.
- Hintenberger H., H. Voshage and H. Sarker (1965) *Z. Naturf.* 20a, 965-967.
- Huch C.A. and M.P. Bacon (1985) *Anal. Chem.* 57, 2138-2142.
- Hulston J.R. and H.G. Thode (1965) *J. Geophys. Res.* 70, 3475-3484.
- Huntress W.T.Jr. (1977) *Astrophys. J. Suppl.* 33, 495-514.
- Huss G.R. and E.C. Alexander Jr. (1987) *Lunar Planet. Sci.* XVII, E710-E716.
- Hutcheon I.D., I.M. Steele, D.E.S. Wachel, J.D. Macdougall and D. Phinney (1984) *Lunar Planet. Sci.* XV, 339-340.
- Imamura M., M. Shima and M. Honda (1980) *Z. Naturf.* 35a, 267-279.
- Ireland T.R. and W. Compston (1987) *Nature* 327, 689-692.
- Ireland T.R., W. Compston and H.R. Heydegger (1985) *Geochim. Cosmochim. Acta* 49, 1989-1993.
- Ireland T.R., W. Compston and T.M. Esat (1986) *Geochim. Cosmochim. Acta* 50, 1413-1421.
- Jacobsen S.B. and G.J. Wasserburg (1984) *Earth Planet. Sci. Lett.* 67, 137-150.
- Jaffe S. and F.S. Klein (1966) *Trans. Faraday Soc.* 62, 3135-3141.
- Jaschek M. and C. Jaschek (1967) in *Magnetic and related stars*, Ed. R.C. Cameron, Baltimore, 381-387.
- Jovanovic S, and G.W. Reed Jr. (1972) *Earth Planet. Sci. Lett.* 16, 257-262.
- Jovanovic S, and G.W. Reed (1976a) *Earth Planet. Sci. Lett.* 31, 95-100.
- Jovanovic S. and G.W. Reed (1976b) *Science* 193, 888-891.



- Jovanovic S. and G.W. Reed (1977a) Lunar Sci. Conf. XIII, 519-521.
- Jovanovic S. and G.W. Reed (1977b) Proc. Lunar Sci. Conf. 7th, 3437-3446.
- Jovanovic S. and G.W. Reed (1980) Geochim. Cosmochim. Acta 44, 1399-1407.
- Jovanovic S. and G.W. Reed (1985) Geochim. Cosmochim. Acta 49, 0001-0009.
- Jovanovic S. and G.W. Reed (1987a) Presented at the 50th Annual Meeting of the Meteoritical Society at NewCastle Upon Tyne, 97.
- Jovanovic S. and G.W. Reed (1987b) Geophys. Res. Lett. 14, 1127.
- Jungck M.H.A. and P. Eberhardt (1979) Meteoritics 14, 439-441.
- Kaiser T. and G.J. Wasserburg (1983) Geochim. Cosmochim. Acta, 47, 43-58.
- Kaiser T., W.R. Kelly and G.R. Wasserburg (1980a) Geophys. Res. Lett. 7, 271-274.
- Kaiser T., W.R. Kelly and G.J. Wasserburg (1980b) Meteoritics 15, 310-311.
- Kerridge J.F. (1983) Earth Planet. Sci. Lett. 64, 186-200.
- Kerridge J.F. (1985) Geochim. Cosmochim. Acta 49, 1707-1714.
- Kiesl W. and F. Hecht (1969) in Meteorite Research, Ed. P.M. Milliman, Reidel.
- Kolodny Y., J.F. Kerridge and I.R. Kaplan (1980) Earth Planet. Sci. Lett. 46, 149-158.
- Kornacki A.S. and B. Fegley (1986) Earth Planet. Sci. Lett. 79, 217-234.
- Kubik P.W., D. Elmore, N.J. Conard., K. Nishiizmi, and J.R. Arnold (1986) Nature 319, 568-570.
- Kuroda P.K. (1985) Geochem. J. 19, 107-112.
- Kuznetsov R.I., N.N. Korotkova and A.K. Lavrukhina (1983) Geochemistry Intl. 20, 1-10.
- Kuznetsov R.A., V.B. Pankratov and V. Styut (1985) Vestn. Leningr. Univ. Geol. Geogr. 85-89.
- Lammerzahl P. and J. Zahringer (1966) Geochim. Cosmochim. Acta 30, 1059-1074.
- Lancet M.S. (1972) Ph.D. Thesis Univ. of Chicago.
- Lancet M. and E. Anders (1970) Science 170, 980-982.
- Larson H.P., M.A. Feierberg and L.A. Lebofsky (1983) Icarus 56, 398-408.

- Laul J.C., M.R. Smith, H. Wanke, E. Jagoutz, G. Driebus, H. Palme, B. Spettel, A. Burghel, R.M. Verkouteren and M.E. Lipschutz (1986) *Geochim. Cosmochim. Acta* **50**, 1422-1450.
- Lavrukhina A.K. and R.A. Kuznetsova (1980) *Geochemistry Intl.* **17**(5), 1-10.
- Lee T. (1979) *Rev. Geophys. Space Phys.* **17**, 1591-1611.
- Lee T., D.M. Schramm, J.P. Wefel, and J.B. Blake (1979) *Astrophys. J.* **232**, 854-862.
- Lewis R. and E. Anders (1983) *Sci. Amer.* **249**, 66-77.
- Lewis R.S., L. Alaerts and E. Anders (1979) *Lunar Planet. Sci. X*, 728-730.
- Lewis R.S., E. Anders, I.P. Wright, S.J. Norris and C.T. Pillinger (1983) *Nature* **305**, 767-771.
- Lichte F.E., J.L. Seeley, L.L. Jackson, D.M. McKown, and J.E. Jaggart (1987) *Anal. Chem.* **59**, 197R-212R.
- Lingner D.W., T.J. Huston, M. Huston and M.E. Lipschutz (1987) *Geochim. Cosmochim. Acta* **51**, 727-739.
- Lipschutz M.E. (1986) *Anal. Chem.* **58**, 968A-974A.
- Luck J.M., J.L. Birck, and C.J. Allegre (1980) *Nature*, **283**, 256-259.
- Lugmair G.W., K. Marti and N.B. Scheinin (1978) *Lunar Planet. Sci. IX*, 672-674.
- Lugmair G.W., T. Shimamura, R.S. Lewis and E. Anders (1983) *Science* **222**, 1015-1018.
- Macdougall J.D. (1977) *Meteoritics* **12**, 301-302.
- MacPherson G.J. and L. Grossman (1984) *Geochim. Cosmochim. Acta* **48**, 29-46.
- Marvin U.B. (1983) *Geophys. Res. Lett.* **10**, 775-778.
- Marvin U.B. (1987) in *Astrochemistry*, Eds. M.S. Vardya and S.P. Tarafdar, 469-484.
- Mathews G.J. and R.A. Ward (1985) *Rep. Prog. Phys.* **48**, 1371-1418.
- McCulloch M.T. and G.J. Wasserburg (1978a) *Astrophys. J.* **220**, L15-L19.
- McCulloch M.T. and G.J. Wasserburg (1978b) *Geophys. Res. Lett.* **5**, 599.
- McFarren E.A., R.J. Lishka, J.H. Parker (1970) *Anal. Chem.* **42**, 358-365.

- McKeegan K.D., R.M. Walker and E. Zinner (1985) *Geochim. Cosmochim. Acta* **49**, 1971-1987.
- McSween H.Y. (1985) *Rev. Geophys.* **23**, 391-416.
- McSween H.Y., and E.M. Stolper (1980) *Sci. Amer.* **242**, 54-63.
- Melosh H.J. (1984) *Icarus* **59**, 234-260.
- Mestel L. (1984) *Phil. Trans. R. Soc. Lond.* **A313**, 19-25.
- Michaud G., H. Reeves and Y. Charland (1974) *Astron. Astrophys.* **37**, 313-324.
- Molini-Velsko C., T.K. Mayeda and R.N. Clayton (1986) *Geochim. Cosmochim. Acta* **50**, 2719-2726.
- Morand P. and C.J. Allegre (1983) *Earth Planet. Sci. Lett.* **63**, 167-176.
- Morgan J.W. and M. Jansseus (1985) *Geochim. Cosmochim. Acta* **49**, 247-259.
- Mullie F. and J. Reisse (1987) in *Topics Curr. Chem.*, Springer-Verlag. **139**, 84-117.
- Murty S.V.S. (1981) Ph.D. Thesis, I.I.T., Kanpur.
- Murty S.V.S., P.N. Shukla and P.S. Goel (1982) *Earth Planet. Sci. Lett.* **60**, 1-7.
- Murty S.V.S., P.S. Goel, D. Yu. Minh and Yu. A. Shukolyukov (1983) *Geochim. Cosmochim. Acta* **47**, 1061-1068.
- Nagahara H. (1984) *Geochim. Cosmochim. Acta* **48**, 2581-2595.
- Nagata T., and M. Funaki (1985) Tenth Symposium on Antarctic Meteorites, Nat.Inst.Pol.Res., Tokyo, 117-119.
- Nakamura N., D.M. UNruch, and M. Tatsumoto (1985) Tenth symposium on Antarctic Meteorites, Nat.Inst.Pol.Res., Tokyo, 103-105.
- Narayan C. and J.I. Goldstein (1985) *Geochim. Cosmochim. Acta* **49**, 397-410.
- Navon O. and G.J. Wasserburg (1985) *Earth Planet. Sci. Lett.* **73**, 1-16.
- Niederer F.R. and D.A. Papanastassiou (1984) *Geochim. Cosmochim. Acta* **48**, 1279-1293.
- Niederer F.R., P. Eberhardt, J. Geiss and R.S. Lewis (1985) *Meteoritics*, **20**, 716-718.
- Niemeyer S. and G.W. Lugmair (1984) *Geochim. Cosmochim. Acta* **48**, 1401-1416.

- Nier A.O. (1950) *Phys. Rev.*, **77**, 789-793.
- Nier A.O. and D.J. Schlutter (1986) *J. Geophys. Res.* **91**, E124-E128.
- Nishiizumi K., J. Klein, R. Middleton, P.W. Kubic, and J.R. Arnold (1986) Eleventh Symp. Antarctic Meteorites, *Nat. Inst. Pol. Res.* Tokyo, 58-59.
- Nyquist L.E., D.D. Bogard, J.L. Wooden, H. Wiesmann, C.Y. Shih, B.M. Bansal and G. McKay (1979) *Meteoritics* **14**, 502.
- Oliver L.L., R.V. Ballad, J.F. Richardson and O.K. Manuel (1981) *J. Inorg. Nucl. Chem.* **43**, 2207-2216.
- Ott U., R. Mack and S. Chang (1981) *Geochim. Cosmochim. Acta* **45**, 1751-1788.
- Ott U., J. Kronenbitter, J. Flores and S. Chang (1984) *Geochim. Cosmochim. Acta* **48**, 267-280.
- Ott U., J. Yang and S. Epstein (1985) *Meteoritics* **20**, 722-723.
- Owen T., B.L. Lutz and C. De. Bergh (1986) *Nature*, **320**, 244-246.
- Papanastassiou D.A. and G.J. Wasserburg (1978) *Geophys. Res. Lett.* **5**, 595-598.
- Parry S.J., (1984) *Proc. Int. Nucl. Meth. Invis. Energy Res.* **5th**, 97-105.
- Patchett P.J. (1980) *Nature* **283**, 438-441.
- Pelas P., A. Ducatel and J.L. Berdot (1973) *Meteoritics* **8**, 418-419.
- Penzias A.A. (1979) *Science* **205**, 549-551.
- Penzias A.A. (1980) *Science* **208**, 663-669.
- Pepin R.O. (1968) in *Origin and Distribution of elements*, Ed. L.H. Ahrens (Pergamon), 379-396.
- Pertel R. and H.E. Gunning (1959) *Can. J. Chem.* **37**, 35-42.
- Pillinger C.T. (1979) *Rep. Prog. Phys.* **42**, 897.
- Pillinger C.T. (1984) *Geochim. Cosmochim. Acta* **48**, 2739-2766.
- Poets H., S.S. Strecker and F. Begemann (1987) *Geochim. Cosmochim. Acta*, 1143-1149.
- Preston G.W. (1971) *Publ. Astron. Soc. Pacific* **83**, 607-612.
- Pritchard J.G. and S.O. Saied (1986) *Analyst*, **111**, 29-35.
- Prombo C.A. and R.N. Clayton (1985) *Science* **230**, 935-937.

- Pruett D.J. (1986) *Sep.Sci.Techn.* **2**, 321-338.
- Reed G.W. (1971) in *Handbook of Elemental Abundances in Meteorites*, Ed. B. Mason, 487-491.
- Reed G.W. and S. Jovanovic (1967) *J. Inorg. Nucl. Chem.* **31**, 3783-3788.
- Reed G.W. and S. Jovanovic (1969) *J. Inorg. Nucl. Chem.* **31**, 3783-3788.
- Reed G.W., K. Kigoshi and A. Turkevich (1960) *Geochim.Cosmochim. Acta* **20**, 122-140.
- Rees C.E. and H.G. Thode (1977) *Geochim.Cosmochim.Acta* **41**, 1679-1682.
- Reeves H. (1978) in *Protostars and Planets*. Ed. T. Gehrels Univ. Arizona, 399.
- Reynolds J.H. (1967) *Ann.Rev.Nucl.Sci.* **17**, 253-316.
- Reynolds J.H. (1977) *Sov.Amer.Conf. Cosmochem. Moon Planets. NASA. SP-370*, 771-780.
- Reynolds J.H., E.C. Alexander, P.K. Davis, and B. Srinivasan (1974) *Geochim. Cosmochim.Acta* **38**, 401-417.
- Reynolds J.H., U. Frick, J.M. Neil and D.L. Phinney (1978) *Geochim.Cosmochim. Acta* **42**, 1775-1797.
- Robert F. (1985) *Meteoritics* **20**, 744-746.
- Robert F. and S. Epstein (1982) *Geochim.Cosmochim.Acta*, **46**, 81-95.
- Robert F., L. Merlivat and M. Javoy (1979) *Nature* **282**, 785-789.
- Robert F., L. Merlivat and M. Javoy (1980) *Meteoritics* **13**, 613-615.
- Rolfs C., H.P. Trautvetter and W.S. Rodney (1987) *Rep.Prog.Phys.* **50**, 233-325.
- Rosman K.J.R., J.R. De Laeter and M.P. Gorton (1980) *Earth Planet.Sci. Lett.* **48**, 166-170.
- Rozanska B and E. Iachowicz (1985) *Anal.Chim.Acta* **175**, 211-217.
- Rubin A.E. (1985) *Rev. Geophys.* **23**, 277-300.
- Rubin A.E., A. Rehfeldt, E. Peterson and K. Keil (1983) *Meteoritics* **18**, 179-196.
- Ryder G. (1987) *Rev.Geophys.* **25**, 277-284.
- Ryder C., H. Reeves, E. Gradsztajn, and J. Audouze (1970) *Astron. Astrophys.*, **8**, 389-397.

- Sander R.K., T.R. Loree, S.D. Rockwood and S.M. Freund (1977) *Appl. Phys. Lett.* **30**, 150-152.
- Sargent W.L.W. (1964) *Ann. Rev. Astron. Astrophys.* **2**, 297-315.
- Schramm D.N. (1978) in *Protostars and Planets*. T. Gehrels, Univ. Arizona, 384.
- Schramm D.N. (1983) in *Essays in Nuclear Astrophys.*, Ed. C.A. Barnes et al., Cambridge, 325-353.
- Scott E.R.D., A.E. Rubin, G.J. Taylor and K. Keil (1984) *Geochim. Cosmochim. Acta* **48**, 1741-1757.
- Scott E.R.D., D. Lusby and K. Keil (1985) *J. Geophys. Res.* **90**, D137-D148.
- Sears D. (1986) *Nature* **322**, 309.
- Seeger P.A., W.A. Fowler and D.D. Clayton (1965) *Astrophys. J. Suppl.* **97**, 121-133.
- Sekine T. and Y. Hasegawa (1977) in *Solvent Extraction Chemistry*, Marcel Dekker Inc. N.Y., 445-449.
- Semenenko V.P., L.G. Samoilovich, and B.V. Tertichnaya (1986) *Mineralog. Mag.* **50**, 317-322.
- Shima M. (1986) *Geochim. Cosmochim. Acta* **50**, 577-584.
- Shima M. and M. Honda (1966) *Shitsuryo Bunseki (Mass Spectroscopy)* **14**, 23-24.
- Shima M., M. Imamura, H. Matsuda and M. Honda (1969) in *Meteorite Research* Ed. P.M. Millman Reidel, 335-347.
- Shimamura T. and G.W. Lugmair (1983) *Earth Planet. Sci. Lett.*, **63**, 177-188.
- Shukolyukov Yu.A., D.V. Minh, P.S. Goel and N.I. Zaslavskaya (1984) *Geokhimiya*, **6**, 771-780.
- Smith J.W. and I.R. Kaplan (1970) *Science* **167**, 1367-1370.
- Snell R.L. and A. Wootten (1979) *Astrophys. J.* **228**, 748-754.
- Srinivasan B. and E. Anders (1978) *Science* **201**, 51-53.
- Stary J. and K. Kratzer (1968) *Anal. Chim. Acta* **40**, 93-100.
- Suess H.E. (1965) *Ann. Rev. Astron. Ap.* **3**, 217-234.
- Suess H.E. and H.C. Urey (1956) *Rev. Mod. Phys.* **28**, 53-74.

- Sutton S.R. (1985) Tenth Symp., Antarctic Meteorites, Natl.Inst.Pol.Res. Tokyo, 111-113.
- Sutton S.R. and G. Crozaz (1983) *Geophys.Res.Lett.* **10**, 809-912.
- Swart P.K., M.M. Grady, C.T. Pillinger, R.S. Lewis, and E. Anders (1983) *Science* **220**, 406-408.
- Szabo A.S. (1985) *J. Radioanal.Nucl.Chem.Lett.* **96**, 241-248.
- Takahashi H., H. Higuchi, J. Gross, J.W. Morgan and E. Anders (1976) *Proc. Natl.Acad.Sci., USA*, **73**, 4253-4256.
- Takaoka N. (1986) Eleventh Symp. Antarctic Meteorites, Natl.Inst.Pol.Meteorites, 114-116.
- Teshima J., G.J. Wasserburg, A. El. Goresy and J.H. Chen (1986) *Geochim. Cosmochim.Acta* **50**, 2073-2087.
- Thakur A.N. and P.S. Goel (1985) *Proc.Radiochem.Radiationchem.Symp.* Dept. of Atomic Energy, IIT Kanpur, 542-554.
- Thakur A.N. and P.S. Goel (1987) Presented to National Space Science Symp. (PRL, Ahmedabad) Dec., 21-24.
- Thiemens M.H. and R.N. Clayton (1979) *Meteoritics* **14**, 545-547.
- Thiemens M.H. and R.N. Clayton (1981) *Earth.Planet.Sci.Lett.* **55**, 363-369.
- Thiemens M.H. and J.E. Heidenreich III (1983) *Science* **219**, 1073-1075.
- Thiemens M.H. and J.D. Jackson (1985) *Meteoritics* **20**, 775-776.
- Thiemens M.H., S. Gupta, and S. Chang (1983) *Meteoritics* **18**, 408-409.
- Turner C., M.C. Enright and P.H. Cadogan (1978) *Proc.Lunar.Planet.Sci.Conf.* **9th**, 989-1025.
- Vogt J.R. and W.D. Ehmann (1965) *Geochim.Cosmochim.Acta* **29**, 373-383.
- Von Helden J. and F. Begemann (1976) *Meteoritics* **11**, 297.
- Voshage H. (1981) *Meteoritics* **16**, 395.
- Voshage H. and H. Hintenberger (1961) *Z. Naturf.* **16a**, 1042-1053.
- Voshage H. and H. Feldmann (1978) *Earth Planet.Sci.Lett.* **39**, 25-36.
- Walker D., E.M. Stolper, and J.F. Hays (1979) *Proc.Lunar Planet.Sci.Conf.* **10th**, 1995-2015.

- Wannier P.G.A. (1980) *Rev. Astr. Astrophys.* **18**, 399-437.
- Warren P.H. and G.W. Kallemeyn (1984) *J.Geophys.Res.* **89**, C16-C24.
- Warren P.H., and G.W. Kallemeyn (1986) Eleventh Symp. Antarctic Meteorites, Nat.Inst.Pol.Res.Tokyo, 31-33.
- Wasserburg G. (1985) in *Protostars and Planets II* (Eds. D.C. Black and M.C. Mathews) Univ.Arizona Press, Tucson, 703-737.
- Wasserburg G.J. and D.A. Papanastasiou (1983) in *Essays in Nuclear Astrophys.* Eds. C.A. Barnes et al., Cambridge Univ.Press.
- Wasserburg G.J., T. Lee and D.A. Papanastasiou (1977) *Geophys.Res.Lett.* **4**, 299-302.
- Wasserburg G.J., D.A. Papanastasiou and T. Lee (1978) *Proc. XXII, Colloq. Intl.d' Astrophysiq.Liege*, 203-255.
- Wasserburg G.J., D.A. Papanastasiou and T. Lee (1980) LXXIII. *Corso.Soc. Ital.deFisica*, Bologna.
- Wasson J.T. (1974) in *Meteorites*, Springer-Verlag. N.Y., Ed. P.J. Wyllie, 84-88.
- Wasson J.T., and G.W. Wetherill (1979) in *Asteroids*, Ed. T. Gehrels, 926-974.
- Wasson J.T. and A.E. Rubin (1985) *Nature* **318**, 168-170.
- Wasson J.T. and J. Wang (1986) *Geochim.Cosmochim.Acta* **50**, 725-732.
- Watson W.D. (1976) *Rev.Mod.Phys.* **48**, 513-520.
- White R.E., A.H. Vaughan, G.W. Preston and J.P. Swings (1976) *Astrophys. J.* **204**, 131-140.
- Wiedenbeck M.E. (1983) in *Proc.NATO.Adv. Std.Inst., Composition and Origin of Cosmic Rays*, NATO ASI Series 65-82.
- Williamson T.G. and W.W. Harrison (1969) in *Modern trends in Activation Analysis*, NBS, Special Publ.No. 312 Vol.1, 283-287.
- Winnewisser G. (1981) in *Topics in Current Chemistry*, Ed. F.L. Boschke, 39-71.
- Winnewisser G. and E. Herbst (1987) in *Topics in Curr.Chem.* **139**, 120-173.
- Winnewisser G., E. Churchwell and C.M. Walmsley (1979) in *Modern Aspects of Microwave Spectroscopy*, Ed. G.W. Chantry, Acad.Press 368-370.



- Wolf R., M. Ebihara, G.R. Richter and E. Anders (1983) *Geochim.Cosmochim. Acta* **47**, 2257-2270.
- Wood C.A., and L.D. Ashwal (1981) *Proc.Lunar Planet.Sci.Conf.* **12B**, 1359-1375.
- Woolfson M.M. (1984) *Phil.Trans.R.Soc.Lond.* **A313**, 5-18.
- Woosley S.E. and W.M. Howard (1977) *Astrophys. J.* **214**, 300-315.
- Woosley S.E. and W.M. Howard (1978) *Astrophys.J.Suppl.* **36**, 285-292.
- Woosley S.E. and T.A. Weaver (1982) in *Essays in Nucl. Astrophys.*, Ed. C.A. Barnes et al. Cambridge 377.
- Woosly S.E., W.D. Arnett. and D.D. Clayton (1973) *Astrophys.J.Suppl.* **26**, 231-312.
- Yang J. and S. Epstein (1983) *Geochim.Cosmochim.Acta* **47**, 2199-2216.
- Yang J. and S. Epstein (1984) *Nature* **311**, 544-547.
- Yeh S.J., J.M. Lo and E.L. Wang (1984) *J.Chinese Chem.Soc.* **31**, 131-142.
- Yu J.C., J.M. Lo and C.M. Wai (1983) *Anal.Chim.Acta* **154**, 307-312.
- Zinner E. and S. Epstein (1987) *Earth Planet.Sci.Lett.* **84**, 359-368.

#### GENERAL REFERENCES

- Anders E. (1987) *Phil.Trans.R.Soc.Lond.* **A323**, 287-304.
- Anders E. (1987) in *Meteorites and the Early Solar System*, Ed. J.F. Kerridge, Univ.Arizona Press, Preprint.
- Arnould M. (1987) *Phil.Trans.R.Soc.Lond.* **A323**, 251-267.
- Graham A.L., A.W.R. Bevan and R. Hutchison (1985) in *Catalogue of Meteorites*, British Museum (Natural History).
- Pillinger C.T. (1987) *Phil.Trans.R.Soc.Lond.* **A323**, 313-322.
- Reus U. and W. Westmeier (1983) *Atomic Data Nucl. Data Tables* **29(1)**, 1-192.
- Reus U. and W. Westmeier (1983) *Atomic Data Nucl. Data Tables* **29(2)**, 193-406.

- Roesmer J. and P. Kruger (1960) in the Radiochemistry of Mercury, NSEC, USA.
- Schramm D. N. (1985) in Nucleosynthesis Challenges and New Developments, Ed. W.D. Arnett and J.W. Truran, Univ. Chicago Press, 106-121.
- Smith D. (1987) Phil.Trans.R.Soc.Lond. A323, 269-286.
- Wood J.A. (1988) Ann.Rev.Earth Planet.Sci. 16, Preprint.
- Wood J.A. and G.E. Morfill (1987) in Meteorites and the Early Solar System, Eds. J.F. Kerridge and M.S. Mathews, Univ.Arizona Press, Preprint.